SCUOLA DI DOTTORATO
UNIVERSITÀ DEGLI STUDI DI MILANO-BICOCCA

Department of Biotechnology and Biosciences

PhD Programme: Converging Technologies for Biomolecular Systems (TeCSBi)

Cycle: XXXIV

Modulation of the Innate Immune Response by Targeting Toll-like Receptor 4 Signalling: Exploring the Role of Natural Products

Surname: Artusa Name: Valentina

Registration number: 848863

Tutor: Prof. Francesco Peri
Co-tutor: Prof. Antonino Bruno

Coordinator: Prof. Paola Branduardi

ACADEMIC YEAR 2020-2021

TABLE OF CONTENTS

Abstract

For centuries, natural products and their derivatives have provided a rich source of compounds for the development of new immunomodulators in the treatment of human diseases. Natural immune modulators may provide the key to control and ultimately defeat disorders affecting the immune system, by either up- or down-regulating the immune response with few adverse side effects. Many of these compounds are currently undergoing clinical trials, particularly as anti-oxidative, anti-microbial, and anti-cancer agents. However, the functions and mechanisms of action of natural products, and how they interact with the immune system, has yet to be extensively explored.

In recent years, the increasing body of knowledge regarding the role of macrophages in the steady-state and in the context of inflammation has opened diverse new avenues of investigation and possibilities for therapeutic intervention targeting the inherent plasticity of macrophages for the treatment of acute and chronic inflammatory disease. Toll-Like Receptors (TLRs), including TLR4, play a crucial role in inflammatory-based diseases, therefore TLR4 signalling has been identified as a therapeutic target for pharmacological intervention.

This work aims to screen and investigate the potential of phytoextracts and phytochemicals to affect TLR4 signalling in a macrophage-like cell model. Specifically, extracts from green (GCE) and roasted (RCE) coffee beans as well as pure chlorogenic acid (5-CQA) were tested. Also, the anti-inflammatory effect of palmitoylethanolamide (PEA), and its synthetic analogue RePEA, was assessed.

Human monocyte-derived macrophages, deriving from the differentiation of a monocytic cell line (THP-1) and/or from human primary $CD14^{+}$ monocytes, were

employed as an *in vitro* model. MTT was used to determine cytotoxic effects of the treatments. TLR4 activation was stimulated by exposure of cells to bacterial endotoxin LPS (*E. coli*), in presence or absence of treatments. Different readouts were evaluated: endpoint pro-inflammatory cytokines production, as well as phosphorylation and nuclear translocation of intracellular signalling mediators. These parameters were measured applying different cellular and molecular techniques, mainly enzyme-linked immunosorbent assay (ELISA), High Content Analysis (immunofluorescence microscopy), and Western blot. Alongside, we employed different commercially available stable transfected cells as tools to investigate the mechanism of action of our tested extract or molecule, THP1-XBlue™, RAW-Blue™ and HEK-Blue™ cells, respectively.

Key findings include a dramatic, dose-dependent, inhibitory effect of both green and roasted coffee extracts towards interferon-β (IFN-β) release, upon LPS stimulation. Consistently, chlorogenic acid, a major polyphenolic component of coffee extracts, showed a comparable biological activity. Additionally, novel evidence towards the immunomodulatory effects and mechanism of action of coffee extracts and chlorogenic acid as modulators of TLR4-related pro-inflammatory signalling have been provided. Alongside, PEA capability of reducing TNF-α release from LPS-stimulated microglial cells, was corroborated in our macrophage model also, confirming its anti-inflammatory potential. Moreover, RePEA, a synthetic PEA analogue designed to be degraded slower, was revealed to be more active than its parent compound.

These experimental data demonstrate that natural products may act as lead molecules for the development of safe and effective immunomodulators.

Taken together, these findings help to validate the above-mentioned natural molecules, 5-CQA and PEA, but also RePEA, as potential novel candidates for further preclinical investigations for the treatment of inflammatory-based disorders.

Riassunto

Per secoli, i prodotti naturali e i loro derivati hanno fornito una ricca fonte di composti per lo sviluppo di nuovi immunomodulatori. Gli immunomodulatori naturali possono fornire la chiave per controllare e, infine, sconfiggere i disturbi che colpiscono il sistema immunitario, stimolando o inibendo la risposta immunitaria con pochi effetti collaterali negativi. Molti di questi composti sono attualmente in fase di sperimentazione clinica, in particolare come agenti antiossidanti, antimicrobici e antitumorali. Tuttavia, la funzione e il meccanismo di azione dei prodotti naturali, e il modo in cui interagiscono con il sistema immunitario, devono ancora essere ampiamente esplorati.

Negli ultimi anni, la conoscenza del ruolo dei macrofagi nel contesto dell'infiammazione ha aperto numerose nuove strade, tra cui la possibilità di intervento terapeutico mirato sfruttando la plasticità intrinseca dei macrofagi per il trattamento di patologie infiammatorie acute e croniche. I recettori Toll-simili (TLR), incluso TLR4, svolgono un ruolo cruciale nelle malattie a base infiammatoria; pertanto, la via di segnalazione di TLR4 è stata identificata come bersaglio terapeutico per l'intervento farmacologico.

Questo lavoro mira a valutare il potenziale dei fitoestratti e delle sostanze fitochimiche di influenzare la via di segnalazione di TLR4 in un modello cellulare di macrofago. Nello specifico, sono stati testati estratti ottenuti da chicchi di caffè verde (GCE) e tostato (RCE), nonché acido clorogenico puro (5-CQA). Inoltre, è stato valutato l'effetto antinfiammatorio della palmitoiletanolamide (PEA) e del suo analogo sintetico RePEA.

Come modello *in vitro* sono stati impiegati macrofagi originati da monociti umani, derivanti dalla differenziazione di una linea cellulare (THP-1) e/o da monociti umani

primari. Il saggio MTT è stato utilizzato per determinare gli effetti citotossici dei trattamenti. L'attivazione di TLR4 è stata stimolata mediante esposizione delle cellule all'endotossina batterica LPS (*E. coli*) in presenza o assenza di trattamento. Sono stati valutati diversi parametri: produzione di citochine pro-infiammatorie, ma anche attivazione e traslocazione nucleare dei mediatori di segnalazione intracellulare. Questi parametri sono stati misurati applicando differenti tecniche di biologia cellulare e molecolare, principalmente test di immunoassorbimento enzimatico (ELISA), immunofluorescenza e immunofissazione (Western blot). Inoltre, abbiamo impiegato diverse cellule transfettate stabilmente disponibili in commercio come strumenti per studiare il meccanismo d'azione del nostro estratto o della nostra molecola, rispettivamente le cellule THP1-XBlue™, RAW-Blue™ e HEK-Blue™.

I risultati chiave includono un marcato effetto inibitorio, dose-dipendente, degli estratti di caffè verde e tostato verso il rilascio di interferone-β (IFN-β) dopo la stimolazione con LPS. Coerentemente, l'acido clorogenico, un importante componente polifenolico degli estratti di caffè, ha mostrato un'attività biologica comparabile. Complessivamente, i risultati ottenuti forniscono nuove prove sugli effetti immunomodulatori e sul meccanismo d'azione degli estratti di caffè e dell'acido clorogenico, in particolare come modulatori della via di segnalazione pro-infiammatoria mediata da TLR4. Inoltre, la capacità della PEA di ridurre il rilascio di TNF-α da parte delle cellule microgliali stimolate con LPS è stata corroborata anche nel nostro modello di macrofagi, confermando il suo potenziale antinfiammatorio. Inoltre, RePEA, un analogo sintetico della PEA progettato per essere degradato più lentamente, si è rivelato più attivo del suo composto originario.

Questi risultati aiutano a convalidare le suddette molecole naturali, 5-CQA e PEA, ma anche RePEA, come potenziali nuovi candidati per ulteriori indagini precliniche per il trattamento delle malattie autoimmuni e infiammatorie.

List of Abbreviations

5-CQA	5-caffeoylquinic acid
AGS	Aicardi–Goutieres syndrome
AIM2	Absent-in-melanoma 2
AP-1	Activator protein 1
ATP	Adenosine triphosphate
ASC	Apoptosis-associated speck-like protein containing a caspase-recruitment domain
CARD	Caspase recruitment domain
CASP	Caspase
CD14	Cluster of differentiation 14
CGA	Chlorogenic acid
CMV	Cytomegalovirus
COX	Cyclooxygenase
CTLD	C-type lectin-like domain
DAMP	Damage-associated molecular pattern
DC	Dendritic cell
dsRNA	double stranded RNA
FAAH	Fatty acid amide hydrolase
FADD	Fas-associated protein with death domain

GCE	Green coffee extract
GM-CSF	Granulocyte/macrophage colony-stimulating factor
GSDMD	Gasdermin D
HIV	Human immunodeficiency virus
HSC	Hematopoietic stem cell
IBD	Inflammatory bowel disease
IFI16	IFNγ-inducible protein 16
IFN	Interferon
IFN-I	Type I interferon
IFNAR	IFN-alpha/beta receptor
IKK	Inhibitor of NF-κB kinase
IL	Interleukin
IL-1β	Interleukin-1 beta
IL-6	Interleukin-6
iNOS	inducible nitric oxide synthase
IRAK	IL-1 receptor-associated kinase
IRF-3	Interferon regulatory transcription factor 3
ISG	Interferon-stimulated gene
ISRE	IFN-stimulated response elements
JNK	c-Jun N-terminal kinase
LBP	LPS-binding protein

LOX	Lipoxygenase
LPS	Lipopolysaccharide
LRR	Leucine-rich repeat motif
MAMP	Microbial-associated molecular pattern
MAPK	Mitogen-activated protein kinase
MCP-1	Monocyte chemoattractant protein-1
MDA5	Melanoma differentiation-associated gene 5
MDM	Monocyte-derived macrophage
MD-2	Myeloid differentiation protein-2
MHC	Major histocompatibility complex
MKK	MAPK kinase
MoDM	Monocyte-derived macrophage
MPS	Mononuclear phagocyte system
MTT	3-(4,5-dimethylthiazol-2-yl)-2,5-diphenyltetrazolium bromide
MYD88	Myeloid differentiation primary response 88
M-CSF	Macrophage colony-stimulating factor
NAAA	*N*-acylethanolamine acid amidase
NAE	*N*-acylethanolamines
NEMO	NF-κB essential modifier
NF-κB	Nuclear factor kappa-light-chain-enhancer of activated B cells
NK	Natural killer cell

NMR	Nuclear magnetic resonance
NLR	Nod-like receptor
NLRP	NOD-, LRR- and pyrin domain-containing
NOD	Nucleotide-binding oligomerization domain
NSAID	Nonsteroidal anti-inflammatory drugs
PAMP	Pathogen-associated molecular pattern
PEA	Palmitoylethanolamide
PPAR-α	Peroxisome proliferator-activated receptor alpha
PRR	Pattern-recognition receptor
PYD	Pyrin domain
PYHIN	Pyrin and HIN domain-containing protein
RA	Rheumatoid arthritis
RCE	Roasted coffee extract
RePEA	Retro-PEA
RIG-I	Retinoid acid-inducible gene I
RIP1	Receptor-interacting protein 1
RIPK1	Receptor-interacting serine/threonine-protein kinase 1
SEAP	Secreted embryonic alkaline phosphatase
SLE	Systemic lupus erythematosus
ssRNA	single stranded RNA
STAT	Signal transducer and activator of transcription

TAB	TAK1-binding protein
TAK1	Transforming growth factor-activated protein kinase 1
TANK	TRAF family member-associated NF-κB activator
TBK1	TANK-binding kinase 1
TBS	Tris-buffered saline
TCM	Traditional Chinese medicine
TGF-β	Transforming growth factor beta
TIR	Toll/interleukin-1 (IL-1) receptor homology domain
TIRAP	TIR domain-containing adaptor protein
TLR	Toll-like receptor
TNF-α	Tumor necrosis factor alpha
TRAF	TNF receptor associated factor
TRAM	TRIF-related adaptor molecule
TRIF	TIR-domain-containing adapter-inducing interferon-β
TRM	Tissue-resident macrophage
TRP	Transient receptor potential
YS	Yolk sac

List of Figures

1. INTRODUCTION

1.1. Immunity and Inflammation in Health and Disease

All living organisms, from bacteria to sea anemones to humans, are constantly exposed of infection by pathogens, and thus have had to evolve a range of defence strategies to persist on Earth. Inflammation, induced by tissue injuries and microbial infection, is one of the most organized biological processes. It can be triggered by a variety of factors, including pathogens, damaged cells, toxic compounds or irradiation.[1] Some inflammatory processes lead to symptoms such as swelling, pain, and redness, but these are, at least initially, completely normal, and protective. However, when inflammation settles in as a permanent feature, it rapidly becomes part of the problem. Thus, quieting long-lasting inflammation is increasingly viewed as critical to health as research firmly establishes that virtually every chronic disease (from Alzheimer's disease to diabetes to hypertension to periodontal disease to inflammatory bowel disease) has an aspect of chronic inflammation at its core. Even though widely demonized, inflammation also plays a critical role in healing. In that context, it appears worthwhile to target the immune system to modulate the risk of certain chronic illnesses.

This introductory section reports a brief overview of the immune system, including a special focus on Toll-like receptor 4 signalling. The pertinence and limitations of targeting the immune system to prevent chronic diseases is also discussed. Finally, a concise review of some of the most studied natural products showing promising immunomodulatory activity is given, as well as the possibilities for translation ethnopharmacology evidence into clinical and therapeutic applications.

1.1.1. Innate and adaptive immunity: barriers and receptor-based recognition

The body's defence system is made up of innate (inborn) and adaptive (acquired) immune systems. Innate immunity is the term given to the set of inherited, germ-line encoded protection mechanisms that operate as the first line of defence for pathogen sensing and host response. The innate immune system is the first line of defence against pathogens and consists of physical and chemical barriers as well as immunological barriers in the form of different cell types able to recognize invading pathogens (monocytes, macrophages, neutrophils, etc.). Physical and chemical defence mechanisms are represented by epidermis, ciliated respiratory epithelium, vascular endothelium, and mucosal surfaces with antimicrobial secretions.[2] On the other hand, the innate immune response is mediated primarily by phagocytic cells and antigen-presenting cells (APCs), such as granulocytes, macrophages, and dendritic cells (DCs), and has been regarded as relatively nonspecific. Contrarily, the adaptive immune response is characterized by specificity developed by clonal gene rearrangements from a broad repertoire of antigen-specific receptors on lymphocytes.[3] The innate immune cells must be able to distinguish "self" (endogenous) from "non-self" (exogenous). This sophisticated immune response relies on the recognition of microorganisms via several distinct receptors known as pattern-recognition receptors or PRRs, such as Toll-like receptors, NOD-like receptor proteins, C-type lectin receptors and RIG-1-like receptors.[4] The activation of PRRs triggers a pro-inflammatory signalling that orchestrates the early response to infection and ultimately leads to subsequent activation of cells of the adaptive immune system (T and B lymphocytes). A major class of molecules involved in many aspects of the inflammatory response and upregulated in response to cellular pathogen recognition consists of immunoreceptors, including cytokine and chemokine receptors, immunoglobulins, TLRs themselves, major histocompatibility complex (MHC) molecules, and costimulatory molecules.[3,5,6]

Together, these proteins participate in the activation and recruitment of leukocytes to sites of inflammation, in enhanced phagocytosis of microbes, in complement- or NK cell-mediated cellular lysis, and in enhanced antigen presentation. Although this immune response is a natural defensive mechanism, a robust and excessive activation of inflammation is clearly associated with numerous immune diseases such as allergic reactions, autoimmune diseases, infectious diseases, cardiovascular disease, atherosclerosis, and cancer.[1]

1.1.2. Pathogen- and Microbial- Associated Molecular Patterns (PAMPs/MAMPs) and the innate immune response

Cells of the innate immune system are responsible for recognizing and responding to the general structural patterns exhibited by pathogens, commonly known as pathogen-associated molecular patterns (PAMPs) and microbial-associated molecular patterns (MAMPs). The innate immune receptors responsible for recognizing PAMPs/MAMPs are known as pattern recognition receptors (PRRs) and offer general protection to the host.[7] Janeway was the first to propose the existence of a class of innate immune receptors recognizing conserved microbial structures or "patterns," even prior to the molecular identification of such a system.[8] The main PRRs and their cognate ligands are depicted in **Figure 1**.

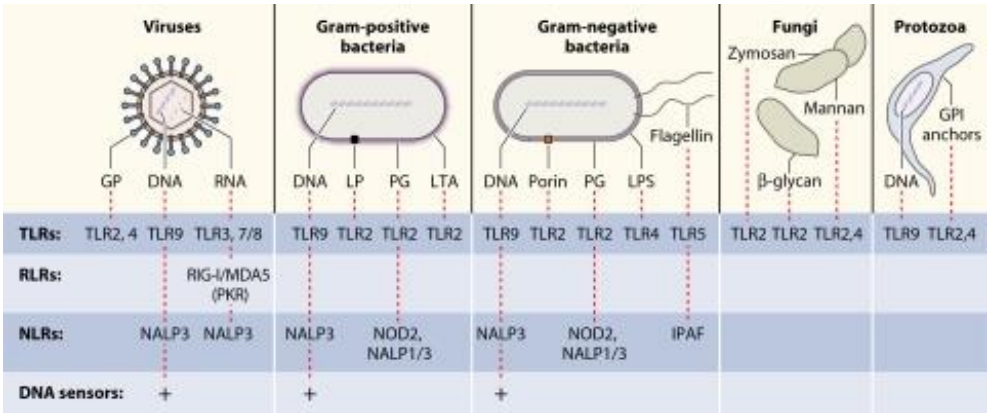

Figure 1. Recognition of PAMPs from different classes of microbial pathogens. Viruses, bacteria, fungi, and protozoa display several different PAMPs, some of which are shared between different classes of pathogens. Major PAMPs are nucleic acids, including DNA, dsRNA, ssRNA, and 5′-triphosphate RNA, as well as surface glycoproteins (GP), lipoproteins (LP), and membrane components (peptidoglycans [PG], lipoteichoic acid [LTA], LPS, and GPI anchors).[9]

Toll-like receptors. Among the PRRs, the Toll-like receptors (TLRs) have been studied most extensively. TLRs derived their name and were originally discovered based on homology to the *Drosophila melanogaster* Toll protein, which plays a role in dorso-ventral patterning during embryogenesis as well as in the antifungal response in Drosophila.[10,11] TLRs play a critical role in sensing both exogenous and endogenous signals that characterize infection and inflammation. TLRs are likely very ancient immune sentinels since two of their characteristic building blocks (LRR and TIR domains) are observed in placozoans (e.g., *Trichoplax* animals) and Porifera (e.g., Sponges). Full TLRs were detected in Cnidarian species, like the starlet sea anemone (*Nematostella vectensis*; one single TLR) and the acroporid corals (*Acropora digitifera*; four TLRs). Interestingly, both developmental and immunological roles of TLRs have been described in Cnidarians. TLRs from both the sea anemone (*Nematostella vectensis*) and the mountainous star coral (*Orbicella faveolata*) have been shown to signal via MyD88 leading to NF-κB activation. In the Bilateria phylum, TLRs can be found in most studied species, however, their

numbers vary greatly among species, ranging from a single TLR in Nematodes like *Caenorhabditis elegans*, to over two hundred in echinoderms like the pacific purple sea urchin *Strongylocentrotus purpuratus*. The expansion of the TLR repertoire in some animals like the sea urchin, reflects the adaptation of their immune arsenal to rapidly changing environmental stressors. In contrast to the very diverse set of TLR repertoires found in other Bilateria species, chordates and more particularly vertebrates contain roughly equal numbers of TLRs, reflecting the reduced need for highly diversified pattern recognition due to the acquisition of adaptive immune components. The reduced number of TLRs in vertebrates does not necessarily mean that the TLR-response in those species cannot be tailored to a particular environment.[12]

To date, a total of 13 TLR members have been identified in mammals.[13] TLRs are generally expressed on immune cells, such as monocytes, macrophages, dendritic cells, B lymphocytes, T lymphocytes, mast cells, neutrophils, and eosinophils, but also on nonimmune cells like epithelial cells, endothelium, fibroblasts, and adipocytes.[14] Despite the central role played by these innate immune cells, recognition of PAMPs by epithelial, endothelial, and hematopoietic cells in different tissues through TLRs is also an integral part of innate immune defences at sites of infection.[3,15] Structurally, TLRs are integral glycoproteins characterized by an extracellular or luminal ligand-binding domain containing three structural elements, a hydrophobic ectodomain containing a variable number of leucine-rich repeat motifs (LRRs), a transmembrane domain and a cytoplasmic signalling Toll/interleukin-1 (IL-1) receptor homology (TIR) domain, which mediates downstream signalling through adaptor proteins.[16]

TLRs can be divided into subfamilies based on the types of ligands they recognize. For instance, TLRs 1, 2, and 6 recognize lipopeptides and glycolipids, TLRs 7, 8, and 9 identify nucleic acids such as single stranded RNA (ssRNA) and unmethylated CpG DNA, TLR3 distinguishes double-stranded RNA (dsRNA) associated with

viral infection, TLR4 recognizes fibronectin, lipopolysaccharides (LPS), heat shock proteins, and responds to endogenous ligands called danger associated molecular patterns (DAMPs). TLR5 identifies bacterial flagellin, and TLRs 11 and 12 recognize profilin, an actin-binding protein. In mammals, one case of TLR adaptation and rapid evolution that is worth mentioning comes from bat species. Analyses of TLR evolution in bats reveal adaptations acquired by TLRs 3, 7, 8 and 9, with unique mutations fixed in ligand-binding sites. These adaptations are thought to stem from the unique lifestyle of bat species, that are the only known flying mammals, and that represent important viral reservoirs.[12]

Another way of grouping TLRs is based on their cellular distribution. Certain TLRs (TLR1, -2, -4, -5, -6, and -10) are expressed at the cell surface and mainly recognize bacterial products unique to bacteria and not produced by the host, whereas others (TLR3, -7, -8, and -9) are located almost exclusively in intracellular compartments, including endosomes and lysosomes, and are specialized in recognition of nucleic acids, with “self” versus “nonself” discrimination provided by the exclusive localization of the ligands rather than solely based on a unique molecular structure different from that of the host.[3] Ligand binding to TLRs through PAMP-TLR interaction induces receptor oligomerization, which subsequently triggers intracellular signal transduction ultimately culminating in in the activation of gene expression and synthesis of a broad range of molecules, including cytokines, chemokines, cell adhesion molecules, and immunoreceptors.[4] The latter together orchestrate the early host response to infection, and also is a prerequisite for the subsequent activation and shaping of adaptive immunity. While an optimum activation of TLRs is a prerequisite to mount immune responses against infection, a well-regulated negative signalling is also crucial to bring the immune responses to homeostatic level. Due to the importance of TLRs in maintaining innate immunity, dysregulation of TLR signalling pathways can lead to aging as well as a wide range

of autoimmune diseases, including diabetes, hepatitis, rheumatoid arthritis (RA), inflammatory bowel disease (IBD), and systemic lupus erythematosus (SLE).[17,18]

Besides TLRs, data from animal studies indicated the existence of other classes of PRRs. More specifically, evidence suggested that receptors other than TLR3 and TLR9 were able to induce type I IFN (IFN-α and IFN-β) production in response to RNA, DNA, or viral infections. Subsequent studies revealed that TLR-independent recognition of pathogens is accomplished by a large group of cytosolic PRRs, which can be broadly divided into retinoid acid-inducible gene I (RIG-I)-like receptors (RLRs) and nucleotide-binding oligomerization domain (NOD)-like receptors (NLRs).[9]

RIG-1-like receptors. RIG-I and melanoma differentiation-associated gene 5 (MDA5) are IFN-inducible RNA helicases that play a pivotal role in sensing of cytoplasmic RNA. These RNA helicases contain an N-terminal caspase recruitment domain (CARD) and a central helicase domain with ATPase activity required for RNA-activated signalling. Binding of dsRNA or 5′-triphosphate RNA to the C-terminal domains of RLRs triggers signalling via CARD-CARD interactions between the helicase and the adaptor protein IFN-β promoter stimulator 1 (IPS-1), ultimately resulting in an antiviral response mediated by type I IFN production.[9]

Although RIG-I and MDA5 function by similar mechanisms, studies have suggested differential roles of these two helicases, with RIG-I being essential for the response to paramyxoviruses and influenza virus, whereas MDA5 seems to be critical for the response to picornavirus and norovirus.[19] At the biochemical level, these differences may be due to length-dependent binding of dsRNA by these two RLRs. Specifically, RIG-I and MDA5 recognize short and long dsRNAs, respectively, and in addition, RIG-I detects 5′-triphosphate RNA. Although the prevailing view is that the major contribution to dsRNA-activated responses is mediated by RLRs, recent data suggesting that the IFN-inducible dsRNA-activated protein kinase (PKR) may be able to amplify RLR signalling, thus illustrating a cross talk between these different

cellular dsRNA-sensing systems involved in antiviral defence.[20] Cytoplasmic localization of DNA is recognized by the innate immune system independently of TLRs, RLRs, and NLRs and seems to be involved in mounting a response to both bacteria and DNA viruses.[9] Considering the large and heterogeneous group of proteins belonging to the family of PRRs, it will not be surprising if even more cytoplasmic DNA receptors are identified. Recently, the identification of the first cytosolic DNA sensor, DAI (DNA-dependent activator of IFN-regulatory factors), was reported.[21]

NOD-like receptors. NLRs belong to a family of innate immune receptors which have gained increasing interest over the past few years and are now considered key sensors of intracellular microbes and danger signals and therefore believed to play an important role in infection and immunity. NLRs are defined by a centrally located NOD that induces oligomerization, a C-terminal LRR that mediates ligand sensing (in analogy with TLRs), and an N-terminal CARD that is responsible for the initiation of signalling. The two best-characterized members of the NLR family are NOD1 and NOD2, which sense bacterial molecules derived from the synthesis and degradation of peptidoglycan. It is currently unresolved whether NOD1 and NOD2 serve as direct receptors of PAMPs or instead detect modifications of host factors as a consequence of the presence of microbial molecules in the cytosol. Irrespective of the specific mechanism, activation of NOD1 and NOD2 induces oligomerization and recruitment of downstream signalling molecules and transcriptional upregulation of inflammatory genes.[22] It is also important to mention that other NLR proteins are involved in activation of caspases. During infection, microbes induce TLR-dependent cytosolic accumulation of inactive IL-1β precursor and activation of caspase-1, the latter of which catalyses the cleavage of the IL-1 precursor pro-IL-1β. The protein complex responsible for this catalytic activity has been identified by Martinon *et al*. and was termed the inflammasome.[23] Inflammasomes are typically formed by a ‘receptor’ protein, the adaptor molecule apoptosis-related speck-like

protein (ASC) and the effector molecule pro-caspase-1. Inflammasome oligomerization results in activation of caspase-1, which subsequently cleaves the accumulated IL-1 precursor, eventually resulting in secretion of biologically active IL-1. Several inflammasome sensor molecules can detect a broad range of molecular signatures to sense microorganisms and tissue stress triggering the formation of inflammasomes. Most of the inflammasomes that have been described to date contain a NLR sensor molecule, namely NLRP1 (NOD-, LRR- and pyrin domain-containing 1), NLRP3, NLRP6, NLRP7, NLRP12 or NLRC4 (NOD-, LRR- and CARD-containing 4; also known as IPAF).[24] Two other inflammasomes have been described that contain the PYHIN (pyrin and HIN domain-containing protein) family members absent in melanoma 2 (AIM2) and IFNγ-inducible protein 16 (IFI16) rather than an NLR.[25] The different inflammasomes differ in their domain organization and composition as depicted in **Figure 2**.

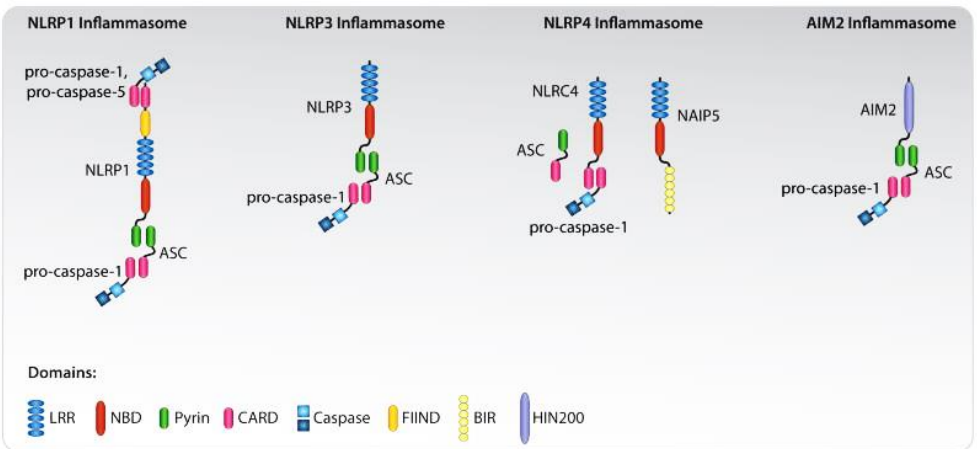

Figure 2. Inflammasomes. Upon their activation inflammasomes form multi-molecular protein complexes that typically consist of an NLR protein, or AIM2, the adapter molecule ASC and the effector pro-caspase-1. The NLRP1 inflammasome contains both a CARD and a PYD domain and can recruit several caspases, while the NLRC4 inflammasome can also contain NAIP5.[26]

Among all, NLRP3 inflammasome is critical for host immune defence against bacterial, fungal, and viral infections. NLRP3 inflammasome can be activated by a plethora of agonists, endogenous and exogenous, sterile or pathogen-derived. NLRP3 is unique among the NLRs in that its basal expression is not sufficient for inflammasome activation in resting cells.[27,28] Canonical activation consists in a two checkpoint activation mechanism for NLRP3 inflammasome activation. In this model, a first signal that is provided by microbial components or endogenous cytokines primes the NLRP3 inflammasome; a second signal from extracellular ATP, pore-forming toxins, or particulate matter activates the NLRP3 inflammasome. In fact, in macrophages, the presence of NLRP3 activators alone is insufficient for inducing inflammasome activation and a priming signal (signal 1) is required for its activation. Macrophages must first be exposed to priming stimuli, such as ligands for toll-like receptors (TLRs), NLRs (e.g., NOD1 and NOD2), or cytokine receptors, which activate the transcription factor NF-κB. NF-κB upregulates the expression of NLRP3, which is thought to exist at concentrations that are inadequate for initiating inflammasome activation under resting conditions, and pro-IL-1β, which is not constitutively expressed in resting macrophages. Moreover, both signalling molecules MyD88 and TRIF of the NF-κB signalling pathway regulate the induction of NLRP3 and pro-IL-1β in response to TLR ligands.[27,28] Thus, NLRP3 undergoes post-translational modifications that license its activation. The activation signal (signal 2) is provided by a variety of stimuli including extracellular ATP, pore-forming toxins, RNA viruses, and particulate matter. However, transcription-independent roles of the priming signal have been recently appreciated. In a rapid priming procedure, acute priming with LPS (10 min stimulation) enhances NLRP3 inflammasome activation in the absence of NLRP3 induction. IL-1 receptor-associated kinase 1 (IRAK-1), which is a signalling molecule downstream of TLRs and MyD88, mediates this rapid transcription-independent priming. LPS-induced phosphorylation of IRAK-1 promotes inflammasome activation in a manner that is independent of the IKK complex, which suggests that downstream NF-κB signalling

is not essential to IRAK-1's role in promoting inflammasome activation. In conclusion, the priming signals regulate NLRP3 inflammasome activation through both transcription-dependent and independent pathways.[29] Moreover, it was discovered that cytoplasmic LPS is sufficient for eliciting endotoxic shock independently of TLR4 signalling. This pathway is called the non-canonical inflammasome and it responds to Gram-negative but not Gram-positive bacteria.[30] The non-canonical inflammasome involves caspases 4/5 in humans and caspase-11 in mice, rather than caspase-1.[31,32] These caspases sense intracellular LPS independently of TLR4 by directly binding to LPS.[33] Priming, as with the canonical pathway, enhances the inflammatory response in mice due to the low basal expression of caspase-11.[34] In contrast, priming is unnecessary for non-canonical inflammasome activation in human cells that express high levels of caspase-4.[33] TLR4-dependent and TRIF-dependent IFN-α/β production are required for caspase-11 activation in macrophages, and they are partially required for pro-caspase-11 expression.[35] Caspases-4/5/11 induce pyroptosis through the processing of GSDMD, and pannexin-1, which is a protein channel that releases ATP from the cell.[29] An alternative pathway was observed to function unlike either the canonical or non-canonical pathways. Human monocytes do not require secondary stimuli following LPS stimulation to activate caspase-1 and induce IL-1β maturation and secretion.[36,37] The alternative inflammasome pathway does not require K^+ efflux, induce ASC speck formation, or lead to subsequent pyroptosis. TLR4-TRIF-RIPK1-FADD-CASP8 signalling is involved in this alternative pathway.[29,38]

C-type lectins. Sugar-dependent receptors such as C-type lectins on macrophages and dendritic cells play important roles in innate immunity also. C-type lectins are an extraordinary superfamily of proteins that recognize a wide diversity of ligands and that are required for numerous essential functions in mammals.[39] They are defined by having one or more characteristic C-type lectin-like domains (CTLDs) that include the EPN (Glu–Pro–Asn) and QPD (Gln–Pro–Asp) motifs, which confer

specificity for mannose-type and galactose-type carbohydrates, respectively. However, the CTLDs of many C-type lectins lack the components required for $Ca2^{+}$-dependent carbohydrate recognition and can recognize a broader repertoire of ligands including proteins, lipids, and even inorganic molecules, such as ice. C-type lectins are found as secreted molecules or as transmembrane proteins, and they have been implicated in a diverse range of physiological functions because of their ability to recognize self and non-self ligands. Many C-type lectins function as PRRs that recognize DAMPs, thereby promoting inflammatory responses. Therefore, it goes without saying that C-type lectins have a key role in the control of immunological tolerance that is responsible for preventing autoimmune disease. In fact, their functions have been implicated at all stages of disease progression because of their ability to recognize endogenous and exogenous ligands, regulate cellular and inflammatory responses and control adaptive immunity.

1.1.3. Molecular mechanism of Toll-like receptor 4 signalling and the initiation of the inflammatory response

TLRs are highly conserved PRRs that activate the innate immune system and participate in initiating the inflammatory response by recognizing non-self-molecules, i.e., pathogen-associated molecular patterns (PAMPs) derived from various pathogens.[40] Lipopolysaccharide (LPS) is an outer membrane component found exclusively in Gram-negative bacteria (**Figure 3**).

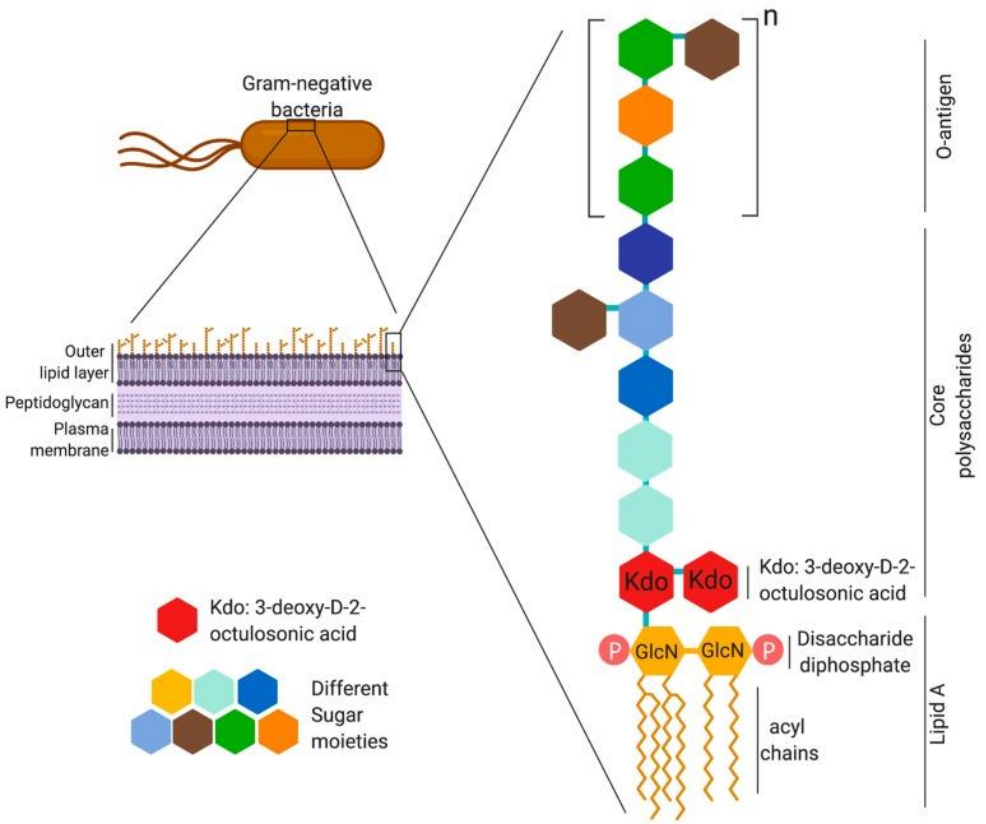

Figure 3. Structural details of lipopolysaccharide from a Gram-negative bacterium. Lipopolysaccharide (LPS) provides structural and functional integrity to outer membrane of Gram-negative bacteria. LPS is an amphipathic molecule with a general structure consisting of three different regions: hydrophobic lipid A, core polysaccharide, and O-antigen (repeats of polysaccharide chain, where n can be up to 40 repeats). Lipid A consists of bisphosphorylated diglucosamine backbone substituted with six acyl chains that are attached by ester or amide linkage.[41]

Extracellular LPS is a potent PAMP recognized primarily by Toll-like receptor-4 (TLR4) which is present on the surface of phagocytic cells like macrophages, neutrophils, and dendritic cells. Recent advances in lipopolysaccharide recognition systems have been recently summarized.[41] While TLR4 was thought to be the only sensor for LPS, recent studies have provided insight into two TLR4-independent LPS recognition systems: transient receptor potential (TRP) channel-dependent sensing of extracellular LPS and caspase-4/5/11-dependent sensing of intracellular LPS.

Efficient LPS recognition and production of inflammatory mediators by TLR4 requires an orchestrated action of various accessory proteins such as LPS-binding protein (LBP), CD14, and MD-2 (**Figure 4**).

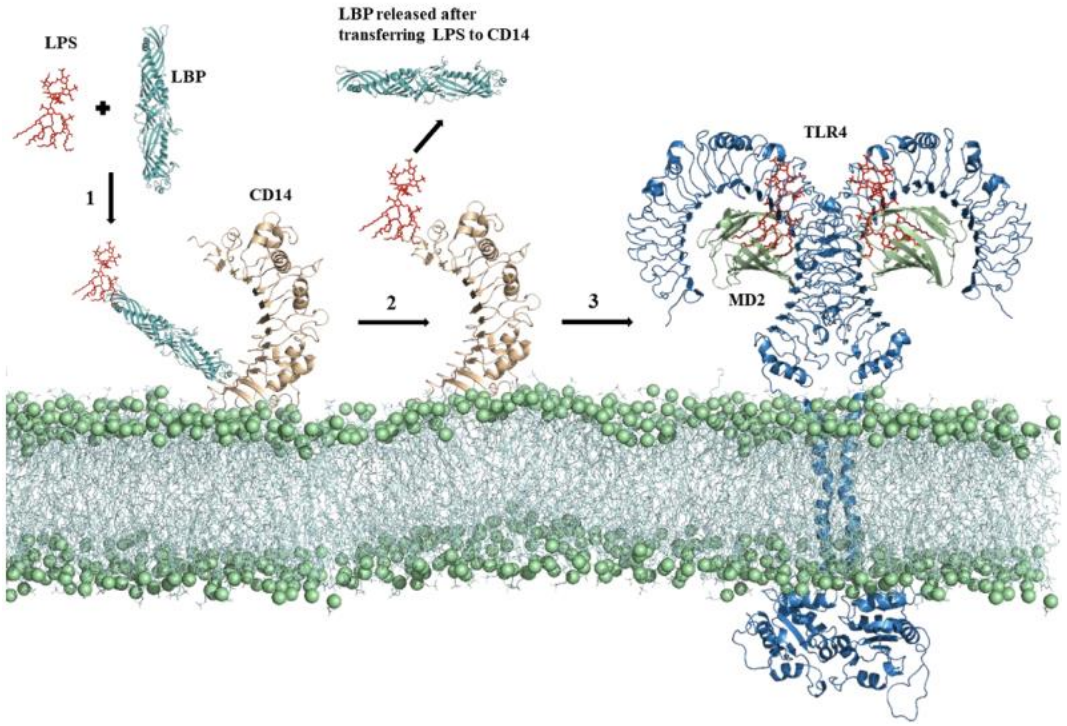

Figure 4. The binding mechanism of LPS for TLR4 activation. A series of events takes place prior to LPS recognition by the TLR4-MD2 complex. (**1**) LBP extracts LPS from the bacterial membrane and (**2**) transfers it to membrane anchored CD14, where it binds to the hydrophobic pocket located at the N-terminus and forms a monomeric complex. (**3**) CD14 facilitates LPS transfer to the TLR4-MD2 complex where it initiated the intracellular pathway.[42]

More in detail, initiation of LPS recognition begins with dissociation of the LPS monomer from the aggregates by LPS-binding protein (LBP) which traffics it to CD14 (glycosylphosphatidylinositol-anchored protein), present on most phagocytic cells (except dendritic cells) that make use of soluble CD14 (sCD14). CD14 then carries and loads LPS to the TLR4/MD-2 receptor complex. Interaction of TLR4 with LPS results in the induction of two distinct pathways. Firstly, TLR4–LPS

binding promotes homodimerization of the ectodomains of TLR4, and the subsequent structural and conformational changes induce dimerization of cytoplasmic TIR (Toll-interleukin-1 receptor) domains. The dimerized TIR domain structure is recognized by the downstream adaptor proteins MyD88 (myeloid differentiation primary response gene 88) and TIRAP (TIR domain-containing adaptor protein), leading to the formation of a protein complex, called Myddosome, along with several other serine-threonine kinases of the IRAK family. Myddosome mediates the signalling cascade that leads to the activation and subsequent translocation of transcription factor NF-κB and expression of pro-inflammatory cytokines such as TNF-α, IL-1β, and IL-6. Furthermore, the MyD88-dependent pathway also activates the downstream MAP kinase pathway that leads to transcription factor activator protein 1 (AP-1) transcription and expression of other pro-inflammatory cytokines.

In addition to signalling at the cell surface, TLR4 signalling within the endosomes begins with the assembly of TRIF (TIR domain-containing adaptor inducing IFN-β) and TRAM (TRIF-related adaptor molecule), leading to the assembly of triffosome which promotes activation of IRF-3 (interferon regulatory factor 3) and induction of type-1 interferons. Indeed, signalling cascades downstream of TLR4 in distinct subcellular sites leads to the production of different pro-inflammatory cytokines.

For this reason, TLR4 is unique among all TLRs, being the only that signal through both a MyD88-dependent and an independent mechanism (**Figure 5**).

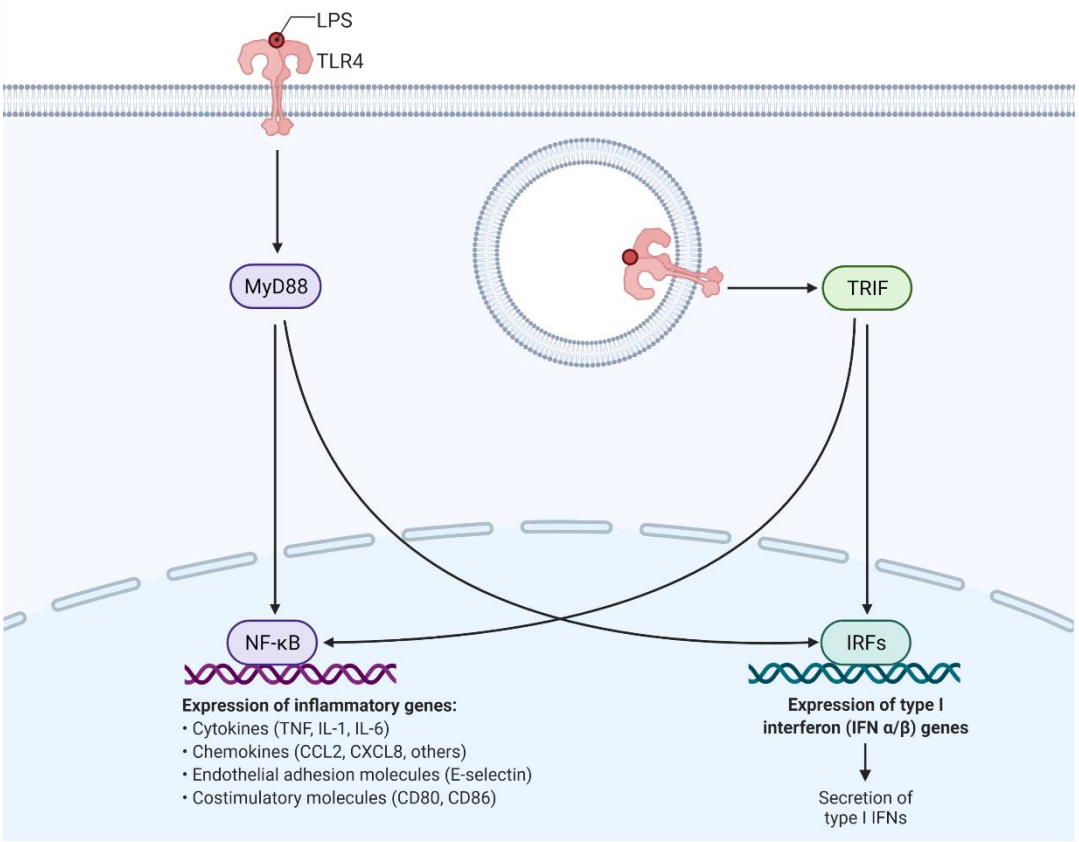

Figure 5. Dual TLR4 signalling. TLR4 activates both the MyD88-dependent and MyD88-independent, TRIF-dependent pathways. The MyD88-dependent pathway is responsible for early-phase NF-κB and MAPK activation, which control the induction of pro-inflammatory cytokines. The MyD88-independent, TRIF-dependent pathway activates IRF-3, which is required for the induction of IFN-β- and IFN-inducible genes. In addition, this pathway mediates late-phase NF-κB as well as MAPK activation, also contributing to inflammatory responses. Created with BioRender.com.

1.1.3.1. The MyD88-dependent signalling pathway

NF-κB and AP-1 are two key transcription factors that drive expression of a bulk of inflammatory genes in macrophages. The intricate network of events occurring downstream of TLR4 activation has been extensively reviewed elsewhere.[9] A simplified scheme is depicted in **Figure 6**. Briefly, in response to TLR4 stimulation by LPS, MyD88 associates with the cytoplasmic part of the receptor and subsequently recruits members of the IL-1 receptor (IL-1R)-associated kinase

(IRAK) family. Following association with MyD88, IRAK4 and IRAK1/2 are sequentially phosphorylated, with IRAK4 being of particular importance, as it has been demonstrated to be indispensable for the response to IL-1 and various TLR ligands. IRAK1 was originally thought to play an essential role in TLR-induced NF-κB activation, but more recent data have emerged suggesting that instead IRAK2 may play a prominent role in NF-κB activation, particularly during the late phase of TLR signalling. Further downstream, IRAK1, or alternatively IRAK2, associates with TRAF6, which acts as a ubiquitin protein ligase (E3) that, together with the ubiquitination enzyme complex (E2), catalyses the synthesis of K63-linked polyubiquitin chains on TRAF6 itself and other substrates, including transforming growth factor-activated protein kinase 1 (TAK1) and the IκB kinase (IKK) subunit NF-κB essential modifier (NEMO). A central step in the downstream signalling events is the recruitment of TAK1-binding protein 2 (TAB2) and TAB3 to ubiquitinated TRAF6, which brings TAK1 into proximity to the signalling complex, leading to its activation. TAK1 then stimulates two distinct pathways involving the IKK complex and the MAPK pathway, respectively. In the first pathway, TAK1-mediated activation of the IKK complex results in site-specific phosphorylation of the inhibitory IκB protein. Being the point of convergence for multiple NF-κB-inducible stimuli, IKK represents an essential component in many inflammatory signalling pathways. This high-molecular-weight kinase is composed of two structurally related kinases, IKKα and IKKβ, as well as the chaperone IKK complex-associated protein and the adaptor NEMO/IKKγ. Despite early reports of IKK dependency upon ubiquitination for optimal kinase activity, it was only recently resolved that direct ubiquitination of NEMO is mediated by TRAF6. Following phosphorylation, IκB undergoes proteasomal degradation to allow activation and translocation of NF-κB to the nucleus, where it binds to κB sites present in promoters and enhancers of a broad range of pro-inflammatory genes, which are then transcribed. In the second pathway, TAK1 phosphorylates members of the MAPK kinase (MKK) family, including MKK3, -4, -6, and -7. MKK3/6 subsequently

phosphorylate and activate p38, whereas MKK4/7 activate c-Jun N-terminal kinase (JNK). However, an alternative mechanism involving p38 autophosphorylation proceeding in a TAK1-dependent and MKK3/6-independent pathway has been described. Ultimately, these signalling pathways lead to activation of the transcription factor activator protein 1 (AP1). Moreover, other members of MKK kinases, most notably MKK kinase 3 and tumor-progression locus 2, have also been implicated in MAPK activation downstream of TLR4. The essential and nonredundant role played by TAK1 is strongly suggested by significantly reduced NF-κB, c-Jun N-terminal kinase (JNK), and p38 responses to various TLR ligands in cells derived from mice deficient in this kinase.[9]

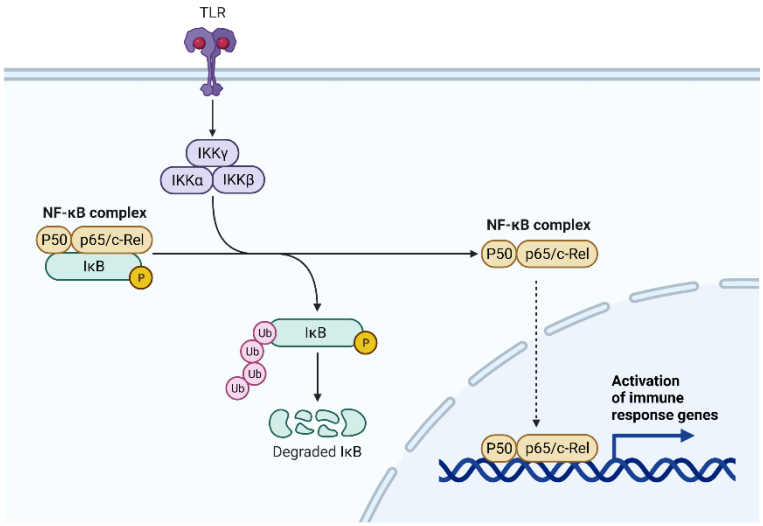

Figure 6. NF-κB following TLR stimulation. MyD88 recruits TRAF6 and members of the IRAK family. TRAF6 activates the TAK1 complex via K63-linked ubiquitination (Ub). The activated TAK1 complex then activates the IKK complex consisting of IKKγ, IKKα and IKKβ, which catalyses the phosphorylation of IκB proteins (P). IκBs are destroyed by the proteasome-dependent pathway, allowing NF-κB (p65/c-Rel–p50 heterodimer) to translocate into the nucleus (canonical pathway). NF-κB controls inflammatory responses through the induction of inflammatory cytokines. Created with BioRender.com.

1.1.3.2. The TRIF-dependent pathway

The existence of a MyD88-independent pathway downstream of TLR3 and TLR4 was indicated by Kaway *et al*. data that showed MyD88-deficient mice displaying normal IFN-β production.[43,44] Extensive molecular studies by Akira and associates then led to the identification of TRIF as the adaptor responsible for signalling in the MyD88-independent pathway.[45] Subsequently, the equally important discovery of two IKK-related kinases, TRAF family member-associated NF-κB activator (TANK)-binding kinase 1 (TBK1) and IKKε, and their essential role in induction of type I IFN were reported.[46] During TLR4-mediated signalling, TRIF, associated with TRAM is responsible for initiating a signalling pathway in which TRAF3 and TANK serve to bridge to the IKK-related kinases TBK1 and IKKε, which mediate direct phosphorylation of IRF-3 and IRF-7. Studies with cells lacking TBK1 or IKKε have revealed that TBK1 and, to a lesser extent, IKKε are responsible for TRIF-mediated IFN responses. It is notable, however, that whereas TBK1 and IKKε are essential for TRIF-dependent IRF-3/7 phosphorylation, these kinases are not involved in TLR-mediated NF-κB activation. As a consequence of phosphorylation, IRF-3 and IRF-7 form hetero- or homodimers, translocate to the nucleus, and bind to target sequences in DNA, such as IFN-stimulated response elements (ISRE). Importantly, IRFs together with NF-κB and AP1 form a multiprotein complex termed the enhanceosome, which induces transcription of the IFN-β gene (**Figure 7**).

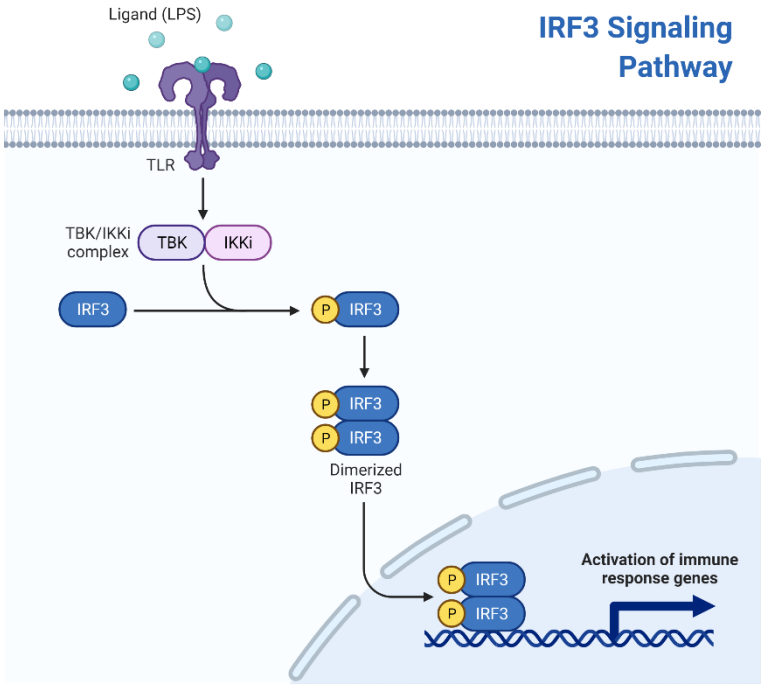

Figure 7. TLR/IRF axis. TRIF recruits TRAF3, which then interacts with TBK1 and IKKi. These kinases mediate phosphorylation of IRF3 (P). Phosphorylated IRF3 dimerizes and translocates into the nucleus to regulate transcription. Activation of the IRF3 is required for induction of type I IFN, particularly IFN-β. Created with BioRender.com.

Noteworthy, there are two types of NF-κB activation in TLR4 signalling: the MyD88-dependent pathway described in the previous paragraph, which mediates early phase activation of NF-κB and the TRIF-dependent pathway, which mediates the late phase activation of NF-κB.[47] TRIF-dependent activation of NF-κB occurs through binding of TRAF6 to TRIF and subsequent ubiquitination-dependent recruitment and activation of TAK1. To obtain robust NF-κB activation, a second molecule, receptor-interacting protein 1 (RIP1), involved in TNF-receptor mediated, is also recruited to TRIF. RIP1 is polyubiquitinated to form a complex with TRAF6, and these two molecules appear to cooperate in facilitating TAK1 activation, resulting in IKK-mediated activation of NF-κB as well as activation of the MAPK pathway.[9]

Shen *et al.*, demonstrate TRIF signalling playing a larger role in the LPS activation of macrophages being critical for IFN-β production.[48] Moreover, their results, in accordance with a previous work[49], indicate that the type I IFNs are major active components of the secreted factors that induce upregulation of costimulatory molecules (UCM) during LPS activation. In fact, after 24h of LPS stimulation, both studies demonstrate that UCM is almost entirely TRIF-dependent.

Although controlled production of the above-mentioned inflammatory mediators is required for clearance of invading pathogens, uncontrolled production of inflammatory cytokines can provoke fatal consequences such as septic shock.[50] Therefore, fine tuning of pro- and anti-inflammatory mediators is required for proper immune function and homeostasis maintenance.

1.1.4. NF-κB-inducible pro-inflammatory mediators

The central role played by NF-κB in both innate and adaptive inflammation and immunity is mediated by the coordinate expression of multiple genes essential for the immune response. The importance of NF-κB is revealed by the extensive list of NF-κB-inducible genes, including those for pro-inflammatory cytokines such as IL-1, IL-6, and TNF-α, as well as chemokines, including IL-8 and RANTES.[5] Moreover, NF-κB governs the expression of cell adhesion molecules, such as intercellular adhesion molecule-1 and E-selectin, is upregulated. Finally, in some instances, it appears to be advantageous for the host to stimulate cell division and inhibit apoptosis, and to achieve these effects, NF-κB induces several growth factors and antiapoptotic proteins.[5,51]

1.1.5. Type I IFN production and the IRF/STAT signalling

Interferons (IFNs) were named for their ability to restrict viral replication ("interference") in vertebrate cells, which has now been shown for many viruses both in human and mouse cells and cell lines.[52] There are three distinct interferon (IFN) families: IFN-I, IFN-II and IFN-III, which differ in their immunomodulatory properties, their structural homology and the group of cells from which they are secreted. IRFs have heterogeneous functions in the regulation of both innate and adaptive immunity and are associated with the recognition of pathogen-associated molecular patterns from TLRs.[53] Notably, only a subset of TLRs, including TLR3, -4, -7, and -9, have the ability to induce IFN, although through different signalling pathways. However, since many pathogens activate several TLRs or additional PRRs, most antimicrobial responses seem to include some degree of IFN production.

The type I IFN (IFN-I) family is a multigene cytokine family, consisting of 13 (in humans, 14 in mice) partially homologous IFN-α subtypes, a single IFN-β, as well as several other poorly defined single gene products including IFNε, IFNτ, IFNκ, IFNω, IFNδ and IFNζ.[54] IFN-I-induced signalling converges on transcription factors, which rapidly induces the expression of hundreds of genes called interferon-stimulated genes (ISGs).[55,56] This antiviral signalling cascade occurs in virtually all cell types exposed to IFN-I. ISGs, along with other downstream molecules controlled by IFN-I (including pro-inflammatory cytokines), have diverse functions, ranging from direct inhibition of viral replication to the recruitment and activation of various immune cells. A robust, well-timed, and localized IFN-I response is thus required as a first line of defence against viral infection because it promotes virus clearance, induces tissue repair, and triggers a prolonged adaptive immune response against viruses.

The type II IFN family consists of the single gene product, IFNγ, that is predominantly produced by T cells and natural killer (NK) cells and can act on a broad range of cell types that express the IFNγ receptor (IFNγR).[57]

Type III IFN family comprises IFNλ1, λ2 and λ3 (also known as IL-29, IL-28A, and IL-28B, respectively) and the recently identified IFNλ4, which have similar functions to cytokines of the type I IFN family but restricted activity as expression of their receptor is largely restricted to epithelial cell surfaces.[58]

IFN regulatory factor (IRF) family include transcription factors that are crucial for the promotion of IFN production.[59] In most cases, IRF-3 and IRF-7 are the fundamental IRFs required, although others such as IRF1, IRF5 and IRF8 can also induce *IFN* gene transcription. The central tenet of IFN-α/β induction is that *IFNB* and *IFNA4* genes are induced in an initial wave of transcription that relies on IRF-3. This initial IFN burst triggers the transcription of IRF7 that then mediates a positive-feedback loop, leading to the induction of a second wave of transcription of genes including additional IFN-α subtypes.[60] Immediately upstream of IRFs, the kinases IκB kinase-ε (IKKε) and TANK-binding kinase 1 (TBK1) are responsible for the phosphorylation of IRF-3 and IRF7. TLR4 use the adaptor molecule TRIF, which associates with TBK1, leading to the activation of IRF-3. Although all 17 type I IFNs bind to a heterodimeric cell surface receptor complex consisting of 2 subunits, type I IFN receptor 1 (IFNAR1) and 2 (IFNAR2)[54], they result in different biological outcomes.[61]

Ligation of the IFNAR activates the receptor associated protein tyrosine kinases Janus kinase 1 (JAK1) and tyrosine kinase 2 (TYK2). In the canonical IFN-α/β signalling, activated JAK1 and TYK2 phosphorylate signal transducer and activator of transcription 1 (STAT1) and STAT2 present in the cytosol, leading to their dimerization, nuclear translocation, and binding to IRF9 to form IFN-stimulated gene factor 3 (ISGF3). ISGF3 complex then binds to IFN-stimulated response elements (ISREs) upstream of ISGs, leading to the activation of their transcription. In this manner, IFNα/β induces the expression of several hundred ISGs, many of which act to induce an antiviral state within the cell. Most viruses devote a part of their limited genome to mechanisms that perturb IFN-α/β production and/or IFN-α/β

signalling to stop these ISGs being induced illustrating the importance of this cytokine family in host cell protection from viral infection.[62]

However, IFN-α/β signalling is not limited to this canonical pathway. In addition to signalling through STAT1–STAT2 heterodimers, IFNα/β can signal through STAT1 homodimers, which are more commonly associated with IFN-γ signalling, that bind to γ-activated sequences (GAS) in gene promoters. IFN-α/β can also signal through other STATs that are usually associated with other cytokine signalling pathways, including STAT3, STAT4 and STAT5. The phosphoinositide 3-kinase (PI3K)–mammalian target of rapamycin (mTOR) pathway and multiple mitogen-activated protein kinase (MAPK) pathways can also be activated downstream of the IFNAR. This diversity of signalling pathways may in part explain the broad effects of IFN-α/β signalling, as it allows for the transcription of a broad range of genes beyond those dedicated to viral restriction.[63] In fact, the role of IFNα/β on boosting the host response to infection are not limited to the acute cell-intrinsic antiviral response, but includes also effects on myeloid cells, B cells, T cells and natural killer (NK) cells that act to enhance the immune response, more effectively resolve viral infection and improve the generation of memory responses for reacting to future viral challenge, making IFN-I being a bridge between innate and adaptive immunity. To complicate the picture, recent studies describe a role for IFNα/β either as mediators of host-microbiota interactions and/or as downstream targets of these interactions, leading to further effects on immune system function.[64]

Accumulating evidence suggests that type I IFN may not only be involved in antiviral defences but also may play a role in antibacterial defences. IFN-α/β can be protective or detrimental to the host during bacterial infection, in an infection-specific manner, although less is known about their role in bacterial infections than viral infections. Two well-described examples of a harmful role for IFN-α/β are in infections with *L. monocytogenes* and *M. tuberculosis*, both of which are intracellular pathogens that preferentially infect macrophages. In the first case, IFN-α/β production which is a

method of self-regulation by immune cells, is subverted by L. monocytogenes for its own advantage. During *L. monocytogenes* infection, aberrant IFN-α/β production potently inhibit responsiveness of macrophages to IFN-γ.[65] On the other hand, patients with active tuberculosis had a prominent whole blood IFN-α/β transcriptional profile that correlated with the extent of radiographic disease and was diminished upon successful treatment.[66] Moreover, Dejager and colleagues' findings reveal that type I IFNs play an important detrimental role during sepsis by negatively regulating neutrophil recruitment. They published a paper providing data that support pharmacologic inhibition of type I IFN signalling as a novel therapeutic treatment in severe sepsis, proposing IFNAR1 as a potential drug target for sepsis.[67]

Dysregulation of IFN-related responses strongly support the linkage between IFN-I and autoimmunity. Dysregulation of the IFN-I system has been well studied in systemic lupus erythematosus (SLE). The common mechanism, by which TLRs play a role in SLE pathogenesis, is believed to be via production of IFN-α. An association between genetic variants of IRF5, which is involved in regulating IFN-α production, and SLE in multiple ethnic groups has been established.[68–70] Biologics that target type I interferons appear effective in SLE and are in phase III trials.[71] Moreover, there is evidence of increased IFN-I activity in many other autoimmune and inflammatory diseases potentially sharing common molecular pathways (e.g., inflammatory myositis, rheumatoid arthritis). Additionally, IFN-I has complex roles in chronic infection (HIV[72], CMV[73]) as well as in cancer and response to radiotherapy.[74] Finally, researcher identified interferonopathies as a heterogeneous group of disorders, mainly presenting an autosomal recessive inheritance pattern, characterized by constitutive upregulation of IFN-I. Among them, the Aicardi–Goutieres syndrome (AGS), the most well-studied interferonopathy, usually presents an early onset during childhood, with symptoms resembling those of SLE.[75] Recent evidence also implicates type I IFN-dependent signalling as a key inflammatory driver in non-autoimmune diseases such as certain solid tumours[76] and myocardial

infarction[77]. Therapeutic strategies that target ligands, receptors, or TLRs may have markedly different clinical effects. As regards the latter, a number of small molecule or oligonucleotide inhibitors of TLRs for potential use in SLE and other autoimmune diseases are in pre-clinical or phase I development.[78]

1.1.5.1. Interplay between SARS-CoV-2 and the type I interferon response

Given the fact that mounting an inflammatory response through PRRs is a prerequisite for containment and eradication of invading pathogens, it is not surprising that most pathogens have developed mechanisms for modulating or interfering with PRR-mediated responses. Viruses are the class of pathogens that have evolved the most diverse and sophisticated molecular mechanisms for interfering with antimicrobial and pro-inflammatory responses. Due to the ability of viruses to exploit the cellular machinery during their replication cycle, an intricate virus-host relationship has developed throughout evolution, and this allows many types of viruses to interfere profoundly with host signalling.[79] Overall, viruses can interfere in multiple ways with NF-κB and IRF pathways to inhibit induction of pro-inflammatory molecules and IFN. Of note, coronaviruses have developed multiple strategies to escape and counteract innate sensing and IFN-I production.

The severe acute respiratory syndrome coronavirus 2 (SARS-CoV-2) is a beta-coronavirus that emerged at the end of 2019 in China and rapidly spread around the world, causing a pandemic.[80,81] COVID-19 is an infectious disease that can lead to severe acute respiratory syndrome. As mentioned above, coronaviruses possess various mechanisms to defeat the IFN-I response within infected cells, and this inhibition ability is associated with clinical severity.[82] Clinical studies showed that coronaviruses evade innate immunity during the first 10 days of infection, which corresponds to a period of widespread inflammation and steadily increasing viral

load. A distinct phenotype was observed in severe and critical patients, consisting of a highly impaired interferon (IFN) type I response (characterized by no IFN-β and low IFN-α production and activity), which was associated with a persistent blood viral load. Elevated virus replication eventually leads to an excessive and uncontrolled inflammatory response which is associated with hypercytokinemia, referred to as a "cytokine storm". The delayed IFN-I response indeed promotes the accumulation of pathogenic monocyte-macrophages. This cell infiltrate results in lung immunopathology, vascular leakage, and suboptimal T cell response. The immune system attacks the host violently, causing multiple organ failure which can lead to death.[83] The cytokine storm associate with COVID-19 is partially driven by the transcriptional factor NF-κB and characterized by increased TNF–α and IL-6 production and signalling, showing similarities with those observed in other pathologies such as sepsis, acute respiratory distress syndrome, acute lung injury and other viral infection including severe cases of influenza.

1.1.6. Macrophages: origins, differentiation, and functions

Macrophages are immune cells with heterogeneous phenotypes and complex functions in tissue homeostasis and innate and acquired immunity. Macrophages are found in tissues, body cavities, and mucosal surfaces. Nobel Prize Ilya Ilich Metchnikoff was the first to describe macrophages in the late 19th century as large phagocytic cells (macro "big" + phage "eat"). Honoured as the "father of innate immunity," Mechnikov was the first to posit that the process of phagocytosis served as a natural immune system.[84,85]

In 1980, van Furth proposed the theory of the "mononuclear phagocyte system" (MPS) suggesting that all macrophages, not only those in inflammatory foci but also those in tissues in the steady-state, are derived from monocytes, which differentiate via promonocytes from monoblasts originating in bone marrow.[86] However,

macrophage origin has been debated extensively during the past years.[87] Researchers have questioned the validity of the MPS model and argued that tissue-resident macrophages are a separate lineage seeded during development and maintained by self-renewal. In 2019, Hume *et al.* reviewed different studies summarizing the evidence that during postnatal life, monocytes can replace resident macrophages in all major organs and adopt their tissue-specific gene expression, concluding that the original MPS lineage concept remains valid and accurate.[88] According to Sheng and colleagues, most of tissue-resident macrophages are progenies of classical hematopoietic stem cells (HSC), being only microglia and, partially epidermal Langerhans cells, the only macrophages that are yolk sac (YS)-derived.[89] Consistently, in both brain and liver, resident population of macrophages plays a role in promoting apoptosis and/or clearance of the infiltrating monocyte-derived macrophage population during the recovery phase, thus infiltrating monocytes do not contribute to the resident macrophage pool rather, during recovery, microglia and Kupffer cells are replenished through local proliferation.[90]

This paradigm was overturned within the last decade due to the results of genetic lineage tracing studies in mice. They found that in many tissues, macrophages originate from precursor cells derived from the yolk sac or foetal liver and differentiate into macrophages as part of prenatal or antenatal development. These "tissue-resident macrophages" can be very long-lived (months to years in the brain, liver, lung, and skin) and self-renewing, maintaining their homeostatic pool without a contribution from circulating monocytes. In other tissues, tissue-resident macrophage populations are replaced by monocyte-derived cells over different time scales. For example, in the intestine, locally maintained tissue-resident macrophages coexist with monocyte-derived populations with relatively short half-life, which have distinct roles in gut homeostasis and intestinal physiology. Indeed, most tissues are now recognized to contain multiple macrophage populations localized to distinct microanatomical domains. Each of these populations differs in its ontogeny, rate of

replacement by monocyte-derived cells, and capacity for self-renewal, and each is likely to play a specialized role in tissue homeostasis, injury, and repair (**Figure 8**).[91]

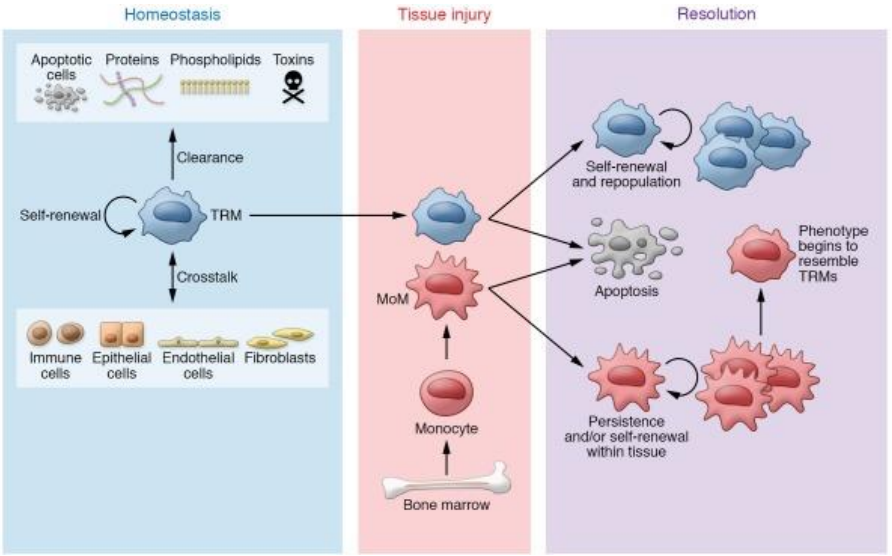

Figure 8. Tissue-resident macrophages and monocyte-derived macrophages play distinct roles in tissue injury and repair. Tissue-resident macrophages (TRMs) originate from the yolk sac and foetal liver during development and persist in many tissues via self-renewal. During homeostasis (left panel), TRMs clear apoptotic cells, proteins, and phospholipids and either clear or respond to toxins, particulates, and pathogens within the local microenvironment. Many TRMs can maintain themselves by local proliferation without the contribution of monocyte-derived macrophages (MoMs). TRMs produce a variety of factors that stimulate the activation, proliferation, and differentiation of immune cells, epithelial cells, endothelial cells, fibroblasts, and stem cells that facilitate tissue homeostasis. In response to tissue injury (middle panel), bone marrow–derived monocytes are recruited to the injured tissue, where they differentiate into MoMs. During injury, TRMs and MoMs play distinct roles; usually MoMs exhibit a more robust inflammatory response. During the resolution of injury (right panel), TRMs may die or expand through self-renewal and repopulate the niche. MoMs either undergo apoptosis or persist, sometimes gaining the capacity for self-renewal. Over time, the phenotypes of TRMs and MoMs become increasingly similar.[91]

Monocytes derive from a common progenitor termed Macrophage Dendritic Cell Precursor (MDP), emphasizing a continuum differentiation potential of monocytes to both inflammatory macrophages and DCs.[92] Relatedness between the two is confirmed also by the fact that monocytes and macrophages share the expression of

many surface markers and dependence upon specific growth factors and transcriptional regulators.[93] Circulating blood monocytes in humans represent about 10% of leukocytes. Circulating monocytes generated in the bone marrow can be divided into three subsets based on differential expression of CD14 and CD16. Approximately 90% of them, termed "classical monocytes," present CD14 but are negative for CD16 ($CD14^{+}CD16^{-}$). The "nonclassical monocytes" are $CD14l^{ow}CD16^{+}$. Finally, a third subtype termed "intermediate" has been defined as $CD14^{+}CD16^{+}$. However, this latter subtype has recently been under debate as certain studies indicate clear transcriptomic[94] and phenotypic[95] differences between the three subtypes while other authors shows that, transcriptionally, only classical and nonclassical subtypes can be distinguished[96], being the intermediate subset a population in transition between the other two subtypes.

Pools of monocytes can be found in the spleen and this reservoir can be mobilized quickly in case of injury or acute inflammation. Leukocyte recruitment is a complex process involving a series of interactions with integrins expressed on vascular endothelium. The sequential rolling, adhesion, and migration of leukocytes into the inflamed tissue is tightly regulated through induced expression of cell adhesion molecules and integrins in response to PRR activation.[3] The acute inflammatory cellular infiltrate consists of monocytes, DCs, neutrophils, and NK cells. Ultimately, the progression of tissue specific pathophysiological insults is dependent on both resident and infiltrating monocyte-derived macrophages. The monocyte subtypes possess differences in their capacity to infiltrate tissues. "Classical" $CD14^{+}$ monocytes tend to be recruited first and at higher levels in inflammatory conditions whereas "nonclassical" monocytes have a monitoring function for tissue damage in the form of dying endothelial cells and promoting recruitment of other immune cells in that case.[97] Traditionally defined and categorized by their anatomical territory (e.g., brain microglia, liver Kupffer cells and lung alveolar, splenic red pulp, and peritoneal macrophages) resident tissue macrophages adapt to each tissue

environment to perform specific functions. They have important roles in organ development, tissue homeostasis and repair. For instance, alveolar macrophages regulate pulmonary surfactant turnover while osteoclasts promote bone resorption, and red-pulp macrophages (RPMs) in the spleen promote red blood cell clearance and regulate iron recycling.[98] Besides their homeostatic functions, tissue-resident macrophages drive local and systemic defensive responses to pathogens as effectors of innate immunity, playing an indispensable role in boosting initial defense.[99]

Macrophages have been implicated in a wide range of diseases, not only those that encompass inflammatory conditions that lead to immune activation, such as atherosclerosis, sepsis, rheumatoid arthritis, and systemic lupus erythematosus, but also those that are accompanied by immune suppression, such as tolerance to bacteria, or cancer. Although it is clear that tissue-resident macrophages are essential in health and disease, the contribution of MDMs to the tissue macrophage population in homeostasis and disease increases over time and strongly affects the course and outcome of subsequent inflammation, immune activation, and disease development.[90]

1.1.7. Macrophage polarization

Two processes that impact on macrophage phenotype can be distinguished: differentiation and polarization. As described in the previous paragraph, the term differentiation indicates the transitions of a monocyte into a more mature state of a macrophage, induced by cytokines, growth factors, or other stimuli. Macrophage polarization, also sometimes referred to as activation, refers to the process by which macrophages produce distinct functional phenotypes as a reaction to specific microenvironmental stimuli and signals, such as pathogen-related molecules (e.g., LPS) or cytokines.

In vivo, macrophages with different polarization and different activation markers coexist in tissues. *In vitro*, macrophages change their polarization state based on diverse stimuli such as cytokines, microbes, microbial products, and other modulators.[100] Literature comprises several terms and definitions to describe the macrophage activation and polarization. Initially, only two closed activation states were considered, M1 (classically activated) or M2 (alternatively activated) (**Figure 9**). The two states represent opposite characteristics and their nomenclature was originally based on Th1 and Th2 cytokines.[101] More specifically, different metabolism of arginine after LPS injection elicits different phenotypes of macrophages in C57BL/6J and Balb/c mice. C57BL/6J peritoneal macrophages induced iNOS resulting in nitric oxide and a T-helper 1 (Th1) CD4 T cell response, while BALB/c mice induced arginase to produce ornithine and a Th2 response.[102]

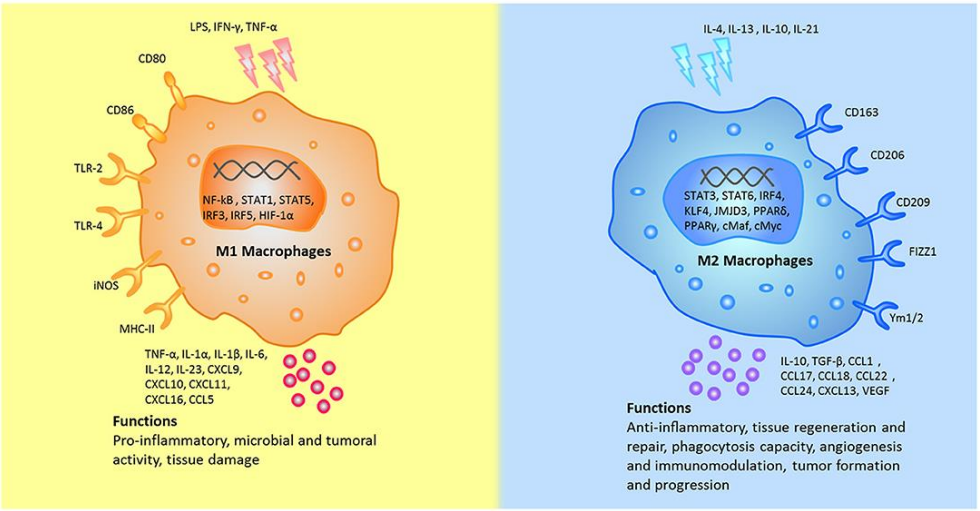

Figure 9. Macrophage classification based upon polarization. Macrophages can be polarized into classically activated (M1) and alternatively activated (M2) macrophages. M1/M2 polarity arises from arginine metabolism via two antagonistic pathways: M1-like macrophages are the products of the iNOS pathway, which produces citrulline and NO from arginine, whereas M2-like macrophages are the products of the arginase pathway, which produces ornithine and urea from arginine.[103] The different stimuli, surface markers, secreted cytokines, and biological functions between M1 and M2 macrophages were depicted.[104]

This classical separation of macrophage activation has been expanded and a spectrum of different activation states have been depicted, from highly pro-inflammatory to pro-fibrotic, pro-tumoral, anti-inflammatory, and many more. Mantovani *et al*. called classically activated macrophages (by IFN-γ combined with LPS or TNF) M1. *In vitro* alternatively activated macrophages (by IL-4) were re-named M2a. Two other M2-like macrophage phenotypes were induced by Fc receptor engagement by immune-complexes (M2b) or by IL-10 and glucocorticoids (M2c). These macrophages differ in their cell surface markers, secreted cytokines, and biological functions (summarized in **Figure 10**). Further clear differences between the phenotype subtypes with respect to size, morphology, and transcriptome has been extensively described elsewhere.[105] Here, for the sake of simplicity, simple dichotomy of M1 and M2 activation will be described.

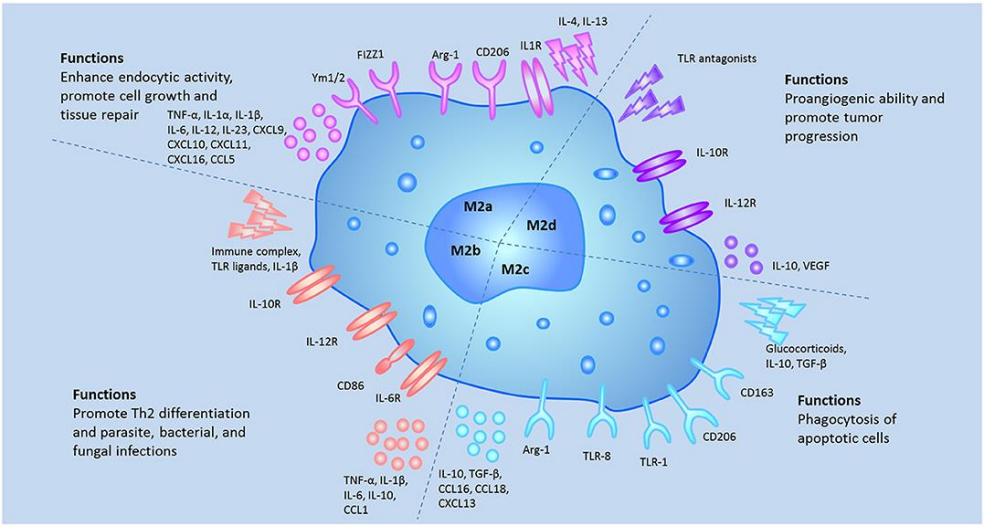

Figure 10. M2 macrophage phenotypes. Different stimuli, surface markers, secreted cytokines, and biological functions characterizing the different subsets.[104]

Following the activation by lipopolysaccharide (LPS) and Th1 cytokines (such as IFN-γ and TNF-α), macrophages are polarized into M1 macrophages and

characterized by TLR2, TLR4, CD80, CD86, iNOS, and MHC-II surface phenotypes. These cells release various cytokines and chemokines (for example, TNF-α, IL-1α, IL-1β, IL-6, IL-12, CXCL9, and CXCL10) which exert positive feedback on unpolarized macrophages. Key transcription factors, such as NF-κB, STAT1, STAT5, IRF-3, and IRF-5 have been shown to regulate the expression of M1 genes. It seems that NF-κB and STAT1 are the two major pathways involved in M1 macrophage polarization and result in microbicidal and tumoricidal functions.[104]

M2 polarization occurs in response to downstream signals of cytokines such as IL-4, IL-13, IL-10, IL-33, and TGF-β. Notably, only IL-4 and IL-13 directly induce M2 macrophage activation, whereas other cytokines (such as IL-33 and IL-25) amplify M2 macrophage activation by producing Th2 cytokines. M2 macrophages can be additionally identified by their expression of surface markers, such as mannitol receptor, CD206, CD163, CD209, FIZZ1, and Ym1/2. Up-regulation of cytokines and chemokines, such as IL-10, TGF-β, CCL1, CCL17, CCL18, CCL22, and CCL24 also attract unpolarized macrophages to polarize into the M2 state. Key transcription factors, such as STAT6, IRF4, JMJD3, PPARδ, and PPARγ have been shown to regulate the expression of M2 genes. Thus far, STAT6 pathway has been considered to be the pathway to activate M2 macrophages.

However, work from many groups in the last decade reveals macrophages as remarkably plastic cells that are epigenetically programmed in response to signals originating from the tissue environment.[99,106] This was definitively shown by Xue *et al*., who found that the M1/M2 paradigm failed to describe the transcriptome of human monocyte-derived and alveolar macrophages stimulated with LPS/IFN-γ or IL-4/IL-13 in the presence of factors known to be present in different tissue or disease microenvironments.[107] Having said that, revisiting the M1/M2 paradigm in the context of macrophage ontogeny will be essential to determine the extent of plasticity of individual populations of macrophages.[90]

1.1.8. The role of macrophages in the resolution of inflammation

As extensively described in the previous paragraphs, during tissue injury, pathogens, infected cells, and cells dying from necroptosis or pyroptosis release PAMPs or DAMPS, which activate inflammatory signalling pathways in macrophages and other resident cell populations that recruit neutrophils, monocytes, and other inflammatory cells to the tissue. Once the acute injury has been controlled, macrophages play a role in suppressing inflammation and initiating wound repair by clearing debris and producing growth factors and mediators that provide trophic support to the tissue in which they reside.[108] In 2019, Watanabe[91] and colleagues suggest two nonexclusive pathways by which tissue macrophages might contribute to repair (**Figure 11**).

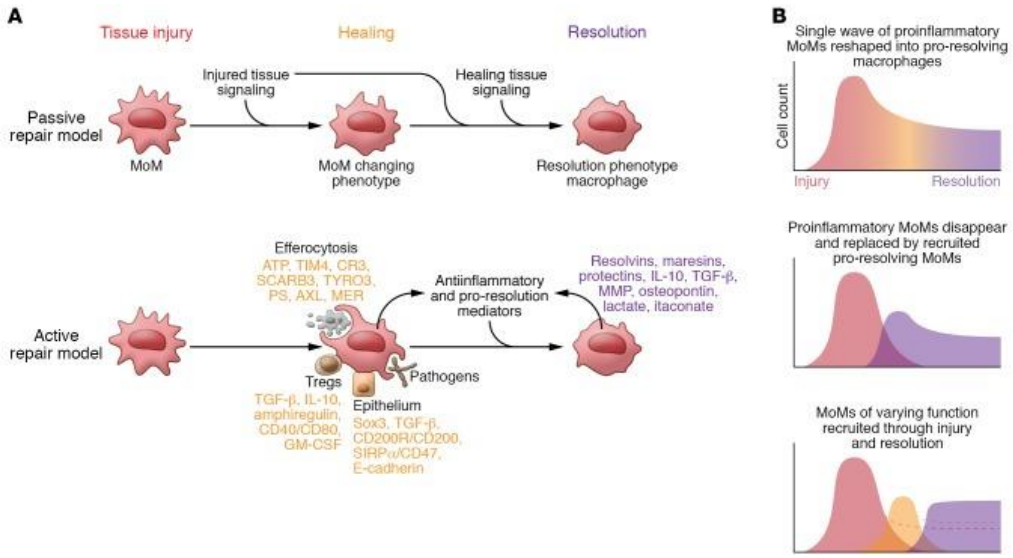

Figure 11. Role and kinetics of macrophages during tissue injury and repair. (**A**) Monocytes are recruited to the tissue during injury, where they differentiate into macrophages in response to cues provided by the injured microenvironment. Watanabe *et al*. propose two models to understand the distinct roles of monocytes in promoting tissue injury and tissue repair during injury resolution, which are not mutually exclusive. In the passive repair model (top panel), tissue regeneration restores signals that promote macrophage differentiation into cells that increasingly resemble tissue-resident macrophages. As the homeostatic function of macrophages is restored, tissue repair is accelerated, creating a feed-forward loop that restores homeostasis. In the active repair model (bottom panel), monocyte-derived macrophages respond to cues in their

microenvironment and express or secrete factors that drive tissue repair. Interactions include the uptake of apoptotic cells (often neutrophils), regulatory T cells, pathogens, and epithelial cells. These monocyte-derived macrophages might promote the resolution of inflammation through secretion of anti-inflammatory and pro-repair mediators including metabolic intermediates, pro-resolution lipid mediators, anti-inflammatory cytokines, and matrix remodelling proteins. (**B**) The kinetics of monocyte-derived macrophage recruitment to tissues is a subject of active investigation. A single wave of monocytes may enter during injury and be progressively reshaped into pro-resolving macrophages in response to cues within the local microenvironment (top panel). Alternatively, distinct waves of monocyte-derived macrophages might be involved in tissue injury (red) and tissue repair (purple) (middle panel), or monocytes with varying functions might be continuously recruited over the course of tissue injury and repair (bottom panel).[91]

The first process, referred to as "passive macrophage repair," involves the progressive differentiation of monocyte-derived macrophages in response to a growing number of "normal" signals originating from the regenerating tissue microenvironment. As this process of differentiation occurs, the macrophages take on phenotype and function increasingly similar to those of homeostatic tissue-resident macrophages. The result is a positive-feedback loop in which an increasing normalization of the tissue microenvironment drives a progressively more homeostatic role for macrophages, which in turn promote tissue repair. Alternatively, monocyte-derived macrophages might die by apoptosis, allowing the restoration of tissue-resident macrophages through proliferation and migration. The second process, called "active macrophage repair," involves activation of specific transcriptional programs in macrophages in response to factors uniquely present in the injured tissue microenvironment. One described mechanisms involves macrophage efferocytosis of apoptotic neutrophils recruited to the tissue during injury that results in a reduced expression of pro-inflammatory cytokines and chemokines from macrophages.[109] In addition to efferocytosis, other factors in the injured tissue microenvironment can activate anti-inflammatory signalling pathways in macrophages. For example, regulatory T cells that expand in the injured tissue can release amphiregulin, TGF-β, and IL-10, or directly interact with macrophages via ligand/surface interactions induced by CD40/CD80.[110] Moreover, microvesicles

originating from macrophages or other recovering cell populations have been reported to carry signalling molecules including SOCS2 or signalling microRNAs that induce reparative phenotypes.[91]

However, as described thoroughly in the previous sections, also those repair mechanisms can be detrimental in case of dysregulation. For example, cell-autonomous activation of mTOR signalling in macrophages induces a systemic granulomatous disease with features suggestive of sarcoidosis in multiple tissues.[111] Furthermore, some pathogens might take advantage from macrophage repair pathways to persist.[112]

Another interesting topic is the study of the relationship between macrophages (dys)functions and aging. Several groups of investigators have observed impaired macrophage transcription and function in normal aging. These include reduced phagocytosis, impaired polarization in vitro, a loss of wound healing response, and a reduced response to Toll-like receptor activation.[113]

It is therefore clear that failure to control macrophage plasticity may result in maladaptive response leading either to inflammatory diseases and tissue damage (in a case of excessive M1-polarized response) or to tissue fibrosis and cancer (in case of extensive M2-polarized response). Hence improving the inflammatory environment by modulating the activation state of macrophages could be an effective therapeutical approach.

1.1.9. Common and different features between macrophages and dendritic cells (DCs)

Although both macrophages and DCs are members of the mononuclear phagocyte system and originate from a common myeloid precursor, they are often considered distinct cell types based on their morphology, functions, and specific transcriptional profiles. Macrophages are defined as large vacuole cells that are highly phagocytic

and modulate immune responses by releasing various immune mediators, while DC are characterized as stellate migratory cells that act as sentinels in non-lymphoid tissues and migrate into lymphoid tissues upon antigen encounter, present antigen, and subsequently activate native T lymphocytes. *In vitro*, macrophage colony-stimulating factor (M-CSF) induces the differentiation of monocytes into macrophages[114], while the combination of granulocyte/macrophage colony-stimulating factor (GM-CSF) and interleukin 4 (IL4) induces the differentiation of monocytes into DCs.[115] While, macrophages are classified into 2 subgroups (M1 and M2 - M2a, M2b, M2c, M2d) depending on their anti- or pro-inflammatory properties[116], DCs comprise two functionally distinct populations: plasmacytoid (pDC) and myeloid (mDC). mDCs have been further subdivided into 2 subsets based on their expression of BDCA3/CD141 (mDC1) and BDCA1/CD1c (mDC2)[117]. Of all the different cell characteristics, surface markers are often used to distinguish DCs from macrophages (**Figure 12**).[104]

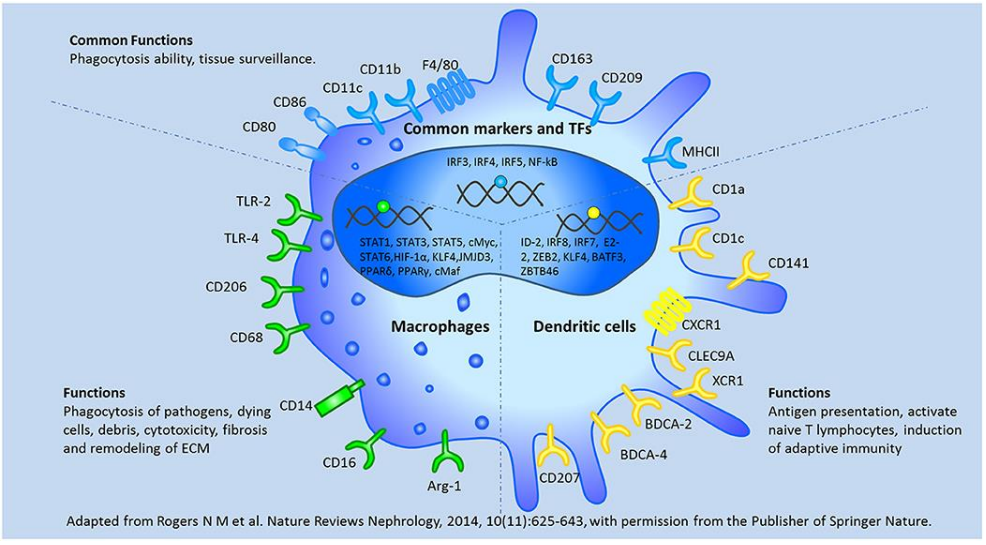

Figure 12. Common and different characteristics between macrophages and dendritic cells. Surface markers, transcription factors, and biological functions.[104,118]

The use of TLR-matured DCs may be an effective therapeutic strategy to treat cancer and provide protection against pathogens.[119] Maximal immune-boosting properties of TLR4-based DC immunotherapy for cancer and infectious diseases may require dual signalling via MyD88 and TRIF.[48]

1.1.10. Pharmacological strategies targeting TLR4 signalling

The pivotal role of TLRs in innate host defences was first indicated by the finding that C3H/HeJ mice with non-functional TLR4 are resistant to LPS-mediated shock[120] and valuable insights into TLR-mediated pathogen recognition and signalling has since been gained from the use of knockout mice and/or *in vitro* single TLR-expressing engineered cells (e.g., human embryonic kidney (HEK) 293 cells) challenged with individual purified PAMPs or entire microbial pathogens. Because of TLR4 signalling cascade's huge role, its extracellular and intracellular components are very attractive therapeutic targets for the treatment of both acute (e. g., sepsis) and chronic disorders, associated with excessive cytokine production (also called cytokine storm, an expression we all have learned due to the COVID-19 pandemic).

In addition to PAMPs, TLR4 can be also triggered by damage-associated molecular patterns (DAMPs) derived from damaged and necrotic tissues (sterile inflammation), such as fibronectins, small fragments of hyaluronan, and even saturated fatty acids in response to cellular damage. Besides the exogenous stimuli, endogenous host molecules, such as the oxidized phospholipids or high-mobility group box 1 (HMGB1) have also been shown to activate TLR4. While different LPS shares a conserved lipid A moiety with chemical determinants that ensure the optimal interaction with CD14 and MD-2 (5 or 6 lipophilic fatty acid chains attached to a disaccharide backbone, and one or two phosphate groups) DAMPs are chemically diverse molecules and the molecular mechanism of TLR4 activation including the

role of CD14 and MD-2 in the sensing of these molecules are not completely understood. DAMPs have been implicated in many pathologies caused by TLR4 activation, including atherosclerosis, rheumatoid arthritis, neuroinflammation, and trauma and haemorrhage. Very recently, our group proposed TLR4 as a promising therapeutic target for amyotrophic lateral sclerosis.[121] Moreover, possible application of TLR4 antagonists in treatment of peripheral neuropathic pain has also been suggested.[122]

Among the diseases caused by TLR4 abnormal activation by bacterial endotoxin, sepsis is the most dangerous because it is a life-threatening acute system inflammatory condition that still lacks specific pharmacological treatment. Septic shock with increased lipopolysaccharide (LPS) levels in blood, overexpression of pro-inflammatory cytokines, activation of blood coagulation system, and accumulation of fibrinogen degradation products leads to a violation of local and general hemodynamic and endothelial dysfunction. In western countries, mortality in patients with severe sepsis is 20-50%, if there is no organ dysfunction it can be diminished (less than 20%).[123]

Numerous compounds have been tested, *in vitro* and/or on animal models, for their capacity to block TLR4-mediated cytokine production. The known TLR4 antagonists belong to various classes of chemical compounds - mainly glycolipids that mimic the natural TLR4 ligand pharmacophore, lipid A, but also heterocycles, peptides, opioids, taxanes, steroids, etc, of natural and synthetic origin.[124] Notably, Professor Peri (University of Milano-Bicocca) has substantially contributed to this field with the development of a series of synthetic glycolipid small molecule modulators of TLR4, referred to as FPs compounds.[125,126] Main synthetic TLR4 antagonists and agonists will be described below.

Synthetic TLR4 antagonists. Several TLR4 antagonists were synthesized. The majority of them are mimetics of lipid A, the natural MD-2 ligand.[124] The most famous lipid A mimetic is Eisai's Eritoran that entered clinical phase. Other TLR4

antagonists with a chemical structure unrelated to lipid A have been recently developed. However, only TAK-242 (resatorvid) entered clinical trials. TAK-242 (resatorvid) is a small-molecule compound that selectively inhibits TLR4 signalling. TAK-242 inhibits the TLR4 pathway by binding directly to a Cys747 in the intracellular TLR4 domain. It has been observed that TAK-242 disrupts the interactions of TLR4 with its adaptor molecules, TIRAP (toll-interleukin 1 receptor (TIR) domain containing adaptor protein), and TRAM (TIR domain-containing adapter inducing IFN-β-related adapter molecule). Treatment of the HEK293 cells transfected with plasmids encoding FLAG-TLR4, MD-2, and FLAG-TIRAP/FLAG-TRAM proteins with TAK-242 inhibited the co-precipitation of TIRAP with TLR4 in a concentration-dependent manner. TAK-242 inhibited the association of TRAM with TLR4 at concentrations similar to those at which it inhibited the association of TIRAP with TLR4.[127,128] Fully deuterated TAK-242 retains TLR4-antagonistic activity, while having better pharmacokinetic and distribution properties than TAK-242.[129]

Eritoran is probably the most known antagonist of TLR4. It mimics the lipid A, but presents four instead of six fatty acid chains, one of them being unsaturated. The crystallographic analysis of the Eritoran/MD-2 complex revealed that Eritoran binds MD-2 more similarly than lipid A, by accommodating the four fatty acid chains into MD-2 binding pocket. However, when bound to MD-2 cavity, Eritoran is rotated 180° respect to lipid A. According to this model, Eritoran acts thus as a classic competitive inhibitor of MD-2 competing with LPS for the binding of the MD-2 pocket.[130] After successful results were obtained on animal models, Eritoran was suggested for testing on humans. However, both TLR4 antagonists Eritoran and TAK-242 failed to pass clinical trials as drugs against acute sepsis and septic shock.[131]

Alongside, cationic amphiphiles (IAXO compounds) based on monosaccharide scaffolds efficiently inhibited TLR4 signalling *in vitro* and *in vivo*.[132] The

mechanism of the antagonist action of this class of compounds was studied in the case of IAXO-102. A direct interaction of hydrophobic fatty acid chains of this compound and MD-2 was found by NMR measurements, confirming that very likely these compounds directly compete with LPS for MD-2 binding. Moreover, it has been observed in *in vitro* binding tests high affinity of IAXO compounds for CD14, so that interaction with CD14 probably reinforces the antagonist effect on the TLR4 signal pathway.[133]

Recently, new synthetic glycolipids, named FP7 and FP12, has been developed as TLR4 antagonists. FP7 and FP12 compete with LPS (and other TLR4 ligands) for the MD-2 binding site, thus inhibiting TLR4 activation (formation of the TLR4/MD-2/LPS complex).[134] In 2018, it has been shown that FP7 can negatively regulate MyD88-dependent TLR4 signalling in both non-haematopoietic and haematopoietic cells, suggesting that this TLR4 antagonist could potentially be used therapeutically for the treatment of inflammatory-related diseases.[135] More recently, the results from a study demonstrated that synthetic TLR4 antagonists FP7 and FP12 were effective in blocking MyD88-independent TLR4 signalling in THP-1 macrophages. Following activation of TLR4 by LPS, data revealed that FP7 and FP12 inhibited TBK1, IRF-3 and STAT1 phosphorylation which was associated with IFN-β and IP-10 down-regulation. Specific blockage of the type I IFN receptor (IFNAR) showed that these novel molecules inhibited IFN-β signalling by interfering with TRIF-dependent TLR4 pathway.[125]

Synthetic TLR4 agonists. On the flip side of the coin, several studies have demonstrated that TLR agonists can act as effective adjuvants for host defence against pathogens and cancer.[126,136] Indeed, an intense interest in developing TLR agonists as adjuvants for clinical vaccines has raised in the past years.[126,137] For instance, TLR4 agonist monophosphoryl lipid A (MPLA) is an approved adjuvant for vaccines against human papilloma virus and hepatitis B.[138] Additionally, new glycolipid-based TLR4 modulators mimicking lipid A chemical structure have been

recently described as innovative vaccine adjuvants by Peri's research group, FP11 and FP18. Mechanistically, FP11 and FP18 were more effective at inducing MyD88-dependent signalling than TRIF-dependent but may still activate signalling via IFNAR.[126]

Among the synthetic molecules we have seen so far, most of them are still in the early stage of preclinical development, a small number is employed for ongoing clinical studies and only a few licensed compounds have been marketed as TLR4-based therapeutics. As mentioned before, TLR4 agonists with a structure related to lipid A (MPL and AS04) have been licenced as vaccine adjuvants. Other lipid A mimetics (AS04, GLA-SE, GSK1795091 and OM-174) are in clinical Phase I or II as anticancer therapeutics. Small molecular TLR4 antagonist AV-411 (Ibudilast) is in Phase II clinical trials for the treatment of asthma and poststroke disorders. NI-0101 is the first anti-TLR4 monoclonal antibody to pass Phase I clinical trials for rheumatoid arthritis, showing safety and tolerability.[131] At this point it becomes clear that extending the chemical variety of TLR4 signalling modulators is an effort that must be addressed, for example by discovering new active molecules drawing from natural sources.

1.2. Natural Products and Immune Modulation

1.2.1. Phytochemicals as phytopharmaceuticals and nutraceuticals

Often patients are given anti-inflammatory drugs for acute or chronic inflammation to ease the suffering. However, sometimes anti-inflammatory drugs worsen the disease processes, is the case of osteoarthritis and rheumatoid arthritis. Also considering their enormous costs (in case of biologics), necessity of utilizing alternatives becomes evident.[139] Classical natural product chemistry methodologies enabled a vast array of bioactive secondary metabolites from terrestrial and marine sources to be discovered. Historically, natural products have been used since ancient times and in folklore for the treatment of many diseases and illnesses.[140] Scientific evidence is also emerging to explain their medicinal uses. Some studies suggest some plant species and their constituents have anti-inflammatory effects relevant for a particular therapeutic use. In these circumstances, plants may be used as phytopharmaceuticals to treat or alleviate inflammatory diseases offering one appealing way to reduce the use of anti- inflammatory drugs. This chapter describes some plant constituents that have been associated with anti-inflammatory effects relevant for use as nutraceuticals, phytopharmaceuticals, or as both. However, before continuing, it is necessary to reflect upon the differences between anti-inflammatory drugs and plant possessing anti-inflammatory properties. Nonsteroidal anti-inflammatory drugs (NSAID), one of the most common categories of such drugs, work primarily (if not exclusively) by inhibiting both isoforms of cyclooxygenase (COX- 1 and COX- 2). Contrarily, herbal medicines have never been demonstrated to act on a single enzyme or receptor. Instead, they have multiple constituents ranging from phenolics, terpenoids, polysaccharides, and proteins that act on multiple targets, and generally to a lesser extent than pharmaceuticals. The result is a gentler, slower onset of action coupled with vastly reduced or absent adverse effects compared to fast-acting, powerful, more toxic drugs and ultimately with long-

lasting effects.[141] Plants have been well documented for their medicinal uses for thousands of years, for example in Traditional Hindu Ayurveda as well as Traditional Chinese medicine (TCM).[142] They have evolved and adapted over millions of years to withstand bacteria, insects, fungi, and weather to produce unique, structurally diverse secondary metabolites. The earliest records of natural products were depicted on clay tablets in cuneiform from Mesopotamia (2600 B.C.) which documented oils from *Cupressus sempervirens* (Cypress) and *Commiphora species* (myrrh) which are still used today for treatment of the common cold, coughs, and inflammation.[143] Examples of drugs derived from natural sources include morphine and codeine, which are isolated from the plant *Papaver somniferum*, artemisinin, a TCM used to treat malaria, and anticancer taxol and halichondrin B, derived from the pacific yew tree and marine sponges, respectively.[17] Another example is *Zingiber officinale*. Ginger is a tropical plant in the *Zingiberaceae* family and is esteemed in natural medicine around the world. The rhizome is used medicinally for many conditions characterized by excessive inflammation. Numerous studies have documented that many constituents of ginger, particularly 6-gingerol and related molecules, inhibit 5-lipoxygenase (5- LOX), COX- 1, COX- 2, NF-κB signalling pathway, and thromboxane synthetase.[144] Due to this wide pattern of activity ginger's action is deeper and broader than simply having multiple effects on inflammation related eicosanoid and cytokine pathways. *Curcuma longa* (turmeric) rhizome is another inflammation modulator from the *Zingiberaceae* family, native to the tropics of Central and South-eastern Asia like its cousin ginger. Much work has investigated the inflammation-modulating aspects of its diarylheptanoid constituents known as curcuminoids. A thorough review of research through 2002 found evidence that curcuminoids inhibit phospholipases, LOX, COX, leukotrienes, thromboxane, prostaglandins, nitric oxide, collagenase, elastase, hyaluronidase, monocyte chemoattractant protein- 1 (MCP- 1), interferon- inducible protein, tumor necrosis factor (TNF), and interleukin- 12 (IL- 12).[145]

Another example is parthenolide, an anti-inflammatory compound, which is naturally present in the plant *Tanacetum parthenium* (also known as feverfew) that is used in herbal remedies. Parthenolide can interfere with the ATPase activity of NLRP3, thereby hindering inflammasome activation.[146]

Nutritional biology can significantly contribute to the discovery of new molecular targets in both health and diseases. Natural bioactive compounds occurring in food that provide medical or health benefits, including the prevention and treatment of a disease, are referred as "nutraceuticals," a hybrid term of "nutrition" and "pharmaceuticals", coined by Stephen DeFelice[147]. In addition to their basic nutritional value, nutraceutical agents have been shown to exert physiological benefits or provide health protection against different diseases. An extensive body of scientific evidence suggests that dietary factors exert their influence largely through their effects on blood pressure, lipids, and lipoproteins, as well as on markers of inflammation and coagulation.[148] This evidence implies that dietary interventions designed to reduce the inflammatory process could be of benefit in reducing the risk of inflammation-related diseases, blurring the line between food and drugs. According to an up-to-date review published in 2021[149], pharmacological modulation of immune responses by nutritional components can occur through three distinct mechanisms. First, nutritional components directly, or their metabolites produced during the digestion process, can interact with intestinal bacteria, and change the gut microbiota composition, leading to physiologic and immunologic changes in the body, which can affect human physiology in both positive and negative ways. The second mechanism by which diet can alter the immunologic response is via epigenetic modifications. Nutritional components can activate or inhibit specific histone deacetylases altering the transcription of proteins and, therefore, the activity of the immune system. The third mechanism is the involvement of pharmacological receptors on the cell surface to which nutritional

molecules can bind and either activate or inhibit the pathway downstream of the receptor.

Given the significance of TLR dysregulation in the onset of disease, there is a need to understand compounds derived from natural sources that modulate TLR signalling pathways, especially in various disease settings. To understand the action of promising molecules treating inflammation, is needed to identify bioactive components of the food matrix or herb extract, mechanisms of their action, and *in vivo* pharmacological effects using appropriate disease models to ultimately adapt the findings for clinical use.

1.2.2. Naturally occurring TLR4 antagonists

Research efforts have begun to focus on plant extracts as potential sources for new therapies in immunology. The first naturally occurring TLR4 antagonist discovered was from a photosynthetic Gram-negative bacterium that was non-pathogenic, known as *Rhodobacter sphaeroides*.[150] The LPS produced from this bacterium, known as *Rhodobacter sphaeroides* lipid A (RsDPLA), was non-toxic towards murine and human cells and was able to compete with toxic LPS for binding sites. RsDPLA was also able to interact with the TLR4/MD2 complex found in rodents and humans with antagonistic effects.[151] Further *in vitro* and *in vivo* studies on the LPS produced by *Rhodobacter sphaeroides* and other bacteria/cyanobacteria have shown potent antagonistic activity of this type of LPS in murine and human cells as well as preventing endotoxic shock in mice.

Additionally, plant-based extracts can have modulatory effects on TLR expression, signalling, and activation, whether by direct activation at the receptor level or further downstream of TLRs.[152] In particular, the study of TLR4 as a target of natural products is gaining popularity among researchers and currently, various natural compounds and their derivatives were found to act as agonists or antagonists for

TLR4 and its downstream signalling molecules. Most TLR4-active natural compounds are polyphenolic and aromatic compounds sharing interesting similarities in their chemical structures and in their mechanism of action, with TLR4 dimerization inhibition being the most characterised.[124] An elegant study published by Shibata *et al.* based on an extensive screening of vegetable extracts for TLR-inhibiting activity in HEK293 cells co-expressing TLR with the NF-κB reporter gene results in the acknowledgement of cabbage and onion extracts as the richest sources of a TLR signalling inhibitor. They identified 3-methylsulfinylpropyl isothiocyanate (iberin) from the cabbage and quercetin and quercetin 4′-*O*-β-glucoside from the onion as the main active substances, among which iberin showed the most potent inhibitory effect. It was revealed that iberin specifically acted on the dimerization step of TLRs in the TLR signalling pathway. To gain insight into the inhibitory mechanism of TLR dimerization, they developed a novel probe combining an isothiocyanate-reactive group and an alkyne functionality for click chemistry and detected the probe bound to the TLRs in living cells, suggesting that iberin disrupts dimerization of the TLRs via covalent binding.[153]

Disruption of TLR4.MD-2 heterodimer by formation of covalent adducts with solvent-exposed MD-2 and/or TLR4 cysteines has been proposed as mechanism of action also for isoliquiritigenin (liquorice), 6-shoagol (ginger), caffeic acid phenethyl ester (CAPE) (honeybee propolis) and cinnamaldehyde (cinnamon), thus suggesting an upstream effect on the extracellular TLR4.MD-2 complex.[124] Also sulforaphane (SFN), obtained from cruciferous vegetables such as broccoli or cabbages, interrupts LPS engagement to TLR4/MD2 complex by direct binding to Cys133 in MD2, attenuating LPS-induced nitric oxide synthase (iNOS), cyclooxigenase-2 (COX-2) and tumor necrosis factor-α (TNF-α) production in macrophage cell lines.[154] Contrarily, (-)-epigallocatechin-3-gallate (EGCG), a green tea polyphenol, do not prevents LPS-induced dimerization of TLR4, but inhibit TLR4 signal downstream, blocking both MyD88- and TRIF-dependent signal pathways by targeting IKKβ and

TBK1 kinases, respectively.[155] Another group in 2015 reported a similar finding, in which natural product dioscin, a saponin derived from various herbs attenuates renal ischemia/reperfusion injury by inhibiting the TLR4/MyD88 signalling pathway via up-regulation of HSP70.[156]

A variety of natural products and their derivatives act via stimulation of multiple TLR signalling pathways. For example, Yi *et al.* reported that ω-3 polyunsaturated fatty acids (PUFAs), abundant in nuts, oils, and fish, suppress the excessive inflammation in patients with severe trauma interacting with TLRs and NF-κB signalling pathways and decreasing levels of COX-2, IL-2, and TNF-α.[157] In particular, Depner *et al.* showed that docosahexaenoic acid (DHA), an omega-3 fatty acid isolated from fish oil, inhibit hepatic inflammation by targeting both TLR4 and TLR9.[158] Additionally, studies have shown that damage or defects in the TLR4 and TLR2 signalling pathways can lead to inflammatory bowel disease (IBD) as a result of sustained chronic inflammation. Nasef *et al.* identified various fruit fractions extracted from strawberries, blackberries, and feijoa that in the context of inflammatory bowel disease act together to mediate the anti-inflammatory response via both the TLR2 and TLR4 pathways.[159] Similarly, Liang and others revealed that sparstolonin B, a compound derived from Chinese herb *Spaganium stoloniferum*, has selective TLR2 and TLR4 antagonist properties, causing inhibition of the inflammatory response.[160] In 2014, Lee and colleagues discovered that ethanol extract from chungkookjang (CHU), a fermented Korean soybean, has anti-inflammatory effects on TLR ligands, particularly on TLRs 2, 3, 4, and 9, via inhibition of NF-κB activation.[161] Moreover, Xu *et al*. observed that total glucosides of paeony (TGP), active compounds of the flowering plant *Paeonia lactiflora*, significantly inhibited TLR2 and TLR4 activation in kidneys of diabetic rats leading to reduced expression of pro-inflammatory cytokines TNF-α and IL-1β.[162] In 2010, Villa *et al.* reported a natural product named malyngamide F acetate, extracted from marine cyanobacterium *Lyngbya majuscule*, that selectively inhibits MyD88-

dependent pathways involving TLR4 and TLR9. Interestingly, the group also observed a unique cytokine expression pattern, in which IL-6 and IL-1β were down-regulated and TNF-α was upregulated.[163]

Nonetheless, plant-derived compounds not only can act inhibiting TLR4-mediated immune response, but also triggering TLR4 signalling. For example, *Li et al.* showed that water extract of the edible mushroom *Pleurotus ferulae*, enhanced the function and maturation of murine bone marrow-derived dendritic cells through TLR4 signalling.[164] Likewise, Tian *et al.*[165] described the mechanism in which *Astragalus mongholicus*, a common traditional Chinese herbal medicine used to alleviate ischemic heart disease and hypertension, acts in inhibiting the growth of human stomach cancer promoting the maturation of dendritic cells through stimulation of TLR4-mediated NF-κB signal transduction pathways. Moreover, a group discovered that an herbal melanin extracted from *Nigella sativa*, or black cumin, modulates cytokine production and suggested it as a agonist for TLR4.[166]

Recent clinical trials on natural products. Various clinical trials have tested the therapeutic use of natural products, particularly in the context of immune regulation. For instance, in 2003 the effect of ganopoly, a *Ganoderma lucidum* polysaccharide extract, on the immune functions was evaluated in 34 advanced-stage cancer patients[167]. In 2015, a randomized dietary intervention in 52 healthy young adults shows that supplementing the diet with 5g or 10g of dried shiitake (*Lentinula edodes*) mushrooms for 4 weeks improved the immune response, decreased levels of acute inflammatory cytokines and modulate the overall cytokine secretion patterns.[168] However, some natural products failed in the clinical trial stage. For example, all the double blinded, placebo controlled clinical trials employing curcumin failed to demonstrate any effect, casting a dark shadow on the results published in the literature demonstrating curcumin activity.[169]

2. AIM OF THE WORK

Macrophages are relevant cells in the context of inflammation, both as direct effectors and regulatory cells. Plasticity of these important myeloid cells place them at the heart of the inflammatory process and, consequently, the possibility to modulate these cells offers great opportunity for novel potential interventions within inflammatory diseases. Considering the important role of both tissue-resident macrophages and MDMs in homeostasis and disease it has always been crucial to develop representative *in vitro* models to study these cells.[170] For such applications, it is worthwhile to differentiate monocytes into specific macrophage phenotypes. Cytokines can polarize macrophages *in vitro*, thus, to generate such macrophages appropriate cytokines are routinely added to culture media. Thereby, monocytic cells will acquire similar morphology and gene expression patterns as macrophages. In our case, we obtain macrophage-like cells through the *in vitro* differentiation of a monocytic cell line (THP-1) and primary $CD14^+$ monocytes isolated from freshly donated human blood. For the *in vitro* generation of macrophages, a range of PMA and M-CSF concentrations can be used, respectively.[114,171] In this this study, we exposed cells to 25 ng/mL PMA or 50 ng/mL M-CSF, to obtain THP-1-derived macrophages (TDM) and $CD14^+$ monocyte-derived macrophages (MDM), respectively.

Lipopolysaccharide (LPS)-induced macrophages activate a variety of inflammatory signalling pathways, which can be widely used to evaluate anti-inflammatory effects. This cellular model of inflammation allows to discriminate between compounds - or mixtures - capable of attenuating the inflammatory response and those that do not.

The current body of work aims to elucidate the immunomodulatory activities of coffee extracts (CE), chlorogenic acid (5-CQA), palmitoylethanolamide (PEA) and its synthetic analogue RePEA, respectively, by studying the influence of each plant

extract or chemical on TLR4-related inflammatory pathways. To this end, macrophage-like cells were obtained through the *in vitro* differentiation of a monocytic cell line (THP-1) and primary $CD14^+$ monocytes isolated from peripheral human blood. MTT was used to determine cytotoxic effects of the treatments. TLR4 activation was triggered by cells exposure to bacterial endotoxin LPS (*E. coli*) in presence or absence of treatments. Different readouts were evaluated: endpoint pro-inflammatory cytokines production, as well as phosphorylation and nuclear translocation of intracellular signalling mediators. These parameters were measured applying different cellular and molecular techniques, mainly enzyme-linked immunosorbent assay (ELISA), High Content Analysis (immunofluorescence microscopy), and Western blot. Alongside, we employed different commercially available stable transfected cells as tools to investigate the mechanism of action of our tested extract or molecule, THP1-XBlue™, RAW-Blue™ and HEK-Blue™ cells, respectively.

3. MATERIAL AND METHODS

3.1. Green and Roasted Coffee Beans Extraction

Coffee extracts from green (GCE) and medium-roasted (RCE) *Coffea canephora* beans (cultivar Robusta, origin Brazil) were obtained using a hydro-alcoholic extraction procedure described in a previous work.[172] Ground coffee beans were received from Beyers Koffie, Belgium. Each sample was analysed in triplicate. Briefly, 200 mg of ground green or roasted coffee beans were extracted with 20 mL of a mixture of acidified (with 0.1 M HCl) water (pH 4.5; 70%) and methanol (30%) by sonication at 37 kHz for 15 min at 30 °C in an ultrasound bath (Elmasonic P 30 H, Elma Schmidbauer GmbH, Singen, Germany). After 1 h, solutions were filtered through cotton wool and 0.45 µm PTFE filters (Pall Corporation, Port Washington, NY, USA), concentrated under reduced pressure at 40 °C and freeze-dried. The extraction yield was calculated for each sample. The lyophilized samples were stored at -20 °C.[173]

3.2. NMR-based Metabolic Profiling

Freeze-dried samples were suspended in 10 mM deuterated phosphate buffer (PB, pH 7.4) at a final concentration of 5 mg/mL, sonicated (37 kHz, 20 min, Elmasonic P 30 H, Elma Schmidbauer GmbH, Singen, Germany) and centrifuged (9425 *x g*, 10 min, 20 °C, ScanSpeed 1730R Labogene, Lynge, Sweden). 4,4-Dimethyl-4-silapentane-1-sulfonic acid (DSS, final concentration 1 mM) was added to the supernatant as an internal reference for concentrations and chemical shift. The pH of each sample was verified with a microelectrode (Mettler Toledo, Columbus, OH, USA) for 5 mm NMR tubes and adjusted to 7.4 with NaOD or DCl. All pH values were corrected for the isotope effect. The acquisition temperature was 25 °C. All

spectra were acquired on an AVANCE III 600 MHz NMR spectrometer (Bruker, Billerica, MA, USA) equipped with a QCI (^{1}H, ^{13}C, ^{15}N/^{31}P and ^{2}H lock) cryogenic probe. ^{1}H-NMR spectra were recorded with water suppression (cpmgpr1d pulse sequences in Bruker library) and 64 scans, spectral width 20 ppm, relaxation delay 30 s. They were processed with 0.3 Hz line broadening, automatically phased and baseline corrected. Chemical shifts were internally calibrated to the DSS peak at 0.0 ppm. Compound identification and assignment were carried out with the support of 2D NMR experiments, comparison with reported assignments[174] and the SMA (Simple Mixture Analysis) analysis tool integrated in MestreNova Software. The ^{1}H,^{1}H-TOCSY (Total Correlation SpectroscopY) spectra were acquired with 48 scans and 512 increments, a mixing time of 80 ms and relaxation delay 2 s. ^{1}H,^{13}C-HSQC (Heteronuclear Single Quantum Coherence) spectra were acquired with 48 scans and 256 increments, relaxation delay 2 s. For coffee bean metabolites quantification, the global spectrum deconvolution (GSD) algorithm, available in the Mnova software package (MestReNova v 14.2.0, 2021, Mestrelab Research, Santiago de Compostela, Spain) was used. Overlapping regions were deconvoluted, and absolute quantification was assessed also for coffee bean metabolites with resonances in rare crowded spectral areas. For each compound, the mean of the different assigned signals was determined.

3.3. Chemicals

3-(4,5-Dimethylthiazol-2-Yl)-2,5-Diphenyltetrazolium Bromide (MTT) and lipopolysaccharide (LPS) from Escherichia coli 055:B5 were purchased from Sigma-Aldrich (Sigma-Aldrich, Inc., Saint Louis, MO 63103, USA). Reagent-grade water used to prepare all solutions was obtained from a Milli-Q purification system (Millipore, Bedford, MA, USA). Palmitoylethanolamide (PEA, CAS N° 544-31-0) was purchased from Cayman Chemical (Ann Arbor, MI, USA) with a declared purity

≥98%. PEA analogue, 3-Hydroxy-N-pentadecylpropanamide (RePEA) was chemically synthetised.[175]

3.4. Cell Cultures

THP-1 cells (ATCC® TIB-202™) were purchased from ATCC® (Manassas, VA 20110 USA), while THP1-XBlue™ cells from InvivoGen (InvivoGen, San Diego, CA 92121, USA). Both cell lines were cultured in RPMI 1640 medium, 2 mM L-glutamine, 10% heat-inactivated foetal bovine serum, 100 U/ml-100 μg/ml Pen-Strep. Cells were maintained in a humidified 37°C, 5% CO_2 incubator. Cells were subcultured every two days. Exponentially growing cells were adjusted to 0.5×10^6/mL according to the routine procedure. RAW-Blue™ and HEK-Blue™-hTLR4 cells were purchased from InvivoGen (InvivoGen, San Diego, CA 92121, USA). Cells were maintained in DMEM, 2 mM L-glutamine, 10% heat-inactivated foetal bovine serum, 100 U/ml-100 μg/ml Pen-Strep and subcultured at 80% confluence. To maintain selection pressure, 100 μg/mL of Zeocin™ and HEK-Blue™ Selection (InvivoGen, San Diego, CA 92121, USA) were added to the growth medium of THP1-XBlue™, RAW-Blue™ and HEK-Blue™ cells, respectively, every other passage. Media and supplements were purchased from Euroclone (Euroclone S.p.A., Pero, Milan, Italy) unless otherwise stated.

3.5. Generation of THP-1-derived macrophages from THP-1 cell lines (TDM)

THP-1-derived macrophages (TDM) were generated from THP-1 or THP1-XBlue™ monocytic cells (3.5×10^5 cells/ml) by exposure to 25 ng/mL phorbol 12-myristate-13-acetate (PMA) (InvivoGen, San Diego, CA 92121, USA). Aliquots (180 μl/well) of the cell suspensions were seeded into a 96-well plate before culture at 37°C, 5%

CO_2. Following 72 h of differentiation, medium was removed and replaced with fresh medium, in absence of PMA, prior to further treatments.

3.6. Primary $CD14^+$ Monocytes Isolation

Human $CD14^+$ monocytes were isolated from total peripheral blood mononuclear cells of healthy donors, by immunomagnetic cell sorting. Samples from healthy donor subjects were obtained within a clinical protocol (n°463-2021), approved by the institutional Ethical Committee at IRCCS MultiMedica Milano, Milan, Italy, in accordance with the Helsinki Declaration of 1975 as revised in 2013. 30 mL of whole blood (< 1 h old), collected into heparinized tubes, were subjected to Ficoll Histopaque®-1077 (Sigma-Aldrich, Inc., Saint Louis, MO 63103, USA) density gradient stratification at 800 x *g*, for 25 minutes, room temperature (RT), without brake. The white ring interface, enriched in mononuclear cells, was collected, and washed in PBS at 300 x *g* for 5 minutes, RT. Residual red blood cells were removed by treating the cell pellets with 1X Red blood lysis buffer solution (10X stock solution: NH_4Cl 83g, $KHCO_3$ 10g, EDTA 1mM, pH 7,2-7,4 in 1 L of H_2O), incubated for 10 minutes at 4°C, then washed in PBS at 300 x *g* for 5 minutes, RT. Monocytes were purified from PBMCs by immunomagnetic cell sorting (positive selection) using CD14 MicroBeads UltraPure (Miltenyi Biotec, Auburn, CA) according to the manufacturer's instructions.

3.7. Generation of $CD14^+$ Monocyte-derived Macrophages (MDM)

Magnetically enriched $CD14^+$ monocytes (3.5×10^5 cells/ml) were differentiated into adherent monocyte-derived macrophages (MDM), by exposure to 50 ng/mL M-CSF (Miltenyi Biotec, Auburn, CA). Aliquots (180 µl/well) of the cell suspensions were loaded into a 96-well plate before culture at 37°C, 5% CO2. Cells were pulsed

with M-CSF every 3 days. Following macrophage differentiation, medium was removed and replaced with fresh RPMI medium, prior to further treatments.

3.8. Cell Viability Assay (MTT)

Cells were treated with increasing concentrations of the tested extract or molecule. After 24 h, cell supernatants were removed and cell viability was assessed by MTT assay, according to the method first described by Tim Mosmann in 1983.[176] This colorimetric assay uses reduction of a yellow tetrazolium salt (3-(4,5-dimethylthiazol-2-yl)-2,5-diphenyltetrazolium bromide, or MTT) to measure cellular metabolic activity as an indicator of cell viability. Viable cells contain NAD(P)H-dependent oxidoreductase enzymes which reduce the MTT reagent to formazan, an insoluble crystalline product with a deep purple colour. After 4 h-incubation with the MTT solution at 37 °C, formazan crystals are then dissolved using a solubilizing solution and absorbance is measured at 570 nm using a plate-reader (LabTech Microplate Reader LT-4000).

3.9. Coffee Extracts and 5-CQA Pre-treatment

In case of GCE, RCE and 5-CQA, cells have been pre-treated with the tested extract or molecule (1 h) and then stimulated with 100 ng/mL LPS. Supernatants and / or cells were collected at different time points after LPS stimulation, adjusted according to further analyses needs. Samples were stored at -20°C prior to be examined.

3.10. PEA and RePEA Post-treatment

In case of PEA and its analogue RePEA, TDM were stimulated with 10 ng/mL LPS for 1 h, then the medium containing LPS was removed, and cells were incubated for 1 h with 100 nM PEA or RePEA. Next, the medium was replaced with fresh complete

RPMI, and supernatants collected after 24 h post LPS administration. Samples were stored at -20°C prior to be analysed.

3.11. PEA pre-treatment

TDM and HEK-Blue™-hTLR4 cells were pre-treated 100 µM PEA (1h) and subsequently challenged with 10 ng/mL LPS. Supernatants were collected after additional 6 h. Samples were stored at -20°C prior to be examined.

3.12. Detection of NF-κB Activation (SEAP assay)

THP1-XBlue™ cells were specifically designed for monitoring the NF-κB signal transduction pathway. THP1-XBlue™ were derived from the human THP-1 monocyte cell line by stable integration of an NF-κB-inducible secreted embryonic alkaline phosphatase (SEAP) reporter construct. THP1-XBlue™ cells are highly responsive to PRR agonists that trigger the NF-κB pathway. HEK-Blue™-hTLR4 cells were obtained by co-transfection of the human TLR4, MD-2 and CD14 co-receptor genes, and an inducible SEAP (secreted embryonic alkaline phosphatase) reporter gene into HEK293 cells. RAW-Blue™ cells are derived from the murine RAW 264.7 macrophages with chromosomal integration of a secreted embryonic alkaline phosphatase (SEAP) reporter construct inducible by NF-κB and AP-1. In general, cell supernatants were collected after 6, 18 or 24 h, depending on the case. Monitoring of NF-κB activation by determining the activity of SEAP in the cell culture supernatant, was assessed with QUANTI-Blue™ reagent according to the manufacturer's instruction (InvivoGen, San Diego, CA, USA). Briefly, 50 µL of the supernatants of SEAP-expressing cells were incubated with 180 µL of QUANTI-Blue™ substrate in a 96-well plate for 0.5 − 4 h at 37 °C, then optical density (OD) was measured at 630 nm.

3.13. Enzyme-linked Immunosorbent Assay (ELISA)

Pro-inflammatory cytokines and interferons released in the medium by human macrophage-like cells were measured by ELISA assays. TDM or MDM were treated as described above. At defined time points of incubation, cell culture supernatants were collected and stored at −20 °C. Samples were analysed in duplicate in each experiment and at least three experiments were performed. The concentrations of IL-1β, IL-6, TNF-α, IFN-β were detected using commercial ELISA kits according to manufacturer's instructions (DuoSet® ELISA Development Systems, R&D Systems, Inc., Minneapolis, MN, Canada, USA). Briefly, 100 µl of standards and samples were added in respective wells of 96 wells antibody coated plate and incubate for 2 h. After incubation and washing steps, conjugated secondary antibodies were added for 2 h followed by same washing steps. Then substrate solution was added in each well followed by addition of stop solution. A standard curve was obtained by using 2-fold dilutions of the standard for each independent experiment. The concentration of cytokines and interferons was calculated using a standard curve.

3.14. Immunofluorescence Analysis

Cellular localization of the phosphorylated form of the transcription factor IRF-3 (p-IRF-3) was examined by confocal immunofluorescence analysis. TDM (2 x 10^4 cells/well) were seeded and differentiated into CellCarrier-96 Ultra Microplates (6055500, PerkinElmer Inc., Milan, Italy). After differentiation, cells have been treated with LPS only or LPS after 1 h pre-treatment with 250 µg/mL GCE or RCE. Cells were exposed to LPS for a maximum of 4 h. Different time points between 0 and 4h have been investigated. Paraformaldehyde 4% (F8775, Sigma-Aldrich, Inc., Saint Louis, MO 63103, USA) fixed cells were permeabilized with ice-cold 100% methanol, blocked, and labelled with Phospho-IRF-3 (Ser386) (E7J8G) XP® Rabbit mAb (E7J8G, Cell Signalling Technology, Inc.). Cells were then tagged with

PhenoVue™ Fluor 568 conjugated anti-rabbit secondary antibody (2GXRB568C1, PerkinElmer Inc., Milan, Italy). The nucleus was counter-labelled with PhenoVue™ Hoechst 33342 Nuclear Stain (CP71, PerkinElmer Inc., Milan, Italy). Images have been acquired using the Operetta CLS™ High-Content Analysis System and analysed through Harmony 4.5 software (PerkinElmer Inc., Milan, Italy).

3.15. Protein Extraction and Western Blot Analysis

TDM and MDM cells were plated into 24-well plates at a density of 0.6×10^6 cells/well. Cells were treated with 250 μM 5-CQA. After 1 h, cells were exposed further for 0 - 4 h to lipopolysaccharide (LPS) to induce inflammation (100 ng/mL). For protein extraction, cells were washed with 1 mL of PBS and then lysate adding 50 + 20 μL of RIPA Buffer (#9806, Cell Signalling Technology, Inc.), containing a protein inhibitor cocktail mixture (SIGMAFAST Protease Inhibitor Cocktail Tablet, S8820, Sigma-Aldrich) and a phosphatase inhibitor cocktail mixture (Phosphatase Inhibitor Cocktail (100X) #5870, Cell Signalling Technology, Inc.), and incubated for 30 min on ice. Then, the whole cell lysates were collected and centrifuged for membrane removal. Protein concentration was measured by spectrophotometric analysis using the Pierce™ BCA Protein Assay Kit (23227, Thermo Scientific™) according to manufacturer instructions. Western blot analysis was performed on 20 μg of total protein extracts. Cell extracts were separated using 10% Mini-Protean TGX Stain-Free Gels reagent kit (Bio-Rad Laboratories) and transferred to membranes using Trans-Blot Turbo Transfer System (Bio-Rad Laboratories). Antibodies against actin (1:1000 dilution/#4970; Cell Signalling Technology, Inc.), p-IRF-3 (1:500 dilution/E7J8G, Cell Signalling Technology, Inc.), and p-STAT1 (1:1000 dilution/#9167, Cell Signalling Technology, Inc.) were diluted in 0.1% TBS-Tween 20 (TBS-T) buffer containing 5% BSA and applied to membranes, followed by overnight incubation at 4°C. The next day, filters were washed three times with TBS-T for 5 min and incubated for 45 min with anti-rabbit secondary antibody

conjugated to peroxidase (#7074, Cell Signalling Technology, Inc.). The antigen–antibody complexes were then detected using ECL Star Enhanced Chemiluminescent Substrate (EMP001005, Euroclone) or LiteAblot Turbo Extra-Sensitive Chemiluminescent Substrate (EMP012001, Euroclone). Quantitative densitometry of bands was carried out through ChemiDoc system (Bio-Rad Laboratories), and the quantification of the signal was performed by ImageJ.

3.16. Statistical Analysis

Data related to biological assays were analysed using GraphPad Prism software (ver.9.0.2, GraphPad Software Inc., San Diego, CA, USA) and the results were shown as means ± standard error of the mean (SEM). Data obtained in three or more independent experiments were compared by one-way analysis of variance (ANOVA) followed by *post hoc* Dunnett's test. Differences between samples were considered statistically significant when $p < 0.05$. Two groups of data were compared using Student's *t*-test (statistically different when, $p < 0.05$).

4. RESULTS AND DISCUSSION

Discussion of the experimental results obtained has been organized into three different chapters. First chapter will introduce to coffee extracts, their chemical composition and health properties associated with coffee consumption. Here, original data concerning the immunological effects of coffee extracts on human macrophages are reported.

The second chapter focuses on the anti-inflammatory bioactivities of chlorogenic acid, as one of the major coffee polyphenols. After a brief introduction regarding the well-known and established biological effects of chlorogenic acid, a newly discovered effect on macrophage inflammatory response modulation is disclosed and new insights into its mechanism of action are described.

Third chapter revolves around palmitoylethanolamide (PEA), an endocannabinoid-like lipid mediator with extensively documented anti-inflammatory, analgesic, antimicrobial, immunomodulatory and neuroprotective effects. Capability of PEA itself, and its synthetic analogue RePEA, to modulate human macrophage response to lipopolysaccharide (LPS) has been investigated and results are given in this section.

CHAPTER I

Coffee Bean Extracts: Inflammation-Modulating Phytochemical Mixtures

Adapted from:

Artusa, V.; Ciaramelli, C.; D'Aloia, A.; Facchini, F.A.; Gotri, N.; Bruno, A.; Costa, B.; Palmioli A,; Airoldi, C.; Peri, F. Green and Roasted Coffee Extracts Inhibit Interferon-β Release in LPS-Stimulated Human Macrophages. *Front. Pharmacol*. **2022**, 13:806010. doi: 10.3389/fphar.2022.806010 (in press) - Appendix I

4.1. Background

With 500 billion cups consumed every year, which is roughly equivalent to about 2.25 billion cups per day, it's no surprise that coffee is one of the world's most popular beverages. In 2020/2021, around 166.63 million bags, which consist of 60 kilograms' worth of coffee each, were consumed worldwide, a slight increase from 164 million bags in the previous year.[177] Finland is the country with the highest coffee consumption per capita.[178] Coffee isn't just one of the most traded goods on the market, it's also one of the oldest. Coffee beverages can be produced using dozens of different techniques that stem from every corner of the globe. Most of all require the mixing of ground coffee beans with hot water, followed by a removal of the coffee grounds prior to drinking. A coffee bean is a seed found inside the red fruit (called the cherry) of a coffee plant (**Figure 13**).

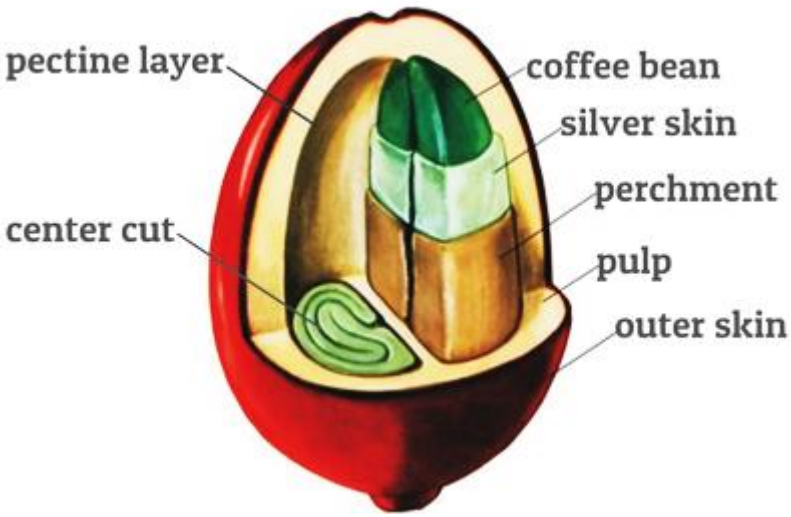

Figure 13. The anatomy of a coffee cherry. The coffee fruit (also called berry or cherry) consists of a smooth, tough outer skin or pericarp, usually green in unripe fruits but that turns red-violet or deep red when ripe. The pericarp covers the soft yellowish, fibrous, and sweet pulp or outer mesocarp. This is followed by a translucent, colourless, thin, viscous, and highly hydrated layer of mucilage (also called the pectin layer). Then, there is a thin endocarp yellowish in colour, also called parchment. Finally, the silverskin covers each hemisphere of the coffee bean (endosperm).[179]

The genus *Coffea* belongs to the family *Rubiaceae*, subfamily *Ixoroideae*, and tribe *Coffeeae*, and include at least 120 species, ranging from shrubs to trees. *Coffea arabica* and *Coffea canephora* var. Robusta plants are the two main source of coffee beans, and, among all the coffee species, the most traded and investigated (**Figure 14**).[180]

Figure 14. Arabica and Robusta coffee beans. Arabica beans (left) are a little longer and oval, while Robusta (right) ones are smaller and rounded.

Coffee beans start out green. They are roasted at a high heat to produce a chemical change that releases the rich aroma and flavour that we associate with coffee. They are then cooled and ground for brewing. Roasting levels range from light to medium to dark. The lighter the roast, the lighter the colour and roasted flavour and the higher its acidity. Dark roasts produce a black bean with little acidity and a bitter roasted flavour.

Beside the high popularity of coffee brews from roasted coffee, green coffee recently came to attention for its nutritional potential. Therefore, green coffee consumption as a dietary supplement or as a beverage is increasing. Green coffee is considered a novel food product because consumers usually consume only roasted coffee. Made with green, unroasted coffee beans, green coffee is an earthy, herbal, tea-like

beverage with light levels of caffeine. To make it, it is necessary to boil green coffee beans in water. Caffeine and especially chlorogenic acids (CGA) in green coffee came into focus because of their beneficial health effects like anti-inflammatory, anti-obesity, and other effects, which were observed in *in vivo* animal and human studies. Green coffee beans can be marketed as such or as an extract obtained from water or alcohol extraction processes.[181] Green coffee products can be sold as powder, capsules, chewing gum, and oils for ingestion or as soaps, body and facial creams, and oils for body massage products for aesthetics purposes.

Health benefits of coffee consumption. Coffee lovers around the world who reach for their favourite morning brew probably aren't thinking about its health benefits or risks. Historically, this beverage has been subject to a long history of debate. Despite nowadays the cumulative research on coffee points in the direction of a health benefit, more research is needed to understand the benefits of coffee. Much of the currently available information on the health effects of coffee is derived from epidemiological research. However, the study of coffee consumption in human populations raises several issues regarding exposure classification and potential confounders that should be considered when interpreting the results of epidemiological studies of coffee consumption. To name but one among others, few epidemiological studies collected information about the brewing process used to prepare coffee. Finally, genetic and lifestyle factors (e.g., cigarette smoking) can affect individual exposure to other bioactive compounds in coffee.[182–184] The identification of biomarkers that accurately reflect the consumption of bioactive compounds in coffee represents an important tool for studying relationships between coffee consumption and health-related endpoints.[185] In the following lines the current updates about the benefits of coffee consumption on health outcomes as well as its side effects were summarized. Coffee consumption has been associated with reductions in the risk of several chronic diseases, including cardiovascular disease[186],

type 2 diabetes mellitus[187], metabolic syndrome[188], cirrhosis[189], Parkinson's disease[190], and cancer[191,192].

Evidence suggests that drinking coffee regularly may lower the risk of heart disease and stroke. Moderate coffee drinking was associated with a 21% reduced risk of heart disease[193], 20% lower risk of stroke[194] and a 21% lower risk of cardiovascular disease deaths[195] compared with non-drinkers. Decaffeinated coffee also showed an association, with 2 or more cups daily and a 11% lower stroke risk, the authors found no such association with other caffeinated drinks such as tea and soda. Thus, these coffee-specific results suggest that components in coffee other than caffeine may be protective.[194] Moreover, a meta-analysis of 36 studies including men and women reviewed coffee consumption and risk of cardiovascular diseases (including heart disease, stroke, heart failure, and deaths from these conditions) revealing that heavier coffee intake of 6 or more cups daily was neither associated with a higher nor a lower risk of cardiovascular disease.[186]

Although ingestion of caffeine can increase blood sugar in the short-term, long-term studies have shown that habitual coffee drinkers have a lower risk of developing type 2 diabetes compared with non-drinkers.[196,197] Inflammation has also been implicated in the biology of type 2 diabetes, therefore, coffee drinking may antagonize the inflammation process by subclinical inflammation.[198,199] Polyphenols and minerals in coffee, such as magnesium, may improve the effectiveness of insulin and glucose metabolism in the body.[200,201]

Metabolic syndrome (MetS) is defined as the co-occurrence of multiple metabolic abnormalities, including central obesity, high blood pressure, hyperglycaemia, and dyslipidaemia.[202] As previously reported in the lines above, coffee consumption has been shown to be associated with a lower risk of type 2 diabetes and CVDs, both of which are likely to appear in people with metabolic syndrome.[203] Additionally, different prospective studies have showed that liver fat accumulation *per se* precedes the onset of the metabolic syndrome.[204] Recently, the association between coffee

consumption and the onset and progression of metabolic disorders, including non-alcoholic fatty liver disease (NAFLD) and metabolic syndrome (MetS) were systematically reviewed.[205] Authors reported that among four studies reporting fibrosis scores, all of them revealed an inverse association of coffee intake with fibrosis severity, although the lack of comparable exposure and outcomes did not allow to perform pooled analysis. Regarding MetS, seven studies met the inclusion criteria to be included in the meta-analysis. The results showed that individuals consuming higher quantities of coffee were less like to have MetS. However, the association of coffee and individual components of MetS was not consistent across the studies.

Liver cirrhosis is a large burden on global health, causing over one million deaths per year. Observational studies have reported an inverse association between coffee and cirrhosis. Five cohort studies and four case–control studies were recently reviewed.[206] The pooled RR of cirrhosis for a daily increase in coffee consumption of two cups was 0.56 thus suggesting that increasing coffee consumption may substantially reduce the risk of cirrhosis.

Parkinson's disease (PD) is mainly caused by low dopamine levels. There is consistent evidence from epidemiologic studies that higher consumption of caffeine is associated with lower risk of developing PD. A systematic review of 26 studies including cohort and case-control studies found a 25% lower risk of developing PD with higher intakes of caffeinated coffee.[207] Likewise, a large cohort of men and women were followed for 10 and 16 years, respectively, to study the relationship between caffeine and coffee intake and PD. The results showed an association in men drinking the most caffeine (6 or more cups of coffee daily) and a 58% lower risk of PD compared with men drinking no coffee. Women showed the lowest risk when drinking moderate intakes of 1-3 cups coffee daily.[190] Turning to Alzheimer's disease (AD), three systematic reviews were inconclusive about coffee's effect on

Alzheimer's disease due to a limited number of studies and a high variation in study types that produced mixed findings.[208–210]

Various polyphenols in coffee have been shown to prevent cancer cell growth. Published in 2021, a recent work demonstrated the antitumor activity of coffee extracts in both 2D and 3D culture cell models, showing that coffee extracts have both antiproliferative and cytotoxic effects on breast cancer cells without affecting viability on human epithelial breast cell lines (noncarcinogens).[211] Previously, Bauer and colleagues, demonstrated that coffee extracts promote a decrease in cell viability, modulate cell cycle and induce apoptosis in human prostate carcinoma cell line (DU-145).[212] Coffee has also been associated with decreased oestrogen levels, a hormone linked to several types of cancer.[213] Regarding human studies on the association between coffee and cancer, a large body of epidemiologic evidence has been recently reviewed.[214]

Most of the clinical trials included in this chapter showed that coffee consumption could benefit human health. In 2021, a systematic review reported similar benefits related to green coffee including improved blood pressure, plasma lipids, and body weight, thus a contribution to the improvement of Metabolic Syndrome's risk components. Also, other effects have been shown, including benefits for the skin and cognitive functions.[215]

Potential risks. A large body of evidence suggests that consumption of caffeinated coffee does not increase the risk of cardiovascular diseases and cancers. In fact, consumption of 3 to 5 standard cups of coffee daily has been consistently associated with a reduced risk of several chronic diseases.[216] However, some individuals may not tolerate higher amounts of caffeine due to symptoms of jitteriness, anxiety, and insomnia. Specifically, those who have difficulty controlling their blood pressure may want to moderate their coffee intake. Pregnant women are also advised to aim for less than 200 mg of caffeine daily because caffeine passes through the placenta

into the foetus and has been associated with pregnancy loss and low birth weight.[217,218]

Green coffee. Reported moisture contents of green coffee beans range from 8 to 13% for arabica and from 12-13% for robusta. The proximate composition of green arabica (A) and robusta (R) coffees (dry basis) includes protein levels ranging from 11 to 17% (A) and from 11 to 13% (R); lipid contents ranging from 9 to 18% (A) and from 9 to 18% (R); carbohydrate (by difference) ranging from 60 to 76% (A) and from 69 to 76% (R); and mineral levels ranging from 4 to 5% (A, R). The reported variations are related to several factors including species/variety, origin, agricultural practices, growth and storage conditions and maturation degree.[219] Caffeine (1 - 4%) and trigonelline (0.8%) are present, but caffeine is in prominence, and its content is related to its quality due to its bitterness. Caffeine has been historically linked to most of the physiological effects of coffee and caffeine levels in green coffees vary mainly with respect to species. Robusta coffees have approximately twice the amount of caffeine found in arabica coffees, with average values ranging from 0.6 to 1.9% for arabica and approximately 2.2% for robusta. The lipids from green coffee include mainly triacylglycerols, sterols, diterpenes, and tocopherols.[220] Cafestol is one of the most abundant diterpenes found in coffee. Kahweol is another relevant compound, and its concentrations may differ substantially in different species of coffee.[215] Phenolic compounds are mainly found in coffee beans as chlorogenic acids (CGA). CGAs represent a family of esters that are structural analogues of quinic acid (QA) carrying one or more cinnamate derivatives such as caffeic, ferulic, and p-coumaric acids.[221] There are at least 30 different types of CGA found in green coffee, including caffeoylquinic acids (CQA), dicaffeoylquinic acids, feruloylquinic acids, and pcoumaroylquinic acids. 5-CQA is the most abundant CGA found in green coffee, representing over 50% of total CGAs. In 2019, Macheiner *et al*. describes green coffee infusion as a novel and emerging food, source of caffeine and chlorogenic acid. They reported the first study on

caffeine and chlorogenic acid content in green coffee infusion as ingested by the consumer. Results of chlorogenic acid ranged from 628 to 1040 mg/L in *C. arabica* infusions, and from 682 and 1210 mg/L in *C. canephora* infusions while caffeine intake can be compared with *Camellia sinensis* green tea beverages.[222] The majority of studies that have been developed so far on the antioxidant potential of green coffee beans or their infusions have associated the significant antioxidant activity to the presence of phenolics, mainly chlorogenic acids. One of the earlier studies on antioxidant activity of green coffee was developed by Daglia and collaborators[223], assessing antioxidant properties of both green and roasted coffee, as affected by species (*C. arabica* and *C. robusta*) and roasting degree. The levels of reducing substances (RS) of green coffee aqueous solutions were significantly higher for *C. robusta* (~11 g/100 g) in comparison to *C. arabica* (~5 g/100 g), whereas *in vitro* antioxidant activity was similar. The significant differences in RS values consistently were attributed to their different content of polyphenol compounds, particularly chlorogenic acids. All green coffee solutions showed an immediate, strong ability to decrease the lipid peroxidation rate in a model system, by at least 90%. Naidu *et al*.[224] also compared the antioxidant potential of *C. arabica* and *C. robusta* green beans. The extracts were prepared with solvent mixtures of isopropanol and water in different ratios. The total polyphenol content (based on Folin-Ciocalteau assay) increased as the amount of water in the mixture was increased, with the best results (~32 g/100 g gallic acid equivalents) obtained from extraction with isopropanol 60/water 40 solution. DPPH-based free radical scavenging activity of the extracts ranged from 92 to 76% inhibition and from 88 to 78% inhibition for arabica and robusta coffees, respectively. Both hydroxyl radical scavenging activity and reducing capacity were also found to be significant for all extracts. Results indicated that extracts obtained from green coffee present potential antioxidant activity and could be used as nutraceuticals as well as preservatives in food formulations. Ramalakshmi *et al*.[225] developed another study on the antioxidant potential of defective green coffee beans. To evaluate the antioxidant potential of green coffee

beans, extracts of beans were prepared using different solvents (hexane, chloroform, acetone, and methanol). The extracts were evaluated through *in vitro* models of radical scavenging activity (α,α-diphenyl-β-picrylhydrazyl radical), antioxidant activity (β-carotene-linoleate model system), reducing power (iron reducing activity) and antioxidant capacity (phosphomolybdenum complex) in comparison to a synthetic antioxidant (butylated hydroxy anisole, BHA). Methanolic extract presented highest activity compared to the other solvents: free radical scavenging activity 92.5% (similar to BHA), antioxidant activity 58.2% (significantly lower than BHA 90%). Results for reducing power were in the following order: ascorbic acid > chlorogenic acid > BHA > methanol extract. The antioxidant capacity of the methanol extract was 1367 ± 54.17 μmol/g as equivalents to ascorbic acid, in comparison to 3587.9 ± 43.87 μmol/g for pure chlorogenic acid and 5098 ± 34.08 μmol/g for propyl gallate. In a subsequent study Ramalakshmi and co-workers further investigated the bioactivity of the methanolic extract of green low-quality beans with reference to antioxidant (ORAC assay), anti-tumour (P388 cell assay) anti-inflammatory (J774A.1 cell assay) and anti-allergenic (RBL-2H3 cell degranulation assay) properties. The ORAC-based antioxidant capacity was significantly high (4416 μmol Trolox eq/g). Anti-tumor activity was observed, with P388 cell viability being reduced to 50.1 ± 3.6%, whereas anti-allergenic activity was not significant. These studies confirmed the potential of green coffee beans as source of antioxidants. It was particularly interesting as a proposition of an alternative use for low quality coffee beans. In 2014, Gawlik-Dziki and co-workers[226] evaluated the antioxidant potential and capacity for inhibition of lipoxygenase of green coffee beans from different origins (Ethiopia, Kenya, Brazil and Colombia). The major antioxidant compounds identified in all the samples were 5-caffeoylquinic acid (5-CQA), 4-caffeoylquinic acid (4-CQA), 3-feruoylquinic acid (3-FQA) and 5-feruoylquinic acid (5-FQA). There were variations in total phenolics contents (TPC) in the following order: Kenya > Brazil > Colombia and Ethiopia. Evaluation of changes in TPC during simulated digestion and absorption was based

on the Folin-Ciocalteau method. Results showed that green coffee beans possessed the ability to protect lipids against oxidation, regardless of origin, this activity was relatively low in the raw extracts. However, digestion *in vitro* released compounds able to protect lipids against oxidation. The authors concluded that green coffee beans are a potential source of bioavailable compounds with multidirectional antioxidant activity. Amigoni *et al*.[173] investigate the chemical composition of green coffee extract by NMR and UPLC/ESI-HRMS analyses. Also, the antioxidant activity of the green coffee extract was assessed. In this study, green coffee extract displayed an anti-aging effect in *Caenorhabditis elegans*, that consisted in increased stress resistance, fertility, and adult mean lifespan. A recent study by Stelmach *et al*.[227] the content of nutritionally important macro (Ca, Mg) and microelements (Fe, Mn, Cu) in infusions of green coffees was evaluated, in order to access a possible correlation with antioxidant activity. It was found that Ca and Mg were present in the highest concentrations in the infusions, with average concentrations of 6.49 and 12.4 μg/g, respectively. Concentrations of minor elements (Cu, Fe, Mn) were in the range from 0.04 to 0.13 μg/mL in the prepared infusions. Moderate positive correlation was observed between the antioxidant activity of green coffee infusions and their total content of phenolic compounds and Ca levels.

Roasted coffee. Several researchers have investigated the difference in chemical composition between green and roasted beans. Coffee roasting is an important step during coffee preparation. During roasting, the green beans are heated at 200-240ºC for 10-15min depending on the degree of roasting required, which is generally evaluated by colour.[228] Temperature, time, and the speed at which coffee is roasted importantly affects the organoleptic properties of coffee. Coffee brew is an intricate chemical mixture reported to contain more than a thousand different chemicals, including carbohydrates, lipids, nitrogenous compounds, vitamins, minerals, alkaloids, and phenolic compounds.[229] The proximate composition remains similar, since changes occur within a specific class of compounds. Slightly higher values and

higher variations of lipids in roasted coffee in comparison to green coffee are attributed to the beans dry matter loss during roasting, which in turn varies with the roasting degree.[230] Studies have shown that roasting can cause caffeine levels to be reduced down to 70% of the amount detected in green coffee.[231,232] Given that the solubility of this compound in water increases with temperature, the caffeine loss can be attributed to dragging, by the water vapor released during roasting. Another substance that is interesting from a nutrition point of view in roasted coffee is nicotinic acid (niacin or vitamin B3), the major non-volatile component resulting from demethylation of trigonelline during roasting. Niacin levels in roasted coffee range from 10 to 40 mg/100 g.[219] coffee roasting could also generate "undesirable" compounds, such as the carcinogenic acrylamide. Robusta coffee upon roasting contained more acrylamide than Arabica coffee.[233] The high temperatures observed in the roasting process mainly led to the decomposition of sugars and decarboxylation of carboxylic acids. CGA may be isomerized, hydrolysed, or degraded into low molecular weight compounds during coffee processing. According to the intensity, coffee roasting leads to reduction in the total CGAs.[234] Such antioxidants will be partly decomposed during roasting and thus it is expected that the antioxidant activity associated to chlorogenic acids for example will decrease upon roasting. Nonetheless, roasting results in the generation of Maillard reaction products (melanoidins), which in turn presents significant antioxidant activities. Moreover, trigonelline can undergo degradation during the roasting process, resulting in *N*-methylpyridinium (NMP).[235] Therefore, there is a significant number of studies that evaluate the antioxidant potential of roasted coffee and the resulting beverages. Some studies have focused on comparing the antioxidant potential of green and roasted coffees as well as the effect of roasting degree. However, results on the effect of roasting on antioxidant activity are contradictory. Some studies report that the antioxidant activity increases from light to medium roasts and then decrease in dark roasts.[236–239] Others concluded that the antioxidant activity increases with roasting[240,241], whereas some claimed the opposite[242]. Recently, our colleagues

developed an experimental protocol that combines NMR spectroscopy and *in vitro* cell assays to detect anti-Aβ molecules naturally occurring in coffee extracts.[172] In fact, in the case of crude extracts, NMR analysis can help in distinguishing differences between relatively similar extracts, enabling the association with a specific (generally *in vitro*) biological activity. They found that both green and roasted coffee extracts show a "multi-target" anti-amyloidogenic activity, hindering Aβ peptide aggregation and cytotoxicity in a human neuroblastoma cell line (SH-SY5Y). Moreover, they identified chlorogenic acids and melanoidins as the most active components of coffee extracts. Additionally, they report that coffee extracts were able to reduce oxidative stress and modulate autophagy *in vitro*. In 2020, Funakoshi-Tago *et al*. investigated the anti-inflammatory activity of roasted coffee extracts analysing the inflammatory response of LPS-stimulated murine macrophages (RAW264.7).[243] They reported that coffee extract significantly inhibited LPS-induced iNOS mRNA expression and NO production in a dose-dependent manner. Coffee extract also markedly inhibited the LPS-induced mRNA expression and secretion of CCL2, CXCL1, IL-6, and TNF-α. Additionally, the LPS-induced expression of IL-10, which is a representative anti-inflammatory cytokine, was found to be decreased. In 2021, Castaldo *et al*.[244] assessed the changes in the anti-inflammatory and antioxidant activity of coffee after simulated gastrointestinal digestion. Digested coffee samples exhibited higher antioxidant capacity and total phenolic content than not-digested coffee samples. Moreover, digested coffee samples showed a higher reduction in IL-6 levels in LPS-stimulated HT-29 cells treated for 48 h (compared to not-digested samples) and fewer cytotoxic effects in the MTT assay.

Coffee by-products. Additionally, industrial processing can generate many coffee by-products such as cherry husks and pulps, silver skin, and spent coffee. Sustainability issues lead to the study of new active ingredients obtained from those by-products. The study conducted by Castro *et al*. found that *Coffee arabica* green

coffee residue extract showed potential as a raw material for dietary supplements, cosmetics, and pharmaceuticals, as a source of antioxidants.[245] In 2012, Murthy and Naidu tested different coffee by-products and found that their antioxidant activity levels ranging from 61% to 70%.[246] In 2014, Bresciani *et al*. analysed *Coffea arabica* silverskin (CSS) and found that its phenolic profile was similar to that of coffee brews. The most abundant quantified phenolics were caffeoylquinic acids, with the 5- and 3-isomers being the most relevant (199 mg/100 g and 148 mg/100 g, respectively). Together, the three caffeoylquinic acid isomers reached a total concentration of 432 mg/100 g, corresponding to 74% of the total chlorogenic acids detected in CSS. To note, caffeine content in CSS was equal to 10 mg/g of product, 3.5 times lower than most coffee brews. Due to the extremely high total antioxidant capacity (139 mmol Fe^{2+}/kg) they observed, authors suggested CSS as an innovative functional ingredient.[247] In 2018, Magoni and co-workers demonstrated that pre-treatments with coffee pulp extracts was effective in preventing IL-8 release by gastric epithelial cells. Chemical evaluation performed by liquid chromatography mass spectrometry showed that quinic acid derivatives are abundant in coffee pulp extract together with procyanidins derivatives, thus those compounds might be responsible for the observed biological activity.[248]

Bioactive Components in Coffee. Coffee may present over 2000 different chemical components. However, the amounts of these compounds may differ in other species, cultivation conditions, time of collection, and storage of fruits.[249] Also the brewing process has a role in this, as "coffee is never 'just coffee'" and that the content of bioactives in a cup of coffee may vary significantly.[250,251] As a mixture of countless bioactive compounds, coffee may exhibit its benefits variously, with its antioxidant[252,253] and anti-inflammatory effects[254–256] having a crucial role. Coffee bioactivity is manly related to caffeine, trigonelline, cafestol, kahweol, chlorogenic acids and melanoidins.[257,258]

Although coffee is appreciated for its aroma and flavour, its caffeine content likely plays a role in its popularity. Caffeine is naturally found in the fruit, leaves, and beans of coffee, cacao, and guarana plants. Its stimulating effect on the central nervous system[259] can cause different reactions in people. Low to moderate doses of caffeine (50–300 mg) may cause increased alertness, energy, and ability to concentrate. Many people appreciate the temporary energy boost after drinking an extra cup of coffee. Moreover, caffeine in coffee has been found to protect cells in the brain that produce dopamine in animal and cell studies.[260] However, in sensitive individuals, higher caffeine doses may have negative effects such as anxiety, restlessness, insomnia, and increased heart rate.[261] There are two most common methods used to remove caffeine from coffee: chemical solvents (methylene chloride or ethyl acetate) or carbon dioxide gas. Both are applied to steamed or soaked beans, which are then allowed to dry. The solvents bind to caffeine, and both evaporate when the beans are rinsed and/or dried. Both methods may cause some loss of flavour as other naturally occurring chemicals in coffee beans that impart their unique flavour and scent may be destroyed during processing.[262] The literature reports several *in vitro* and *in vivo* studies reporting the effect of caffeine on BDNF, whereas the effect of a *Coffea arabica* extract from fruits was investigated only in one clinical study.[263]

The acknowledgment that coffee and caffeine are not equivalent has increased the interest in whether other components of coffee might contribute to the protective action in the human body.

Another substance that has been reported not only as an important precursor of important flavour compounds (furans, pyrazine, alkyl-pyridines, and pyrroles), but also as a beneficial nutritional factor is trigonelline, a pyridine derivative.[264–266] Trigonelline levels are reduced during roasting, with *N*-methylpyridinium and nicotinic acid (niacin or vitamin B3) being the major non-volatile decomposition products. To note, vitamin B3 is highly bioavailable in coffee, more than in other food sources.[267] Concerning their biological effects, trigonelline and its derivatives

have been related to anti-diabetic, neuroprotective, and anti-proliferative activities.[268]

Kahweol, together with cafestol was first isolated in coffee oil and identified as cholesterol-raising factors.[269] As reported in a meta-analysis of 14 randomized controlled trials examining the effect of coffee consumption on serum cholesterol concentrations, the consumption of boiled coffee dose-dependently increased serum total and LDL cholesterol concentrations, while the consumption of filtered coffee resulted in very little increase in serum cholesterol.[270] Thus, these diterpenes are extracted from ground coffee during brewing but are mostly removed from coffee by paper filters. However, succeeding studies have demonstrated that cafestol and kahweol can have a two-faced effect, exhibiting a wide variety of pharmacological activities, including anti-inflammatory, anti-angiogenic and anti-tumorigenic properties which were recently reviewed.[271]

The unroasted, green coffee beans are a rich source of polyphenols such as chlorogenic acids. The content of chlorogenic acids in unprocessed coffee bean declines with fruit maturation and the ripe and fully ripe fruit has a marked distinction. The various degrees of maturity are ascribed to an increase in 3-caffeoylquinic acid and a decrease in 5-caffeoylquinic acids.[272] Of the two varieties of coffee that are commercially cultivated, *Coffea arabica* contains 3.5 - 7.5% (w/w of dry matter) chlorogenic acids, while *Coffea canephora* chlorogenic acids content range is 7–14%. Three main classes of chlorogenic acids: caffeoylquinic acid (CQA), dicaffeoylquinic acid (diCQA) and feruoylquinic acid (FQA), together account for more than 80% of the total chlorogenic acids (CGAs) present in green coffee.[273] According to the IUPAC nomenclature, CGA is referred as 5-CQA and its isomers are 3-CQA and 4-CQA, while according to the IUPAC numbering system, the carbon 1 and 3 of the quinic acid contain axial hydroxyl groups whereas carbon 4 and 5 contain equatorial hydroxyl groups. 5-CQA is the most abundant CGA found in green coffee, representing over 50% of total CGAs, followed by 3- and 4-CQAs.

During coffee processing, CGAs are primarily hydrolysed to quinic acid and caffeic acids.[274] Moreover, chlorogenic acid lactones are built up as a consequence of roasting.[179] Generally, CGAs have been endorsed with several biological activities, such as inhibiting reactive oxygen species production, improving endothelial function by modulating nitric oxide (NO) production and/or thromboxane activation, and reducing blood LDL-cholesterol levels.[275] Additional details regarding the biological properties of chlorogenic acids, especially those linked to inflammation are given in CHAPTER II – Pharmacologic Overview of Chlorogenic Acid in Inflammation.

Positive biological activities of the coffee brew have been associated to compounds built during the roasting process. Rearrangement and reactions between amino acids and sugars via Maillard and Strecker reactions generate new compounds of very different chemical classes, including hydroxyphenylindans, hydroxyl-dihydrocaffeic acid, and cinnamoyl-shikimic acids, and melanoidins, that can affect the overall antioxidant capacity and anti-inflammatory effect of coffee.[241,257,276,277]

Coffee brew is one of the main natural sources of melanoidins of the daily diet worldwide (**Figure 15**). These complex macromolecules possess multiple health-promoting properties, such as antioxidant, anti-inflammatory, and prebiotic capacity, which make them very interesting from a nutritional point of view.[278] For instance, coffee melanoidins act as an anticariogenic agent since they inhibit the adhesion of *Streptococcus mutans*, the major causative agent of dental caries in humans, almost completely at a concentration of 6 mg/ml.[279] Moreover, melanoidins have been demonstrated to confer to human HepG2 cells a significant protection against oxidative insults and prevent oxidative endogenous formation of oxidative DNA damage by reducing TNF-α, tissue transglutaminase, and transforming growth factor beta (TGF-β) expression in the liver.[277] Interestingly, they are also able to lower the blood glucose peak and insulin response due to the chlorogenic acids linked to their structure (**Figure 15B**).[280] Moreover, a study revealed that polyphenol-rich

melanoidins, such coffee melanoidins, can scavenge α-dicarbonyl compounds (DCs), thus mitigating the negative consequences of their reaction with other macromolecules in physiological conditions.[281]

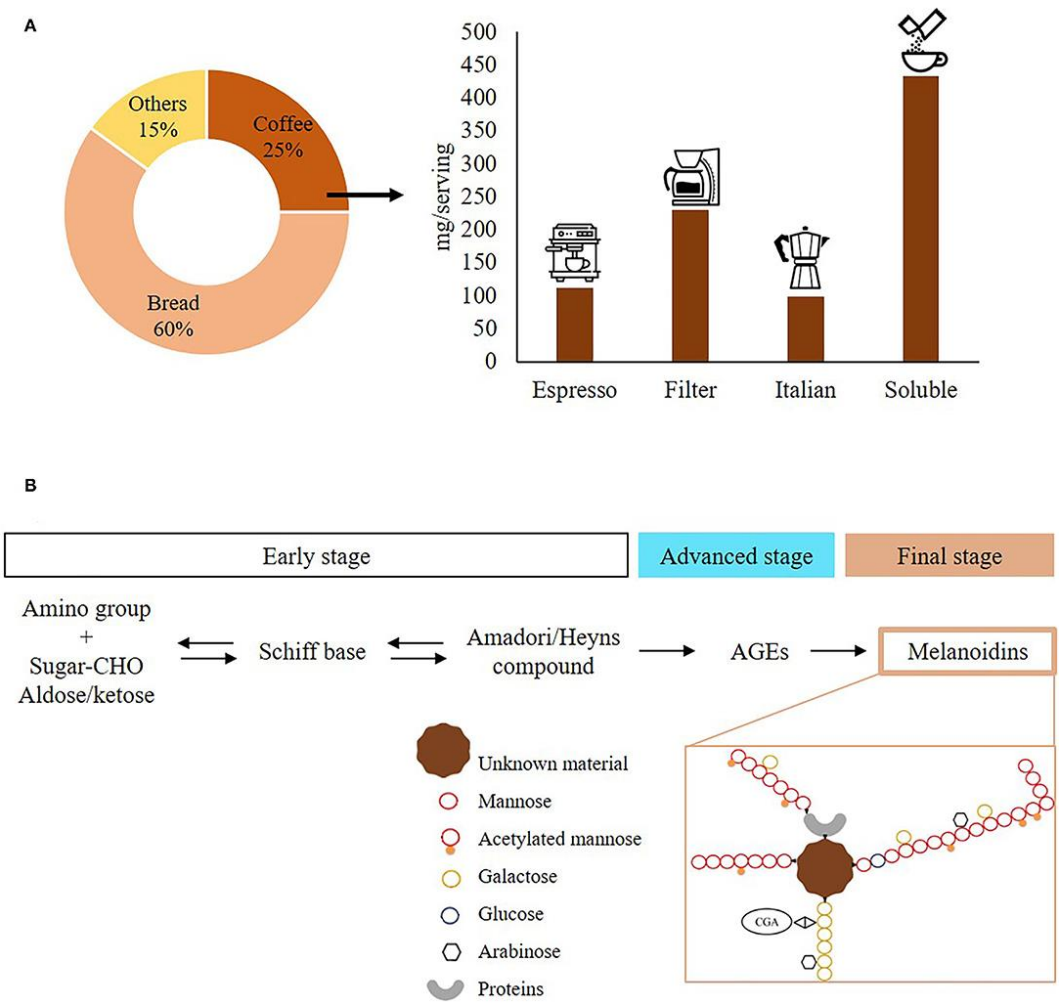

Figure 15. Coffee melanoidins. (**A**) Dietary intake of coffee brew melanoidins. (**B**) Pathway of formation and structure of coffee brew melanoidins.[278]

Interestingly, in 2021 Ribeiro *et al*.[282] evaluated protein extracts of green and roasted coffee beans as sources of bioactive peptides. Their findings showed that 11S coffee globulin is a precursor of bioactive peptides.

Coffee-derived compounds as inflammation modulators. Even though a plethora of evidence linked coffee consumption and the reduced risk of the onset of inflammation-related diseases, few studies have explored the detailed mechanism of action of the coffee-derived products involved, thus it will be interesting to determine whether the TLR signalling pathways are at least partially involved.

Caffeine (1,3,7-trimethylxanthine) is the most widely consumed psychostimulant substance in the world. At nontoxic doses, caffeine acts as a nonselective adenosine receptor antagonist. Besides its well-known psychoactive effects, caffeine has a broad range of actions. It regulates several physiological mechanisms as well as modulates both native and adaptive immune responses by various ways. In humans, 99% of caffeine is absorbed from the gastrointestinal tract in about 45 min after ingestion.[283] Chavez Valdez *et al*. provide observations on the relationship between serum caffeine levels and cytokine concentrations in tracheal aspirates and peripheral blood in a cohort of preterm infants. The results show that serum caffeine levels were higher after more than a week of treatment than they were after the initial doses. The relationship between caffeine levels and pro-inflammatory cytokines was U-shaped, meaning that at low serum caffeine levels TNF-a, IL-1 and IL-6 were reduced in concentration but at higher caffeine levels their levels were increased.[284] In 2020, a Spanish group investigated the effects of caffeine and green coffee extract (GCE) on hepatic lipids in lean female rats with steatosis. Interestingly, their conclusion was that a low dose of caffeine alone did not reduce hepatic steatosis in lean female rats, but the same dose provided as a green coffee extract led to lower liver triglyceride levels.[285] To note, in 2021 Kovács and colleagues[286] reported a comparative analysis of the effect of caffeine on two subpopulations of human monocyte-derived macrophages differentiated in the presence of macrophage colony-stimulating factor

(M-CSF) or granulocyte-macrophage colony-stimulating factor (GM-CSF), M-MΦs and GM-MΦs, respectively. They showed that although TNF-α secretion was downregulated in both LPS-activated MΦ subtypes by caffeine, the secretion of IL-8, IL-6, and IL-1β as well as the expression of Nod-like receptors was enhanced in M-MΦs, while it did not change in GM-MΦs. Moreover, they showed that caffeine (1) altered adenosine receptor expression, (2) changed Akt/AMPK/mTOR signalling pathways, and (3) inhibited STAT1/IL-10 signalling axis in M-MΦs, concluding that these alterations could play an important modulatory role in the upregulation of NLRP3 inflammasome-mediated IL-1β secretion in LPS-activated M-MΦs following caffeine treatment.

In a model of inflamed and dysfunctional human adipocytes, *N*-methylpyridinium (NMP) at concentrations as low as 1 µmol/L reduced the TNF-α-triggered expression of several pro-inflammatory mediators, including C-C Motif chemokine ligand (CCL)-2, C-X-C Motif chemokine ligand (CXCL)-10, and intercellular adhesion Molecule (ICAM)-1, but left the induction of prostaglandin G/H synthase (PTGS)2, interleukin (IL)-1β, and colony stimulating factor (CSF)1 unaffected. Moreover, NMP reduces adipose dysfunction in pro-inflammatory activated adipocytes, suggesting that bioactive NMP in coffee may improve the inflammatory and dysmetabolic milieu associated with obesity.[287]

Cafestol and kahweol can significantly reduce the mRNA levels of COX-2 and iNOS and decrease the expression of COX-2 and iNOS protein, therefore inhibiting the synthesis of PGE2 and NO in a dose-dependent manner. Further experiments demonstrate that coffee diterpenes can inhibit the activation of IKK in LPS-induced macrophages in a dose-dependent manner (within the concentration range of 0.5–10 µM) indicating the inhibition of NF-κB activation as the primary mechanism of action.[288] Later, Shen and colleagues discovered that Kahweol can down-regulates phosphorylation of signal transducers and activators of transcription 1 (STAT1) without altering its total level. However, the inhibition of JAK2 phosphorylation by

kahweol was not stronger than that of JAK2 inhibitor AG490, so there may be other pathways to block phosphorylation of STAT1.[289] Similarly, another study suggested that the suppression of the transcriptional activation of iNOS by kahweol might be mediated through the inhibition of NF-κB activation.[290]

Pyrocatechol, a component of roasted coffee, exhibits anti-inflammatory activity. Moon and Shibamoto reported that pyrocatechol was released from chlorogenic acid under reactive conditions (250 °C, 30 min)[291], which resemble coffee roasting conditions. A recent study showed that pyrocatechol inhibits LPS-induced NF-κB activation and induces Nrf2 activation, which negatively regulates LPS-induced inflammatory responses. As a result, pyrocatechol in roasted coffee beans suppresses NO production by inhibiting the mRNA expression of iNOS as well as CCL2, CXCL1, and IL-6. However, the direct target protein in the LPS signalling pathway for pyrocatechol has not yet been identified.[243]

Coffee melanoidins were found to contribute to reduce liver damage in a rat model of steatohepatitis.[277] In this study, 1.5 mL/day of decaffeinated coffee or its polyphenols or melanoidins were added for 8 weeks to the drinking water of rats who were being fed a high-fat, high-calorie solid diet (HFD) for the previous 4 weeks. Percentage variations of cytokine concentration of HFD-fed rats versus control rats were assessed. Several pro-inflammatory cytokines (except IL-6 and IFN-γ, which were unchanged) were significantly less abundant in HFD-fed rats drinking melanoidins than those drinking water. The effect of melanoidins was more important in TNF-α, IL-1α, and IL-1b, because reductions of 58%, 31%, and 15%, respectively, were found in melanoidin-drinking versus water-drinking rats.

4.2. Hypothesis

Numerous epidemiological studies have reported a relationship between coffee consumption and reduced incidence of chronic diseases. Experimentally, *in vivo* and

in vitro studies demonstrate the ability of coffee and coffee-related components to modulate inflammation. However, most of them have employed murine cell models or specimens.

In the present study we investigate the putative immune modulatory properties of both green and roasted coffee beans extracts, employing both immortalized and primary human macrophages. We also aim at determining whether the coffee processing have an impact or not.

4.3. Experimental Design

First, we performed an NMR-based metabolic profiling of green and roasted Robusta (*Coffee canephora*) coffee bean extracts (GCE and RCE). Then, we evaluated coffee extracts (CE) cytotoxicity on human macrophages. To this end, cell viability after coffee extracts treatment was estimated by MTT assay. Next, we investigated CE immune modulatory activities, measuring the production of both inflammatory cytokines and type I interferons in human LPS-stimulated THP-1-derived macrophages (TDM). Moreover, High Content Analysis was performed to visualise the intracellular effects of coffee extracts. Finally, primary $CD14^+$ monocyte-derived macrophages (MDM) were employed.

4.4. Results

4.4.1. NMR-based Metabolic Profiling of Coffee Extracts

Green (GCE) and roasted (RCE) coffee beans hydroalcoholic extracts were prepared as previously described.[172,173,292,293] The methodology is described in section 3.1. They were characterized by NMR spectroscopy. ^{1}H-NMR metabolic profiles of GCE and RCE are depicted in **Figure 16**.

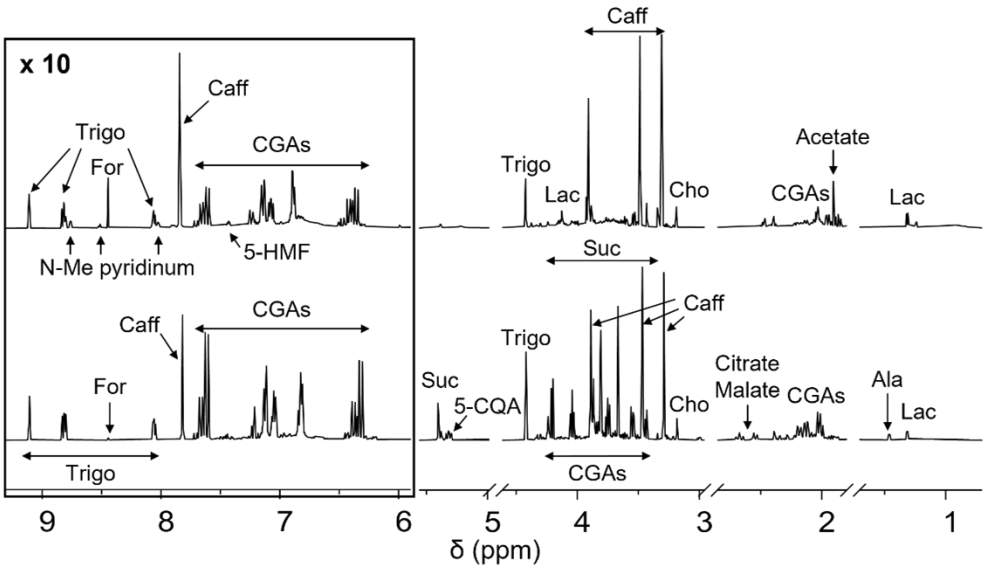

Figure 16. NMR profiling of coffee samples. ^{1}H-NMR spectra of Robusta green (bottom) and roasted (up) coffee extracts from Brazil. Each sample, containing 5 mg/mL of extract, was dissolved in a 10 mM deuterated phosphate buffer, pH 7.4, DSS 1 mM. Spectra were acquired at 25 °C and 600 MHz. Assignments of the resonances of the most important metabolites are shown (5-HMF, 5-hydroxymethylfurfural; Trigo, trigonelline; *N*-Me pyridinium, *N*-methyl pyridinium; For, formate; Caff, caffeine; CGAs, chlorogenic acids; Suc, sucrose; 5-CQA, 5-*O*-caffeoylquinic acid; Cho, choline; Ala, alanine; Lac, lactate).

As previously reported[172,293], the main differences among GCE and RCE rely in the complete disappearance of sucrose in RCE, together with a significant reduction of the amount of CGAs, due to melanoidin formation occurring during the roasting process, and the formation of *N*-methyl pyridinium, nicotinic acid, 5-hydroxy-methyl furfural and 2-furylmethanol. Moreover, a significant decrease in trigonelline and choline content can be observed. Metabolites identification was based on the analysis of mono (^{1}H) and bi-dimensional (^{1}H,^{1}H-TOCSY, ^{1}H,^{13}C-HSQC) NMR spectra and by the use of specific libraries built in-house for the Simple Mixture Analysis (SMA) tool implemented in the MestReNova 14.2.0 software.[294,295] Data were in agreement with those previously reported by our and other groups.[172,293,296–298] SMA allowed not only the identification but also the simultaneous quantitation of all the

metabolites over the detection limit (about 50 nM). Quantification values are reported in **Table 1**. Melanoidin content in RCE was quantified by UV spectroscopy as 683.89 ± 33.99 µg/mg of RCE.

TABLE 1 | Metabolite quantification in GCE and RCE.

Metabolites	GCE		RCE	
	Mean	SD	Mean	SD
1,3-arabinofuranose unit	—	—	10.18	0.31
1,5-arabinofuranose unit	—	—	7.31	0.37
2-furylmethanol	—	—	0.59	0.08
5-CQA	128.5	2.61	42.54	1.64
5-hydroxymethyl-furfural	—	—	1.02	0.72
Acetate	0.67	0.06	4.12	0.18
Alanine	1.92	0.13	—	—
Caffeine	83.89	3.81	70.3	3.49
CGAs	349.59	6.68	148.57	13.96
Choline	16.31	0.15	2.2	0.04
Citrate	—	—	15.74	0.16
Formate	0.25	0.08	1.81	0.17
Lactate	12.62	0.48	6.71	0.68
Myoinositol	—	—	36.63	0.34
N-methylpyridinium	—	—	1.47	0.15
Nicotinic acid	—	—	0.27	0.06
Sucrose	204.01	2.79	—	—
Trigonelline	22.9	0.85	12.16	1.14

Results were expressed as µg/mg of extract and reported as mean and standard deviation (SD) of three-independent determinations (n = 3).

4.4.2. Effect of Coffee Extracts on THP-1-derived Macrophages (TDM) Viability

Toxicity of coffee extracts on cells was first tested by treating THP-1-derived macrophages (TDM) with increasing concentrations of GCE and RCE (10 to 500 µg/mL). After 24 h, cell supernatants were removed, and the remaining cell

monolayers were immediately used to assess cytotoxicity via the MTT assay. The integrity of cell morphology before and after treatment was inspected by a light microscope. Treatment effect on cell viability was expressed by setting the percentage of non-treated cells at 100%. As shown in **Figure 17**, viability of cells was generally unaffected by coffee extracts, except for RCE treatment of TDM at the highest concentration of 500 µg/mL. Therefore, for TDM, the highest concentration limit was set at 250 µg/mL in subsequent experiments.

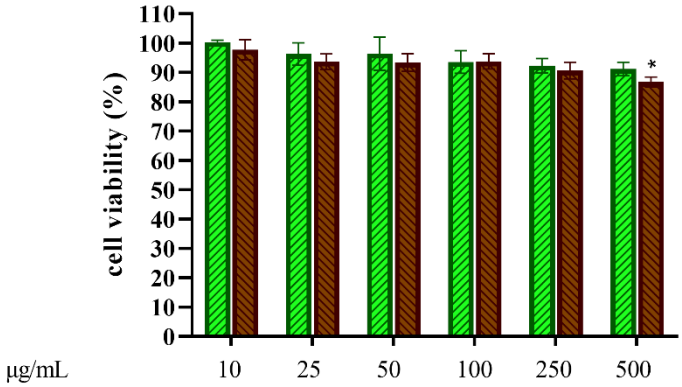

Figure 17. THP-1-derived macrophages viability. THP-1-derived macrophages (TDM) cell viability after treatment with increasing concentrations of GCE (green, down-up diagonal pattern) and RCE (brown, up-down diagonal pattern) was evaluated by MTT assay (24 h). Data are represented as mean ± SEM of three independent experiments (n=3). Results are referred to untreated control (100%) (one-way ANOVA, followed by *post hoc* Dunnett's test *p<0.05).

4.4.3. Effects of Coffee Extracts on NF-κB Activation in THP1-XBlue™ cells

LPS stimulation of cells induces NF-κB activation by phosphorylation and subsequent activation of downstream cytokines gene expression. To assess the activity of molecules on the LPS-induced NF-κB activation, a transcriptional reporter assay was used. In the absence of stimuli, NF-κB is associated with the

inhibitory protein IκBα, which restrains translocation of the transcription factor from cytoplasm to the nucleus. LPS stimulation causes rapid IκBα degradation, allowing NF-κB activation by phosphorylation. The ability of GCE and RCE to counteract the activation of NF-κB occurring upon LPS-stimulation was assessed by using THP1-XBlue™ cells, an engineered THP-1 cell line which expresses a reporter gene under the control of the NF-κB promoter. In these experimental conditions, LPS markedly increased the activation of NF-κB compared to the unstimulated control (**Figure 18A**). Both extracts inhibited NF-κB-driven transcription in a dose-dependent manner. GCE appear to be more active than RCE, GCE pre-treatment results in a 50% inhibition at the maximum dose of 250 μg/mL, while with RCE pre-treatment 20% inhibition was observed at the same concentration.

4.4.4. Effects of Coffee Extracts on Pro-inflammatory Cytokines Release in THP-1-derived Macrophages

The effects of GCE and RCE on the production of the main inflammatory cytokines TNF-α, IL-6 and interleukin-1-β (IL-1β) produced downstream to the TLR4/MyD88 signal pathway was investigated in TDM. Cells were treated with coffee extracts, then stimulated with LPS and cytokines were quantified in cell supernatants after 24 h from LPS stimulation. Pro-inflammatory cytokines levels of negative (non-treated) and positive (treated with LPS only) samples were compared with samples pre-treated with increasing concentrations of both GCE and RCE (10, 25, 50, 100, and 250 μg/mL) as depicted in **Figure 18**. Coffee extracts treatment of TDM resulted in a weak dose-dependent reduction of TNF-α release in response to LPS (**Figure 18B**). Contrarily, IL-1β and IL-6 production was more effectively inhibited by coffee extracts. IL-1β release was more strongly reduced by CGE compared to RCE pre-treatment (**Figure 18C**). This different behaviour was also confirmed by the Pearson's correlation analysis, which show a significant linear correlation for GCE treatment but not for RCE treatment (Pearson $r = -0.7391$, $p = 0.0932$). IL-6

production in TDM was markedly reduced in a dose-dependent manner by both CGE and RCE pre-treatments (**Figure 18D**).

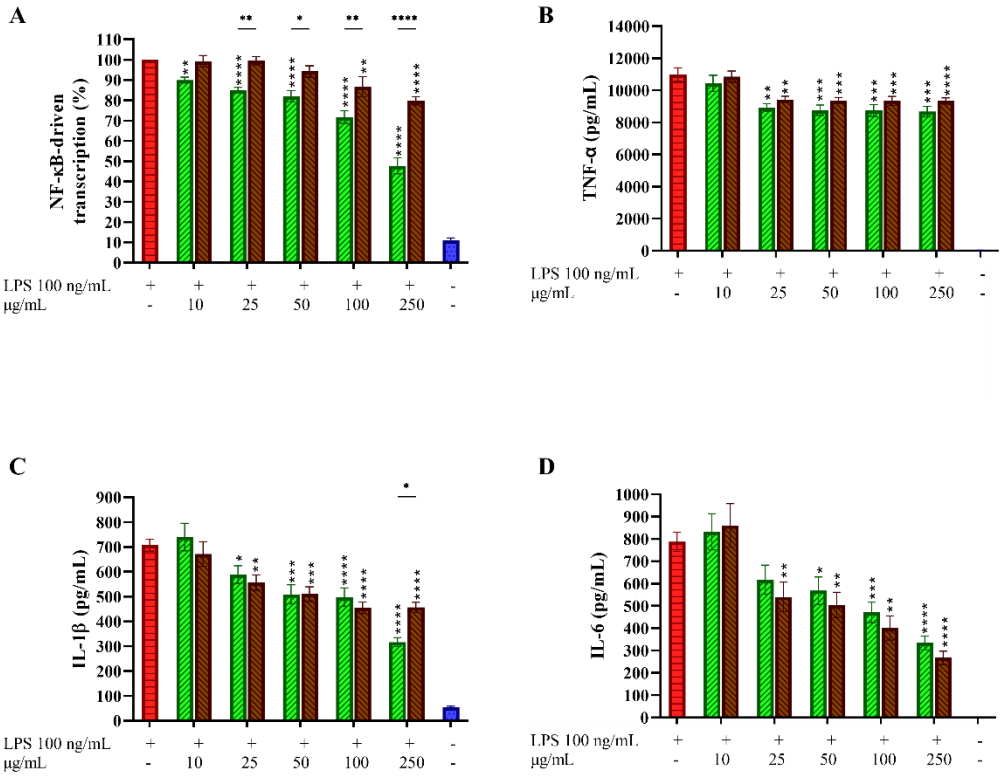

Figure 18. NF-κB-dependent transcription and pro-inflammatory cytokines profiling in LPS-stimulated THP-1-derived macrophages. THP-1-derived macrophages (TDM) cells were pre-treated with increasing concentrations of GCE (green, down-up diagonal pattern) and RCE (brown, up-down diagonal pattern) for 1 h and then challenged with 100 ng/mL LPS. Activation of NF-κB pathway **(A)** was assessed by using THP1-XBlue™ cells as a reporter cell line and quantifying the activity of SEAP released in the medium after 18 h. Percentage is referred to positive control (red, 100%) Negative control (unstimulated cells) is indicated in blue. TNF-α **(B)**, IL-1β **(C)** and IL-6 **(D)** release in the medium after 24 h were quantified via ELISA. Data are represented as mean ± SEM of three independent experiments (n=3). (one-way ANOVA, followed by *post hoc* Dunnett's test **p*<0.05, ***p*<0.01, ****p*<0.001, *****p*<0.0001).

4.4.5. Coffee Extracts Inhibit IFN-β Release in THP-1-derived Macrophages

TLR4 activation and signalling through the MyD88-independent TRAM/TRIF pathway leads to the activation of TBK1 and IRF-3 thus inducing the IFN-β gene transcription. As for other cytokines, IFN-β release was assessed by monitoring its concentration in cell supernatants, after 3 h LPS stimulation. The IFN-β levels of negative (non-treated cells) and positive (cells treated with LPS only) samples were compared with samples pre-treated with increasing concentrations of GCE or RCE (10, 25, 50, 100, 250 or 500 μg/mL), as indicated in **Figure 19**. A strong dose-dependent inhibition of IFN-β release was observed upon pre-treatment with CGE and RCE.

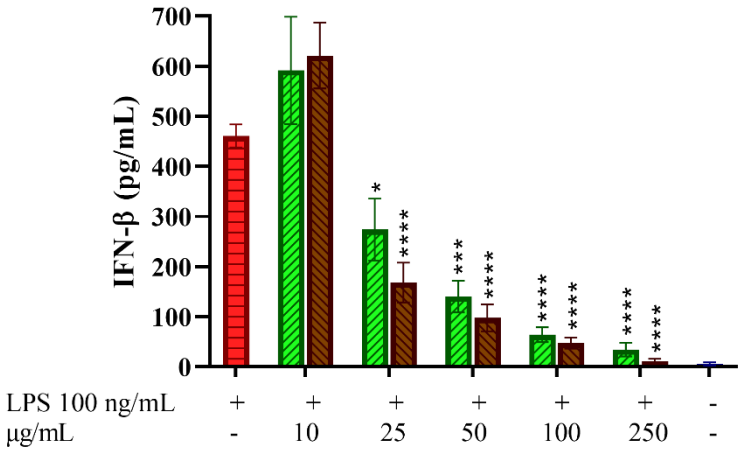

Figure 19. Effect of coffee extracts on THP-1-derived macrophages release of IFN-β upon LPS stimulation. THP-1-derived macrophages (TDM) cells were pre-treated with increasing concentrations of GCE (light green, down-up diagonal pattern) and RCE (brown, up-down diagonal pattern) for 1 h and then challenged with 100 ng/mL LPS. Supernatants were collected after 3 h. IFN-β released in the medium was quantified via ELISA. Negative control (unstimulated cells) is indicated in blue. Data are represented as mean ± SEM of three independent experiments (n=3) (one-way ANOVA, followed by *post hoc* Dunnett's test *p<0.05, ***p<0.001, ****p<0.0001).

4.4.6. Green and Roasted Coffee Extracts Inhibit p-IRF-3 Nuclear Translocation in THP-1-derived Macrophages

To investigate the subcellular events linked to the effects of GCE and RCE on inflammatory pathways, in particular on TLR4-mediated IFN-β production, we performed confocal microscopy analyses by using an automated screening microscope, the Operetta CLS™ High-Content Analysis System. We investigated the effect of coffee extracts pre-treatment on LPS-triggered nuclear translocation of the phosphorylated form of IRF-3. In fact, TLR4/TRIF pathway leads mainly to IRF-3 activation,[299,300] and subsequent production of IFN-β. We therefore verified the activation of TLR4/TRIF pathway by monitoring the downstream activation of IRF-3. LPS stimulation of TDM cells (0-4h) triggered the phosphorylation of IRF-3 resulting in a fluorescence signal. Nuclei-located fluorescence signal of LPS-stimulated samples was higher compared to non-treated samples, peaking at 2h. Treatment with RCE and GCE turned out to inhibit p-IRF-3 nuclear translocation, resulting in a significant reduction of the p-IRF-3-associated nuclei-located fluorescence (**Figure 20**). This observation parallels with the observation of the strong inhibitory effect of RCE, and GCE, on IFN-β release. Images (2000 cells/sample) were analysed using the built-in Harmony® high-content analysis software and percentage of positive nuclei for p-IRF-3 (PhenoVue™ Fluor 568 intensity threshold: 7000) was calculated. RCE and GCE pre-treatment resulted in a marked inhibition of p-IRF-3 nuclear translocation (about 40%).

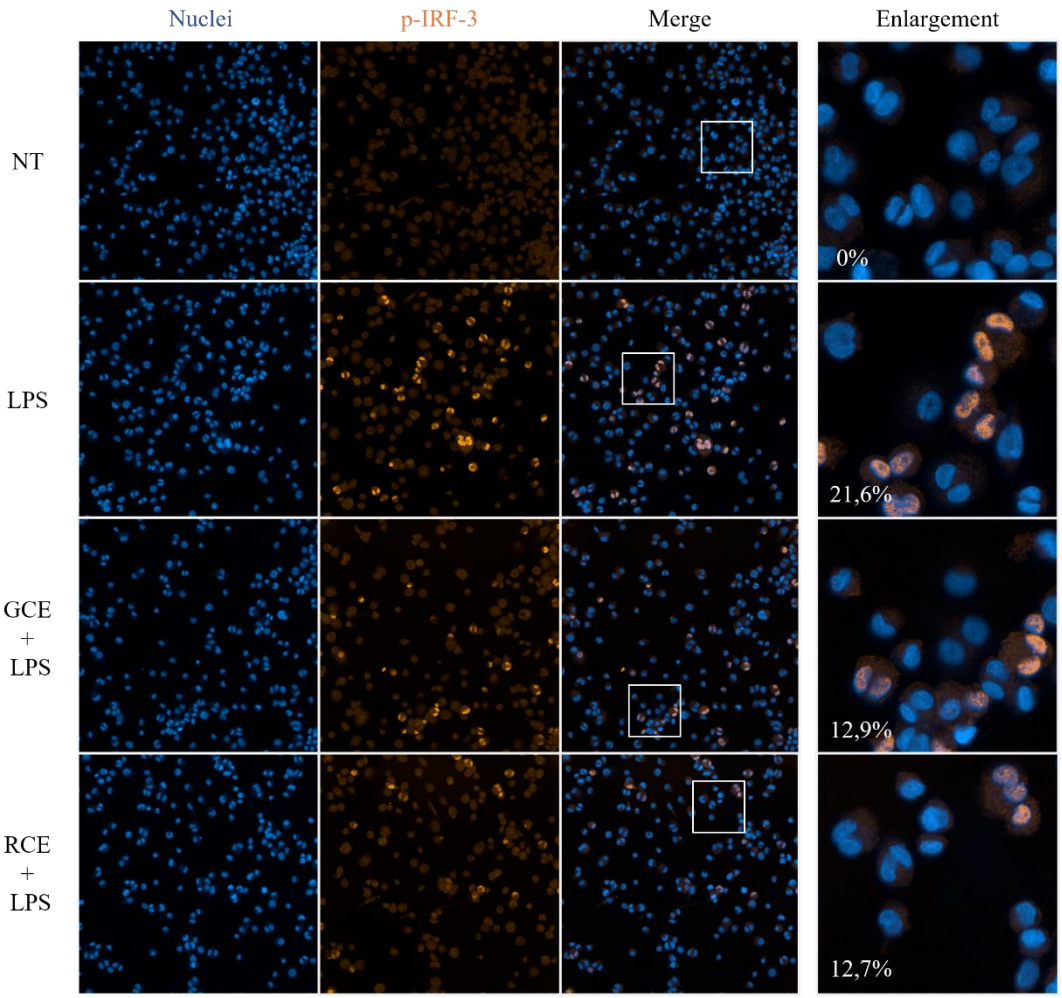

Figure 20. Immunofluorescence analysis of p-IRF-3 nuclear translocation. Phospho-IRF-3 localization in THP-1-derived macrophages (TDM) after 250 µg/mL GCE or RCE pre-treatment (1 h) and LPS stimulation (2 h). Images have been acquired using the Operetta CLS™ High-Content Analysis System and analysed through Harmony 4.5 software with the following settings: original magnification 20X, water objective, confocal mode. Pictures are representative. Data represent the percentage of positive nuclei (PhenoVue™ Fluor 568 intensity threshold: 7000) of different acquired fields of view/sample (fov=9).

4.4.7. Green and Roasted Coffee Extracts Inhibit Interferon-β Release in CD14$^+$ Monocyte-derived Macrophages

Macrophage-like cells differentiated from purified CD14$^+$ monocytes (MDM) were treated with increasing concentrations of GCE and RCE (10 to 500 µg/mL) to first assess toxicity of coffee extracts on primary cells. Cell viability after treatment is depicted in **Figure 21A**. None of the concentration used negatively affect cell viability, therefore the entire dose curve was maintained in subsequent experiments. Given the remarkable results obtained regarding the inhibition of IFN-β release in THP-1-derived macrophages, we were strongly encouraged to see if this effect should be confirmed on primary cells also. Thus, we treated MDM with GCE or RCE for 1 h and then we add LPS. As in previous experiments, we collected supernatant after 3h and we measured the IFN-β released in the medium. As shown in **Figure 21B**, GCE and RCE are both able to decrease the amount of IFN-β released in a dose-dependent manner. These data are consistent with those obtained using TDM (Figure 19).

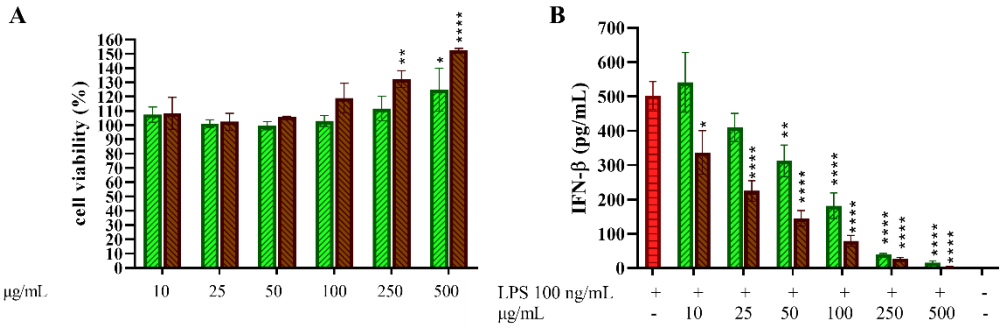

Figure 21. Effect of 5-CQA on CD14$^+$ monocytes-derived macrophages cell viability and IFN-β release. (A) CD14$^+$ monocytes-derived macrophages (MDM) cell viability after treatment with increasing concentrations of GCE (**A**, green, down-up diagonal pattern) and RCE (**A**, brown, up-down diagonal pattern) was evaluated by MTT assay (24 h). **(B)** MDM cells were pre-treated with increasing concentrations of GCE (light green, down-up diagonal pattern) and RCE (brown, up-down diagonal pattern) for 1 h and then challenged with 100 ng/mL LPS. Supernatants were collected after 3 h. IFN-β released in the medium was

quantified via ELISA. Negative control (unstimulated cells) is indicated in blue. Data are represented as mean ± SEM of three independent experiments (n=3) (one-way ANOVA, followed by *post hoc* Dunnett's test *p<0.05, **p<0.01, ****p<0.0001).

4.5. Discussion

Several studies showed the anti-inflammatory properties of coffee extracts in terms of inhibition of the main inflammatory mediators released upon LPS stimulation, both *in vitro* and *in vivo*, employing mainly murine models and focusing on the MyD88-dependent pathway. As far as we know, this is the first investigation of coffee extracts effects on another important inflammatory pathway occurring after LPS challenge, the TRIF-dependent cascade that led to Type I interferon production. First, this study reports a qualitative and quantitative characterization of the GCE and RCE molecular components by NMR. To summarize, the roasting process results in a reduction of total CGAs, and the formation of polymeric melanoidins together with other small molecules, such as *N*-methyl pyridinium, nicotinic acid, 5-hydroxy-methyl furfural and 2-furylmethanol. On the contrary some small molecular components such as trigonelline and choline are reduced during the roasting process. The main molecular components of both GCE and RCE are the chemically heterogeneous CGAs, among them 5-CQA is the most abundant isomer. Cell-based assays showed that both GCE and RCE were able to modulate inflammation in LPS-stimulated human TDM. Interestingly, the release of IL-1β and IL-6 was clearly inhibited by coffee extracts while TNF-α production was only slightly affected. NF-κB activation in macrophages derived from THP1-XBlue™ cells was inhibited as well. Those data are in line with previous studies on coffee extract anti-inflammatory effects performed *in vitro* and in experimental animals' models.[301,302] Interestingly, we report for the time that also the TRIF-dependent TLR4 signalling was modulate by coffee extracts. Specifically, IFN-β release was inhibited in human TDM. Inhibition of interferon-β was much more pronounced compared to the other cytokine examined: whether we observed a 50% inhibition of IL-6 and IL-1β release

with extracts concentration of 250 μg/mL, the same IFN-β inhibition occurred with 25 μg/mL coffee extracts. Molecular mechanism of IFN-β inhibition was further investigated by immunofluorescence confocal microscopy analysis that showed a diminished nuclear translocation of p-IRF-3, the main transcription factor responsible for IFN-β synthesis. The inhibition of IFN-β release by RCE and GCE was also confirmed by using human primary cells, specifically $CD14^+$ monocytes-derived macrophages (MDM), opening striking translational perspectives. Taken together, our findings support the role of coffee extract as putative immunonutrient supplements, particularly in relation to those pathological conditions characterised by an impaired type I interferon activity, e.g., SLE and other autoimmune diseases.

CHAPTER II

Pharmacologic Overview of Chlorogenic Acid in Inflammation

Adapted from:

Artusa, V.; Ciaramelli, C.; D'Aloia, A.; Facchini, F.A.; Gotri, N.; Bruno, A.; Costa, B.; Palmioli A,; Airoldi, C.; Peri, F. Green and Roasted Coffee Extracts Inhibit Interferon-β Release in LPS-Stimulated Human Macrophages. *Front. Pharmacol*. **2022**, 13:806010. doi: 10.3389/fphar.2022.806010 (in press) - Appendix I

4.6. Background

Although greater knowledge about the chemical composition of coffee extracts could help to understand the possible compounds responsible for the observed effects, attribute to a single compound in the bioactive properties of the complex mixture obtained when preparing coffee remain a difficult task. Hence, many authors have investigated the effect of isolated compounds (caffeine, phenolic compounds, trigonelline, flavonoids, chlorogenic acid, caffeic acid, etc.). This second chapter aims to give an insight of the various studies conducted to understand the biological properties of chlorogenic acid.

History and nomenclature. The term chlorogenic acid often refers to 5-*O*-caffeoylquinic acid (5-CQA), an ester of caffeic acid with quinic acid. However, the term chlorogenic acids (CGAs) stand for the whole set of hydroxycinnamic esters with quinic acid, including caffeoyl-, feruloyl-, dicaffeoyl- and coumaroylquinic acids.

Plant dietary sources. Coffee is one of the well-known dietary sources of CGAs and among the most highly consumed drinks worldwide. Accordingly, dietary intake of CGAs is closely associated with coffee consumption. The most common isomer in green coffee beans (76–84% of the total CGA) or coffee beans (10 g/100 g) is 5-caffeoylquinic acid (5-CQA) (**Figure 22**).[303]

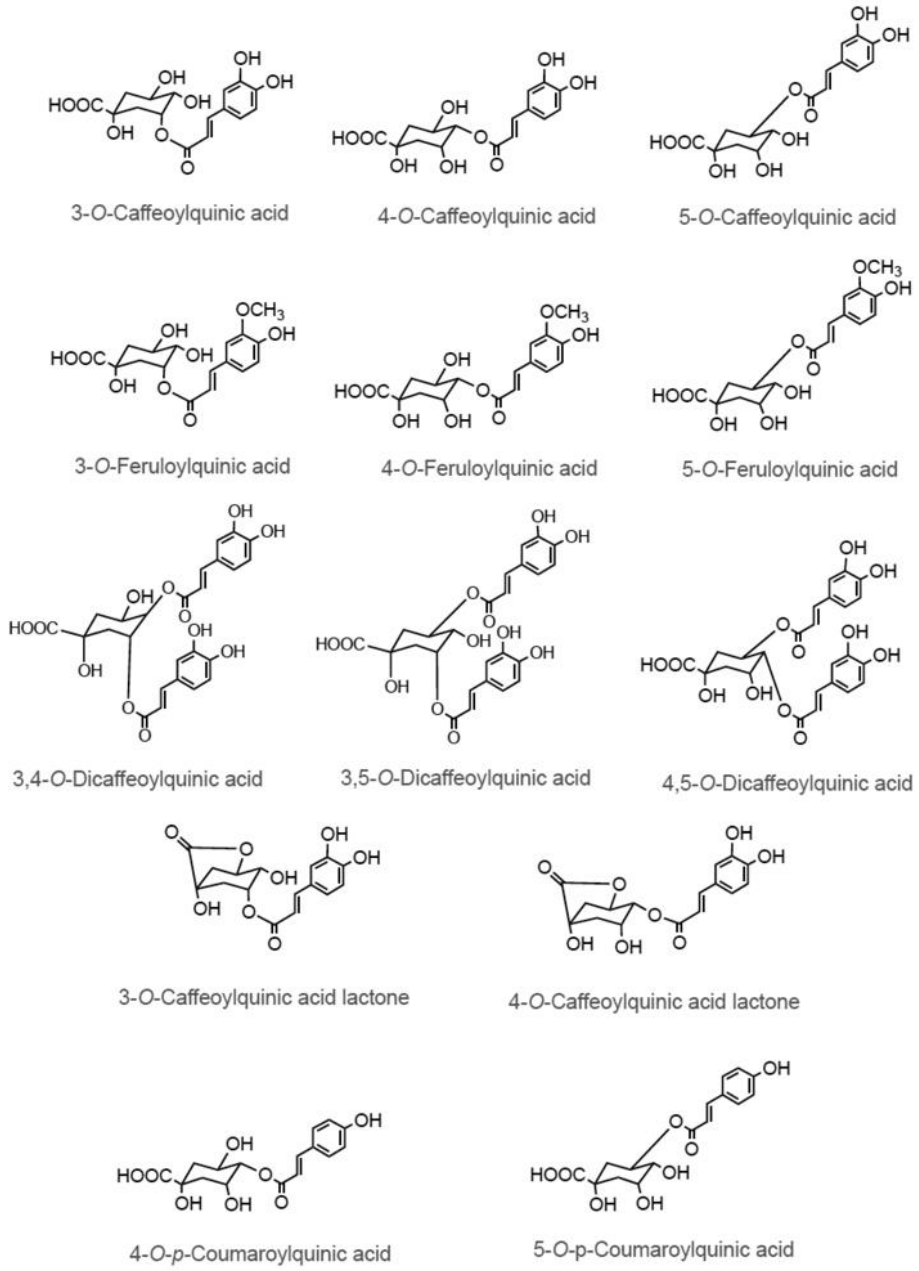

Figure 22. Structures of chlorogenic acids occurring in coffee. Phenolic acids are the most abundant polyphenols in coffee. Caffeic acid, which is unrelated to caffeine, is the main phenolic acid in coffee. Caffeic acid may be converted to ferulic acid. Both compounds may form an ester bond with quinic acid and generate any of the many isomers included in the family of the chlorogenic acids. The most frequent isomer is the 5-*O*-caffeoylquinic acid that, because of that, is commonly called chlorogenic acid.[304,305]

Green *Coffea canephora* var. Robusta beans contain higher amount of CGA on average compared to green *Coffea arabica* beans.[306] While much of the CGAs are degraded during the roasting process, for those who drink it, coffee beans are still considered the main source of CGAs in the human diet (up to 1750 mg/L) and 5-CQA still remained the major CGAs isomer in roasted coffee.[307] Besides coffee, vegetables and fruits also contribute to 5-CQA dietary consumption. Eggplant has also been reported to contain a high concentration of 5-CQA (1.4 to 28.0 mg/g), accounting for between 80 and 95% of the total hydroxycinnamic acids.[308] In addition, carrot (0.3 to 18.8 mg/g), artichoke (1.1 to 1.8 mg/g), and pepper (0.7 to 0.9 mg/g) also make a substantial contribution to 5-CQA intake in the human diet. Additionally, 5-CQA is also found in apples, pears, peaches, plums, cherries, tomatoes, and potatoes.[309] The content of 5-CQA in various dietary sources was extensively reviewed.[310] About two–thirds of ingested chlorogenic acid reaches the colon where it may be metabolized by the colonic microflora. Here, chlorogenic acid is likely hydrolysed to caffeic acid and quinic acid. Studies in colostomy patients indicate that about 33% of ingested chlorogenic acid and 95% of caffeic acid are absorbed intestinally.[311,312]

Chlorogenic acid in green coffee and roasted coffee. As evident from most methods of coffee preparation, chlorogenic acids are freely and easily solubilized in water. Chlorogenic acids are soluble in ethanol, methanol, water, and acetonitrile, owing to their polar nature due to the presence of numerous hydroxyl groups. The primary groups of CGA observed in green coffee beans include caffeoylquinic acids, dicaffeoylquinic acids, feruloylquinic acids, p-coumaroylquinic acids, and quinic acid blended diesters, each group having at least three isomers. Other than its biological properties, CGA also contributes for the colour, flavour, aroma, and phenolic derivatives during roasting.[313,314] During this process of roasting, some part of the CGA isomerizes, while another small part is converted to quinolactones by dehydration and intra-molecular bonds, while still another part is hydrolysed and

decomposed into compounds of low molecular weight. Intense roasting conditions lead to losses of up to 95% of CGA.[313] An Italian study evaluated chlorogenic acids content in 65 different capsule-brewed coffees, commercialised by 5 of the most representative brands in Italy. Large (*lungo*) coffees have the highest average amount of CQAs (60.4 ± 26.6 mg/serving), followed by regular (49.6 ± 16.0 mg/serving) and decaffeinated (43.0 ± 17.4 mg/serving) expresso coffees.[251] After coffee consumption, chlorogenic acids undergo extensive metabolism prior to absorption, first in the small intestine (~30%) and then in the large intestine (~70%) where the colonic microflora produces a unique spectrum of colonic catabolites which are then excreted in urine (~29%).[315] Even though absorption occurs in the small intestine, substantial quantities pass to the large intestine where the parent compounds and their catabolites can impact on both colonic health and the colonic microflora. Also, the level of urinary excretion indicates that substantial quantities of the colonic catabolites are absorbed into the portal vein and pass through the body in the circulatory system prior to excretion.[305]

Pharmacological effects and safety evaluation. Among CGAs, 5-CQA has received increasing attention due to its multiple pharmacological effects and biological activities such as antioxidant, anti-inflammatory, anti-obesity, antitumor, antihypertensive, improvement of metabolic disorders, and gastrointestinal tract-protective effects.[316] In 2018, a study was conducted to explicate the effects of decaffeinated green coffee bean extract (GCE) on patients with markers of metabolic syndrome. In a total of 50 subjects, 25 were randomly assigned to consume 400 mg decaffeinated GCE capsules (each capsule contained 186 mg chlorogenic acid) and 25 consumed placebo capsules twice per day for 8 weeks. Chlorogenic acid consumption resulted in reduction of all the investigated markers, including anthropometric indices, blood pressure, lipid profile, glycaemic control, insulin resistance and their appetite.[317]

Animal studies have shown that chlorogenic acid is effective against obesity. Cho *et al*. studied the impact of chlorogenic acid on body weight, visceral fat mass, plasma leptin and insulin levels, triglycerides in liver and heart, and cholesterol in adipose tissue and heart in mice, discovering that those parameters were significantly reduced ($p< 0.05$) due to the effect of chlorogenic acid and caffeic acid when compared with the high-fat control group.[318] Similarly, Huang *et al*. reported comparable outcomes: chlorogenic acid repressed the increase in weights of body and visceral fat and hepatic free fatty acids caused by high-fat diet in male Sprague-Dawley rats.[319] Another study investigated effects of decaffeinated green coffee bean extract for prevention of obesity and improvement in insulin resistance. The results indicated that mice within the group fed with high fat diet supplemented with 0.3% green coffee bean extract (decaffeinated) showed reduced body weight gain and increased plasma lipids, glucose and insulin levels when induced due to the high fat diet. The extract also assisted in down-regulation of genes involved in WNT10b- and galanin-mediated adipogenesis and TLR4-mediated pro-inflammatory pathway. Translocation of GLUT4 to the plasma membrane in white adipose tissue was also stimulated.[320] Hypercholesterolemia often occurs in obesity and leads development of cardiovascular disease and non-alcoholic fatty liver disease. The results of an *in vivo* research performed to demonstrate the hypocholesterolemic and hepatoprotective impacts of chlorogenic acid intake showed that chlorogenic acid is able to reduce the HDL level caused by a hypercholesterolemic diet showing reduced lipid depositions in the liver of hypercholesterolemic rats.[321]

Very recently, an Italian research group investigated the putative protective role that coffee phenolic metabolites may have in counteracting diesel exhaust particles (DEPs)-induced oxidative stress in rat C6 glioma cells.[322] The authors reported that the pre-treatment of cells with two different coffee metabolites mix (0.5 μM Mix 1, 1 μM Mix 2) or 1 μM caffeic acid for 48 h followed by DEP exposure, successfully prevented oxidative stress and cytotoxicity induced by DEP treatment. Notably, ROS

production and cell viability were kept almost at the control's value. The MEK-ERK1/2 pathway is involved in the antioxidant response in C6 glioma cells after DEP exposure, resulting in Nrf2 activation, thus causing an increase in antioxidant enzymes such as HO-1. While the ERK1/2 expression levels did not change significantly following any treatment, authors data suggested that p-ERK2/ERK2 ratio decreased after pre-treatment with coffee phenolic metabolites. Thus, authors claimed that coffee phenolic metabolites can be promising molecules to protect against oxidative stress induced by daily exposure to air pollution generated by motor vehicle traffic.

In 2019, Amano *et al*. used *in vitro* and *ex vivo* profiling assays according to ICH S7A guideline to evaluate the safety of 5-CQA and found that 5-CQA and its metabolites were safe to use and could have beneficial effects as a pharmaceutical[323], however, literature lack a pharmacological safety evaluation of 5-CQA to determine the maximum effective and safe doses of 5-CQA in both animals and humans.

Immunomodulatory effects. Intravenous administration of chlorogenic acid protected C57BL/6 mice from septic shock after intraperitoneal LPS challenge. At the dosage 3 mg/kg chlorogenic acid, the survival rate was increased up to 70%. In addition, the cytokine levels in blood of treated animals were decreased, too. *In vitro*, kinase assays demonstrated that MAPK activation was blocked by chlorogenic acid, as well as auto-phosphorylation of IRAK4. Protein or mRNA levels of TNF-α, IL-1α, and HMGB-1 (high-mobility group box-1) in the peritoneal macrophages, induced by LPS, were also attenuated by CGA treatment.[324]

Chlorogenic acid inhibits staphylococcal exotoxin (SE)-induced inflammatory cytokines and chemokines, e.g., IL-1β, TNF, IL-6, IFN-γ, monocyte chemotactic protein I (MCP-l), macrophage inflammatory protein (MIP)-lα, and MIP-lβ by human peripheral blood mononuclear cells and inhibits SE-induced T-cell proliferation (by 98%)[325].

Notably, among chlorogenic acid-derived catabolites, ferulaldehyde, a ferulic acid catabolite, had been tested in a murine lipopolysaccharide (LPS)-induced septic shock model. When intraperitoneally administered, ferulaldehyde (6 mg/kg every 12 h) prolonged the lifespan of LPS-treated mice, decreasing the inflammatory response (pro-inflammatory cytokines TNF-α and IL-1β), increasing anti-inflammatory IL-10 levels in serum, and inhibiting LPS-induced activation of NF-κB in the liver of the mice.[326]

4.7. Hypothesis

In the previous chapter, we demonstrate for the first time a novel biological activity of green and roasted coffee extracts. In fact, we showed that hydroalcoholic extracts obtained from both unroasted and roasted coffee beans were able to dramatically decrease LPS-induced IFN-β release in human macrophages. In the current chapter, we aimed to elucidate the contribution of 5-CQA, one of the most abundant phytochemicals in coffee extract, to this biological effect. Moreover, we performed mechanistic studies to better explain how chlorogenic acid modulatory effects occur.

4.8. Experimental Design

In the previous chapter, we demonstrated that macrophage-like cells pre-treated with 250 μg/mL GCE showed a diminished LPS-induced IFN-β release. In the following experiments, the concentration of pure 5-CQA used (88.5 μg/mL) reproduce the total concentration of chlorogenic acids present in 250 μg/mL GCE. Also, in an attempt to preliminarily explore the underlying mechanisms of its action, we performed Western blot analyses assessing the capability of 5-CQA to modulate the phosphorylation of IRF-3 and STAT1, two key events occurring before and after IFN-β release, respectively. Additionally, we evaluate 5-CQA capability to counteract the inflammatory cascade that led to NF-κB activation using both stimuli

different from LPS (TNF-α and IL-1β) and different cell models, a macrophage murine cell line (RAW-Blue™) and HEK293 cells expressing the human TLR4 receptor (HEK-Blue™ hTLR4).

4.9. Results

4.9.1. Effect of 5-CQA on THP-1-derived Macrophages (TDM) Viability

Toxicity of coffee extracts on cells was first tested by treating THP-1-derived macrophages (TDM) with increasing concentrations of 5-CQA (10 to 500 µM). After 24 h, cell supernatants were removed, and the remaining cell monolayers were immediately used to assess cytotoxicity via the MTT assay. The integrity of cell morphology before and after treatment was inspected by a light microscope. Treatment effect on cell viability was expressed by setting the percentage of non-treated cells at 100%. As shown in **Figure 23**, viability of cells was generally unaffected.

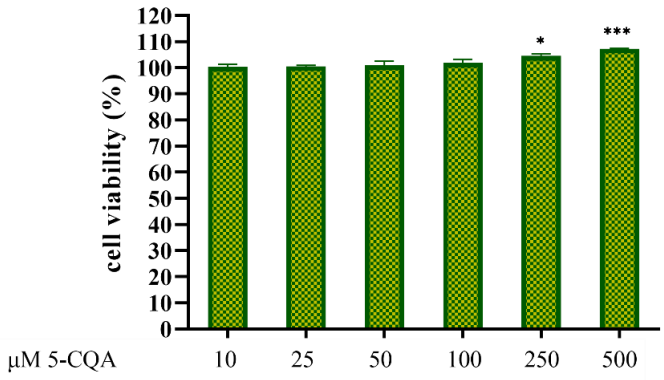

Figure 23. THP-1-derived macrophages viability. THP-1-derived macrophages (TDM) cell viability after treatment with increasing concentrations of 5-CQA (square pattern) was evaluated by MTT assay (24 h). Data are represented as mean ± SEM of three independent experiments (n=3). Results are referred to untreated control (100%) (one-way ANOVA, followed by *post hoc* Dunnett's test *p<0.05, ***p<0.001).

4.9.2. 5-CQA Inhibits IFN-β Release in THP-1-derived Macrophages

TLR4 activation and signalling through the MyD88-independent TRAM/TRIF pathway leads to the activation of TBK1 and IRF-3 thus inducing the IFN-β gene transcription and its subsequent expression. We started from the assumption that, in our experimental conditions: (i) GCE and RCE exhibited the ability to diminish IFN-β release; (ii) the main molecular components of both GCE and RCE are the chemically heterogeneous CGAs, among them 5-CQA is the most abundant isomer. Thus, we perform a comparison between the two extracts (mixtures) and pure 5-CQA. TDM cells were treated with 250 µg/mL GCE, 250 µg/mL RCE and 250 µM 5-CQA (88.5 µg/mL - corresponding to the 5-CQA content in 250 µg/mL GCE). IFN-β release was assessed by monitoring its concentration in cell supernatants collected 3 h after LPS stimulation. As shown in **Figure 24**, although 5-CQA was able to diminish IFN-β release, it seemed to be less effective if compared with GCE and RCE, suggesting an additive or synergistic effect may occur within the mixtures.

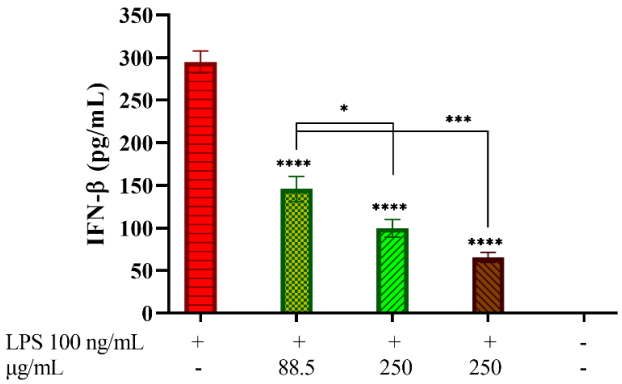

Figure 24. Effect of 5-CQA and coffee extracts on THP-1-derived macrophages release of IFN-β upon LPS stimulation. TDM cells were pre-treated with 88.5 µg/mL 5-CQA (dark green, square pattern), 250 µg/mL GCE (light green, down-up diagonal pattern) and 250 µg/mL RCE (brown, up-down diagonal pattern) for 1 h and then challenged with 100 ng/mL LPS. Cells treated with LPS only served as positive control. Supernatants were collected after 3 h. IFN-β released in the medium was quantified via ELISA. Negative control

(unstimulated cells) is indicated in blue. Data are represented as mean ± SEM of three independent experiments (n=3) (one-way ANOVA, followed by *post hoc* Dunnett's test vs LPS group, ****p<0.0001). Differences between 5-CQA vs GCE and 5-CQA vs RCE were tested using Student's *t*-test and comparison visualized as bars placed above columns (*p<0.05, ***p<0.001).

5-CQA ability to counteract IFN-β release was also investigated in time course experiments, by pre-treating cells with 5-CQA (1h), challenging them with LPS and then collecting supernatant at different time points (0-4 h). Cells treated with LPS only were used as positive control. **Figure 25** shows that LPS-induced IFN-β release started between 1 and 1.5 h and increased up to 4 h. Pre-treatment with 5-CQA dramatically decreases IFN-β release over time.

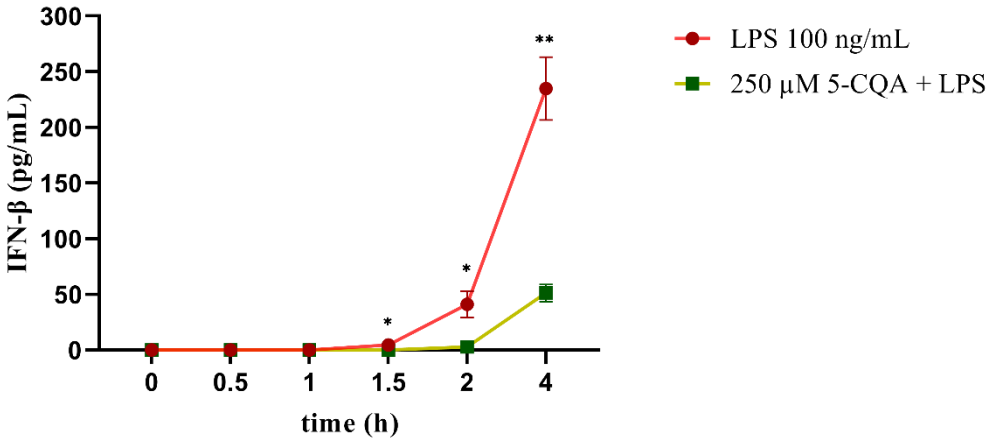

Figure 25. Effect of 5-CQA on THP-1-derived macrophages release of IFN-β upon LPS stimulation. THP-1-derived macrophages (TDM) cells were pre-treated with 250 µM 5-CQA (green squares) for 1 h and then challenged with 100 ng/mL LPS. TDM treated with LPS only are depicted in red circles. Supernatants were collected at different time points (0-4 h). IFN-β released in the medium was quantified via ELISA. Data are represented as mean ± SEM of three independent experiments (n=3) (*t*-test, *p<0.05, **p<0.01).

4.9.3. 5-CQA Effects on IRF-3 and STAT1 Phosphorylation in THP-1-derived Macrophages

Since we observed that 5-CQA pre-treatment results in a dramatic reduction of LPS-induced IFN-β release we asked ourselves two challenging questions: (i) is this a result of a reduced activation of its transcriptional factor IRF-3? (ii) will the IFN-β release reduction have consequences on the canonical IFN signalling? Thus, we performed time course western blot analyses on untreated cells (negative control), cells treated with LPS only (positive control) and cells pre-treated with 250 μM 5-CQA (1h) and subsequently challenged with 100 ng/mL LPS. As shown in **Figure 26**, untreated cells and cells treated with 5-CQA only did not show any activation of IRF-3. Phosphorylated IRF-3 (p-IRF-3) begins to be appreciable after 1 h post LPS stimulation and increased over time reaching a peak at 2 h, before slowing down again. This phenomenon seemed to be not affected by 5-CQA pre-treatment (**Figure 26B**). IFN-β released in the medium can act in both autocrine and paracrine manner activating the JAK-STAT pathway in the cell itself and/or in neighbouring cells. Phosphorylation of STAT-1 triggered by IFN-β recognition started 1.5 h after LPS administration and peaked at 2 h. As expected, cells pre-treated with 5-CQA before receiving LPS showed a less pronounced activation of STAT1, which we conjecture is as a direct consequence of a reduced amount of IFN-β released (**Figure 26C**).

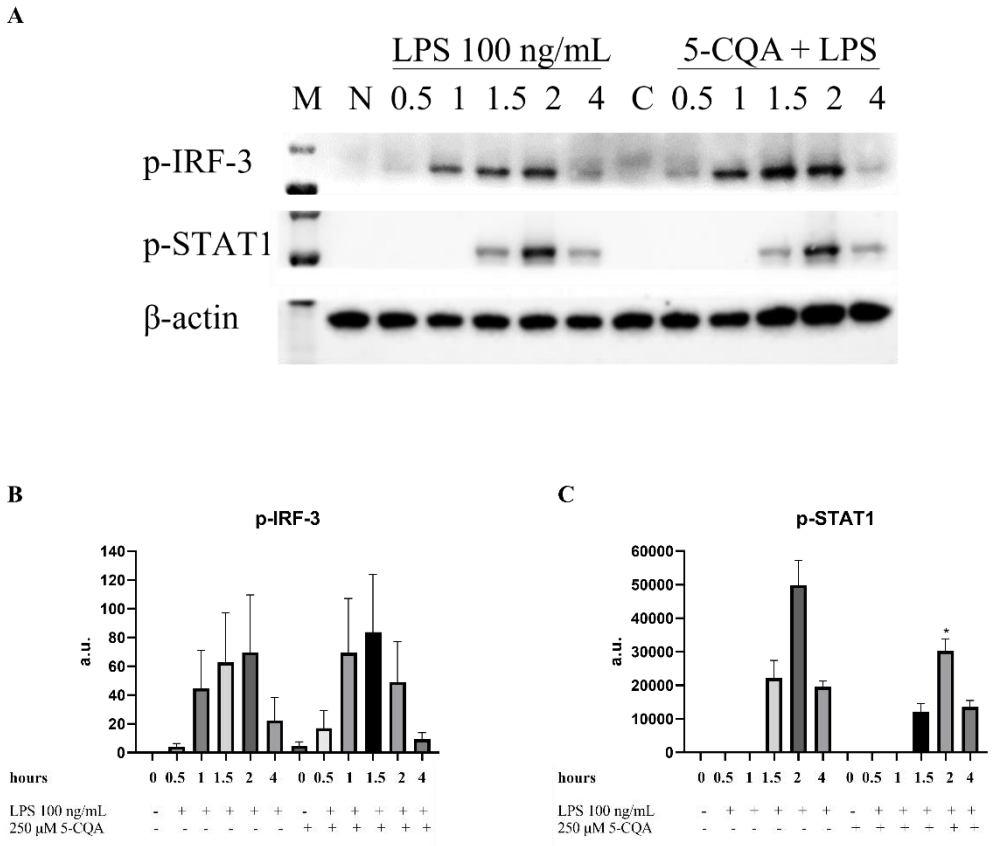

Figure 26. Phosphorylation of IRF-3 and STAT1 in cells treated with 5-CQA and LPS or LPS only. Western blot analyses were performed on the total protein content of untreated cells (negative control), cells treated with LPS only (positive control) and cells pre-treated with 250 μM 5-CQA (1h) and subsequently challenged with 100 ng/mL LPS. Proteins were separated by SDS-PAGE and transferred to a nitrocellulose membrane; membranes were then probed with anti-p-IRF-3 and anti-p-STAT1. β-actin was used to normalize sample loading. A representative membrane is shown (**A**). Densitometric analysis was carried out through ChemiDoc system (Bio-Rad Laboratories), and the quantification of the signal area was performed by ImageJ. Numerical data corresponding to p-IRF-3 and p-STAT1 were normalised on β-actin expression and expressed as arbitrary units. Mean ± SEM of three independent experiments (n=3) are depicted in panel (**B**) and (**C**), respectively. Corresponding groups of data were compared using Student's *t*-test **p*<0.05. M: markers, N: non-treated cells, C: cells treated with 5-CQA only. 0.5-4: time points (h).

4.9.4. 5-CQA Inhibits NF-κB Pathway Downstream to TLR4

To better characterize the biological effects of 5-CQA observed on TDM we perform a transcriptional reporter assay employing THP1-XBlue™ cells (as described in section 3.12). After differentiation into macrophages, cells were treated with increasing concentration of 5-CQA (10-500 μM) and then stimulated with 100 ng/mL LPS. Treatment with LPS result in a prominent release of SEAP as a consequence of NF-κB-driven transcription, while cells treated with 5-CQA only do not exhibit NF-κB activation (**Figure 27A**). On the contrary, pre-treatment of cells with 5-CQA 1 h before the addition of LPS significantly inhibit NF-κB-driven transcription of SEAP in a dose-dependent manner (**Figure 27B**). Two pro-inflammatory stimuli different from LPS and capable of trigger the NF-κB pathway without targeting TLR4 were used, namely the cytokines TNF-α and IL-1β. In fact, although structurally different, Toll-like receptors as well as receptor for TNF-α and IL-1, use similar signal transduction mechanisms that include activation of IkB kinase (IKK) and NF-κB.[327] In both cases, 5-CQA pre-treatment was able to inhibit NF-κB-driven transcription of SEAP causes by both the stimulation with 10 ng/mL TNF-α (**Figure 27C**) and 100 ng/mL IL-1β (**Figure 27D**).

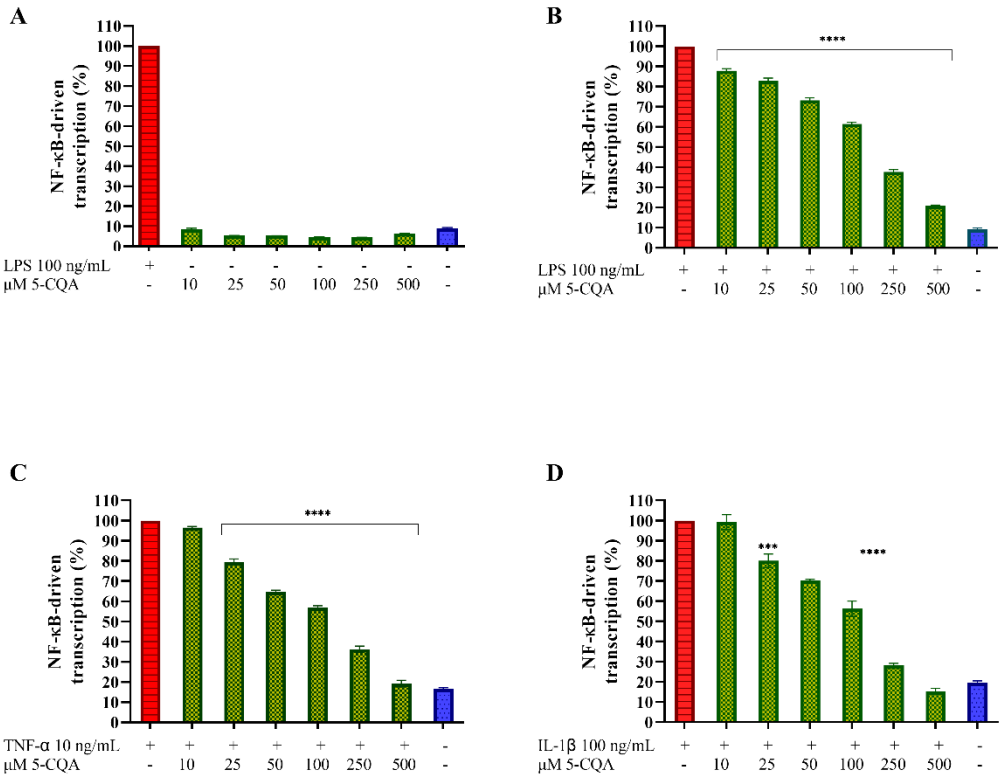

Figure 27. Effect of 5-CQA on THP1-XBlue™-derived macrophages treated with different pro-inflammatory stimuli. (A) THP-1-derived macrophages (TDM) cells treated with increasing concentrations of 5-CQA (dark green, square pattern) for 1 h or challenged with 100 ng/mL LPS. **(B)** TDM cells pre-treated with increasing concentrations of 5-CQA (dark green, square pattern) for 1 h and then challenged with 100 ng/mL LPS. **(C)** TDM cells pre-treated with increasing concentrations of 5-CQA (dark green, square pattern) for 1 h and then challenged with 10 ng/mL TNF-α. **(D)** TDM cells pre-treated with increasing concentrations of 5-CQA (dark green, square pattern) for 1 h and then challenged with 100 ng/mL IL-1β. Activation of NF-κB pathway was assessed by using THP1-XBlue™ cells as a reporter cell line and quantifying the activity of SEAP released in the medium after 18 h. Results are referred to positive control (red, 100%). Negative control (unstimulated cells) is indicated in blue. Data are represented as mean ± SEM of three independent experiments (n=3). Results are referred to untreated control (100%) (one-way ANOVA, followed by *post hoc* Dunnett's test ***p<0.001, ****p<0.0001).

To unveil the role of TLR4, we applied the same experimental setting on murine macrophages RAW-Blue™ that naturally express TLR4, and HEK-Blue™ cells, cells co-transfected with the human TLR4, MD-2 and CD14 co-receptor genes, as well as the inducible SEAP. Our data indicated that 5-CQA weakly inhibited LPS-stimulated NF-κB activation in murine macrophages (**Figure 28A**) and was totally inactive in HEK-Blue™-hTLR4 cells (**Figure 28B**).

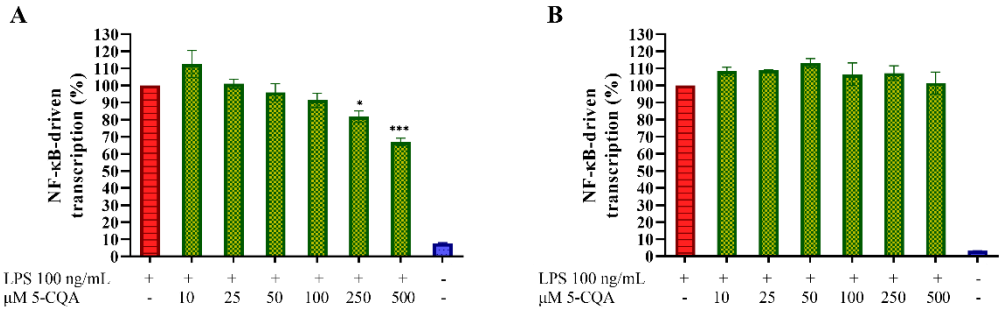

Figure 28. Effect of 5-CQA on LPS-stimulated RAW-Blue™ and HEK-Blue™ cells. (A) RAW-Blue™ cells treated with increasing concentrations of 5-CQA (dark green, square pattern) for 1 h or challenged with 100 ng/mL LPS. **(B)** HEK-Blue™ cells pre-treated with increasing concentrations of 5-CQA (dark green, square pattern) for 1 h and then challenged with 100 ng/mL LPS. Activation of NF-κB pathway was assessed by using RAW-Blue™ or HEK-Blue™ cells as a reporter cell line and quantifying the activity of SEAP released in the medium after 18 h. Results are referred to positive control (red, 100%). Negative control (unstimulated cells) is indicated in blue. Data are represented as mean ± SEM of three independent experiments (n=3). Results are referred to untreated control (100%) (one-way ANOVA, followed by *post hoc* Dunnett's test *p<0.05, ***p<0.001).

4.10. Discussion

To discover the bioactive component of coffee extracts responsible for the previously denoted immunomodulatory activity (Chapter I), we performed experiments on TDM using pure 5-CQA. Results shown the capability of 5-CQA to counteract IFN-β release upon LPS stimulation (0-4h), clearly indicating its involvement in the biological effect exerted by coffee extracts. However, pure 5-CQA was less effective in diminishing IFN-β compared to GCE or RCE total extract. A further characterization of the mechanism of action of 5-CQA was performed involving the use of different cell reporter assays. Human macrophages obtained from the differentiation of THP1-XBlue™ cells shown the ability of 5-CQA to inhibit the activation of the NF-κB pathway not only upon stimulation with LPS, but also with inflammatory stimulus different from LPS, TNF-α and IL-1β, which recognition and initiation of the signalling is independent from TLR4, thus suggesting that the molecular target of this compounds belong to the inflammatory cascade downstream to TLR4. This behaviour was observed, even if to a less extent, also in murine RAW-Blue™ macrophages. The observation that 5-CQA is inactive in inhibiting the LPS-triggered NF-κB pathway in HEK-Blue™-hTLR4 cells also imply that the molecular target of this compound is not the membrane TLR4/MD-2 complex but another intracellular protein involved in inflammatory response, with a cell-type-specific effect on innate immune cells. Notably, whereas TBK1 is expressed in a wide variety of tissues, IKKi expression is restricted to immune cells and is further upregulated in response to various stimuli, including LPS, TNF-α, IL-1β, IFN-γ and IL-6.[328] Moreover, IKKi functions not only as an IRF-3 kinase but also as a STAT1 kinase. In fact, IKKi can phosphorylate a serine residue in STAT1 that is crucial for its transcriptional activity. We noted that 5-CQA pre-treatment did not resulted in a reduced phosphorylation of IRF-3, while p-STAT1 level at its peak was diminished. Together, these observations open interesting perspectives for the investigation of the role of IKKi and its related downstream signalling in 5-CQA mechanism of action. TLR4 recognition of lipopolysaccharide (LPS) from bacteria

is the most potent type I IFN inducer, signalling through the adaptor protein TIR-domain-containing adaptor protein inducing IFNβ (TRIF).[329] Numerous studies investigated the role of type I IFN in the immunopathology of autoimmune and inflammatory diseases (reviewed in[71]). Qin and colleagues, indicate that direct LPS induction of NF-κB activation and LPS-induced production of IFN-β, which subsequently activates STAT-1α, are important events for CD40 gene expression in macrophages and microglia.[330] In addition, the partial inhibition of LPS-induced CD40 expression on inclusion of IFN-β–neutralizing antibody demonstrates the importance of this signalling pathway in CD40 gene expression. In this perspective the possibility to modulate IFN-β secretion by chlorogenic acid could be beneficial in those autoimmune inflammatory diseases that share aberrant expression of CD40, such as multiple sclerosis and rheumatoid arthritis.

CHAPTER III

Palmitoylethanolamide: A Natural Body-Own Anti-Inflammatory Agent

Adapted from:

D'Aloia, A.; Molteni, L.; Gullo, F.; Bresciani, E.; **Artusa, V.**; Rizzi, L.; Ceriani, M.; Meanti, R.; Lecchi, M.; Coco, S.; Costa, B.; Torsello, A. Palmitoylethanolamide Modulation of Microglia Activation: Characterization of Mechanisms of Action and Implication for Its Neuroprotective Effects. *Int. J. Mol. Sci*. **2021**, 22, 3054. https://doi.org/10.3390/ijms22063054 - Appendix II

D'Aloia, A.; Arrigoni, F.; Tisi, R.; Palmioli, A.; Ceriani, M.; **Artusa, V.**; Airoldi, C.; Zampella, G.; Costa, B.; Cipolla, L. Synthesis, Molecular Modeling and Biological Evaluation of Metabolically Stable Analogues of the Endogenous Fatty Acid Amide Palmitoylethanolamide. *Int. J. Mol. Sci.* **2020**, 21, 9074. https://doi.org/10.3390/ijms21239074 - Appendix III

4.11. Background

Since a decade, *N*-acylethanolamines (NAEs), both as saturated fatty amides and as poly-unsaturated forms, are found to play an important physiological role in the modulation of immune reactions in several autoimmune disorders via a number of different receptors. Among this class of compounds, we must mention: (i) *N*-arachidonoyl-ethanolamine (anandamide, AEA), the first endocannabinoid that was discovered; (ii) the anorectic mediator *N*-oleoyl-ethanolamine (OEA); (iii) *N*-palmitoyl-ethanolamine (PEA) (depicted in **Figure 29**).[331]

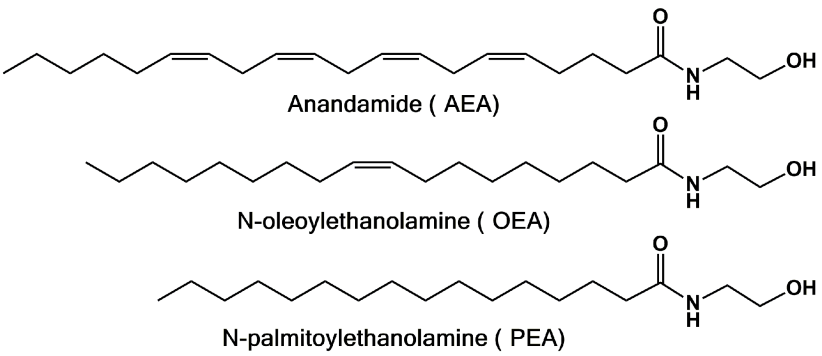

Figure 29. Chemical structures of some of the most studied bioactive *N*-acyl-ethanolamines (NAEs).[331]

One of them, worth of particular attention is palmitoylethanolamide (PEA), an endogenous fatty acid amide with the chemical structure of *N*-(2-hydroxyethyl)-esadecanamides. PEA is a food component known since 1957.[332] In that year, Kuehl and colleagues succeeded in isolating a crystalline anti-inflammatory factor first from soybean lecithin and then also from a phospholipid fraction of egg yolk and from hexane-extracted peanut meal.

The crystalline material had a melting point of 98-99°C and was described as neutral, optically inactive, and possessing the chemical formula $C_{18}H_{37}O_2N$, which hydrolysis resulted in palmitic acid and ethanolamine. Kuehl *et al*. further analysed the anti-inflammatory activity of several derivatives of PEA and could prove that the basic moiety of the molecule was responsible for its anti-inflammatory activity.[332] Pea was then found in a wide variety of food sources (recently summarised by Petrosino and Di Marzo,[333] **Table 2**).

Table 1. PEA content in different food sources.[333]

Food source	Concentration of PEA ($ng \cdot g^{-1}$ fresh weight)	Reference
Bovine milk	0.25	Gouveia-Figueira and Nording, 2014
Elk milk	1.81	Gouveia-Figueira and Nording, 2014
Human breast milk	8.98 ± 3.35 nmol·L^{-1}	Lam *et al.*, 2010
Human breast milk (110 ± 32.3 lactation days)	23.4 ± 7.2 nmol·L^{-1}	Schuel *et al.*, 2002
Common bean (*Phaseoulus vulgaris*)	53.5	Venables *et al.*, 2005
Garden pea (Pisum sativum)	100	Venables *et al.*, 2005; Kilaru *et al.*, 2007
Southern or blackeyed peas (Vigna unguiculata)	138	Venables *et al.*, 2005
Tomato	100	Kilaru *et al.*, 2007
Medicago sativa	1150	Venables *et al.*, 2005
Corn	200	Kilaru *et al.*, 2007
Soybean (Glycine max)	6700	Venables *et al.*, 2005; Kilaru *et al.*, 2007
Soy lecithin	950 000	Kilaru *et al.*, 2007
Peanut (Arachis hypogaea)	3730	Venables *et al.*, 2005; Kilaru *et al.*, 2007

In animals, the biosynthesis of PEA occurs through the hydrolysis of its direct phospholipid precursor, *N*-palmitoyl-phosphatidyl-ethanolamine, by the action of *N*-acyl-phosphatidyl-ethanolamine-selective phospholipase D (NAPE-PLD) (**Figure 30A**). The degradation of PEA to palmitic acid and ethanolamine occurs by the action of two different hydrolytic enzymes, that is, fatty acid amide hydrolase (FAAH) and, more specifically, *N*-acylethanolamine-hydrolysing acid amidase (NAAA) (**Figure 30A**).

Interestingly, the biosynthesis and degradation of PEA, as well as other *N*-acylethanolamines, in plants, where these compounds exert quite different physiological functions, seem to occur via identical routes and often similar enzymes.[333] PEA exerts a multitude of physiological functions related to metabolic and cellular homeostasis. It is an interesting anti-inflammatory therapeutic substance and might also hold great promise for the treatment of several (auto)immune disorders, including inflammatory bowel disease and inflammatory diseases of the central nervous system (CNS).[334,335] Several efforts have been made to identify the molecular mechanism of action of PEA and explain its multiple effects both in the central and the peripheral nervous system. Nobel laureate Rita Levi-Montalcini's clarified PEA's mechanism of action, analysing the role of PEA as an anti-inflammatory agent. In fact, Rita Levi-Montalcini's research group suggested that PEA acts via 'Autacoid Local Injury Antagonism (ALIA)' to down-regulate mast cell activation.[336] Further research has revealed that PEA can act via multiple mechanisms, depicted in **Figure 30B–E**).[337] The anti-inflammatory effects of PEA have also been investigated in numerous inflammatory *in vitro* and *in vivo* models. In 2009, Hoareau *et al*. investigate the anti-inflammatory effect of PEA on human adipocytes, as well as in a murine model.[338] TNF-α production by LPS-treated human subcutaneous adipocytes in primary culture and CF-1 mice, an ideal *in vivo* infectious disease model, was investigated by enzyme-linked immunosorbent assay. The effects of PEA on adipocyte TNF-α secretion were explored as well as some suspected PEA anti-inflammatory pathways: the NF-κB pathway, PPAR-α gene expression, and TNF-α-converting enzyme (TACE) activity. The effects of PEA on the TNF-α serum concentration in intraperitoneally LPS-treated mice were also studied. They demonstrate that the LPS induced secretion of TNF-α by human adipocytes is inhibited by PEA. This action is neither linked to a reduction in TNF-α gene transcription nor to the inhibition of TACE activity. Moreover, PPAR-α is not implicated in this anti-inflammatory activity. Lastly, PEA exhibits a wide-reaching anti-inflammatory action as the molecule can completely inhibit the strong

increase in TNF-α levels in the serum of mice treated with high doses of LPS. In 2015, Impellizzeri and colleagues investigate the effects of PEA, in rats subjected to LPS-induced uveitis.[339] PEA treatment decreased the inflammatory cell infiltration and improved histological damage of eye tissues. In addition, PEA treatment reduced pro-inflammatory TNF-α levels, protein extravasation and lipid peroxidation. Immunohistochemical analysis showed ICAM-1 and nitrotyrosine was significantly reduced in eye sections from LPS-injected rats treated with PEA. In addition, PEA strongly inhibited iNOS expression and nuclear NF-κB translocation.

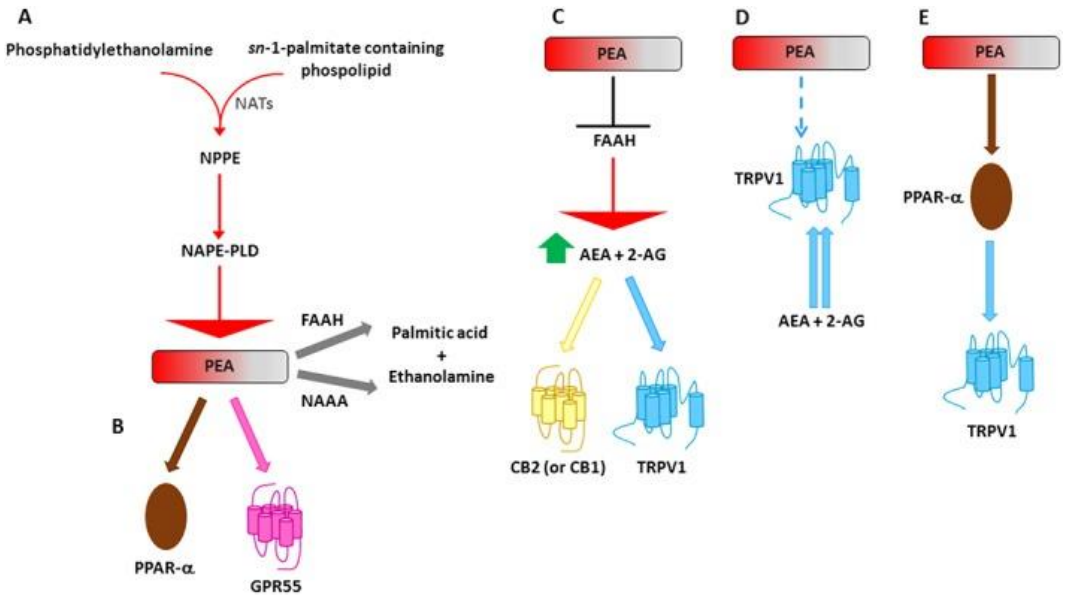

Figure 30. Metabolic pathways and molecular targets of PEA. (**A**) PEA is biosynthesized from a membrane phospholipid, *N*-palmitoylphosphatidylethanolamine (NPPE), via several routes, the most investigated of which is through the direct hydrolysis by NAPE-PLD. PEA can be then degraded to palmitic acid and ethanolamine by either FAAH or NAAA. (**B**) PEA can directly activate PPAR-α or, more controversially, GPR55. (**C**) PEA, for example through the inhibition of the expression of FAAH, may increase the endogenous levels of AEA and 2-AG, which directly activate CB2 (or CB1) receptors and TRPV1 channels (entourage effect). (**D**) PEA, possibly through an allosteric modulation of TRPV1 channels, potentiates the activation and desensitization by AEA and 2-AG of TRPV1 channels (entourage effect). (**E**) PEA may also activate TRPV1 channels via PPAR-α. NAT, N-acyl-transferase.[333]

Inflammation is a key element in the pathobiology of neurodegenerative diseases. Different neuronal and non-neuronal cells are involved as players able to respond to inflammatory signals of immune origin. Among them, microglial cells, parenchymal tissue-resident macrophages resident in the central nervous system, plays a central role in mediating tissue homeostasis in health and disease.[340] Microglia are characterized by morphological features that reflect their functional capacity. In a healthy brain, microglia are in a quiescent state, or have a "down-regulated" phenotype, and exhibit a ramified shape, with short fine processes and thus increased surface area for tissue surveillance.[341] This down-regulated phenotype is characterized by an attenuated innate immune function correlated with homeostatic tissue remodelling and steady-state wound healing functions.[342] Early in disease progression, microglial cells develop an altered inducible "activated" state that is functionally different from steady-state microglia. This activated state is then further subdivided into a classical pro-inflammatory M1 and alternative M2 state. Same as peripheral macrophages, *in vitro* studies demonstrate that M1 and M2 activation can be induced in microglia by LPS and IL-4, respectively.[343,344] Morphologically, activated microglia exhibit an amoeboid shape in contrast to the quiescent ramified shape of steady-state microglia.[345] In the brain, infiltrating monocyte-derived macrophages promote nodal demyelination[90,346] and exhibit a highly phagocytic and inflammatory behaviour, while resident microglia, required for the initiation of disease, are relatively quiescent upon disease onset[347]. Lipopolysaccharide (LPS) is widely known to induce potent neuroinflammatory responses in the brain.[348] In 2020, an *in vitro* study was performed on different neuronal (SH-SY5Y) and non-neuronal cell lines (C6, BV-2, and Mo3.13) subjected to NAAA enzyme silencing and then treated with PEA ultra-micronized (PEA-um) (1, 3, and 10 μM).[349] Results showed that concomitant treatment of neuronal and non-neuronal cells with PEA-um, after NAAA genic downregulation, successfully counteracted LPS/INF-γ-provoked neuroinflammation without affecting cell viability.

4.12. Hypothesis

Microglia-mediated inflammatory response is associated with the majority of neurodegenerative conditions. PEA is licensed for use in humans as nutraceutical, food supplement, or food for medical purposes for its analgesic and anti-inflammatory properties demonstrating efficacy and tolerability. However, exogenously administered PEA is rapidly inactivated by fatty acid amide hydrolase (FAAH) enzyme, that plays a key role both in hepatic metabolism and in intracellular degradation. Costa's research group extensively investigated PEA pharmacological activity in pain perception and inflammatory diseases.[350–356] Recently they conducted a study where they synthetized a small library of PEA analogues designed to be more resistant to FAAH-mediated hydrolysis. Molecular docking and density functional theory calculations were applied to find the more stable analogue. The computational investigation identified RePEA as the best candidate in terms of both synthetic accessibility and metabolic stability to FAAH-mediated hydrolysis. The selected compound was synthesized and assayed *ex vivo* to monitor its enhanced resistance to FAAH-mediated hydrolysis. ^{1}H-NMR spectroscopy performed on membrane samples containing FAAH in integral membrane protein demonstrated that RePEA is not processed by FAAH, in contrast with PEA. Moreover, RePEA retained PEA's ability to inhibit LPS-induced cytokine release in murine N9 microglial cells. The rationale for our study was to examine the role of PEA and its analogue RePEA in the regulation of pro-inflammatory cytokines released by LPS-challenged macrophages. The ultimate goal was obtaining a comparison between the effect of PEA and its analogue RePEA on microglial cells and on macrophage cells.

Later, they explored the possibility that PEA could exert its neuroprotective and anti-inflammatory effects through the modulation of microglia reactive phenotypes. They found that in N9 microglial cells, the pre-incubation with PEA blunted the increase of LPS-induced M1 pro-inflammatory markers, concomitantly increasing M2 anti-inflammatory markers. They also acquired and processed microglial cells images to

obtain a set of morphological parameters that can be used to distinguish different phenotypes. They found that PEA is able to inhibit the LPS-induced M1 polarization and suggested that PEA might induce the anti-inflammatory M2a phenotype. Microglia function strongly relies on intracellular calcium signalling. PEA prevented Ca^{2+} transients in both N9 cells and primary microglia and antagonized the neuronal hyperexcitability induced by LPS, as revealed by multi-electrode array (MEA) measurements on primary cortical neurons, microglia, and astrocytes. Since LPS is a TLR4 ligand, we thought it could be interesting to obtain further insight about the role of the TLR4/NF-κB axis in the previously observed PEA-induced inhibition of pro-inflammatory cytokines. Thus, our contribute to this work consisted in the investigation of the putative effects of PEA on the NF-κB activation triggered by TLR4 stimulation in human macrophage-like cells obtained from the *in vitro* differentiation of THP1-XBlue™ cells. Moreover, we employed HEK-Blue™-hTLR4 cells as a tool to investigate whether PEA acts involving TLR4 directly.

4.13. Experimental Design

THP-1 and THP1-XBlue™ cells were differentiated into macrophage-like cells (as described in section 3.5.), referred as PMA-THP-1 and PMA-THP-1 X-Blue™ cells, correspondingly. Cells were treated with PEA and/or RePEA and cytotoxicity was assessed via MTT assay. Then, cells were challenged with LPS, either before or after PEA/RePEA administration (sections 3.10. and 3.11.). Supernatant concentration of different pro-inflammatory cytokines, and also SEAP (as a result of its NF-κB-driven transcription), were measured by ELISA and SEAP assay, respectively. SEAP released by LPS-stimulated HEK-Blue™-hTLR4 cells pre-treated with PEA was also assessed.

4.14. Results

4.14.1. PEA and RePEA Post-treatment Effects on Cell Viability and NF-κB Activation in Human Macrophages

As PEA and its analogue RePEA are intended to be used on human beings, we executed the same experiments previously performed on murine microglial cells (N9) on macrophage-like cells of human origin. First, cell viability was assessed at 24 h. Results showed that both PEA and RePEA were not cytotoxic (**Figure 31B**). To further explore the role of the TLR4/NF-κB axis in the previously observed inhibition of pro-inflammatory cytokines, NF-κB activation triggered by TLR4 stimulation was investigated using THP-1 X-Blue™-derived macrophages (PMA-THP-1 X-Blue™ cells) as a tool to investigate whether PEA and/or RePEA act involving TLR4 directly. Cells were treated as described in section 3.10. As shown in **Figure 31A** both PEA and RePEA were able to inhibit NF-κB activation triggered by TLR4 stimulation. RePEA was more effective in decreasing SEAP release compared with its parent compound PEA, 50% versus 30%, respectively.

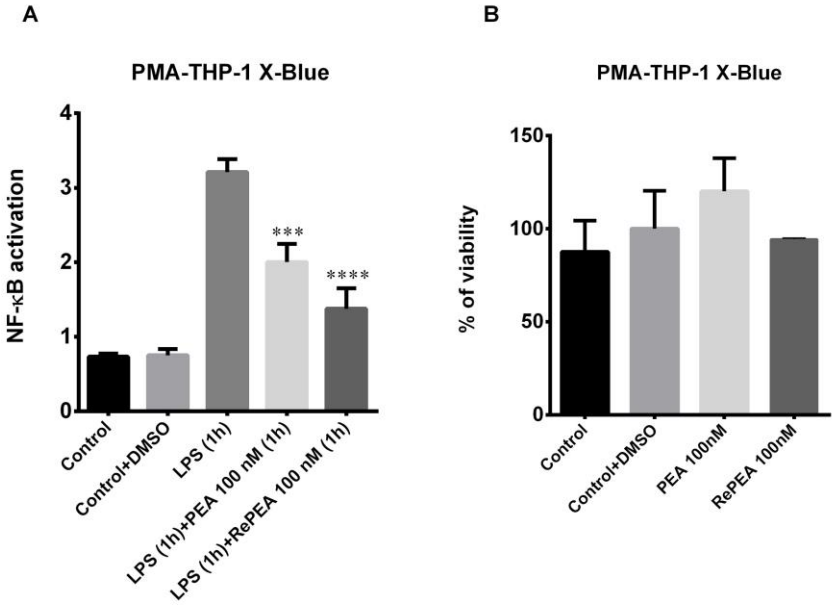

Figure 31. PEA and RePEA effect on cell viability and NF-κB activation. (**A**) PMA-THP-1 X-Blue™ cells were challenged with 10 ng/mL LPS for 1 h; then, the LPS-containing medium was removed, and cells were incubated for 1 h with 100 nM PEA and RePEA, respectively. Then, the medium was replaced with fresh RPMI. The amount of SEAP (Secreted Embryonic Alkaline Phosphatase) released into the culture medium was quantified after 24 h as a measure of NF-κB activation. Data are presented as mean ± SEM (n = 3 independent experiments), normalized on MTT data (the activity of SEAP, expressed as OD, was normalized on the MTT OD value of each corresponding well, as a measure of cell viability). Differences between treated groups (PEA and RePEA) and the positive control (LPS) were determined using nonparametric one-way analysis of variance (ANOVA) with *post hoc* Dunnett's multiple comparison tests. *** $p < 0.001$, **** $p < 0.0001$. (**B**). PMA-THP-1 X-Blue™ cells were incubated for 1 h with 100 nM PEA and RePEA. Then, medium was replaced with fresh RPMI. Cell viability was assessed after 24 h. Data are presented as mean ± SEM (n = 3 independent experiments).

4.14.2. PEA and RePEA Post-treatment Effect on Pro-inflammatory Cytokines Release in Human Macrophages

Furthermore, PEA and RePEA ability to counteract TNF-α release was evaluated. LPS markedly induce TNF-α release in PMA-THP-1 cells. Both PEA and RePEA showed to be effective in reducing TNF-α content in supernatants after LPS stimulation. Notably, RePEA was more efficient in inhibiting TNF-α release compared to PEA, corroborating previously obtained data on NF-κB activation assessment (**Figure 32A**). These results support the hypothesis that RePEA is slower hydrolysed by FAAH. Finally, other cytokines associated with microglial activation have been measured, specifically IL-6 and IL-1β. PEA and RePEA treatment after LPS challenge significantly decreased IL-6 release, compared with LPS only (**Figure 32B**). RePEA only was able to diminish IL-1β release (**Figure 32C**). These results were closely related with those obtained using N9 cells.

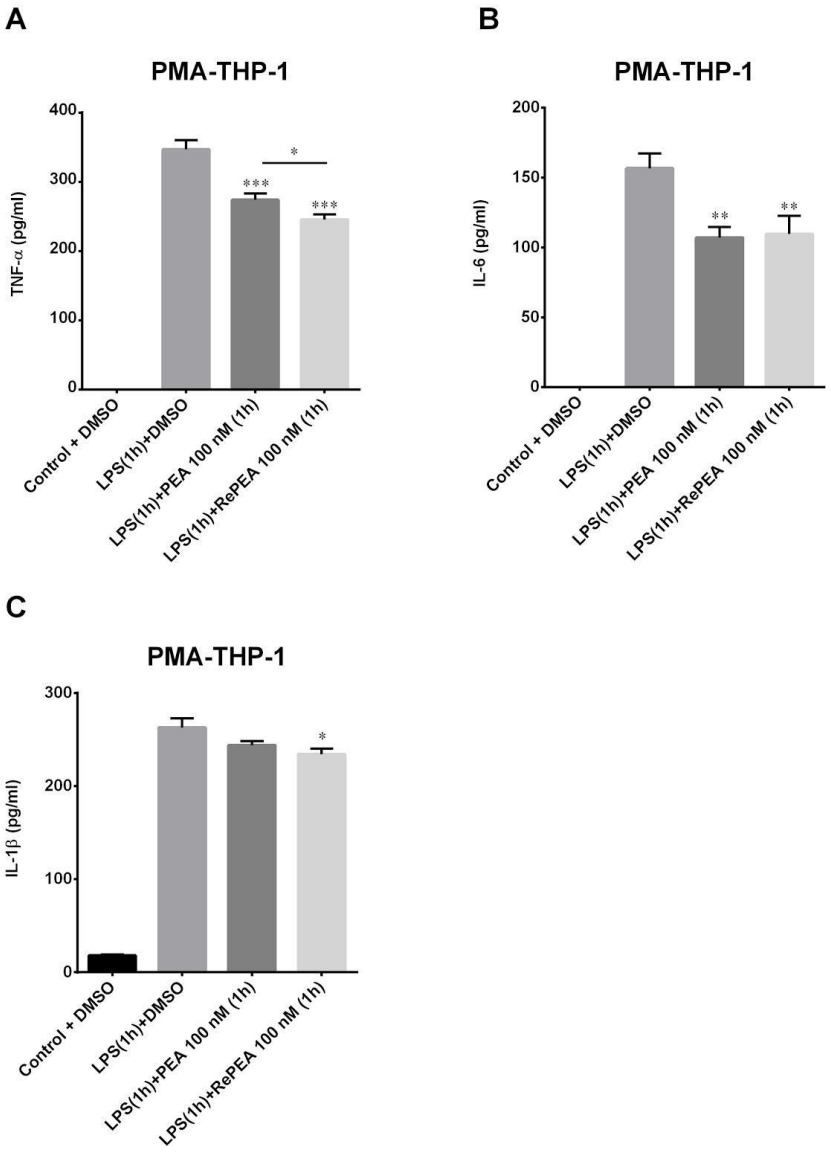

Figure 32. TNF-α, IL-6, and IL-1β release after 24 h post LPS administration. Human macrophage-like cells (PMA-THP-1) were stimulated with 10 ng/mL LPS for 1 h; then, LPS-containing medium was removed, and cells were incubated for an additional 1 h with 100 nM PEA and its analogue, RePEA. Next, medium was replaced with fresh RPMI. The amount of TNF-α (**A**), IL-6 (**B**), and IL-1β (**C**) released in the medium was quantified after 24 h post LPS administration. Data are presented as mean ± SEM (n = 3 independent experiments). Differences between treated groups (PEA and RePEA) and the positive control (LPS) were determined using nonparametric one-way analysis of variance (ANOVA) with *post hoc* Dunnett's multiple comparison tests. * $p < 0.05$; ** $p < 0.01$; *** $p < 0.001$. Difference between PEA and RePEA treatment was determined using unpaired *t*-test * $p < 0.05$.

4.14.3. PEA Pre-treatment Counteracts LPS-Induced NF-κB Activation in Human Macrophages Without Directly Involving TLR4

PEA pre-treatment was showed to inhibit LPS-triggered M1 pro-inflammatory markers (including iNOS, IL-1β, TNF-α, IL-6 and MCP-1), concomitantly increasing M2 anti-inflammatory markers (Arg-1 expression), thus inducing an M2a anti-inflammatory phenotype in murine microglial cell (N9).[357] Hence, we investigated PEA effect on NF-κB activation triggered by TLR4 stimulation in human macrophages. PMA-THP1-XBlue™ cells were pre-incubated with 100 µM PEA (1h) before administering 10 ng/mL LPS. As shown in **Figure 33A**, SEAP expression significantly decreased (40%) in human macrophages when cells are pre-treated with PEA, compared to cells treated with LPS only. Thus, PEA is not only capable to inhibit NF-κB activation if administered after LPS (section 4.14.1.), but also if it is added before LPS stimulation occur in THP-1-derived macrophages.

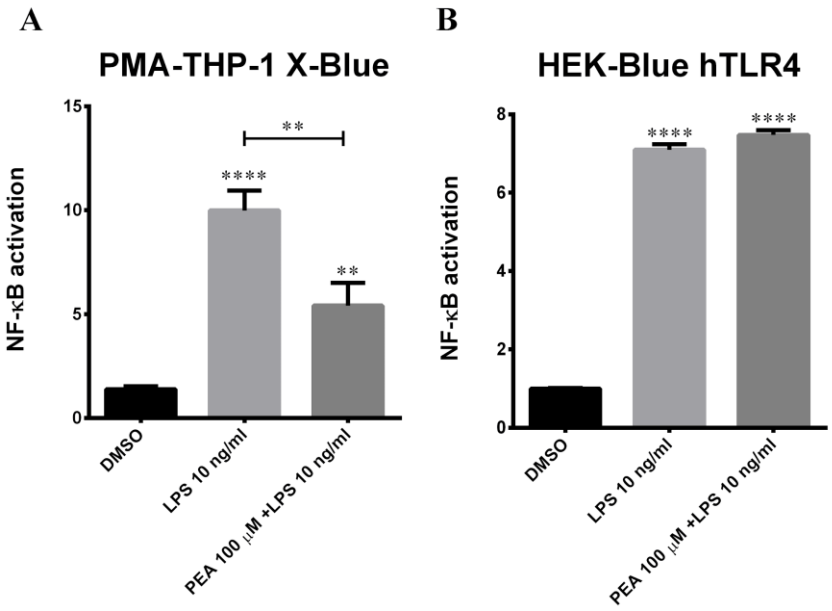

Figure 33. PEA pre-treatment effect on NF-κB activation in LPS-stimulated PMA-THP1-XBlue™ and HEK-Blue™-hTLR4 cells. PMA-THP1-XBlue™ (**A**) and HEK-Blue™-hTLR4 (**B**) cells were incubated with 100 µM PEA (1h) before treatment with 10 ng/mL LPS. The amount of SEAP released in the medium was quantified 6h later as a measure of NF-κB activation. Data are presented as mean ± SEM (n = 3 independent

experiments) normalized on the control sample. Differences between groups were evaluated applying the ANOVA test and Tukey's test for *post hoc* analysis. ** $p < 0.01$, **** $p < 0.0001$.

To assess whether TLR4 is directly involved in PEA mechanism of action, we investigated NF-κB activation in HEK-Blue™-hTLR4 cells. Results indicated that PEA pre-treatment did not affect NF-κB activation induced by LPS (**Figure 33B**). Taken together, our findings suggested that PEA is able to inhibit NF-κB activation triggered by LPS administration in human macrophages, but this effect is not mediated by its direct interaction with TLR4. Further experiments suggested a partial involvement of CB2R in the PEA mechanism of action. Briefly, SR144528, a selective CB2R inverse agonist, significantly reduced the ability of PEA to inhibit LPS stimulation of iNOS expression in N9 cells. Similarly, SR144528 was able to antagonize PEA capability to shift the morphology of N9 cells treated with LPS from the M1 to M2 shape.[357]

4.15. Discussion

Nowadays, *N*-palmitoyl-ethanolamine (PEA) is recognized worldwide for its efficient anti-inflammatory and analgesic effects in experimental models of visceral, neuropathic, and inflammatory diseases, acting through several possible mechanisms.[333] However, so far scarce experimental data have been reported about PEA's use in animals, or particularly, humans. PEA naturally occur in several food sources. Moreover, under inflammatory and neurodegenerative conditions, it can be produced as a "on-demand" protective endogenous mediator to counteract inflammation, neuronal damage, and pain itself. Our collaborators in Costa's research group deeply investigate PEA potential as an anti-inflammatory drug in several *in vitro* models of neuroinflammation induced by LPS and ATP. The aim of our work was employing our well-established human macrophage-like cell models to prove or disprove the hypothesis that PEA could act similarly on human macrophages. Our results demonstrated that: (i) both PEA and RePEA post-treatment were able to inhibit NF-κB activation triggered by TLR4 stimulation; (ii) PEA post-treatment decreased TNF-α and IL-6 release, while RePEA post-treatment significantly inhibited TNF-α, IL-6 and IL-1β release, also; (iii) RePEA seemed to be more effective compared with its parent compound PEA, suggesting a slower degradation rate caused by FAAH; (iv) PEA can counteract NF-κB activation also if it is added before LPS stimulation occur; (v) PEA capability to interfere within the TLR4/NF-κB axis is not attributable to a direct interaction between PEA and TLR4. Our results contributed to unravel PEA mechanism of action in human macrophages. Moreover, we reported the *in vitro* evaluation of the biological activity of a newly synthetized PEA analogue, RePEA. Although the specific mechanism of action and the *in vivo* evaluation of its metabolic stability need further investigation, RePEA could represents a good candidate for pre-clinical studies aiming at developing a drug with the same well-known therapeutic properties of PEA but with a better pharmacokinetic profile.

5. CONCLUSIONS

Toll-Like Receptor 4 (TLR4) plays a key role in the host defence mechanism and can recognize a variety of PAMPs and DAMPs. On the other hand, any dysregulation of the TLR4 pathway can initiate various diseases. The inhibition of TLR4 by a small-molecule can be achieved by blocking (1) ligand-receptor interaction, (2) dimerization of the TLR4-MD2 complex, or (3) downstream signalling. Botanical extracts present a large source of natural immune modulators, many of which have been used in traditional medicine for centuries. At the intersection between nutrition and immunomodulation, plant extracts turned out to be a promising source of new therapies directed toward TLR-related diseases. Goal of the present work is to contribute with new insights on innate immunity modulation by natural compounds. Intake of coffee is hypothesized to reduce the risk of several chronic diseases, but current scientific evidence is not conclusive. Also, the health effects of consuming chlorogenic acid have been studied but its exact mechanism of action is yet to be elucidated. In our study, we investigated the capability of coffee extracts to counteract LPS-induced inflammation employing different cell-based assays. After a chemical characterization of both green (GCE) and roasted (RCE) coffee extracts, we tested their ability to inhibit the release of pro-inflammatory cytokines and interferons by human macrophages. We found that GCE and RCE pre-treatment were effective in mildly modulate the MyD88-dependent pathway downstream of TRL4 LPS recognition, resulting in a reduced NF-κB activation and a lower release of TNF-α, IL-6 and IL-1β, in THP-1-derived macrophages. Then, we focused our attention on the TLR4/TRIF/IRF axis. We reported here the unprecedented observation that GCE and RCE pre-treatment dramatically inhibited IFN-β release, in a dose-dependent manner. Thus, we explored GCE and RCE intracellular effects and we observed that both extracts could reduce LPS-triggered IRF-3 nuclear

translocation, the latter being the main transcriptional factor responsible for IFN-β expression. Subsequently, the same experimental setting was carried out employing primary human macrophages, derived from the *in vitro* differentiation of $CD14^+$ monocytes isolated from human peripheral blood. In this conditions, macrophage-like cells pre-treated with GCE or RCE and then challenged with LPS exhibited a lower IFN-β release, paralleling the results obtained using THP-1-derived macrophages. This observation could bring interesting information for a translational point of view. Moreover, IFN-β release inhibition by coffee extracts parallels with the activity of their main phytochemical component, 5-CQA, thus suggesting that this compound is involved in the immunomodulatory effect observed. Further experiments, aiming at clarifying the molecular mechanism of 5-CQA, revealed that 5-CQA was able to modulate NF-κB-driven transcription triggered not only by LPS stimulation, but also upon TNF-α and IL-1β administration. Additionally, 5-CQA pre-treatment counteracted LPS-induced NF-κB activation in murine macrophages. On the contrary 5-CQA was not effective in HEK cells expressing human TLR4. This observation led us to conclude that 5-CQA molecular target it is not TLR4 itself but, instead, could be an effector molecule downstream of TLR4 shared by both human and murine immune cells. Additionally, we provided the results of western blot analyses that showed 5-CQA pre-treatment did not resulted in a reduced phosphorylation of IRF-3, but rather in a variation of p-STAT1 level at its peak. Taken together, our insights on 5-CQA bioactivity will complement the information currently available[310], offering new perspectives for considering 5-CQA as a preclinical drug candidate, functional food additive, and natural health promoter. Additionally, our work carried out in tandem with the pharmacologists of our department, highlighted how chemical modification of a natural compound could improve its biological activity. It has been observed that RePEA, a PEA analogue rationally designed to be more resistant to FAAH-mediated degradation, was more effective than PEA in modulating macrophage and microglial activity. Moreover, we provided additional information about PEA mechanism of action, demonstrating that

do not directly involve TLR4. To summarize, we demonstrate PEA capability to modulate human macrophage activation triggered by LPS, corroborating previous data obtained using murine microglial cells.

In conclusion, two important considerations should be addressed. First, it should be pointed out that in case of natural products, health benefits are actually related to synergic effects of the whole matrix as opposed to individual substances or classes of compounds. Hereby, not only synergistic but also additive effects were observed.[358] In our case, coffee extracts immunomodulatory effects likely rely not only on the presence of 5-CQA but also on the synergistic effect with other bioactive compounds. Second, some might doubt the physiological relevance of a direct treatment of macrophages with food-derived extracts without considering their pharmacokinetic and metabolic transformation in the body. Regarding this aspect, recent literature provided more in-depth knowledge about the absorption and bioavailability process, pharmacokinetic activity and the mechanisms underlying coffee-derived bioactives absorption.[359–363] Moreover, to increase distribution and pharmacokinetic properties of natural compound, macrophage-specific delivery of selected phytochemicals might be enhanced through nanomaterials that are avidly phagocytosed by tissue macrophages. This approach has already been exploited for the delivery of therapeutics to tumour-associated macrophages, for example.[364] Taking everything into consideration, future work will be required to completely unveil how macrophages immune response can be regulated by the phytochemicals presented in this thesis, and their possible therapeutic implications.

6. OUTLOOKS

Unravelling Plant Natural Chemical Diversity for Drug Discovery Purposes

The biosynthesis and breakdown of proteins, fats, nucleic acids, and carbohydrates, which are essential to all living organisms, is known as primary metabolism with the compounds involved in the pathways known as “primary metabolites”. The mechanism by which an organism biosynthesizes compounds called ‘secondary metabolites’ (natural products) is often found to be unique to an organism or is an expression of the individuality of a species and is referred to as “secondary metabolism”. Secondary metabolites are generally not essential for the growth, development or reproduction of an organism and are produced either as a result of the organism adapting to its surrounding environment or are produced to act as a possible defence mechanism against predators to assist in the survival of the organism. The biosynthesis of secondary metabolites is derived from the fundamental processes of photosynthesis, glycolysis, and the Krebs cycle to afford biosynthetic intermediates which, ultimately, results in the formation of secondary metabolites. The most important building blocks employed in the biosynthesis of secondary metabolites are those derived from the intermediates: Acetyl coenzyme A (acetyl-CoA), shikimic acid, mevalonic acid and 1-deoxyxylulose-5-phosphate. They are involved in countless biosynthetic pathways, involving numerous different mechanisms and reactions (e.g., alkylation, decarboxylation, aldol, Claisen and

Schiff base formation.[140] Although the number of building blocks are limited, the formation of novel secondary metabolites is infinite, thus plant secondary metabolism provides an endless source of chemically diverse bioactive and pharmacologically active compounds. The screening and testing of extracts against a variety of pharmacological targets to benefit from the immense natural chemical diversity is a concern in many laboratories worldwide. Several successes have been recorded in finding new actives in natural products, some of which have become new drugs or new sources of inspiration for drugs. Between 1940 and 2014, 49% of anticancer molecules approved were natural products or chemical derivatives worldwide.[365] However, less than 10% of the world's biodiversity has been evaluated for potential biological activity, many more useful natural lead compounds await discovery.[140]

With this work, we aimed to give a contribute to this field of research with novel insights about coffee extracts, chlorogenic acid and palmitoylethanolamide as potential natural immune modulators of the TLR4 signalling. In the future, sustained research into the inflammation realm will lead to further discoveries about TLR biology and aid in the development of novel TLR modulators for clinical applications. Within this context, future investments in the identification of natural molecules that target TLR4 intracellular signalling platforms or the receptor itself could generate a novel class of highly effective anti-inflammatory phytotherapeutics.

As a Plant, Food and Agri-environmental Biotechnologist passionate about Food research and Immunonutrition, with this experimental thesis I hope have added a puzzle piece to the vast area of research that focuses on the molecular mechanisms of action of natural immune modulators.

---

7. LIST OF PUBLICATIONS AND AUTHOR CONTRIBUTION

- **Artusa, V.**; Ciaramelli, C.; D'Aloia, A.; Facchini, F.A.; Gotri, N.; Bruno, A.; Costa, B.; Palmioli A,; Airoldi, C.; Peri, F. Green and Roasted Coffee Extracts Inhibit Interferon-β Release in LPS-Stimulated Human Macrophages. *Front. Pharmacol*. **2022**, 13:806010. doi: 10.3389/fphar.2022.806010 (in press) - Appendix I

- D'Aloia, A.; Molteni, L.; Gullo, F.; Bresciani, E.; **Artusa, V.**; Rizzi, L.; Ceriani, M.; Meanti, R.; Lecchi, M.; Coco, S.; Costa, B.; Torsello, A. Palmitoylethanolamide Modulation of Microglia Activation: Characterization of Mechanisms of Action and Implication for Its Neuroprotective Effects. *Int. J. Mol. Sci*. **2021**, 22, 3054. https://doi.org/10.3390/ijms22063054 - Appendix II

- D'Aloia, A.; Arrigoni, F.; Tisi, R.; Palmioli, A.; Ceriani, M.; **Artusa, V.**; Airoldi, C.; Zampella, G.; Costa, B.; Cipolla, L. Synthesis, Molecular Modeling and Biological Evaluation of Metabolically Stable Analogues of the Endogenous Fatty Acid Amide Palmitoylethanolamide. *Int. J. Mol. Sci.* **2020**, 21, 9074. https://doi.org/10.3390/ijms21239074 - Appendix III

Main body of my investigation as a Doctoral Researcher was included in a recently accepted manuscript (Appendix I). Specifically, I have dealt with the: (i) designing of the experimental settings, (ii) execution of cellular and biochemical assays, (iii) data management, (iv) data analysis, (v) data visualization, (vi) writing of the original manuscript and its final revisioning.

Additionally, being involved in a multidisciplinary collaborative project, I had the chance to contributed to the publication of two different Research Articles, here annexed as Appendix II and Appendix III, respectively. Providing my expertise with the handling of the *in vitro* differentiation of human macrophages and the establishment of an LPS-induced inflammation model, I was able to collect useful data that supported the previous observation obtained using microglial cells.

8. REFERENCES

1. Chen, L. *et al.* Inflammatory responses and inflammation-associated diseases in organs. *Oncotarget* **9**, 7204–7218 (2018).
2. Basset, C., Holton, J., O'Mahony, R. & Roitt, I. Innate immunity and pathogen–host interaction. *Vaccine* **21**, S12–S23 (2003).
3. Iwasaki, A. & Medzhitov, R. Toll-like receptor control of the adaptive immune responses. *Nat. Immunol.* **5**, 987–995 (2004).
4. Akira, S., Uematsu, S. & Takeuchi, O. Pathogen recognition and innate immunity. *Cell* **124**, 783–801 (2006).
5. Ghosh, S., May, M. J. & Kopp, E. B. NF-kappa B and Rel proteins: evolutionarily conserved mediators of immune responses. *Annu. Rev. Immunol.* **16**, 225–260 (1998).
6. Miettinen, M., Sareneva, T., Julkunen, I. & Matikainen, S. IFNs activate toll-like receptor gene expression in viral infections. *Genes Immun.* **2**, 349–355 (2001).
7. Medzhitov, R. & Biron, C. A. Innate immunity. *Curr. Opin. Immunol.* **15**, 2–4 (2003).
8. Janeway, C. A., Jr. Approaching the asymptote? Evolution and revolution in immunology. *Cold Spring Harb. Symp. Quant. Biol.* **54 Pt 1**, 1–13 (1989).

9. Mogensen, T. H. Pathogen recognition and inflammatory signaling in innate immune defenses. *Clin. Microbiol. Rev.* **22**, 240–73, Table of Contents (2009).

10. Medzhitov, R., Preston-Hurlburt, P. & Janeway, C. A., Jr. A human homologue of the Drosophila Toll protein signals activation of adaptive immunity. *Nature* **388**, 394–397 (1997).

11. Lemaitre, B., Nicolas, E., Michaut, L., Reichhart, J. M. & Hoffmann, J. A. The dorsoventral regulatory gene cassette spätzle/toll/cactus controls the potent antifungal response in Drosophila adults. *Cell* **86**, 973–983 (1996).

12. Majzoub, K., Wrensch, F. & Baumert, T. F. The innate antiviral response in animals: An evolutionary perspective from flagellates to humans. *Viruses* **11**, 758 (2019).

13. Bowie, A. & O'Neill, L. A. The interleukin-1 receptor/Toll-like receptor superfamily: signal generators for pro-inflammatory interleukins and microbial products. *J. Leukoc. Biol.* **67**, 508–514 (2000).

14. Dolasia, K., Bisht, M. K., Pradhan, G., Udgata, A. & Mukhopadhyay, S. TLRs/NLRs: Shaping the landscape of host immunity. *Int. Rev. Immunol.* **37**, 3–19 (2018).

15. Matzinger, P. The danger model: a renewed sense of self. *Science* **296**, 301–305 (2002).

16. O'Neill, L. A. J. & Bowie, A. G. The family of five: TIR-domain-containing adaptors in Toll-like receptor signalling. *Nat. Rev. Immunol.* **7**, 353–364 (2007).

17. Chen, L. & Yu, J. Modulation of Toll-like receptor signaling in innate immunity by natural products. *Int. Immunopharmacol.* **37**, 65–70 (2016).

18. Duffy, L. & O'Reilly, S. C. Toll-like receptors in the pathogenesis of autoimmune diseases: recent and emerging translational developments. *ImmunoTargets Ther.* **5**, 69–80 (2016).

19. Kato, H. *et al.* Differential roles of MDA5 and RIG-I helicases in the recognition of RNA viruses. *Nature* **441**, 101–105 (2006).

20. Sadler, A. J. & Williams, B. R. G. Structure and function of the protein kinase R. *Curr. Top. Microbiol. Immunol.* **316**, 253–292 (2007).

21. Takaoka, A. *et al.* DAI (DLM-1/ZBP1) is a cytosolic DNA sensor and an activator of innate immune response. *Nature* **448**, 501–505 (2007).

22. Kanneganti, T.-D., Lamkanfi, M. & Núñez, G. Intracellular NOD-like receptors in host defense and disease. *Immunity* **27**, 549–559 (2007).

23. Martinon, F., Burns, K. & Tschopp, J. The inflammasome: a molecular platform triggering activation of inflammatory caspases and processing of proIL-beta. *Mol. Cell* **10**, 417–426 (2002).

24. Latz, E., Xiao, T. S. & Stutz, A. Activation and regulation of the inflammasomes. *Nat. Rev. Immunol.* **13**, 397–411 (2013).

25. Hornung, V. & Latz, E. Intracellular DNA recognition. *Nat. Rev. Immunol.* **10**, 123–130 (2010).

26. Horvath, G. L., Schrum, J. E., De Nardo, C. M. & Latz, E. Intracellular sensing of microbes and danger signals by the inflammasomes. *Immunol. Rev.* **243**, 119–135 (2011).

27. Bauernfeind, F. G. *et al.* Cutting edge: NF-kappaB activating pattern recognition and cytokine receptors license NLRP3 inflammasome activation by regulating NLRP3 expression. *J. Immunol.* **183**, 787–791 (2009).

28. Franchi, L., Eigenbrod, T. & Núñez, G. Cutting edge: TNF-alpha mediates sensitization to ATP and silica via the NLRP3 inflammasome in the absence of microbial stimulation. *J. Immunol.* **183**, 792–796 (2009).

29. Kelley, N., Jeltema, D., Duan, Y. & He, Y. The NLRP3 inflammasome: An overview of mechanisms of activation and regulation. *Int. J. Mol. Sci.* **20**, 3328 (2019).

30. Kayagaki, N. *et al.* Noncanonical inflammasome activation by intracellular LPS independent of TLR4. *Science* **341**, 1246–1249 (2013).

31. Kayagaki, N. *et al.* Non-canonical inflammasome activation targets caspase-11. *Nature* **479**, 117–121 (2011).

32. Baker, P. J. *et al.* NLRP3 inflammasome activation downstream of cytoplasmic LPS recognition by both caspase-4 and caspase-5. *Eur. J. Immunol.* **45**, 2918–2926 (2015).

33. Shi, J. *et al.* Inflammatory caspases are innate immune receptors for intracellular LPS. *Nature* **514**, 187–192 (2014).

34. Hagar, J. A., Powell, D. A., Aachoui, Y., Ernst, R. K. & Miao, E. A. Cytoplasmic LPS activates caspase-11: implications in TLR4-independent endotoxic shock. *Science* **341**, 1250–1253 (2013).

35. Broz, P. *et al.* Caspase-11 increases susceptibility to Salmonella infection in the absence of caspase-1. *Nature* **490**, 288–291 (2012).

36. Piccini, A. *et al.* ATP is released by monocytes stimulated with pathogen-sensing receptor ligands and induces IL-1beta and IL-18 secretion in an autocrine way. *Proc. Natl. Acad. Sci. U. S. A.* **105**, 8067–8072 (2008).

37. Netea, M. G. *et al.* Differential requirement for the activation of the inflammasome for processing and release of IL-1beta in monocytes and macrophages. *Blood* **113**, 2324–2335 (2009).

38. Gaidt, M. M. *et al.* Human monocytes engage an alternative inflammasome pathway. *Immunity* **44**, 833–846 (2016).

39. Brown, G. D., Willment, J. A. & Whitehead, L. C-type lectins in immunity and homeostasis. *Nat. Rev. Immunol.* **18**, 374–389 (2018).

40. Takeda, K. Toll-like Receptors and their Adaptors in Innate Immunity. *Curr. Med. Chem. Anti Inflamm. Anti Allergy Agents* **4**, 3–11 (2005).

41. Mazgaeen, L. & Gurung, P. Recent advances in lipopolysaccharide recognition systems. *Int. J. Mol. Sci.* **21**, 379 (2020).

42. Ain, Q. U., Batool, M. & Choi, S. TLR4-targeting therapeutics: Structural basis and computer-aided drug discovery approaches. *Molecules* **25**, 627 (2020).

43. Kawai, T., Adachi, O., Ogawa, T., Takeda, K. & Akira, S. Unresponsiveness of MyD88-deficient mice to endotoxin. *Immunity* **11**, 115–122 (1999).

44. Kawai, T. *et al.* Lipopolysaccharide stimulates the MyD88-independent pathway and results in activation of IFN-regulatory factor 3 and the expression of a subset of lipopolysaccharide-inducible genes. *J. Immunol.* **167**, 5887–5894 (2001).

45. Yamamoto, M. *et al.* Role of adaptor TRIF in the MyD88-independent toll-like receptor signaling pathway. *Science* **301**, 640–643 (2003).

46. Fitzgerald, K. A. *et al.* IKKepsilon and TBK1 are essential components of the IRF3 signaling pathway. *Nat. Immunol.* **4**, 491–496 (2003).

47. Kawai, T. & Akira, S. Signaling to NF-kappaB by Toll-like receptors. *Trends Mol. Med.* **13**, 460–469 (2007).

48. Shen, H., Tesar, B. M., Walker, W. E. & Goldstein, D. R. Dual signaling of MyD88 and TRIF is critical for maximal TLR4-induced dendritic cell maturation. *J. Immunol.* **181**, 1849–1858 (2008).

49. Hoebe, K. *et al.* Upregulation of costimulatory molecules induced by lipopolysaccharide and double-stranded RNA occurs by Trif-dependent and Trif-independent pathways. *Nat. Immunol.* **4**, 1223–1229 (2003).

50. Munoz, C. *et al.* Dysregulation of in vitro cytokine production by monocytes during sepsis. *J. Clin. Invest.* **88**, 1747–1754 (1991).

51. Karin, M. Nuclear factor-kappaB in cancer development and progression. *Nature* **441**, 431–436 (2006).

52. Yan, N. & Chen, Z. J. Intrinsic antiviral immunity. *Nat. Immunol.* **13**, 214–222 (2012).

53. Honda, K. & Taniguchi, T. IRFs: master regulators of signalling by Toll-like receptors and cytosolic pattern-recognition receptors. *Nat. Rev. Immunol.* **6**, 644–658 (2006).

54. Pestka, S., Krause, C. D. & Walter, M. R. Interferons, interferon-like cytokines, and their receptors. *Immunol. Rev.* **202**, 8–32 (2004).

55. Schoggins, J. W. Interferon-stimulated genes: What do they all do? *Annu. Rev. Virol.* **6**, 567–584 (2019).

56. Schneider, W. M., Chevillotte, M. D. & Rice, C. M. Interferon-stimulated genes: a complex web of host defenses. *Annu. Rev. Immunol.* **32**, 513–545 (2014).

57. Schoenborn, J. R. & Wilson, C. B. Regulation of interferon-gamma during innate and adaptive immune responses. *Adv. Immunol.* **96**, 41–101 (2007).

58. Witte, K., Witte, E., Sabat, R. & Wolk, K. IL-28A, IL-28B, and IL-29: promising cytokines with type I interferon-like properties. *Cytokine Growth Factor Rev.* **21**, 237–251 (2010).

59. Honda, K., Takaoka, A. & Taniguchi, T. Type I Inteferon Gene Induction by the Interferon Regulatory Factor Family of Transcription Factors. *Immunity* **25**, 349–360 (2006).

60. Tamura, T., Yanai, H., Savitsky, D. & Taniguchi, T. The IRF family transcription factors in immunity and oncogenesis. *Annu. Rev. Immunol.* **26**, 535–584 (2008).

61. de Weerd, N. A., Samarajiwa, S. A. & Hertzog, P. J. Type I interferon receptors: Biochemistry and biological functions. *J. Biol. Chem.* **282**, 20053–20057 (2007).

62. Versteeg, G. A. & García-Sastre, A. Viral tricks to grid-lock the type I interferon system. *Curr. Opin. Microbiol.* **13**, 508–516 (2010).

63. Ivashkiv, L. B. & Donlin, L. T. Regulation of type I interferon responses. *Nat. Rev. Immunol.* **14**, 36–49 (2014).

64. Belkaid, Y. & Hand, T. W. Role of the Microbiota in immunity and inflammation. *Cell* **157**, 121–141 (2014).

65. *during infection with L. monocytogenes, IFNα/β potently inhibit these pathways by blocking responsiveness of macrophages to IFNγ.*

66. Berry, M. P. R. *et al.* An interferon-inducible neutrophil-driven blood transcriptional signature in human tuberculosis. *Nature* **466**, 973–977 (2010).

67. Dejager, L. *et al.* Pharmacological inhibition of type I interferon signaling protects mice against lethal sepsis. *J. Infect. Dis.* **209**, 960–970 (2014).

68. Graham, R. R. *et al.* A common haplotype of interferon regulatory factor 5 (IRF5) regulates splicing and expression and is associated with increased risk of systemic lupus erythematosus. *Nat. Genet.* **38**, 550–555 (2006).

69. Kelly, J. A. *et al.* Interferon regulatory factor-5 is genetically associated with systemic lupus erythematosus in African Americans. *Genes Immun.* **9**, 187–194 (2008).

70. Takaoka, A. *et al.* Integral role of IRF-5 in the gene induction programme activated by Toll-like receptors. *Nature* **434**, 243–249 (2005).

71. Psarras, A., Emery, P. & Vital, E. M. Type I interferon–mediated autoimmune diseases: pathogenesis, diagnosis and targeted therapy. *Rheumatology (Oxford)* kew431 (2017).

72. Bosinger, S. E. *et al.* Gene expression profiling of host response in models of acute HIV infection. *J. Immunol.* **173**, 6858–6863 (2004).

73. Amsler, L., Verweij, M. C. & DeFilippis, V. R. The tiers and dimensions of evasion of the type I interferon response by human Cytomegalovirus. *J. Mol. Biol.* **425**, 4857–4871 (2013).

74. Fuertes, M. B., Woo, S.-R., Burnett, B., Fu, Y.-X. & Gajewski, T. F. Type I interferon response and innate immune sensing of cancer. *Trends Immunol.* **34**, 67–73 (2013).

75. Crow, Y. J. & Manel, N. Aicardi–Goutières syndrome and the type I interferonopathies. *Nat. Rev. Immunol.* **15**, 429–440 (2015).

76. Budhwani, M., Mazzieri, R. & Dolcetti, R. Plasticity of type I interferon-mediated responses in cancer therapy: From anti-tumor immunity to resistance. *Front. Oncol.* **8**, 322 (2018).

77. King, K. R. *et al.* IRF3 and type I interferons fuel a fatal response to myocardial infarction. *Nat. Med.* **23**, 1481–1487 (2017).

78. Wu, Y.-W., Tang, W. & Zuo, J.-P. Toll-like receptors: potential targets for lupus treatment. *Acta Pharmacol. Sin.* **36**, 1395–1407 (2015).

79. Hiscott, J., Nguyen, T.-L. A., Arguello, M., Nakhaei, P. & Paz, S. Manipulation of the nuclear factor-kappaB pathway and the innate immune response by viruses. *Oncogene* **25**, 6844–6867 (2006).

80. Wang, C., Horby, P. W., Hayden, F. G. & Gao, G. F. A novel coronavirus outbreak of global health concern. *Lancet* vol. 395 470–473 (2020).

81. Zhu, N. *et al.* A novel Coronavirus from patients with pneumonia in China, 2019. *N. Engl. J. Med.* **382**, 727–733 (2020).

82. de Wit, E., van Doremalen, N., Falzarano, D. & Munster, V. J. SARS and MERS: recent insights into emerging coronaviruses. *Nat. Rev. Microbiol.* **14**, 523–534 (2016).

83. Li, X., Geng, M., Peng, Y., Meng, L. & Lu, S. Molecular immune pathogenesis and diagnosis of COVID-19. *J. Pharm. Anal.* **10**, 102–108 (2020).

84. Metschnikoff, E. Leçons sur la pathologie comparée de l'inflammation. *Dtsch. Med. Wochenschr.* **19**, 17–18 (1893).

85. Schmalstieg, F. C., Jr & Goldman, A. S. Ilya ilich Metchnikoff (1845-1915) and Paul Ehrlich (1854-1915): The centennial of the 1908 Nobel Prize in Physiology or Medicine. *J. Med. Biogr.* **16**, 96–103 (2008).

86. van Furth, R. The mononuclear phagocyte system. *Verh. Dtsch. Ges. Pathol.* **64**, 1–11 (1980).

87. Ginhoux, F. & Guilliams, M. Tissue-resident macrophage ontogeny and homeostasis. *Immunity* **44**, 439–449 (2016).

88. Hume, D. A., Irvine, K. M. & Pridans, C. The mononuclear phagocyte system: The relationship between monocytes and macrophages. *Trends Immunol.* **40**, 98–112 (2019).

89. Sheng, J., Ruedl, C. & Karjalainen, K. Most tissue-resident macrophages except microglia are derived from fetal hematopoietic stem cells. *Immunity* **43**, 382–393 (2015).

90. Dey, A., Allen, J. & Hankey-Giblin, P. A. Ontogeny and polarization of macrophages in inflammation: blood monocytes versus tissue macrophages. *Front. Immunol.* **5**, 683 (2014).

91. Watanabe, S., Alexander, M., Misharin, A. V. & Budinger, G. R. S. The role of macrophages in the resolution of inflammation. *J. Clin. Invest.* **129**, 2619–2628 (2019).

92. Fogg, D. K. *et al.* A clonogenic bone marrow progenitor specific for macrophages and dendritic cells. *Science* **311**, 83–87 (2006).

93. Rojo, R., Pridans, C., Langlais, D. & Hume, D. A. Transcriptional mechanisms that control expression of the macrophage colony-stimulating factor receptor locus. *Clin. Sci. (Lond.)* **131**, 2161–2182 (2017).

94. Gren, S. T. *et al.* A single-cell gene-expression profile reveals inter-cellular heterogeneity within human monocyte subsets. *PLoS One* **10**, e0144351 (2015).

95. Ong, S.-M. *et al.* A novel, five-marker alternative to CD16-CD14 gating to identify the three human monocyte subsets. *Front. Immunol.* **10**, 1761 (2019).

96. Villani, A.-C. *et al.* Single-cell RNA-seq reveals new types of human blood dendritic cells, monocytes, and progenitors. *Science* **356**, (2017).

97. Ginhoux, F. & Jung, S. Monocytes and macrophages: developmental pathways and tissue homeostasis. *Nat. Rev. Immunol.* **14**, 392–404 (2014).

98. Davies, L. C., Jenkins, S. J., Allen, J. E. & Taylor, P. R. Tissue-resident macrophages. *Nat. Immunol.* **14**, 986–995 (2013).

99. Wynn, T. A., Chawla, A. & Pollard, J. W. Macrophage biology in development, homeostasis and disease. *Nature* **496**, 445–455 (2013).

100. Murray, P. J. *et al.* Macrophage activation and polarization: Nomenclature and experimental guidelines. *Immunity* **41**, 14–20 (2014).

101. Martinez, F. O., Sica, A., Mantovani, A. & Locati, M. Macrophage activation and polarization. *Front. Biosci.* **13**, 453–461 (2008).

102. Mills, C. D., Kincaid, K., Alt, J. M., Heilman, M. J. & Hill, A. M. M-1/M-2 macrophages and the Th1/Th2 paradigm. *J. Immunol.* **164**, 6166–6173 (2000).

103. Lampiasi, N., Russo, R. & Zito, F. The alternative faces of macrophage generate osteoclasts. *Biomed Res. Int.* **2016**, 9089610 (2016).

104. Yao, Y., Xu, X.-H. & Jin, L. Macrophage polarization in physiological and pathological pregnancy. *Front. Immunol.* **10**, 792 (2019).

105. Murray, P. J. Macrophage polarization. *Annu. Rev. Physiol.* **79**, 541–566 (2017).

106. Lavin, Y. *et al.* Tissue-resident macrophage enhancer landscapes are shaped by the local microenvironment. *Cell* **159**, 1312–1326 (2014).

107. Xue, J. *et al.* Transcriptome-based network analysis reveals a spectrum model of human macrophage activation. *Immunity* **40**, 274–288 (2014).

108. Vannella, K. M. & Wynn, T. A. Mechanisms of organ injury and repair by macrophages. *Annu. Rev. Physiol.* **79**, 593–617 (2017).

109. Rosas, M. *et al.* The transcription factor Gata6 links tissue macrophage phenotype and proliferative renewal. *Science* **344**, 645–648 (2014).

110. Arpaia, N. *et al.* A distinct function of regulatory T cells in tissue protection. *Cell* **162**, 1078–1089 (2015).

111. Linke, M. *et al.* Chronic signaling via the metabolic checkpoint kinase mTORC1 induces macrophage granuloma formation and marks sarcoidosis progression. *Nat. Immunol.* **18**, 293–302 (2017).

112. Bah, A. & Vergne, I. Macrophage autophagy and bacterial infections. *Front. Immunol.* **8**, 1483 (2017).

113. Linehan, E. & Fitzgerald, D. Ageing and the immune system: focus on macrophages. *Eur. J. Microbiol. Immunol. (Bp.)* **5**, 14–24 (2015).

114. Jin, X. & Kruth, H. S. Culture of macrophage colony-stimulating factor differentiated human monocyte-derived macrophages. *J. Vis. Exp.* (2016) doi:10.3791/54244.

115. Sallusto, F. & Lanzavecchia, A. Efficient presentation of soluble antigen by cultured human dendritic cells is maintained by granulocyte/macrophage colony-stimulating factor plus interleukin 4 and downregulated by tumor necrosis factor alpha. *J. Exp. Med.* **179**, 1109–1118 (1994).

116. Shapouri-Moghaddam, A. *et al.* Macrophage plasticity, polarization, and function in health and disease. *J. Cell. Physiol.* **233**, 6425–6440 (2018).

117. Macri, C., Pang, E. S., Patton, T. & O'Keeffe, M. Dendritic cell subsets. *Semin. Cell Dev. Biol.* **84**, 11–21 (2018).

118. Rogers, N. M., Ferenbach, D. A., Isenberg, J. S., Thomson, A. W. & Hughes, J. Dendritic cells and macrophages in the kidney: a spectrum of good and evil. *Nat. Rev. Nephrol.* **10**, 625–643 (2014).

119. Gilboa, E. DC-based cancer vaccines. *J. Clin. Invest.* **117**, 1195–1203 (2007).

120. Poltorak, A. *et al.* Defective LPS signaling in C3H/HeJ and C57BL/10ScCr mice: mutations in Tlr4 gene. *Science* **282**, 2085–2088 (1998).

121. De Paola, M. *et al.* Synthetic and natural small molecule TLR4 antagonists inhibit motoneuron death in cultures from ALS mouse model. *Pharmacol. Res.* **103**, 180–187 (2016).

122. Bettoni, I. *et al.* Glial TLR4 receptor as new target to treat neuropathic pain: efficacy of a new receptor antagonist in a model of peripheral nerve injury in mice. *Glia* **56**, 1312–1319 (2008).

123. Suarez De La Rica, A., Gilsanz, F. & Maseda, E. Epidemiologic trends of sepsis in western countries. *Ann. Transl. Med.* **4**, 325 (2016).

124. Peri, F. & Calabrese, V. Toll-like receptor 4 (TLR4) modulation by synthetic and natural compounds: an update. *J. Med. Chem.* **57**, 3612–3622 (2014).

125. Palmer, C. *et al.* Synthetic glycolipid-based TLR4 antagonists negatively regulate TRIF-dependent TLR4 signalling in human macrophages. *Innate Immun.* **27**, 275–284 (2021).

126. Facchini, F. A. *et al.* Synthetic glycolipids as molecular vaccine adjuvants: Mechanism of action in human cells and in vivo activity. *J. Med. Chem.* **64**, 12261–12272 (2021).

127. Takashima, K. *et al.* Analysis of binding site for the novel small-molecule TLR4 signal transduction inhibitor TAK-242 and its therapeutic effect on mouse sepsis model. *Br. J. Pharmacol.* **157**, 1250–1262 (2009).

128. Matsunaga, N., Tsuchimori, N., Matsumoto, T. & Ii, M. TAK-242 (resatorvid), a small-molecule inhibitor of Toll-like receptor (TLR) 4 signaling, binds selectively to TLR4 and interferes with interactions between TLR4 and its adaptor molecules. *Mol. Pharmacol.* **79**, 34–41 (2011).

129. Thomas, G. G. S. S. C. Z. Preparation of Deuterated Cyclohexenes as Modulators of TLR4 Signaling for Disease Treatment. *U.S. Patent No. US* (2009).

130. Kim, H. M. *et al.* Crystal structure of the TLR4-MD-2 complex with bound endotoxin antagonist Eritoran. *Cell* **130**, 906–917 (2007).

131. Zaffaroni, L. & Peri, F. Recent advances on Toll-like receptor 4 modulation: new therapeutic perspectives. *Future Med. Chem.* **10**, 461–476 (2018).

132. Piazza, M. *et al.* Glycolipids and benzylammonium lipids as novel antisepsis agents: synthesis and biological characterization. *J. Med. Chem.* **52**, 1209–1213 (2009).

133. Piazza, M. *et al.* Evidence of a specific interaction between new synthetic antisepsis agents and CD14. *Biochemistry* **48**, 12337–12344 (2009).

134. Facchini, F. A. *et al.* Structure–activity relationship in monosaccharide-based toll-like receptor 4 (TLR4) antagonists. *J. Med. Chem.* **61**, 2895–2909 (2018).

135. Palmer, C. *et al.* The synthetic glycolipid-based TLR4 antagonist FP7 negatively regulates in vitro and in vivo haematopoietic and non-haematopoietic vascular TLR4 signalling. *Innate Immun.* **24**, 411–421 (2018).

136. Li, J.-K., Balic, J. J., Yu, L. & Jenkins, B. TLR Agonists as Adjuvants for Cancer Vaccines. *Adv. Exp. Med. Biol.* **1024**, 195–212 (2017).

137. Romerio, A. & Peri, F. Increasing the Chemical Variety of Small-Molecule-Based TLR4 Modulators: An Overview. *Front. Immunol.* **11**, 1210 (2020).

138. Casella, C. R. & Mitchell, T. C. Putting endotoxin to work for us: monophosphoryl lipid A as a safe and effective vaccine adjuvant. *Cell. Mol. Life Sci.* **65**, 3231–3240 (2008).

139. Gautam, R. & Jachak, S. M. Recent developments in anti-inflammatory natural products. *Med. Res. Rev.* **29**, 767–820 (2009).

140. Dias, D. A., Urban, S. & Roessner, U. A historical overview of natural products in drug discovery. *Metabolites* **2**, 303–336 (2012).

141. Modulation of Inflammation by Botanical Medicines. in *Clinical Botanical Medicine* 389–401 (Mary Ann Liebert, Inc., publishers, 2009).

142. Patwardhan, B. Ethnopharmacology and drug discovery. *J. Ethnopharmacol.* **100**, 50–52 (2005).

143. Cragg, G. M. & Newman, D. J. Natural products: a continuing source of novel drug leads. *Biochim. Biophys. Acta* **1830**, 3670–3695 (2013).

144. Nigam, N., George, J. & Shukla, Y. Ginger (6-gingerol). in *Molecular Targets and Therapeutic Uses of Spices* 225–256 (WORLD SCIENTIFIC, 2009).

145. Chainani-Wu, N. Safety and anti-inflammatory activity of curcumin: A component of tumeric (Curcuma longa). *J. Altern. Complement. Med.* **9**, 161–168 (2003).

146. Juliana, C. *et al.* Anti-inflammatory compounds parthenolide and Bay 11-7082 are direct inhibitors of the inflammasome. *J. Biol. Chem.* **285**, 9792–9802 (2010).

147. DeFelice, S. L. The nutraceutical revolution: its impact on food industry R&D. *Trends Food Sci. Technol.* **6**, 59–61 (1995).

148. Ruiz-León, A. M., Lapuente, M., Estruch, R. & Casas, R. Clinical advances in immunonutrition and atherosclerosis: A review. *Front. Immunol.* **10**, 837 (2019).

149. van Daal, M. T., Folkerts, G., Garssen, J. & Braber, S. Pharmacological modulation of immune responses by nutritional components. *Pharmacol. Rev.* **73**, 198–232 (2021).

150. Strittmatter, W., Weckesser, J., Salimath, P. V. & Galanos, C. Nontoxic lipopolysaccharide from Rhodopseudomonas sphaeroides ATCC 17023. *J. Bacteriol.* **155**, 153–158 (1983).

151. Anwar, M. A., Panneerselvam, S., Shah, M. & Choi, S. Insights into the species-specific TLR4 signaling mechanism in response to Rhodobacter sphaeroides lipid A detection. *Sci. Rep.* **5**, 7657 (2015).

152. Chahal, D. S., Sivamani, R. K., Isseroff, R. R. & Dasu, M. R. Plant-based modulation of Toll-like receptors: an emerging therapeutic model. *Phytother. Res.* **27**, 1423–1438 (2013).

153. Shibata, T. *et al.* Toll-like receptors as a target of food-derived anti-inflammatory compounds. *J. Biol. Chem.* **289**, 32757–32772 (2014).

154. Koo, J. E., Park, Z.-Y., Kim, N. D. & Lee, J. Y. Sulforaphane inhibits the engagement of LPS with TLR4/MD2 complex by preferential binding to Cys133 in MD2. *Biochem. Biophys. Res. Commun.* **434**, 600–605 (2013).

155. Youn, H. S. *et al.* Suppression of MyD88- and TRIF-dependent signaling pathways of Toll-like receptor by (-)-epigallocatechin-3-gallate, a polyphenol component of green tea. *Biochem. Pharmacol.* **72**, 850–859 (2006).

156. Qi, M. *et al.* Dioscin attenuates renal ischemia/reperfusion injury by inhibiting the TLR4/MyD88 signaling pathway via up-regulation of HSP70. *Pharmacol. Res.* **100**, 341–352 (2015).

157. Yi, C. *et al.* Effect of ω-3 polyunsaturated fatty acid on toll-like receptors in patients with severe multiple trauma. *J. Huazhong Univ. Sci. Technolog. Med. Sci.* **31**, 504 (2011).

158. Depner, C. M., Philbrick, K. A. & Jump, D. B. Docosahexaenoic acid attenuates hepatic inflammation, oxidative stress, and fibrosis without decreasing hepatosteatosis in a Ldlr(-/-) mouse model of western diet-induced nonalcoholic steatohepatitis. *J. Nutr.* **143**, 315–323 (2013).

159. Nasef, N. A., Mehta, S., Murray, P., Marlow, G. & Ferguson, L. R. Anti-inflammatory activity of fruit fractions in vitro, mediated through toll-like receptor 4 and 2 in the context of inflammatory bowel disease. *Nutrients* **6**, 5265–5279 (2014).

160. Liang, Q. *et al.* Characterization of sparstolonin B, a Chinese herb-derived compound, as a selective Toll-like receptor antagonist with potent anti-inflammatory properties. *J. Biol. Chem.* **286**, 26470–26479 (2011).

161. Lee, W. H. *et al.* Specific oligopeptides in fermented soybean extract inhibit NF-κB-dependent iNOS and cytokine induction by toll-like receptor ligands. *J. Med. Food* **17**, 1239–1246 (2014).

162. Xu, X.-X. *et al.* Effects of total glucosides of paeony on immune regulatory toll-like receptors TLR2 and 4 in the kidney from diabetic rats. *Phytomedicine* **21**, 815–823 (2014).

163. Villa, F. A., Lieske, K. & Gerwick, L. Selective MyD88-dependent pathway inhibition by the cyanobacterial natural product malyngamide F acetate. *Eur. J. Pharmacol.* **629**, 140–146 (2010).

164. Li, J. *et al.* Pleurotus ferulae water extract enhances the maturation and function of murine bone marrow-derived dendritic cells through TLR4 signaling pathway. *Vaccine* **33**, 1923–1933 (2015).

165. Tian, Y. *et al.* Astragalus mongholicus regulate the Toll-like-receptor 4 meditated signal transduction of dendritic cells to restrain stomach cancer cells. *Afr. J. Tradit. Complement. Altern. Med.* **11**, 92–96 (2014).

166. Öberg, F. *et al.* Herbal melanin activates TLR4/NF-κB signaling pathway. *Phytomedicine* **16**, 477–484 (2009).

167. Gao, Y., Zhou, S., Jiang, W., Huang, M. & Dai, X. Effects of ganopoly (a Ganoderma lucidum polysaccharide extract) on the immune functions in advanced-stage cancer patients. *Immunol. Invest.* **32**, 201–215 (2003).

168. Dai, X. *et al.* Consuming Lentinula edodes (shiitake) mushrooms daily improves human immunity: A randomized dietary intervention in healthy young adults. *J. Am. Coll. Nutr.* **34**, 478–487 (2015).

169. Nelson, K. M. *et al.* The essential medicinal chemistry of curcumin. *J. Med. Chem.* **60**, 1620–1637 (2017).

170. Luque-Martin, R., Mander, P. K., Leenen, P. J. M. & Winther, M. P. J. Classic and new mediators for in vitro modelling of human macrophages. *J. Leukoc. Biol.* **109**, 549–560 (2021).

171. Starr, T., Bauler, T. J., Malik-Kale, P. & Steele-Mortimer, O. The phorbol 12-myristate-13-acetate differentiation protocol is critical to the interaction of THP-1 macrophages with Salmonella Typhimurium. *PLoS One* **13**, e0193601 (2018).

172. Ciaramelli, C. *et al.* NMR-driven identification of anti-amyloidogenic compounds in green and roasted coffee extracts. *Food Chem.* **252**, 171–180 (2018).

173. Amigoni, L. *et al.* Green coffee extract enhances oxidative stress resistance and delays aging in Caenorhabditis elegans. *J. Funct. Foods* **33**, 297–306 (2017).

174. Wei, F. *et al.* 13C NMR-Based Metabolomics for the Classification of Green Coffee Beans According to Variety and Origin. *J. Agric. Food Chem.* **60**, 10118–10125 (2012).

175. D'Aloia, A. *et al.* Synthesis, molecular modeling and biological evaluation of metabolically stable analogues of the endogenous fatty acid amide palmitoylethanolamide. *Int. J. Mol. Sci.* **21**, 9074 (2020).

176. Mosmann, T. Rapid colorimetric assay for cellular growth and survival: application to proliferation and cytotoxicity assays. *J. Immunol. Methods* **65**, 55–63 (1983).

177. Global coffee consumption, 2020/21. *Statista* https://www.statista.com/statistics/292595/global-coffee-consumption/.

178. Coffee consumption by country 2021. https://worldpopulationreview.com/country-rankings/coffee-consumption-by-country.

179. Esquivel, P. & Jiménez, V. M. Functional properties of coffee and coffee by-products. *Food Res. Int.* **46**, 488–495 (2012).

180. Davis, A. P., Govaerts, R., Bridson, D. M. & Stoffelen, P. An annotated taxonomic conspectus of the genus Coffea (Rubiaceae). *Bot. J. Linn. Soc.* **152**, 465–512 (2006).

181. Marcason, W. What is green coffee extract? *J. Acad. Nutr. Diet.* **113**, 364 (2013).

182. Carrillo, J. A. & Benitez, J. Clinically significant pharmacokinetic interactions between dietary caffeine and medications. *Clin. Pharmacokinet.* **39**, 127–153 (2000).

183. Joeres, R. *et al.* Influence of smoking on caffeine elimination in healthy volunteers and in patients with alcoholic liver cirrhosis. *Hepatology* **8**, 575–579 (1988).

184. Cook, D. G. *et al.* Relation of caffeine intake and blood caffeine concentrations during pregnancy to fetal growth: prospective population based study. *BMJ* **313**, 1358–1362 (1996).

185. Hodgson, J. M., Chan, S. Y. & Puddey, I. B. *Phenolic acid metabolites as biomarkers for tea-and coffee-derived polyphenol exposure in human subjects*. (2004).

186. Ding, M., Bhupathiraju, S. N., Satija, A., van Dam, R. M. & Hu, F. B. Long-term coffee consumption and risk of cardiovascular disease: a systematic review and a dose-response meta-analysis of prospective cohort studies. *Circulation* **129**, 643–659 (2014).

187. Salazar-Martinez, E. *et al.* Coffee consumption and risk for type 2 diabetes mellitus. *Ann. Intern. Med.* **140**, 1–8 (2004).

188. Shang, F., Li, X. & Jiang, X. Coffee consumption and risk of the metabolic syndrome: A meta-analysis. *Diabetes Metab.* **42**, 80–87 (2016).

189. Vecchia, L. Coffee, liver enzymes, cirrhosis and liver cancer. *J. Hepatol* (2005).

190. Ascherio, A. *et al.* Prospective study of caffeine consumption and risk of Parkinson's disease in men and women. *Ann. Neurol.* **50**, 56–63 (2001).

191. Wang, A. *et al.* Coffee and cancer risk: A meta-analysis of prospective observational studies. *Sci. Rep.* **6**, 33711 (2016).

192. Godos, J. *et al.* Coffee consumption and risk of biliary tract cancers and liver cancer: A dose–response meta-analysis of prospective cohort studies. *Nutrients* **9**, 950 (2017).

193. de Koning Gans, J. M. *et al.* Tea and coffee consumption and cardiovascular morbidity and mortality. *Arterioscler. Thromb. Vasc. Biol.* **30**, 1665–1671 (2010).

194. Lopez-Garcia, E. *et al.* Coffee consumption and risk of stroke in women. *Circulation* **119**, 1116–1123 (2009).

195. Crippa, A., Discacciati, A., Larsson, S. C., Wolk, A. & Orsini, N. Coffee consumption and mortality from all causes, cardiovascular disease, and cancer: a dose-response meta-analysis. *Am. J. Epidemiol.* **180**, 763–775 (2014).

196. Ding, M., Bhupathiraju, S. N., Chen, M., van Dam, R. M. & Hu, F. B. Caffeinated and decaffeinated coffee consumption and risk of type 2 diabetes: a systematic review and a dose-response meta-analysis. *Diabetes Care* **37**, 569–586 (2014).

197. Iang, X., Zhang, D. & Jiang, W. Coffee and caffeine intake and incidence of type 2 diabetes mellitus: a meta-analysis of prospective studies. *Eur J Nutr* (2014).

198. Donath, M. Y. & Shoelson, S. E. Type 2 diabetes as an inflammatory disease. *Nat. Rev. Immunol.* **11**, 98–107 (2011).

199. Kempf, K. *et al.* Effects of coffee consumption on subclinical inflammation and other risk factors for type 2 diabetes: a clinical trial. *Am. J. Clin. Nutr.* **91**, 950–957 (2010).

200. Williamson, G. & Sheedy, K. Effects of polyphenols on insulin resistance. *Nutrients* **12**, 3135 (2020).

201. Takaya, J., Higashino, H. & Kobayashi, Y. Intracellular magnesium and insulin resistance. *Magnes. Res.* **17**, 126–136 (2004).

202. Alberti, K. G. M. M. *et al.* Harmonizing the metabolic syndrome: A joint interim statement of the International Diabetes Federation task force on epidemiology and prevention; National Heart, Lung, and Blood Institute;

American Heart Association; World heart federation; International atherosclerosis society; And international association for the study of obesity. *Circulation* **120**, 1640–1645 (2009).

203. Eckel, R. H., Alberti, K., Grundy, S. M. & Zimmet, P. Z. The metabolic syndrome. *Lancet* **375**, 181–183 (2010).
204. Lonardo, A., Ballestri, S., Marchesini, G., Angulo, P. & Loria, P. Nonalcoholic fatty liver disease: a precursor of the metabolic syndrome. *Dig. Liver Dis.* **47**, 181–190 (2015).
205. Marventano, S. *et al.* Coffee and tea consumption in relation with non-alcoholic fatty liver and metabolic syndrome: A systematic review and meta-analysis of observational studies. *Clin. Nutr.* **35**, 1269–1281 (2016).
206. Kennedy, O. J. *et al.* Systematic review with meta-analysis: coffee consumption and the risk of cirrhosis. *Aliment. Pharmacol. Ther.* **43**, 562–574 (2016).
207. Costa, J., Lunet, N., Santos, C., Santos, J. & Vaz-Carneiro, A. Caffeine exposure and the risk of Parkinson's disease: A systematic review and meta-analysis of observational studiess. *J. Alzheimers. Dis.* **20**, S221–S238 (2010).
208. Panza, F. *et al.* Coffee, tea, and caffeine consumption and prevention of late-life cognitive decline and dementia: a systematic review. *J. Nutr. Health Aging* **19**, 313–328 (2015).
209. Santos, C., Costa, J., Santos, J., Vaz-Carneiro, A. & Lunet, N. Caffeine intake and dementia: systematic review and meta-analysis. *J. Alzheimers. Dis.* **20 Suppl 1**, S187-204 (2010).

210. Carman, A. J., Dacks, P. A., Lane, R. F., Shineman, D. W. & Fillit, H. M. Current evidence for the use of coffee and caffeine to prevent age-related cognitive decline and Alzheimer's disease. *J. Nutr. Health Aging* **18**, 383–392 (2014).

211. Nigra, A. D. *et al.* Antitumor effects of freeze-dried Robusta coffee (Coffea canephora) extracts on breast cancer cell lines. *Oxid. Med. Cell. Longev.* **2021**, 5572630 (2021).

212. Bauer, D. *et al.* Effect of roasting levels and drying process of Coffea canephora on the quality of bioactive compounds and cytotoxicity. *Int. J. Mol. Sci.* **19**, 3407 (2018).

213. Je, Y. & Giovannucci, E. Coffee consumption and risk of endometrial cancer: findings from a large up-to-date meta-analysis. *Int. J. Cancer* **131**, 1700–1710 (2012).

214. Arab, L. Epidemiologic evidence on coffee and cancer. *Nutr. Cancer* **62**, 271–283 (2010).

215. Bosso, H., Barbalho, S. M., de Alvares Goulart, R. & Otoboni, A. M. M. B. Green coffee: economic relevance and a systematic review of the effects on human health. *Crit. Rev. Food Sci. Nutr.* 1–17 (2021).

216. van Dam, R. M., Hu, F. B. & Willett, W. C. Coffee, caffeine, and health. *N. Engl. J. Med.* **383**, 369–378 (2020).

217. Grosso, G., Godos, J., Galvano, F. & Giovannucci, E. L. Coffee, caffeine, and health outcomes: An umbrella review. *Annu. Rev. Nutr.* **37**, 131–156 (2017).

218. Committee on Obstetric Practice, American College of Obstetricians and Gynecologists. ACOG committee opinion no. 462. Moderate caffeine consumption during pregnancy. *Obstet. Anesth. Dig.* **31**, 147 (2011).

219. Franca, A. S. & Oliveira, L. S. Coffee Processing Solid Wastes: Current Uses and Future Perspectives. in *Agricultural Wastes* (eds. Ashworth, G. S. & Azevedo, P.) 155–189 (Nova Publishers, 2009).

220. Speer, K. & Kölling-Speer, I. The lipid fraction of the coffee bean. *Braz. J. Plant Physiol.* **18**, 201–216 (2006).

221. Narita, Y. & Inouye, K. Chlorogenic acids from coffee. in *Coffee in Health and Disease Prevention* 189–199 (Elsevier, 2015).

222. Macheiner, L., Schmidt, A., Schreiner, M. & Mayer, H. K. Green coffee infusion as a source of caffeine and chlorogenic acid. *J. Food Compost. Anal.* **84**, 103307 (2019).

223. Daglia, M., Papetti, A., Gregotti, C., Bertè, F. & Gazzani, G. In vitro antioxidant and ex vivo protective activities of green and roasted coffee. *J. Agric. Food Chem.* **48**, 1449–1454 (2000).

224. Madhava Naidu, M., Sulochanamma, G., Sampathu, S. R. & Srinivas, P. Studies on extraction and antioxidant potential of green coffee. *Food Chem.* **107**, 377–384 (2008).

225. Ramalakshmi, K., Rahath Kubra, I. & Jagan Mohan Rao, L. Antioxidant potential of low-grade coffee beans. *Food Res. Int.* **41**, 96–103 (2008).

226. Gawlik-Dziki, U. *et al.* Lipoxygenase inhibitors and antioxidants from green coffee—mechanism of action in the light of potential bioaccessibility. *Food Res. Int.* **61**, 48–55 (2014).

227. Stelmach, E., Pohl, P. & Szymczycha-Madeja, A. The content of Ca, Cu, Fe, Mg and Mn and antioxidant activity of green coffee brews. *Food Chem.* **182**, 302–308 (2015).

228. Andriot, I., Le Quéré, J.-L. & Guichard, E. Interactions between coffee melanoidins and flavour compounds: impact of freeze-drying (method and time) and roasting degree of coffee on melanoidins retention capacity. *Food Chem.* **85**, 289–294 (2004).

229. Spiller, M. A. The Chemical Components of Coffee". in *Caffeine* 97–161 (1998).

230. Speer, K. & Kölling-Speer, I. Non-volatile compounds - lipids. in *Coffee: Recent Developments* (eds. Clarke, R. J. & Vitzhum, O. G.) 33–49 (Blackwell Science, 2001).

231. Franca, A. S., Oliveira, L. S., Mendonça, J. C. F. & Silva, X. A. Physical and chemical attributes of defective crude and roasted coffee beans. *Food Chem.* **90**, 89–94 (2005).

232. Franca, A. S., Mendonça, J. C. F. & Oliveira, S. D. Composition of green and roasted coffees of different cup qualities. *Lebenson. Wiss. Technol.* **38**, 709–715 (2005).

233. Bagdonaite, K., Derler, K. & Murkovic, M. Determination of acrylamide during roasting of coffee. *J. Agric. Food Chem.* **56**, 6081–6086 (2008).

234. Moon, J.-K., Yoo, H. S. & Shibamoto, T. Role of roasting conditions in the level of chlorogenic acid content in coffee beans: correlation with coffee acidity. *J. Agric. Food Chem.* **57**, 5365–5369 (2009).

235. Riedel, A. *et al.* N-methylpyridinium, a degradation product of trigonelline upon coffee roasting, stimulates respiratory activity and promotes glucose utilization in HepG2 cells. *Food Funct.* **5**, 454–462 (2014).

236. Castillo, M. D. del, Gordon, M. H. & Ames, J. M. Peroxyl radical-scavenging activity of coffee brews. *Eur. Food Res. Technol.* **221**, 471–477 (2005).

237. Silveira-Duarte, S. M., Abreu, C. M. P., Castle De Menezes, H., Santos, M. H. & Paivagouvea, C. M. C. Effect of processing and roasting on the antioxidant activity of coffee brews. *Ciência e Tecnologia de Alimentos* **25**, 387–393 (2005).

238. Cämmerer, B. & Kroh, L. W. Antioxidant activity of coffee brews. *Eur. Food Res. Technol.* **223**, 469–474 (2006).

239. Vignoli, J. A., Viegas, M. C., Bassoli, D. G. & Benassi, M. de T. Roasting process affects differently the bioactive compounds and the antioxidant activity of arabica and robusta coffees. *Food Res. Int.* **61**, 279–285 (2014).

240. Nicoli, M. C., Anese, M., Parpinel, M. T., Franceschi, S. & Lerici, C. R. Loss and/or formation of antioxidants during food processing and storage. *Cancer Lett.* **114**, 71–74 (1997).

241. Borrelli, R. C., Visconti, A., Mennella, C., Anese, M. & Fogliano, V. Chemical characterization and antioxidant properties of coffee melanoidins. *J. Agric. Food Chem.* **50**, 6527–6533 (2002).

242. Richelle, M., Tavazzi, I. & Offord, E. Comparison of the antioxidant activity of commonly consumed polyphenolic beverages (coffee, cocoa, and tea) prepared per cup serving. *J. Agric. Food Chem.* **49**, 3438–3442 (2001).

243. Funakoshi-Tago, M. *et al.* Pyrocatechol, a component of coffee, suppresses LPS-induced inflammatory responses by inhibiting NF-κB and activating Nrf2. *Sci. Rep.* **10**, 2584 (2020).

244. Castaldo, L. *et al.* Antioxidant and anti-inflammatory activity of coffee brew evaluated after simulated gastrointestinal digestion. *Nutrients* **13**, 4368 (2021).

245. Castro, A. C. C. M. *et al.* Green coffee seed residue: A sustainable source of antioxidant compounds. *Food Chem.* **246**, 48–57 (2018).

246. Murthy, P. S. & Naidu, M. M. Recovery of phenolic antioxidants and functional compounds from coffee industry by-products. *Food Bioproc. Tech.* **5**, 897–903 (2012).

247. Bresciani, L., Calani, L., Bruni, R., Brighenti, F. & Del Rio, D. Phenolic composition, caffeine content and antioxidant capacity of coffee silverskin. *Food Res. Int.* **61**, 196–201 (2014).

248. Magoni, C. *et al.* Valorizing coffee pulp by-products as anti-inflammatory ingredient of food supplements acting on IL-8 release. *Food Res. Int.* **112**, 129–135 (2018).

249. Farah, A. & Ferreira, T. The coffee plant and beans: An introduction. in *Coffee in health and disease prevention* (2015).

250. Sumner, L. W. *et al.* Proposed minimum reporting standards for chemical analysis Chemical Analysis Working Group (CAWG) Metabolomics Standards Initiative (MSI). *Metabolomics* **3**, 211–221 (2007).

251. Angelino, D., Tassotti, M., Brighenti, F., Del Rio, D. & Mena, P. Niacin, alkaloids and (poly)phenolic compounds in the most widespread Italian capsule-brewed coffees. *Sci. Rep.* **8**, 17874 (2018).

252. Bhagat, A. R. *et al.* Review of the role of fluid dairy in delivery of polyphenolic compounds in the diet: Chocolate milk, coffee beverages, matcha green tea, and beyond. *J. AOAC Int.* **102**, 1365–1372 (2019).

253. Nogaim, Q. A. *et al.* Protective effect of Yemeni green coffee powder against the oxidative stress induced by Ochratoxin A. *Toxicol. Rep.* **7**, 142–148 (2020).

254. Cosola, C., Sabatino, A., di Bari, I., Fiaccadori, E. & Gesualdo, L. Nutrients, nutraceuticals, and xenobiotics affecting renal health. *Nutrients* **10**, (2018).

255. Rajaram, S., Jones, J. & Lee, G. J. Plant-based dietary patterns, plant foods, and age-related cognitive decline. *Adv. Nutr.* **10**, S422–S436 (2019).

256. Li, H.-Y. *et al.* Plant-based foods and their bioactive compounds on fatty liver disease: Effects, mechanisms, and clinical application. *Oxid. Med. Cell. Longev.* **2021**, 6621644 (2021).

257. Ludwig, I. A., Clifford, M. N., Lean, M. E. J., Ashihara, H. & Crozier, A. Coffee: biochemistry and potential impact on health. *Food Funct.* **5**, 1695–1717 (2014).

258. Socała, K., Szopa, A., Serefko, A., Poleszak, E. & Wlaź, P. Neuroprotective effects of coffee bioactive compounds: A review. *Int. J. Mol. Sci.* **22**, 107 (2020).

259. Klingel, T. *et al.* A review of coffee by-products including leaf, flower, cherry, husk, silver skin, and spent grounds as novel foods within the European Union. *Foods* **9**, 665 (2020).

260. Manalo, R. V. M. & Medina, P. M. B. Caffeine protects dopaminergic neurons from dopamine-induced neurodegeneration via synergistic adenosine-dopamine D2-like receptor interactions in transgenic Caenorhabditis elegans. *Front. Neurosci.* **12**, 137 (2018).

261. Eskelinen, M. H. & Kivipelto, M. Caffeine as a protective factor in dementia and Alzheimer's disease. *J. Alzheimers. Dis.* **20 Suppl 1**, S167-74 (2010).

262. Katz, S. N. Decaffeination of Coffee. in *Coffee: Volume 2: Technology* (eds. Clarke, R. J. & Macrae, R.) 59–71 (Springer Netherlands, 1987).

263. Sangiovanni, E., Brivio, P., Dell'Agli, M. & Calabrese, F. Botanicals as modulators of neuroplasticity: Focus on BDNF. *Neural Plast.* **2017**, 5965371 (2017).

264. Ghule, A. E., Jadhav, S. S. & Bodhankar, S. L. Trigonelline ameliorates diabetic hypertensive nephropathy by suppression of oxidative stress in kidney and

reduction in renal cell apoptosis and fibrosis in streptozotocin induced neonatal diabetic (nSTZ) rats. *Int. Immunopharmacol.* **14**, 740–748 (2012).

265. Ilavenil, S. *et al.* Trigonelline attenuates the adipocyte differentiation and lipid accumulation in 3T3-L1 cells. *Phytomedicine* **21**, 758–765 (2014).
266. Makowska, J. *et al.* Preliminary studies on trigonelline as potential anti-Alzheimer disease agent: determination by hydrophilic interaction liquid chromatography and modeling of interactions with beta-amyloid. *J. Chromatogr. B Analyt. Technol. Biomed. Life Sci.* **968**, 101–104 (2014).
267. Stadler, R. H., Varga, N., Hau, J., Vera, F. A. & Welti, D. H. Alkylpyridiniums. 1. Formation in model systems via thermal degradation of trigonelline. *J. Agric. Food Chem.* **50**, 1192–1199 (2002).
268. Perrone, D., Donangelo, C. M. & Farah, A. Fast simultaneous analysis of caffeine, trigonelline, nicotinic acid and sucrose in coffee by liquid chromatography-mass spectrometry. *Food Chem.* **110**, 1030–1035 (2008).
269. Urgert, R. & Katan, M. B. The cholesterol-raising factor from coffee beans. *Annu. Rev. Nutr.* **17**, 305–324 (1997).
270. Jee, S. H. *et al.* Coffee consumption and serum lipids: a meta-analysis of randomized controlled clinical trials. *Am. J. Epidemiol.* **153**, 353–362 (2001).
271. Ren, Y., Wang, C., Xu, J. & Wang, S. Cafestol and kahweol: A review on their bioactivities and pharmacological properties. *Int. J. Mol. Sci.* **20**, 4238 (2019).

272. Smrke, S., Kroslakova, I., Gloess, A. N. & Yeretzian, C. Differentiation of degrees of ripeness of Catuai and Tipica green coffee by chromatographical and statistical techniques. *Food Chem.* **174**, 637–642 (2015).

273. Pimpley, V., Patil, S., Srinivasan, K., Desai, N. & Murthy, P. S. The chemistry of chlorogenic acid from green coffee and its role in attenuation of obesity and diabetes. *Prep. Biochem. Biotechnol.* **50**, 969–978 (2020).

274. Jaiswal, R., Matei, M. F., Golon, A., Witt, M. & Kuhnert, N. Understanding the fate of chlorogenic acids in coffee roasting using mass spectrometry based targeted and non-targeted analytical strategies. *Food Funct.* **3**, 976–984 (2012).

275. Tajik, N., Tajik, M., Mack, I. & Enck, P. The potential effects of chlorogenic acid, the main phenolic components in coffee, on health: a comprehensive review of the literature. *Eur. J. Nutr.* **56**, 2215–2244 (2017).

276. Perrone, D., Farah, A. & Donangelo, C. M. Influence of coffee roasting on the incorporation of phenolic compounds into melanoidins and their relationship with antioxidant activity of the brew. *J. Agric. Food Chem.* **60**, 4265–4275 (2012).

277. Vitaglione, P. *et al.* Coffee reduces liver damage in a rat model of steatohepatitis: the underlying mechanisms and the role of polyphenols and melanoidins. *Hepatology* **52**, 1652–1661 (2010).

278. Iriondo-DeHond, A., Rodríguez Casas, A. & Del Castillo, M. D. Interest of coffee melanoidins as sustainable healthier food ingredients. *Front. Nutr.* **8**, 730343 (2021).

279. Daglia, M. *et al.* Antiadhesive effect of green and roasted coffee on Streptococcus mutans' adhesive properties on saliva-coated hydroxyapatite beads. *J. Agric. Food Chem.* **50**, 1225–1229 (2002).

280. Walker, J. M. *et al.* Melanoidins from coffee and bread differently influence energy intake: A randomized controlled trial of food intake and gut-brain axis response. *J. Funct. Foods* **72**, 104063 (2020).

281. Zhang, H., Zhang, H., Troise, A. D. & Fogliano, V. Melanoidins from coffee, cocoa, and bread are able to scavenge α-dicarbonyl compounds under simulated physiological conditions. *J. Agric. Food Chem.* **67**, 10921–10929 (2019).

282. Ribeiro, E., Rocha, T. de S. & Prudencio, S. H. Potential of green and roasted coffee beans and spent coffee grounds to provide bioactive peptides. *Food Chem.* **348**, 129061 (2021).

283. Fredholm, B. B., Bättig, K., Holmén, J., Nehlig, A. & Zvartau, E. E. Actions of caffeine in the brain with special reference to factors that contribute to its widespread use. *Pharmacol. Rev.* **51**, 83–133 (1999).

284. Chavez Valdez, R. *et al.* Correlation between serum caffeine levels and changes in cytokine profile in a cohort of preterm infants. *J. Pediatr.* **158**, 57–64, 64.e1 (2011).

285. Velázquez, A. M. *et al.* Effects of a Low Dose of Caffeine Alone or as Part of a Green Coffee Extract, in a Rat Dietary Model of Lean Non-Alcoholic Fatty Liver Disease without Inflammation. *Nutrients* **12**, (2020).

286. Kovács, E. G. *et al.* Caffeine has different immunomodulatory effect on the cytokine expression and NLRP3 inflammasome function in various human macrophage subpopulations. *Nutrients* **13**, 2409 (2021).

287. Quarta, S. *et al.* Coffee bioactive N-methylpyridinium attenuates tumor necrosis factor (TNF)-α-mediated insulin resistance and inflammation in human adipocytes. *Biomolecules* **11**, 1545 (2021).

288. Kim, J. Y., Jung, K. S. & Jeong, H. G. Suppressive effects of the kahweol and cafestol on cyclooxygenase-2 expression in macrophages. *FEBS Lett.* **569**, 321–326 (2004).

289. Shen, T., Park, Y. C., Kim, S. H., Lee, J. & Cho, J. Y. Nuclear factor-kappaB/signal transducers and activators of transcription-1-mediated inflammatory responses in lipopolysaccharide-activated macrophages are a major inhibitory target of kahweol, a coffee diterpene. *Biol. Pharm. Bull.* **33**, 1159–1164 (2010).

290. Kim, J. Y. *et al.* The coffee diterpene kahweol suppress the inducible nitric oxide synthase expression in macrophages. *Cancer Lett.* **213**, 147–154 (2004).

291. Moon, J.-K. & Shibamoto, T. Formation of volatile chemicals from thermal degradation of less volatile coffee components: quinic acid, caffeic acid, and chlorogenic acid. *J. Agric. Food Chem.* **58**, 5465–5470 (2010).

292. Palmioli, A. *et al.* Natural Compounds in Cancer Prevention: Effects of Coffee Extracts and Their Main Polyphenolic Component, 5-O-Caffeoylquinic Acid, on Oncogenic Ras Proteins. *Chem.--Asian J.* **12**, 2457–2466 (2017).

293. Ciaramelli, C., Palmioli, A. & Airoldi, C. Coffee variety, origin and extraction procedure: Implications for coffee beneficial effects on human health. *Food Chem.* **278**, 47–55 (2019).

294. mestrelab. SMA - Mestrelab. https://mestrelab.com/software/mnova/sma/.

295. Airoldi, C. SMA libraries for metabolite identification and quantification in coffee extracts. (2018) doi:10.17632/fs3vf7jbg5.1.

296. Arana, V. A. *et al.* Coffee's country of origin determined by NMR: the Colombian case. *Food Chem.* **175**, 500–506 (2015).

297. Consonni, R., Cagliani, L. R. & Cogliati, C. NMR based geographical characterization of roasted coffee. *Talanta* **88**, 420–426 (2012).

298. Wei, F., Furihata, K., Hu, F., Miyakawa, T. & Tanokura, M. Two-Dimensional 1H–13C Nuclear Magnetic Resonance (NMR)-Based Comprehensive Analysis of Roasted Coffee Bean Extract. *J. Agric. Food Chem.* **59**, 9065–9073 (2011).

299. Akira, S. & Takeda, K. Toll-like receptor signalling. *Nature Reviews Immunology* vol. 4 499–511 (2004).

300. Satoh, T. & Akira, S. Toll-Like Receptor Signaling and Its Inducible Proteins. *Microbiology Spectrum* vol. 4 (2016).

301. Weber, L., Hammoud Mahdi, D., Jankuhn, S., Lipowicz, B. & Vissiennon, C. Bioactive Plant Compounds in Coffee Charcoal (Coffeae carbo) Extract Inhibit Cytokine Release from Activated Human THP-1 Macrophages. *Molecules* **24**, (2019).

302. Choi, S., Jung, S. & Ko, K. S. Effects of Coffee Extracts with Different Roasting Degrees on Antioxidant and Anti-Inflammatory Systems in Mice. *Nutrients* **10**, (2018).

303. Perrone, D., Donangelo, R., Donangelo, C. M. & Farah, A. Modeling weight loss and chlorogenic acids content in coffee during roasting. *J. Agric. Food Chem.* **58**, 12238–12243 (2010).

304. Cano-Marquina, A., Tarín, J. J. & Cano, A. The impact of coffee on health. *Maturitas* **75**, 7–21 (2013).

305. Del Rio, D., Stalmach, A., Calani, L. & Crozier, A. Bioavailability of Coffee Chlorogenic Acids and Green Tea Flavan-3-ols. *Nutrients* **2**, 820–833 (2010).

306. Perrone, D., Farah, A., Donangelo, C. M., de Paulis, T. & Martin, P. R. Comprehensive analysis of major and minor chlorogenic acids and lactones in economically relevant Brazilian coffee cultivars. *Food Chem.* **106**, 859–867 (2008).

307. Manach, C., Scalbert, A., Morand, C., Rémésy, C. & Jiménez, L. Polyphenols: food sources and bioavailability. *Am. J. Clin. Nutr.* **79**, 727–747 (2004).

308. Plazas, M. *et al.* Breeding for chlorogenic acid content in eggplant: Interest and prospects. *Not. Bot. Horti Agrobot. Cluj Napoca* **41**, 26 (2013).

309. Kumar, R., Sharma, A., Iqbal, M. S. & Srivastava, J. K. Therapeutic promises of chlorogenic acid with special emphasis on its anti-obesity property. *Curr. Mol. Pharmacol.* **13**, 7–16 (2020).

310. Lu, H., Tian, Z., Cui, Y., Liu, Z. & Ma, X. Chlorogenic acid: A comprehensive review of the dietary sources, processing effects, bioavailability, beneficial properties, mechanisms of action, and future directions. *Compr. Rev. Food Sci. Food Saf.* **19**, 3130–3158 (2020).

311. Olthof, M. R., Hollman, P. C. H., Buijsman, M. N. C. P., van Amelsvoort, J. M. M. & Katan, M. B. Chlorogenic acid, quercetin-3-rutinoside and black tea phenols are extensively metabolized in humans. *J. Nutr.* **133**, 1806–1814 (2003).

312. Olthof, M. R., Hollman, P. C. & Katan, M. B. Chlorogenic acid and caffeic acid are absorbed in humans. *J. Nutr.* **131**, 66–71 (2001).

313. Montavon, P., Duruz, E., Rumo, G. & Pratz, G. Evolution of green coffee protein profiles with maturation and relationship to coffee cup quality. *J. Agric. Food Chem.* **51**, 2328–2334 (2003).

314. Natella, F., Nardini, M., Di Felice, M. & Scaccini, C. Benzoic and cinnamic acid derivatives as antioxidants: structure-activity relation. *J. Agric. Food Chem.* **47**, 1453–1459 (1999).

315. Del Rio, D. *et al.* Dietary (poly)phenolics in human health: structures, bioavailability, and evidence of protective effects against chronic diseases. *Antioxid. Redox Signal.* **18**, 1818–1892 (2013).

316. Naveed, M. *et al.* Chlorogenic acid (CGA): A pharmacological review and call for further research. *Biomed. Pharmacother.* **97**, 67–74 (2018).

317. Roshan, H., Nikpayam, O., Sedaghat, M. & Sohrab, G. Effects of green coffee extract supplementation on anthropometric indices, glycaemic control, blood pressure, lipid profile, insulin resistance and appetite in patients with the metabolic syndrome: a randomised clinical trial. *Br. J. Nutr.* **119**, 250–258 (2018).

318. Cho, A.-S. *et al.* Chlorogenic acid exhibits anti-obesity property and improves lipid metabolism in high-fat diet-induced-obese mice. *Food Chem. Toxicol.* **48**, 937–943 (2010).

319. Huang, K., Liang, X.-C., Zhong, Y.-L., He, W.-Y. & Wang, Z. 5-Caffeoylquinic acid decreases diet-induced obesity in rats by modulating PPARα and LXRα transcription. *J. Sci. Food Agric.* **95**, 1903–1910 (2015).

320. Song, S. J., Choi, S. & Park, T. Decaffeinated green coffee bean extract attenuates diet-induced obesity and insulin resistance in mice. *Evid. Based. Complement. Alternat. Med.* **2014**, 718379 (2014).

321. Wan, C.-W. *et al.* Chlorogenic acid exhibits cholesterol lowering and fatty liver attenuating properties by up-regulating the gene expression of PPAR-α in hypercholesterolemic rats induced with a high-cholesterol diet. *Phytother. Res.* **27**, 545–551 (2013).

322. Botto, L. *et al.* Study of the antioxidant effects of coffee phenolic metabolites on C6 glioma cells exposed to diesel exhaust particles. *Antioxidants (Basel)* **10**, 1169 (2021).

323. Amano, Y. *et al.* Safety pharmacological evaluation of the coffee component, caffeoylquinic acid, and its metabolites, using ex vivo and in vitro profiling assays. *Pharmaceuticals (Basel)* **12**, 110 (2019).

324. Park, S. H. *et al.* IRAK4 as a molecular target in the amelioration of innate immunity-related endotoxic shock and acute liver injury by chlorogenic acid. *J. Immunol.* **194**, 1122–1130 (2015).

325. Krakauer, T. The polyphenol chlorogenic acid inhibits staphylococcal exotoxin-induced inflammatory cytokines and chemokines. *Immunopharmacol. Immunotoxicol.* **24**, 113–119 (2002).

326. Radnai, B. *et al.* Ferulaldehyde, a water-soluble degradation product of polyphenols, inhibits the lipopolysaccharide-induced inflammatory response in mice. *J. Nutr.* **139**, 291–297 (2009).

327. Ghosh, S. & Karin, M. Missing pieces in the NF-κB puzzle. *Cell* **109**, S81–S96 (2002).

328. Shimada, T. *et al.* IKK-i, a novel lipopolysaccharide-inducible kinase that is related to IkappaB kinases. *Int. Immunol.* **11**, 1357–1362 (1999).

329. Moynagh, P. N. TLR signalling and activation of IRFs: revisiting old friends from the NF-kappaB pathway. *Trends Immunol.* **26**, 469–476 (2005).

330. Qin, H., Wilson, C. A., Lee, S. J., Zhao, X. & Benveniste, E. N. LPS induces CD40 gene expression through the activation of NF-kappaB and STAT-1alpha in macrophages and microglia. *Blood* **106**, 3114–3122 (2005).

331. Saturnino, C. *et al.* Anti-inflammatory, antioxidant and crystallographic studies of N-palmitoyl-ethanol Amine (PEA) derivatives. *Molecules* **22**, 616 (2017).

332. Kuehl, F. A., Jr, Jacob, T. A., Ganley, O. H., Ormond, R. E. & Meisinger, M. A. P. The identification of n-(2-hydroxyethyl)-palmitamide as a naturally occurring anti-inflammatory agent. *J. Am. Chem. Soc.* **79**, 5577–5578 (1957).

333. Petrosino, S. & Di Marzo, V. The pharmacology of palmitoylethanolamide and first data on the therapeutic efficacy of some of its new formulations. *Br. J. Pharmacol.* **174**, 1349–1365 (2017).

334. Russo, R. *et al.* Gut-brain Axis: Role of Lipids in the Regulation of Inflammation, Pain and CNS Diseases. *Curr. Med. Chem.* **25**, 3930–3952 (2018).

335. Cordaro, M., Cuzzocrea, S. & Crupi, R. An Update of Palmitoylethanolamide and Luteolin Effects in Preclinical and Clinical Studies of Neuroinflammatory Events. *Antioxidants (Basel)* **9**, (2020).

336. Aloe, L., Leon, A. & Levi-Montalcini, R. A proposed autacoid mechanism controlling mastocyte behaviour. *Agents Actions* **39 Spec No**, C145-7 (1993).

337. Iannotti, F. A., Di Marzo, V. & Petrosino, S. Endocannabinoids and endocannabinoid-related mediators: Targets, metabolism and role in neurological disorders. *Prog. Lipid Res.* **62**, 107–128 (2016).

338. Hoareau, L. *et al.* Anti-inflammatory effect of palmitoylethanolamide on human adipocytes. *Obesity (Silver Spring)* **17**, 431–438 (2009).

339. Impellizzeri, D. *et al.* The anti-inflammatory effects of palmitoylethanolamide (PEA) on endotoxin-induced uveitis in rats. *Eur. J. Pharmacol.* **761**, 28–35 (2015).

340. Perry, V. H. & Teeling, J. Microglia and macrophages of the central nervous system: the contribution of microglia priming and systemic inflammation to chronic neurodegeneration. *Semin. Immunopathol.* **35**, 601–612 (2013).

341. Olah, M., Biber, K., Vinet, J. & Boddeke, H. W. G. M. Microglia phenotype diversity. *CNS Neurol. Disord. Drug Targets* **10**, 108–118 (2011).

342. Prinz, M., Tay, T. L., Wolf, Y. & Jung, S. Microglia: unique and common features with other tissue macrophages. *Acta Neuropathol.* **128**, 319–331 (2014).

343. Eggen, B. J. L., Raj, D., Hanisch, U.-K. & Boddeke, H. W. G. M. Microglial phenotype and adaptation. *J. Neuroimmune Pharmacol.* **8**, 807–823 (2013).

344. Cherry, J. D., Olschowka, J. A. & O'Banion, M. K. Neuroinflammation and M2 microglia: the good, the bad, and the inflamed. *J. Neuroinflammation* **11**, 98 (2014).

345. Boche, D., Perry, V. H. & Nicoll, J. A. R. Review: activation patterns of microglia and their identification in the human brain. *Neuropathol. Appl. Neurobiol.* **39**, 3–18 (2013).

346. Yamasaki, R. *et al.* Differential roles of microglia and monocytes in the inflamed central nervous system. *J. Exp. Med.* **211**, 1533–1549 (2014).

347. Vainchtein, I. D. *et al.* In acute experimental autoimmune encephalomyelitis, infiltrating macrophages are immune activated, whereas microglia remain immune suppressed. *Glia* **62**, 1724–1735 (2014).

348. Andersson, P. B., Perry, V. H. & Gordon, S. The acute inflammatory response to lipopolysaccharide in CNS parenchyma differs from that in other body tissues. *Neuroscience* **48**, 169–186 (1992).

349. Casili, G. *et al.* Synergic therapeutic potential of PEA-um treatment and NAAA enzyme silencing in the management of neuroinflammation. *Int. J. Mol. Sci.* **21**, 7486 (2020).

350. Costa, B. *et al.* Targeting mast cells in neuropathic pain with the endogenous modulator palmitoylethanolamide. *J. Peripher. Nerv. Syst.* **14**, (2009).

351. Donvito, G., Bettoni, I., Comelli, F., Colombo, A. & Costa, B. Palmitoylethanolamide relieves pain and preserves pancreatic islet cells in a murine model of diabetes. *CNS Neurol. Disord. Drug Targets* **14**, 452–462 (2015).

352. Bettoni, I., Comelli, F., Colombo, A., Bonfanti, P. & Costa, B. Non-neuronal cell modulation relieves neuropathic pain: efficacy of the endogenous lipid palmitoylethanolamide. *CNS Neurol. Disord. Drug Targets* **12**, 34–44 (2013).

353. Skaper, S. D. *et al.* Palmitoylethanolamide, a naturally occurring disease-modifying agent in neuropathic pain. *Inflammopharmacology* **22**, 79–94 (2014).

354. Costa, B., Conti, S., Giagnoni, G. & Colleoni, M. Therapeutic effect of the endogenous fatty acid amide, palmitoylethanolamide, in rat acute inflammation: inhibition of nitric oxide and cyclo-oxygenase systems. *Br. J. Pharmacol.* **137**, 413–420 (2002).

355. Conti, S., Costa, B., Colleoni, M., Parolaro, D. & Giagnoni, G. Antiinflammatory action of endocannabinoid palmitoylethanolamide and the synthetic cannabinoid nabilone in a model of acute inflammation in the rat. *Br. J. Pharmacol.* **135**, 181–187 (2002).

356. Costa, B., Comelli, F., Bettoni, I., Colleoni, M. & Giagnoni, G. The endogenous fatty acid amide, palmitoylethanolamide, has anti-allodynic and anti-hyperalgesic effects in a murine model of neuropathic pain: involvement of CB(1), TRPV1 and PPARgamma receptors and neurotrophic factors. *Pain* **139**, 541–550 (2008).

357. D'Aloia, A. *et al.* Palmitoylethanolamide Modulation of Microglia Activation: Characterization of Mechanisms of Action and Implication for Its Neuroprotective Effects. *Int. J. Mol. Sci.* **22**, (2021).

358. Wink, M. Modes of action of herbal medicines and plant secondary metabolites. *Medicines (Basel)* **2**, 251–286 (2015).

359. Bresciani, L. *et al.* Absorption, pharmacokinetics, and urinary excretion of pyridines after consumption of coffee and cocoa-based products containing coffee in a repeated dose, crossover human intervention study. *Mol. Nutr. Food Res.* **64**, e2000489 (2020).

360. Mena, P. *et al.* Effect of different patterns of consumption of coffee and a cocoa-based product containing coffee on the nutrikinetics and urinary excretion of phenolic compounds. *Am. J. Clin. Nutr.* **114**, 2107–2118 (2021).

361. Favari, C. *et al.* Metabolomic changes after coffee consumption: New paths on the block. *Mol. Nutr. Food Res.* **65**, e2000875 (2021).

362. Mena, P. *et al.* A comprehensive approach to the bioavailability and cardiometabolic effects of the bioactive compounds present in espresso coffee and confectionery-derived coffee. *Proc. Nutr. Soc.* **79**, (2020).

363. Mena, P. *et al.* The Pocket-4-Life project, bioavailability and beneficial properties of the bioactive compounds of espresso coffee and cocoa-based confectionery containing coffee: study protocol for a randomized cross-over trial. *Trials* **18**, 527 (2017).

364. Ovais, M., Guo, M. & Chen, C. Tailoring nanomaterials for targeting tumor-associated macrophages. *Adv. Mater.* **31**, e1808303 (2019).

365. Newman, D. J. & Cragg, G. M. Natural products as sources of new drugs from 1981 to 2014. *J. Nat. Prod.* **79**, 629–661 (2016).

9. AKNOWLEDGEMENTS

Appendix I

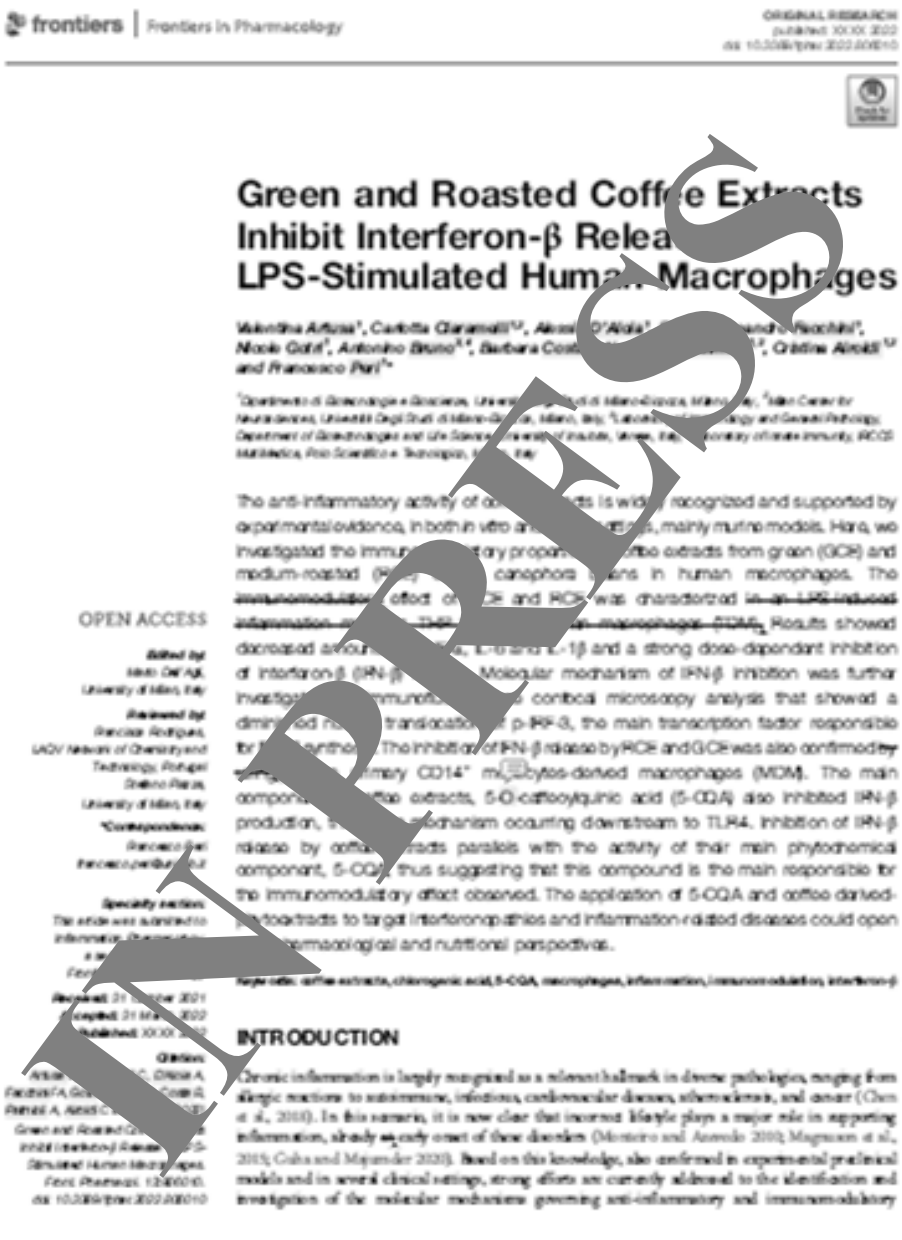

frontiers | Frontiers in Pharmacology

ORIGINAL RESEARCH

Green and Roasted Coffee Extracts Inhibit Interferon-β Release in LPS-Stimulated Human Macrophages

Valentina Artusa[1], Carlotta Caramelli[1,2], Alessia D'Alvia[1], Nicole Gold[3], Antonino Bruno[3,4], Barbara Costa[1], Cristina Airoldi[1,2] and Francesco Peri[1,2]*

[1]Department of Biotechnology and Biosciences, University of Milano-Bicocca, Milano, Italy, [2]Milan Center for Neuroscience, Università degli Studi di Milano-Bicocca, Milano, Italy, [3]Laboratory of Allergology and General Pathology, Department of Biomedicine and Life Sciences, University of Insubria, Varese, Italy, [4]Laboratory of Innate Immunity, IRCCS Humanitas, Pieve Emanuele e Tecnologie, [illegible] Italy

The anti-inflammatory activity of coffee extracts is widely recognized and supported by experimental evidence, in both in vitro and in vivo models, mainly murine models. Here, we investigated the immunomodulatory properties of coffee extracts from green (GCE) and medium-roasted (RCE) Coffea canephora beans in human macrophages. The immunomodulatory effect of GCE and RCE was characterized in an LPS-induced inflammation model on THP1-derived macrophage-like cells (TDMs). Results showed decreased amounts of TNF-α, IL-6 and IL-1β and a strong dose-dependent inhibition of interferon-β (IFN-β) release. Molecular mechanism of IFN-β inhibition was further investigated by immunofluorescence confocal microscopy analysis that showed a diminished nuclear translocation of p-IRF-3, the main transcription factor responsible for IFN-β synthesis. The inhibition of IFN-β release by RCE and GCE was also confirmed by experiments on primary CD14+ monocytes-derived macrophages (MDM). The main component of coffee extracts, 5-O-caffeoylquinic acid (5-CQA) also inhibited IFN-β production, suggesting a mechanism occurring downstream to TLR4. Inhibition of IFN-β release by coffee extracts parallels with the activity of their main phytochemical component, 5-CQA, thus suggesting that this compound is the main responsible for the immunomodulatory effect observed. The application of 5-CQA and coffee derived-phytoextracts to target interferonopathies and inflammation-related diseases could open [illegible] pharmacological and nutritional perspectives.

Keywords: coffee extracts, chlorogenic acid, 5-CQA, macrophages, inflammation, immunomodulation, interferon-β

Edited by:
Mario Dell'Agli,
University of Milan, Italy

Reviewed by:
Patrícia Rijo,
LAQV Network of Chemistry and Technology, Portugal
Stefano Piazza,
University of Milan, Italy

***Correspondence:**
Francesco Peri
francesco.peri@unimib.it

Specialty section:
This article was submitted to Inflammation Pharmacology, a section of the journal Frontiers in Pharmacology

Received: 21 October 2021
Accepted: 31 March 2022
Published: XXXX 2022

Citation:
Artusa V, Caramelli C, D'Alvia A, Gold N, Bruno A, Costa B, Airoldi C and Peri F (2022) Green and Roasted Coffee Extracts Inhibit Interferon-β Release in LPS-Stimulated Human Macrophages. Front. Pharmacol. 13:XXXXXX. doi: 10.3389/fphar.2022.XXXXXX

INTRODUCTION

Chronic inflammation is largely recognized as a relevant hallmark in diverse pathologies, ranging from allergic reactions to autoimmune, infectious, cardiovascular diseases, atherosclerosis, and cancer (Chen et al., 2018). In this scenario, it is now clear that incorrect lifestyle plays a major role in supporting inflammation, already at early onset of these disorders (Monteiro and Azevedo 2010; Magnusson et al., 2015; Cuba and Majumder 2020). Based on this knowledge, also confirmed in experimental preclinical models and in several clinical settings, strong efforts are currently addressed to the identification and investigation of the molecular mechanisms governing anti-inflammatory and immunomodulatory

Appendix II

International Journal of *Molecular Sciences*

MDPI

Article

Palmitoylethanolamide Modulation of Microglia Activation: Characterization of Mechanisms of Action and Implication for Its Neuroprotective Effects

Alessia D'Aloia [1,†], Laura Molteni [2,†], Francesca Gullo [1], Elena Bresciani [2], Valentina Artusa [1], Laura Rizzi [2], Michela Ceriani [1], Ramona Meanti [2], Marzia Lecchi [1], Silvia Coco [2], Barbara Costa [1,*] and Antonio Torsello [2,*]

[1] Department of Biotechnology and Biosciences, University of Milano-Bicocca, 20126 Milano, Italy; alessia.daloia@unimib.it (A.D.); francesca.gullo@unimib.it (F.G.); v.artusa@campus.unimib.it (V.A.); michela.ceriani@unimib.it (M.C.); marzia.lecchi1@unimib.it (M.L.)

[2] School of Medicine and Surgery, University of Milano-Bicocca, 20900 Monza, Italy; laura.molteni@unimib.it (L.M.); elena.bresciani@unimib.it (E.B.); laura.rizzi@unimib.it (L.R.); r.meanti@campus.unimib.it (R.M.); silvia.coco@unimib.it (S.C.)

* Correspondence: barbara.costa@unimib.it (B.C.); antonio.torsello@unimib.it (A.T.)

† These authors contributed equally to the work.

Abstract: Palmitoylethanolamide (PEA) is an endogenous lipid produced on demand by neurons and glial cells that displays neuroprotective properties. It is well known that inflammation and neuronal damage are strictly related processes and that microglia play a pivotal role in their regulation. The aim of the present work was to assess whether PEA could exert its neuroprotective and anti-inflammatory effects through the modulation of microglia reactive phenotypes. In N9 microglial cells, the pre-incubation with PEA blunted the increase of M1 pro-inflammatory markers induced by lipopolysaccharide (LPS), concomitantly increasing those M2 anti-inflammatory markers. Images of microglial cells were processed to obtain a set of morphological parameters that highlighted the ability of PEA to inhibit the LPS-induced M1 polarization and suggested that PEA might induce the anti-inflammatory M2a phenotype. Functionally, PEA prevented Ca^{2+} transients in both N9 cells and primary microglia and antagonized the neuronal hyperexcitability induced by LPS, as revealed by multi-electrode array (MEA) measurements on primary cortical cultures of neurons, microglia, and astrocyte. Finally, the investigation of the molecular pathway indicated that PEA effects are not mediated by toll-like receptor 4 (TLR4); on the contrary, a partial involvement of cannabinoid type 2 receptor (CB2R) was shown by using a selective receptor inverse agonist.

Keywords: palmitoylethanolamide; microglia; morphotypes; neuroinflammation; cytokines; cannabinoid receptor; LPS; electrophysiology

check for updates

Citation: D'Aloia, A.; Molteni, L.; Gullo, F.; Bresciani, E.; Artusa, V.; Rizzi, L.; Ceriani, M.; Meanti, R.; Lecchi, M.; Coco, S.; et al. Palmitoylethanolamide Modulation of Microglia Activation Characterization of Mechanisms of Action and Implication for Its Neuroprotective Effects. *Int. J. Mol. Sci.* **2021**, *22*, 3054. https://doi.org/10.3390/ijms22063054

Academic Editor: Stefania Petrosino

Received: 1 March 2021
Accepted: 15 March 2021
Published: 17 March 2021

Publisher's Note: MDPI stays neutral with regard to jurisdictional claims in published maps and institutional affiliations.

1. Introduction

Microglia are resident macrophage-like cells of the central nervous system (CNS). For a long time, they were considered to be quiescent in healthy conditions, becoming activated in pathological situations. However, it is now accepted that microglia in "resting" state participate in fundamental aspects of neuronal homeostasis and act to surveil the CNS; this surveillant/non-polarized phenotype is also known as M0 [1]. Upon injury, microglia become activated, switching between pro-inflammatory (M1) phenotype, producing cytokines such as tumor necrosis factor alpha (TNF-α) and interleukin-1 beta (IL-1β), and anti-inflammatory/neuroprotective (M2) phenotype, expressing interleukin-10 (IL-10). M2 microglia are further characterized into sub-classificatices: anti-inflammatory (M2a), inflammation modulatory (M2b), and immunosuppressive (M2c), even if microglia phenotype is not absolute since microglial cells show high plasticity [2]. The presence of multiple activation phenotypes for microglia is a relatively new concept; therefore, the roles they

play are still not fully characterized. However, it is well established that during chronic neuroinflammation, which underlies many neurodegenerative diseases, microglial cells are continually activated by proinflammatory stimuli. These chronically activated microglia will continue to produce inflammatory cytokines and reactive oxygen/nitrogen species, which lead to neuronal death [3]. This makes microglia modulation an attractive therapeutic tool in pathological conditions where detrimental polarization may contribute to disease. Thus, the identification of compounds acting as microglia modulators, i.e., able not only to prevent the detrimental proinflammatory phenotype, but also to promote the beneficial alternative phenotype, can be a therapeutic tool to mitigate various neuro-pathologies that share chronic microglia hyper-reactivity (Alzheimer's disease, multiple sclerosis, stroke).

Palmitoylethanolamide (PEA) belongs to the class of the *N*-acylethanolamine and is an endogenous lipid potentially useful in a wide range of therapeutic areas. PEA is produced on-demand by neurons and glial cells in the CNS and is involved in the endogenous neuroprotective mechanisms that are activated following tissue damage or inflammation [4], suggesting that its exogenous contribution may favor the process of resolution of inflammation and the restoration of tissue homeostasis. Many studies have demonstrated that the anti-inflammatory property of PEA is accomplished through the inhibition of the release of pro-inflammatory molecules from mast cells and macrophages [5,6]. More recently, the PEA ability to induce microglia changes associated with increased migration and phagocytic activity has been reported [7]. Even though some studies have suggested that PEA can exert its neuroprotective effect through the microglia modulation, no extensive characterization has been done. The aim of this study was to assess whether PEA could control microglia polarization in order to furnish further insights on endogenous PEA protective and pro-homeostatic mechanism and to suggest its exogenous administration as a useful pharmacological tool for controlling neuroinflammatory conditions.

In this work, we studied the effect of PEA on lipopolysaccharide (LPS)-induced microglia activation by (1) evaluating the markers defining microglia phenotypes; (2) performing a morphometric analysis, which is considered as a valuable method to better understand form and function relationships in microglia; (3) analyzing the microglial Ca^{2+} signals as a rapid functional tool of microglia activation; (4) assessing neuron–glia cross-talk through the multi-electrode array (MEA) recording method; and (5) studying the possible receptor involved.

2. Results

2.1. PEA Pre-Treatment Counteracts M1 Microglia Polarization Induced by LPS Treatment

The effects of PEA were first assessed on the pro-inflammatory activity of LPS in N9 microglia cells. Dose-response and time-course experiments were first performed to select the optimal concentration of PEA and incubation time to be used. The results of these preliminary experiments indicated that 100 µM PEA, administered 1 h before LPS treatment, was the best condition to observe reduction of the effects induced by LPS. These conditions were maintained in the subsequent experiments. The activation states of microglia were assessed by measuring the levels of inducible nitric oxide synthase (iNOS), a M1 marker, and those of arginase-1 (Arg1), a M2a marker, in N9 cells incubated for 6 h with LPS. Levels of iNOS and Arg1 were measured by Western blot. LPS significantly increased iNOS levels and concomitantly inhibited those of Arg1 compared to controls (Figure 1A). The LPS-induced iNOS increase was significantly blunted in cells pre-treated with 100 µM PEA for 1 h (Figure 1B). Of particular interest is that PEA pre-treatment antagonized LPS-induced Arg1 reduction and restored it to control values (Figure 1B). Given that the increase of Arg1 is considered a specific marker of the subtype anti-inflammatory M2a phenotype, these data highlight the ability of PEA to inhibit the LPS-induced M1 polarization of microglia and suggest that PEA might induce a M2a phenotype upon injury. To further strengthen these hypotheses, N9 cells were treated with 100 µM PEA alone for 1 h (Figure S1), and results demonstrated a trend toward an increase in Arg1 levels, even if it did not reach statistical significance.

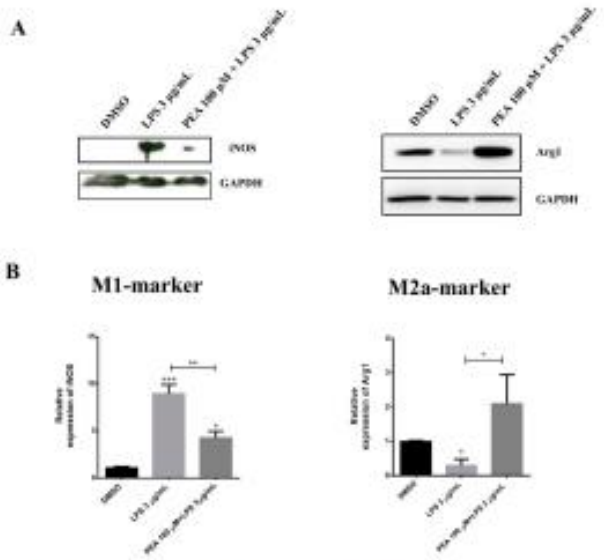

Figure 1. Effect of palmitoylethanolamide (PEA) on M1/M2 markers in lipopolysaccharide (LPS)-stimulated N9 cells. Cells were incubated with 100 μM PEA at 1 h before treatment with 3 μg/mL lipopolysaccharide (LPS) for 6 h. Total protein extract from N9 cells were separated on SDS-PAGE and transferred to a polyvinylidene difluoride (PVDF) membrane; membranes were probed with anti-iNOS and anti-Arg1. GAPDH was used to normalize sample loading. Panel (**A**): A representative Western blot is shown. Panel (**B**): Histograms relative to the quantification of bands of inducible nitric oxide synthase (iNOS) and arginase-1 (Arg1) after dimethyl sulfoxide (DMSO), LPS, and PEA + LPS treatments. Data are shown as the mean ± S.E.M. (n = three independent experiments). Differences among groups were tested for significance by the one-way analysis of variance (ANOVA) followed by Tukey post hoc test (for iNOS) or by Kruskal–Wallis test followed by Dunn's multiple comparisons test (for Arg1). * $p < 0.05$, ** $p < 0.01$, *** $p < 0.001$.

To further characterize the role of PEA on microglia activation and polarization, inflammatory cytokine levels were measured in N9 cells after LPS incubation. LPS stimulated an increase of mRNA levels for TNF-α, interleukin-6 (IL-6), and IL-1β (Figure 2A,B,D, respectively), as well as those for monocyte chemoattractant protein-1 (MCP-1; Figure 2C), which are all markers of the M1 phenotype. In addition, LPS induced an increase also in mRNA levels for interleukin-10 (IL-10) (Figure 2E), which is a marker of the M2b microglia sub-phenotype. The pre-treatment with PEA 100 μM significantly antagonized LPS stimulation of mRNA levels for pro-inflammatory cytokines, as well as the increase in IL-10. Moreover, PEA effectively reduced TNF-α release in the culture medium (Figure 2G) and the cellular content of pro-IL-1β protein (Figure 2H). These findings suggest that PEA pre-treatment largely counteracts microglia activation induced by LPS, preventing the classical M1 microglia polarization. It is well known that LPS polarizes microglia to a mixed M1/M2b phenotype through the toll-like receptor (TLR) signaling. Thus, we measured the mRNA levels of TLR4 in N9 cells. The incubation with LPS induced a significant reduction of TLR4 mRNA levels, and this effect was not inhibited by the pre-incubation for 1 h with

PEA (Figure 2F). The ability of LPS to downregulate TLR4 has been already demonstrated in immortalized microglia cells [8], in primary culture [9], and in macrophages [10], and it has been suggested that this may be a mechanism to prevent over stimulation of the innate response.

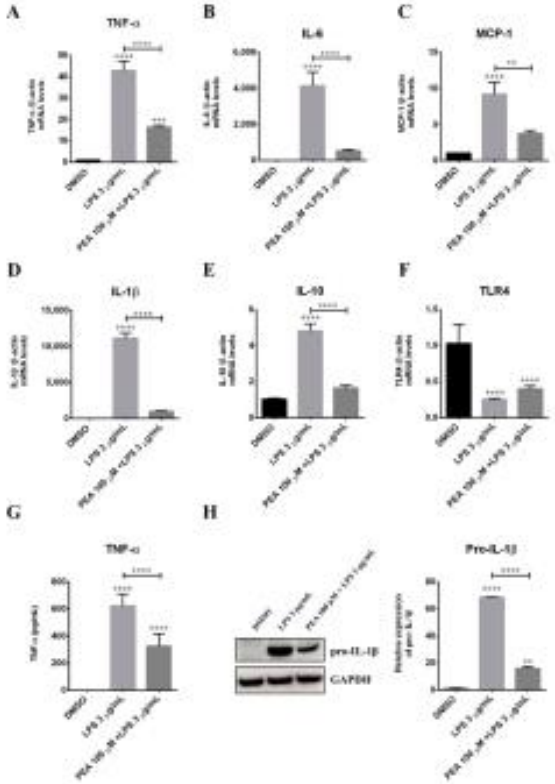

Figure 2. Effect of PEA on LPS stimulation of inflammatory cytokines in N9 cells. Cells were incubated with PEA 100 μM for 1 h and then LPS 3 μg/mL was added for 6 h. mRNA levels of (**A**) tumor necrosis factor alpha (TNF-α), (**B**) interleukin-6 (IL-6), (**C**) monocyte chemoattractant protein-1 (MCP-1), (**D**) interleukin-1 beta (IL-1β), (**E**) interleukin-10 (IL-10) and (**F**) toll-like receptor 4 (TLR4) were examined by real-time PCR. β-actin mRNA was used for data normalization. Data are shown as the mean ± S.E.M. of measurements obtained in three independent experiments ($n = 18$). (**G**) Release of TNF-α into the culture medium was quantified by using a specific enzyme-linked immunosorbent assay (ELISA). Data are shown as the mean ± S.E.M. of measurements obtained in three independent experiments ($n = 3$). (**H**) IL-1β protein expression was measured by Western blotting. To ensure equal loading, blots were also probed with anti-GAPDH. Data are shown as the mean ± S.E.M. of measurements obtained in three independent experiments ($n = 3$). Differences between groups were tested for significance by applying the ANOVA test and Tukey post hoc test. ** $p < 0.01$, *** $p < 0.001$, **** $p < 0.0001$.

2.2. PEA Pre-Treatment Prevents Microglia De-Ramification Induced by LPS Treatment

In order to further evaluate microglia polarization, N9 cell morphologies were analyzed after LPS exposure. Microglia morphology was visualized by a confocal microscope. As shown in Figure 3A, under control condition, microglia exhibited the typical ramified morphology of resting microglia (M0 stage) with numerous long branches and multiple filopodia [11]. As expected, LPS administration changed microglia morphology from the typical branched and ramified morphology to amoeboid with loss of most branches (M1 stage). The morphological changes in microglia reflect profound functional changes in these cells, because it is known that the release of cytokines and other signaling factors into the surrounding tissue is enhanced when microglia acquire amoeboid morphology [12], in agreement with our previous results on cytokine expression. PEA pre-treatment prevents LPS-induced microglia shift into M1 state, keeping cells in ramified morphology. On this basis, microglia ramified morphology changes were measured by quantifying the number of microglia endpoints and process length per cell. As shown in Figure 3B, microglia endpoints and process length significantly decreased with LPS treatment compared to control, while these effects were no present in cells pre-treated with 100 µM PEA for 1 h. Therefore, skeleton analysis of microglia morphologies revealed that microglia became de-ramified (fewer and shorter processes per cell) in LPS treatment while PEA pre-treatment counteracted this situation maintaining cells in ramified form.

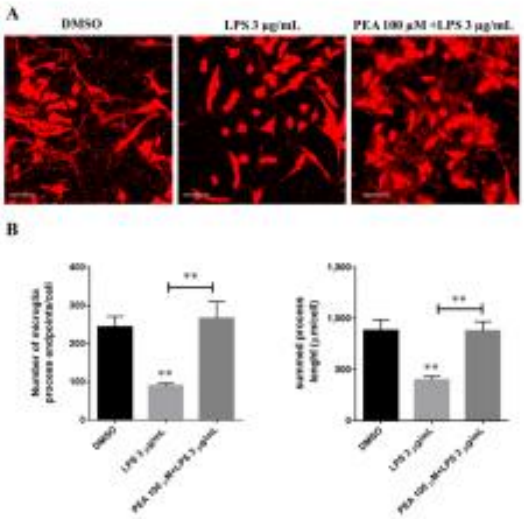

Figure 3. Effect of PEA on microglia ramification in LPS-stimulated N9 cells. N9 cells were seeded on porcine gelatin pre-treated coverslips and then were incubated with 100 µM PEA at 1 h before treatment with 3 µg/mL LPS for 6 h. (**A**) Cells were stained with the membrane dye DiI and fixed. Fluorescence images were acquired by a 63× magnification on Leica TCSSP2 laser scanning confocal microscope. Scale bar: 50 µm. (**B**) Histograms relative to the quantification of process endpoints/cells and process length/cells. Data are shown as the mean ± S.E.M. of different images analyzed ($n = 5$, total number of cells present in each image $n = 30$, total number of cells analyzed for each group $n = 150$). Differences between groups were tested for significance by applying the ANOVA test and Tukey post hoc test. ** $p < 0.01$.

Furthermore, to better analyze microglia morphological changes, FracLac analysis was performed. Examples of microglia (made binary and outlined) in each treatment are shown in Figure 4.

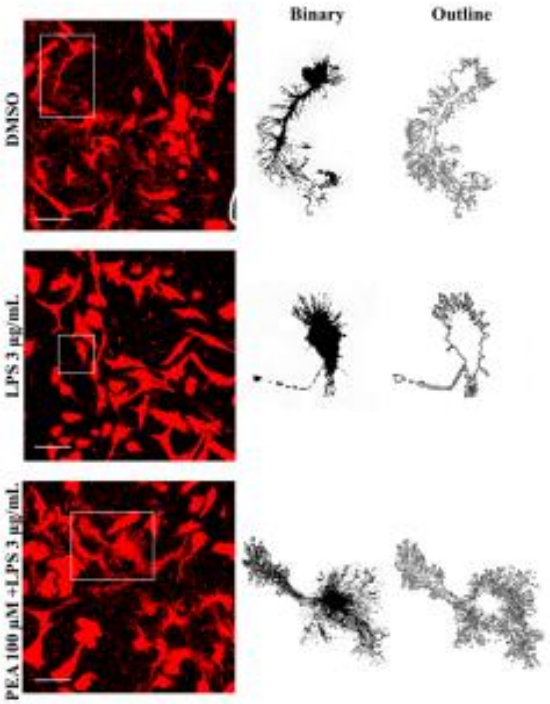

Figure 4. Effect of PEA on microglia morphology in LPS-stimulated N9 cells. N9 cells were seeded on porcine gelatin pre-treated coverslips and then were incubated with 100 µM PEA at 1 h before treatment with 3 µg/mL LPS for 6 h. Cells were stained with the membrane dye DiI and fixed. Fluorescence images were acquired by a 63× magnification on Leica TCSSP2 laser scanning confocal microscope. On the right, examples of cell outlines. Scale bar: 50 µm.

Application of FracLac for ImageJ to microglia outlines resulted in fractal dimensions that ranged from 1.33 and 1.532–1.542 (available range is 1–2), with the lowest value occurring in LPS treatment and the highest in control and PEA pre-treatment. Indeed, microglia complexity significantly decreased with LPS administration, while PEA pre-incubation counteracted it (Figure 5A). Fractal dimension scores suggest that PEA pre-treatment is able to maintain complexity of microglia shape, which characterizes control cells. Using FracLac for ImageJ, additional measures of microglia morphology related to cell shape were investigated: span ratio, density, cell area, perimeter, lacunarity, and circularity. Span ratio is a measure of microglia elongation. Therefore, this parameter, together with cell circularity, is relevant to define microglia shape (rod or circle). As shown in Figure 5C,G, span ratio and cell circularity were unchanged among different groups. Density, cell area,

and perimeter are used to report microglia size. LPS administration decreased density, cell area, and perimeter compared to control, while they were significantly preserved in cells pre-treated with 100 µM PEA for 1 h (Figure 5B,D,E). Lacunarity (Λ) is a measure of microglia shape changing; since Λ assesses heterogeneity or translational and rotational invariance in an image, lower Λ values imply homogeneity [13]. As shown in Figure 5F, PEA pre-treatment significantly increased lacunarity compared to LPS administration.

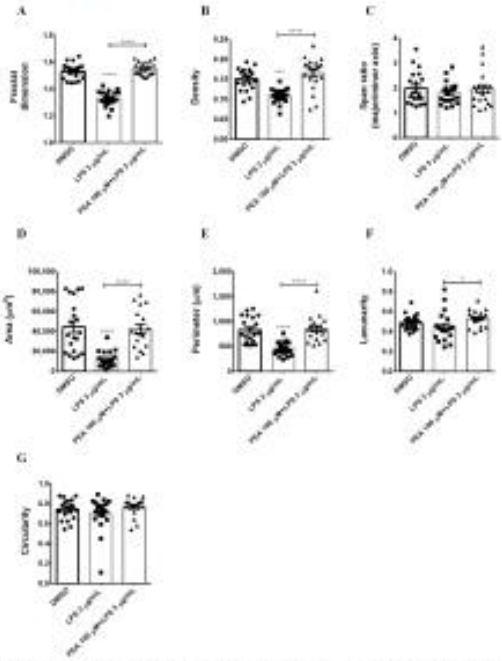

Figure 5. Effect of PEA on microglia complexity, elongation, and size in LPS-stimulated N9 cells. Summary data and statistical analysis of fractal dimension (**A**), density (**B**), span ratio (**C**), area (**D**), perimeter (**E**), lacunarity (**F**), and circularity (**G**). Total number of cells analyzed for each condition $n = 20$. Data are shown as the mean ± S.E.M. Differences between groups were tested for significance by applying the ANOVA test and Tukey post hoc test. * $p < 0.05$, *** $p < 0.001$, **** $p < 0.0001$.

To properly categorize the different morphotypes of microglia present in this experimental model and correlate them with their activation state, hierarchical cluster analysis (HCA) was performed (Figure 6A). For this mathematical approach to classify microglia in different groups, parameters calculated by FracLac analysis were used. Based on these measures, and following Thorndike's procedure [14], microglia were classified in three clusters or morphotypes (Figure 6B). Especially, as shown in Figure 6A, there were two big clusters, Cluster 1 and 2, with Cluster 2 further ramified in two sub-groups, 2.1 and 2.2. Cluster 1 included cells from LPS-treatment, while Cluster 2 included a mixture of cells from both control and PEA pre-treatment. Notably, whereas control cells were equally

distributed between Cluster 2.1 and Cluster 2.2, the greatest part of cells derived from PEA pre-incubation were grouped in Cluster 2.2.

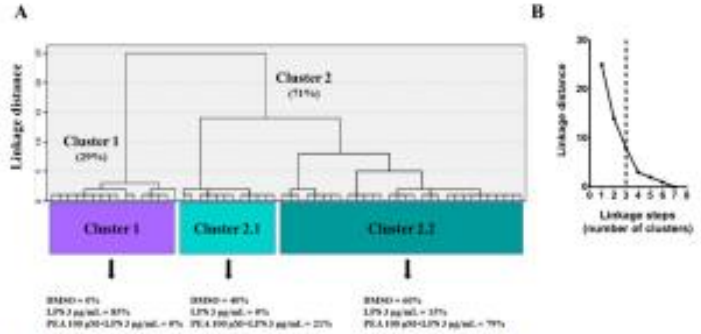

Figure 6. Classification of microglia according to FracLac parameters. (**A**) Hierarchical cluster analysis (HCA) of microglial cells, treated as described above, based on parameters calculated by FracLac analysis. Dendrogram for 59 cells, where the abscissa represents individual microglia, and the ordinate corresponds to the linkage distance measured by Euclidean distance. As shown, data were classified as two main clusters (Cluster 1 and 2). Cell morphology of LPS-treated microglia fit into Cluster 1; on the contrary, both not treated cells and cells pre-treated with PEA belong to the second Cluster (Clusters 2.1 and 2.2) (**B**) Three was identified as an appropriate number of clusters according to the linkage distance (Euclidean distance) vs linkage steps (number of clusters) analysis performed following Thorndike's procedure, as indicated by the vertical dashed line.

To better understand microglia morphology and its changes, which reflect profound functional modifications, endpoints/cell, fractal dimension, and lacunarity score from different treatments were plotted on a 3D graph; data were averaged for each group. These three measures were chosen as single variables to represent cell ramification, complexity, and shape changing, respectively. Including all variables would be redundant. Plotting these three parameters on a scatter plot (Figure 7) allowed us to categorize PEA pre-treatment in the same group of control (ramified group) as opposed to LPS treatment (de-ramified and rod group). Even though PEA and control group were near in the plot, PEA group displayed a higher lacunarity. Lacunarity defines the polarization of the cells, which is where their prolongations are oriented toward a specific point, and this characteristic is typical of the M2a phenotype.

2.3. *PEA Inhibits ATP-Induced Intracellular Ca^{2+} Increase in N9 and Primary Microglial Cells*

Microglia function strongly relies on intracellular calcium signaling. Unable to observe substantial increase in calcium following LPS application, we studied the calcium elevation induced by ATP. In particular, microglia expressed receptors for ATP that regulate microglial motility. After local damage, the release of ATP induced microgliosis and activated microglial cell migration to the site of injury, proliferation, and phagocytosis of cells and cellular compartments [15]. To investigate if PEA could affect the calcium signaling in microglia, we evaluated intracellular Ca^{2+} mobilization in N9 cells. Stimulation of cells with 10 µM ATP caused a transient increase of intracellular Ca^{2+} that was significantly reduced (approximately 45%) by the pre-treatment with 100 µM PEA (Figure 8A). Increase in cytoplasmic Ca^{2+} ion concentration creates that phenomenon called intercellular Ca^{2+} wave (ICW), which is the main communication approach by which glial cells interact and coordinate with each other to execute immune defense [16,17]. In order to obtain further insight about the role of PEA in counteracting intracellular Ca^{2+} increase induced by ATP,

we repeated the experiment in primary microglial cells. According to what we observed for N9 cells, pre-treatment of primary microglia with 100 µM PEA inhibited (49%) the rise in intracellular Ca^{2+} concentration induced by ATP (Figure 8B). These data suggest that PEA is able to prevent generalized Ca^{2+} transients that in microglia are a signal of damage.

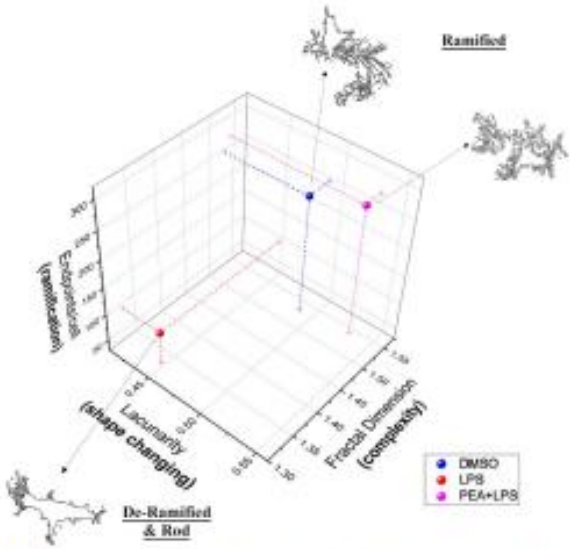

Figure 7. Effect of PEA on different microglia morphologies in LPS-stimulated N9 cells. Fractal dimension (D_B), endpoints/cell, and lacunarity data were analyzed by Pearson's correlation and then averages for each group were used for visualization. The figure summarizes the relationship between all three variables. Fractal dimension (D_B) is directly related to endpoints/cell ($r = 0.9994$, $p = 0.0108$) and lacunarity (Λ) ($r = 0.2637$, $p = 0.08954$); lacunarity (Λ) is not significantly correlated with endpoints/cells ($r = 0.9161$, $p = 0.1313$). Two groupings emerge: ramified and de-ramified and rod.

2.4. PEA Prevents LPS-Induced Hyperexcitability in Primary Cortical Cultures

LPS treatment of cultures of neurons, astrocytes, and microglia causes atypical seizure-like activity in the neuronal network, which we have characterized in detail in our previous studies [18,19]. To investigate if PEA could counteract the hyperexcitability induced by LPS, we pre-incubated primary cortical cultures with 100 µM PEA 1 h before administering 3 µg/mL LPS. The electrical activity of the network, recorded by the MEA system, is shown in the raster plots in Figure 9A for a representative culture in control, during LPS administration, and during PEA pre-administered to LPS. In the raster plot, each line corresponds to one cell, and the small vertical ticks represent the spikes. PEA abolished the atypical hyperactivity induced by LPS and, in some cultures, it even showed a trend to reduce the network activity compared to control condition. In order to more precisely characterize the effect of PEA, we evaluated the cumulative distribution of the burst durations (cumBD) of the network, which in our previous papers was considered as the principal variable for describing the atypical seizure-like events induced by LPS. The typical effect of LPS on cumBD was a right-shift of the curve with respect to control (Figure 9B, upper panel). From the figure it is evident that, in control, 95% of the bursts had BD < 4 s,

whereas in LPS, only ~80% of the bursts had BD < 4 s and the rest of the bursts had longer BDs. Pre-incubation with PEA increased to 100% the probability of having BD < 4 s (Figure 9B, lower panel), showing a preventive effect of PEA on the LPS treatment. In order to compare different experiments, the value of cumBD at 95%, which represented the duration of 95% of the bursts (cumBD95), was extracted for LPS and PEA + LPS from each experiment and was normalized on cumBD95 of its respective control; thus, data from $n = 3$ independent experiments were averaged. Data at different time points (0, 1, 2, 4, and 6 h from LPS administration) were represented in Figure 9C in order to show the time course of LPS administration without and with PEA pre-incubation. PEA counteracted LPS-induced increase in cumBD95 at all the investigated time points ($p < 0.05$ at 1 and 4 h, $p < 0.01$ at 2 h, $p < 0.001$ at 6 h), suggesting a long-lasting preventive action of PEA on network hyperexcitability caused by LPS. The reduction of network activity shown by PEA administration versus control was not significant ($p > 0.05$, multiple t-test corrected for multiple comparisons by using the Holm–Sidak method).

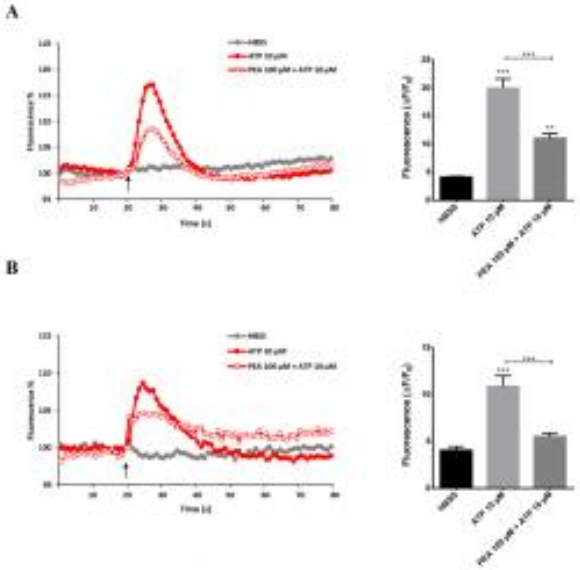

Figure 8. Effect of PEA on ATP-mediated intracellular Ca^{2+} increase in primary microglia and N9 cells. Cells were loaded with FLUO-4 NW and fluorescence emission was measured at 535 nm every 0.5 s for the 20 s preceding and the 60 s following the injection of the stimuli. (left) ATP was injected in (**A**) N9 cells and in (**B**) primary microglia at the time indicated by the arrow. Results are the means of measurements obtained in at least six different wells for each experiment. All experiments were repeated at least three times. One representative experiment is shown (right). Graphs show intracellular Ca^{2+} increase (expressed as fluorescence intensity) in (**A**) N9 cells and (**B**) primary microglia stimulated with ATP. Data are shown as the mean ± S.E.M. of measurements obtained in three independent experiments ($n = 18$). Differences between groups were tested for significance by applying the ANOVA test and Tukey post hoc test. ** $p < 0.01$, *** $p < 0.001$.

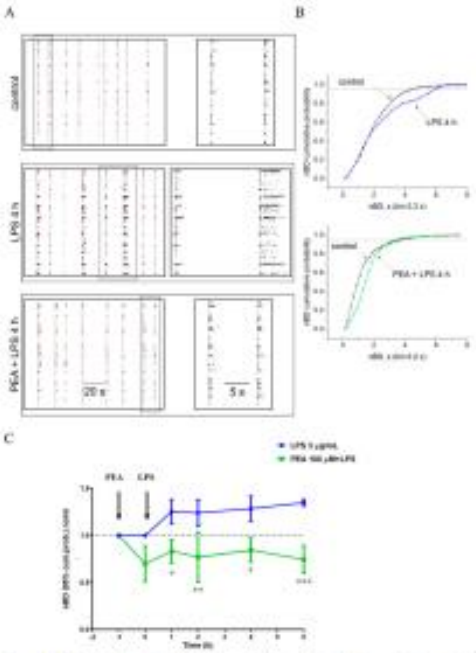

Figure 9. Protective effect of PEA on LPS-induced inflammation and hyperexcitability of cortical network. (**A**) Representative example of raster plot of patterns of spontaneous burst activity in control condition after 4 h of 3 µg/ml. LPS administration and during 100 µM PEA + LPS. PEA was administered 1 h before LPS. In each condition, a couple of bursts were boxed and shown in a new window with a time scale enlarged, on the right of panel A. Each vertical line is a timestamp representing a single spike, and the global network burst duration (BD) is computed considering all neurons (distributed on the row). (**B**) Plots of superimposed BD cumulative probability histograms in control (black line), after 4 h of LPS administration (upper panel) and LPS with PEA pre-administered (lower panel). The data are obtained, computing all the BDs in temporal windows of 30 min, then, the cumulative probabilities of the time lapse of interest were normalized to the maximum value. Number of analyzed bursts in represented experimental steps were 110 in control, 103 in LPS, and 108 in PEA + LPS. On cumulative distribution, the statistical significance, obtained by Kruskal–Wallis non parametric test, was $p < 0.01$ for LPS vs control and $p > 0.05$ for PEA + LPS vs control. The value of cumulative distribution of the burst durations (cumBD) at 95% of probability (dot line) in the upper panel changed from 4.4 s, in control, to 6 s, in LPS; in the lower panel the same value is 3.6 s in control and 3.55 s in PEA + LPS condition. (**C**) Time plot of cumBD data at 95% of probabilities; each point in the indicated time lapse represents averaged data normalized at the control (dot line). Significant differences for PEA + LPS (green line) vs LPS (blue line) were determined at all experimental steps by Holm–Sidak method. 0.832 ± 0.123 and 1.253 ± 0.128, 0.769 ± 0.267 and 1.240 ± 0.139, 0.844 ± 0.127 and 1.285 ± 0.132, 0.745 ± 0.146 and 1.347 ± 0.034 were, respectively, the values for PEA + LPS and LPS at 1, 2, 4, and 6 h ($n = 3$ independent experiments for each condition). No significant effect was observed in PEA versus control. Data are expressed as mean ± S.E.M. * $p < 0.05$, ** $p < 0.01$, *** $p < 0.001$.

2.5. PEA Counteracts LPS-Induced TNF-α Release in Primary Cortical Cultures

As described above, TNF-α is an inflammatory cytokine marker of the M1 microglia polarization state. To verify whether PEA pre-treatment is able to counteract the microglial-release of TNF-α induced by LPS treatment in primary cortical neuron/astrocyte/microglia cultures, we performed an ELISA. The amount of this cytokine in the presence of PEA was, at 6 h after LPS treatment, significantly smaller than that found when PEA was absent (Figure 10A). Thus, to assess if PEA pre-treatment activates anti-inflammatory processes in primary cortical cultures, we measured the level of brain derived neurotrophic factor (BDNF). As shown in Figure 10B, the amount of this neurotrophin did not increase compared to control. These findings confirm what we previously observed in N9 microglia cells, namely, that PEA pre-treatment can counteract inflammation induced by LPS treatment.

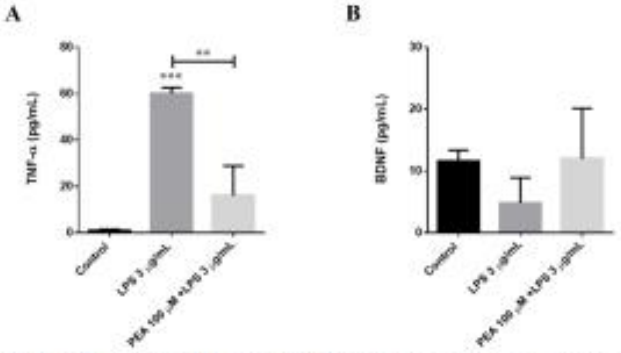

Figure 10. Release of TNF-α (**A**) and BDNF (**B**) at 6 h after LPS application. The mouse primary cortical cultures were incubated with 100 μM PEA at 1 h before treatment with 3 μg/mL LPS. The amount of TNF-α and brain derived neurotrophic factor (BDNF) released into the culture medium was quantified after 6 h from LPS treatment. Data are shown as the mean ± S.E.M. of measurements obtained in three independent experiments ($n = 3$). Differences between groups were tested for significance by applying the ANOVA test and Tukey post hoc test. ** $p < 0.01$, *** $p < 0.001$.

2.6. PEA Counteracts LPS-Induced Nf-κB Activation in Human PMA-THP-1 X-Blue Cells and This Effect Is Not Mediated by Interaction with TLR4

LPS is a ligand for TLR4. When LPS is bound together with TLR4, a cascade of signaling pathways is triggered, which can activate the expression of pro-inflammatory cytokines, including interleukin (IL)-1, IL-6, and TNF-α [20]. Although structurally different, TNF-α, IL-1, and TLR receptors use similar signal transduction mechanisms that include activation of IkB kinase (IKK) and nuclear factor kappa-light-chain-enhancer of activated B cells (NF-κB) [21]. In recent years, it has become clear that there are at least two separate pathways for NF-κB activation. The "canonical" pathway is triggered by microbial products and proinflammatory cytokines such as TNF-α and IL-1, usually leading to activation of RelA- or cRel-containing complexes [22]. Moreover, preclinical studies showing the therapeutic effect of synthetic small molecules acting as TLR4 antagonists, both in vitro and in vivo, confirmed its central role in the regulation of inflammation [23]. In order to obtain further insight about the role of TLR4/NF-κB axis in the previously observed PEA-induced inhibition of pro-inflammatory cytokines, we investigated NF-κB activation triggered by TLR4 stimulation in human macrophages PMA-THP-1 X-Blue cells. Cells were pre-incubated with 100 μM PEA 1 h before administering 10 ng/mL LPS. As shown in Figure 11A, secreted embryonic alkaline phosphatase (SEAP) expression significantly

decreased (40%) in human macrophages upon PEA pre-treatment as compared to LPS, accordingly to previous report [24]. PEA is able to inhibit activation of NF-κB even if PEA is administered after LPS in THP-1 derived macrophages. Taken together, these findings could suggest a possible involvement of the TLR4/NF-κB axis in the PEA mechanism of action in human macrophages.

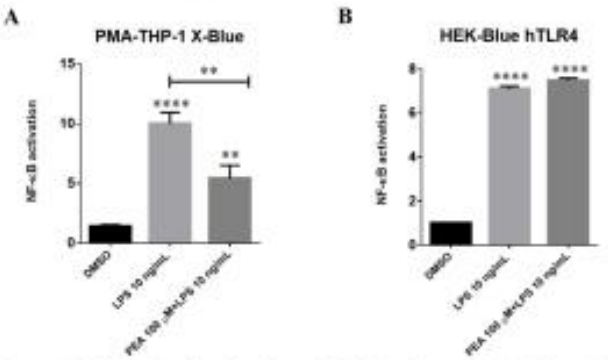

Figure 11. Inhibition of nuclear factor kappa-light-chain-enhancer of activated B cells (NF-κB) activation in LPS-stimulated PMA-THP-1 X-Blue cells by PEA. PMA-THP-1 X-Blue (**A**) and HEK-Blue hTLR4 (**B**) cells were incubated with 100 μM PEA at 1 h before treatment with 10 ng/mL LPS. The amount of secreted embryonic alkaline phosphatase (SEAP) released into the culture medium was quantified after 6 h as a measure of NF-κB activation. Data are presented as mean ± S.E.M. ($n = 3$ independent experiments) normalized on the control sample. Differences between groups were tested for significance by applying the ANOVA test and Tukey post hoc test. ** $p < 0.01$, **** $p < 0.0001$.

To confirm this hypothesis, we investigated NF-κB activation in HEK-Blue hTLR4 cells. HEK-Blue hTLR4 cells served as a tool to investigate whether PEA acts involving TLR4 directly. Pre-treatment with PEA did not affect NF-κB activation induced by LPS (Figure 11B). These data indicated that PEA is able to inhibit NF-κB activation triggered by LPS administration in human macrophages, but this effect is not mediated by interaction with TLR4.

2.7. CB2 Receptor Is Partially Involved in PEA-Induced Effects on Microglia

Microglia express both the cannabinoid type 1 (CB1R) and type 2 (CB2R) receptors; however, CB2R is more abundantly expressed in microglial cells [25], and its expression is further increased during activation in vitro and in disease animal models [26]. Therefore, it is expected that CB2R plays a crucial role in the anti-inflammatory microglial response. In fact, upregulation of the alternative M2 markers by CB2R activation in microglial cells has been reported [27]. To investigate the role of CB2R in PEA-neuroprotective effects, a selective CB2R inverse agonist SR144528 was used. The expression of iNOS was measured as the marker of microglial activation by Western blot analysis. As shown in Figure 12A, pre-administration of SR144528 100 nM significantly increased iNOS expression compared to PEA treatment. The ability of SR144528 to partially antagonize PEA effects could be due to a possible action of PEA on CB2R. As described above, the morphological changes in microglia reflect profound functional modifications. On this basis, microglia ramified morphology changes were quantified. The benefits induced by PEA pre-treatment, which counteracted the de-ramified form induced by LPS, were completely reversed in presence of SR144528 (Figure 12B). Moreover, in primary cortical neuron/astrocyte/microglia cultures,

pre-incubation with SR144528 100 nM significantly increased TNF-α release compared to control, partially antagonizing PEA preventive effects (Figure 12C). Taken together, these findings suggest a partial involvement of CB2R in the PEA mechanism of action.

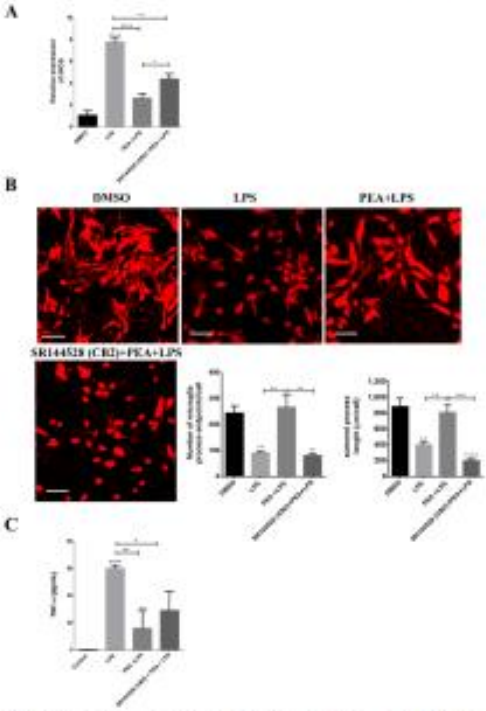

Figure 12. Involvement of cannabinoid type 2 receptor (CB2R) in PEA-neuroprotective effects. N9 cells and mouse primary cortical cultures were incubated with 100 nM SR144528 at 1 h before 100 μM PEA pre-treatment. After 1 h, they were then exposed to 3 μg/mL LPS. (**A**) Histograms relative to the quantification of Western blot bands of iNOS in N9 cells, after DMSO, LPS, PEA + LPS and SR144328 + PEA + LPS treatments. Data are shown as the mean ± S.E.M. ($n = 3$ independent experiments) (**B**) N9 cells were seeded on porcine gelatin pre-treated coverslips and treated as described above. Cells were stained with the membrane dye DiI and fixed. On the left, fluorescence images acquired by a 63× magnification on Leica TCS SP2 laser scanning confocal microscope. Scale bar: 50 μm. On the right, histograms relative to the quantification of process endpoints/cells and process length/cells. Data are shown as the mean ± S.E.M. of different images analyzed ($n = 5$, total number of cells present in each image $n = 30$, total number of cells analyzed for each group $n = 150$). (**C**) The amount of TNF-α released into the culture medium in mouse primary cortical cultures. Cells were treated as described above, and the amount of this cytokine was quantified at 6 h from LPS application. Data are shown as the mean ± S.E.M. of measurements obtained in three independent experiments ($n = 3$). Differences between groups were tested for significance by applying the ANOVA test and Tukey post hoc test. * $p < 0.05$, ** $p < 0.01$, *** $p < 0.001$, **** $p < 0.001$.

3. Discussion

In this study, characterized the effects of PEA in several in vitro models of neuroinflammation induced by LPS and ATP. Our results demonstrated that: (i) PEA induced a switch from M1 to M2 phenotype in N9 microglia stimulated with LPS; (ii) PEA blunted the increase of intracellular calcium stimulated by ATP in N9 and primary microglia; (iii) PEA antagonized the hyperexcitability in cultures of primary cortical neurons, astrocytes and microglia induced by LPS; and (iv) PEA inhibited NF-κB activation by modulating the activation of CB2R signaling but not through interactions with TLR4.

PEA is an endogenous lipid messenger which displays key properties in many biological processes, showing not only anti-inflammatory activities but also analgesic and neuroprotective ones [28]. For this reason, PEA is potentially effective in a wide range of therapeutic areas, as demonstrated by many preclinical and clinical studies that highlighted its efficacy in neurodegenerative diseases [29], chronic pain conditions [30], and epilepsy [4]. The efficacy and the tolerability of PEA explain why it has been marketed in different countries as a nutraceutical food supplement since 2008. Different molecular mechanisms have been proposed so far to explain the biological effects of PEA, including direct action on proliferator-activated receptor-α (PPAR-α) [31] and many indirect cannabinoid receptor-mediated actions through the so-called entourage effect [32]. In spite of this multiple mechanism of action, the effect of PEA on cell types involved in inflammatory responses has not been yet fully characterized. In the present study, we focused on the mechanisms by which PEA modulates the release of pro- and anti-inflammatory mediators from microglia and its capability to shift microglia from M1 to M2 polarization.

A growing body of evidence suggests an important role for neuroinflammation in the pathogenesis of several neurological diseases, including, among others, amyotrophic lateral sclerosis, Alzheimer's, and Parkinson's diseases [33]. It is generally acknowledged that acute neuroinflammation plays a protective role in the CNS by activating microglial phagocytosis of harmful agents, whereas the chronicization of neuroinflammation assumes a detrimental role because of the excessive release of inflammatory cytokines and cytotoxic factors [34]. Microglia are derived from myeloid cells in the periphery and comprise approximately 12% of cells in the brain, where they typically exist in a resting state characterized by ramified morphology [35]. Microglia are highly plastic cells, and classification of activated microglia into the three classical phenotypes [i.e., (i) resting M0; (ii) pro-inflammatory M1; and (iii) immunosuppressive M2] is the most commonly used approach to represent a simplified model of polar extremes of inflammatory response [36]. A switch from M1 to M2 microglia is thought to occur during natural resolution of inflammation, and M2 microglia are often described as having anti-inflammatory or reparative functions [37]. In the present study, we used LPS to stimulate pro-inflammatory responses in the N9 murine microglia cells, which were previously demonstrated to be a suitable model for pharmacological and toxicological studies on microglia [38,39]. Our results in N9 microglia demonstrated that LPS stimulated an increase in the expression of pro-inflammatory mediators, including iNOS, IL-1β, TNF-α, IL-6 and MCP-1, and inhibited the expression of Arg1. Interestingly, LPS stimulation inhibited the expression of TLR4, which exists as a complex with the co-receptor myeloid differentiation protein-2 (MD-2) [40]. The binding of LPS to TLR4-MD-2 complexes activated downstream mediator pathways, including NF-κB. This ability of LPS to downregulate TLR4 may be a negative feedback mechanism to prevent over stimulation of the innate response [8–10]. Also, at the morphological level, LPS induced a shift of N9 microglia from the M0 to M1 amoeboid shape. The morphological changes in microglia morphology are indicative of primary functional modification since it is known that the release of cytokines and other signaling factors into the surrounding tissue is enhanced when microglia acquire amoeboid morphology [12]. Interestingly, PEA effectively antagonized the effects of LPS on pro-inflammatory mediators and IL-10 expression and significantly stimulated the anti-inflammatory Arg-1 expression. These effects were also reflected in the ability of PEA to induce LPS-stimulated amoeboid microglia to switch toward the M2 shape. Additionally, fractal dimension analysis suggested that PEA was capable to

preserve the complexity of microglia shape, similar to control, and also in cells stimulated with LPS. However, N9 treated with PEA displayed a higher lacunarity, a characteristic that defines cell polarization, indicating that their prolongations were oriented toward a specific point, and this characteristic is typical of M2a phenotype. Interestingly, PEA was unable to restore TLR4 expression reduced by LPS, suggesting that its intracellular mechanism of action is at least in part independent from that of LPS.

Microglia function strongly relies on intracellular calcium signaling. In fact, release of ATP from damaged cells stimulates microglial cell migration to the site of injury, proliferation, and phagocytosis of cells [15]. Extracellular ATP is an important signal for the intercellular Ca^{2+} wave (ICWs) [41–43], which is the primary mechanism by which microglia [16,17], astrocytes [44], and neurons [45] communicate to maintain homeostasis of the CNS. In N9 cells, stimulation with ATP caused a significant transient increase of intracellular Ca^{2+} that lasted for about 30 s. PEA pre-treatment significantly inhibited the increase of intracellular Ca^{2+} stimulated by ATP. Almost superimposable effects were obtained also in murine primary microglia, demonstrating that: (i) PEA can modulate the intracellular activation initiated by binding of ATP to purinergic receptors; and (ii) N9 cells are a reliable experimental model to study the effects of pharmacological treatments on microglia.

In cultures of neurons, astrocytes, and microglia, we evaluated the cumulative distribution of the burst durations (cumBD) of the network, which can be assumed as the principal variable for describing the atypical seizure-like events [18,19]. In the control group, about 95% of the bursts had BD < 4 s, but in the group stimulated with LPS, only ~80% of the bursts had BD < 4 s. This effect could be mediated, at least in part, by LPS stimulation of TNF-α release in the culture medium. TNF-α was previously shown to control basal synaptic functions [46] as well as plasticity [47,48]. In this setting, PEA effectively increased to 100% the probability of having BD < 4 s in cultures stimulated with LPS, and significantly inhibited the release of TNF-α in the culture medium. These data demonstrated that PEA has important modulatory activity and can prevent network hyperexcitability caused by LPS treatment.

More insights into the PEA mechanism of action were obtained using both the PMA-THP-1 X-Blue cell and HEK-Blue hTLR4 models. These cells have been modified for measuring NF-κB activation in terms of SEAP release in the culture medium. Our results showed that LPS significantly increased NF-κB activation in PMA-THP-1 X-Blue cells, and this effect could be significantly inhibited by PEA pre-incubation. However, in HEK-Blue hTLR4, PEA was unable to inhibit LPS stimulation of NF-κB activation, suggesting that its effects are not mediated by a direct effect on TLR4 receptors. Previous evidence suggested a role of CB2 receptor in the mechanism of action of PEA. To investigate the role of CB2R in PEA-anti-inflammatory effects, we used SR144528, a selective CB2R inverse agonist. SR144528 significantly reduced the ability of PEA to inhibit LPS stimulation of iNOS expression in N9 cells. Similarly, SR144528 was able to antagonize PEA capability to shift the morphology of N9 cells treated with LPS from the M1 to M2 shape. It has been reported that PEA does not directly bind CB1R or CB2R, and our results are in agreement with those suggesting that PEA anti-inflammatory effects could result by its ability to stimulate a yet unknown CB2-like receptor [49].

In conclusion, the present study provides evidence that PEA is an effective inhibitor of the pro-inflammatory effects of LPS in microglia. PEA can also modulate microglia activation induced by ATP stimulation. We also demonstrated that PEA can effectively counteract microglial morphological changes induced by LPS and hyperactivation of neurons–microglia–astrocyte networks. PEA effects are likely mediated by its interaction with a still unknown CB2-like receptor. These findings suggest that PEA could be a useful drug to prevent the consequences of chronic neuroinflammation in neurodegenerative disorders.

4. Materials and Methods

4.1. Cell Cultures

The murine microglial N9 cells were cultured in Iscove Modified Dulbecco's Medium (IMDM, Sigma-Aldrich, St. Louis, MO, USA) supplemented with 5% heat-inactivated fetal bovine serum (FBS), 100 U/mL penicillin, 100 µg/mL streptomycin, 2 mM L-glutamine (all Euroclone, Pero, Italy), and Mycozap Prophylactic (Lonza, Walkersville, MD, USA) under standard cell culture conditions (37 °C, 5% CO_2).

Primary microglial cells were isolated from P2 neonatal rats as previously described [50]. Briefly, isolated hippocampi and cortices were triturated and suspended in complete glial medium, composed of Minimum Essential Medium (MEM, Sigma-Aldrich, St. Louis, MO, USA), 20% FBS (Euroclone, Pero, Italy), 33 mM glucose (Sigma-Aldrich, St. Louis, MO, USA), 2 mM ultra-glutamine (Lonza, Walkersville, MD, USA), 100 U/mL penicillin, and 100 µg/mL streptomycin (Euroclone, Pero, Italy). Cells were then seeded in 0.02 mg/mL poly-D-lysine pre-coated flasks and cultured under standard cell culture conditions (37 °C, 5% CO_2) for 15 days. After this period, microglial cells were isolated from mixed glial cultures by shaking flasks and then seeded onto 0.05 mg/mL poly-ornithinated plates at the desired concentration.

THP-1 X-Blue cells (InvivoGen, San Diego, CA, USA), derived from a human peripheral blood monocyte cell line by stable integration of an NF-κB-inducible SEAP reporter construct, were obtained. Cells were maintained in RPMI 1640 Medium without L-Glutamine with Phenol Red (Euroclone, Pero, Italy), supplemented with 10% heat-inactivated FBS, 2 mM L-Glutamine, and 100 U/mL Penicillin/Streptomycin (all Euroclone, Pero, Italy). Before treatments, cells were seeded into a 96-well plate and differentiated into macrophages by 72 h incubation with 100 ng/mL phorbol 12-myristate 13-acetate (PMA; Enzo Life Sciences, New York, NY, USA), followed by 24 h incubation in RPMI medium without PMA.

HEK-Blue hTLR4 cells (InvivoGen, San Diego, CA, USA) were obtained by co-transfection of the human TLR4, MD-2 and CD14 co-receptor genes, and an inducible SEAP reporter gene into HEK293 cells. Cells were maintained in DMEM medium without L-Glutamine with Phenol Red (Euroclone, Pero, Italy), supplemented with 10% heat-inactivated FBS, 2 mM L-Glutamine, 100 U/mL Penicillin/Streptomycin (all Euroclone, Pero, Italy), and HEK-Blue Selection (InvivoGen, San Diego, CA, USA), a solution that combines several selective antibiotics to maintain selection pressure.

4.2. Chemicals

PEA was purchased from Cayman Chemical (Ann Arbor, MI, USA). It was dissolved in dimethyl sulfoxide (DMSO) at a concentration of 67 mM or 100 mM and then serially diluted in culture medium immediately prior to experiments. Adenosine 5′-triphosphate (ATP) and lipopolysaccharides (LPS; *Escherichia coli* O55:B5) were obtained from Sigma-Aldrich (St. Louis, MO, USA). SR144528 was purchased from Tocris (Bristol, UK).

4.3. Real-Time PCR Analysis

N9 cells were plated in 24-well culture plates at a density of 80×10^5 cells/well and incubated at 37 °C for 48 h. Cells were then treated with 3 µg/mL LPS diluted in culture medium for 6 h. PEA (100 µM) was applied 1 h before LPS and maintained in contact with the cells throughout the whole LPS exposure. After the incubation period, total RNA was extracted from N9 cells using EuroGOLD Trifast reagent (Euroclone, Pero, Italy) according to the manufacturer's instructions and quantified using Nanodrop ND-1000 spectrophotometer (Thermo Fisher Scientific, Waltham, MA, USA). Reverse transcription was performed using iScript cDNA Synthesis Kit (Bio-Rad, Hercules, CA, USA). Real-time PCR (RT-PCR) was carried out on a QuantStudio 7 Flex Real-Time PCR System (Applied Biosystem, Foster City, CA, USA) using the iTaq Universal Probes Supermix (Bio-Rad, Hercules, CA, USA). Pairs of primers and Taqman probes (Taqman Gene Expression Assays) were obtained from Applied Biosystem (Foster City, CA, USA). RT-PCR was

performed as follows: 50 °C for 2 min, followed by 95 °C for 10 min, and lastly 40 cycles at 95 °C for 15 s and 60 °C for 1 min. Relative mRNA concentrations of the target genes were normalized to the corresponding β-actin internal control and calculated using the $2^{-\Delta\Delta Ct}$ method. Data were analyzed using GraphPad v6.0 software (San Diego, CA, USA), employing ANOVA, followed by Tukey's test for group comparison. $p < 0.05$ was considered statistically significant.

4.4. Western Blot Analysis

N9 cells were plated in 6-well culture plates at a density of 35×10^4 cells/well, incubated at 37 °C for 48 h, and then treated as indicated on PCR analysis; for the experiments with selective inverse agonist of CB2, cells were incubated with 100 nM SR144528 1 h before the treatment with PEA and LPS. After incubation, cells were collected and lysed in radioimmunoprecipitation assay (RIPA) buffer (Cell Signaling Technology, Danvers, MA, USA). The total protein concentration was determined using the Pierce BCA Protein Assay Kit (Thermo Fisher Scientific, Waltham, MA, USA). Equal amounts of proteins were heated at 95 °C for 10 min, loaded on precast 4–12% gradient gels (Twin Helix, Rho, Italy), separated by electrophoresis, and transferred to a polyvinylidene difluoride (PVDF) membrane (Thermo Fisher Scientific, Waltham, MA, USA). Non-specific binding was blocked with 5% dried fat-free milk dissolved in phosphate-buffered saline (PBS) supplemented with 0.1% Tween-20 (PBS-T) for 1 h at room temperature (RT). After washes in PBS-T, membranes were incubated with the primary antibody overnight at 4 °C and then with a peroxidase-coupled secondary antibody for 1 h at RT. Blots were probed with anti-IL-1β (#31202, Cell Signaling Technology, Danvers, MA, USA, 1:1000), anti-iNOS (#13120, Cell Signaling Technology, Danvers, MA, USA, 1:1000) and anti-Arg1 (#93668, Cell Signaling Technology, Danvers, MA, USA, 1:1000). Rabbit primary anti-GAPDH antibody (#2118, Cell Signaling Technology, Danvers, MA, USA, 1:3000) was used for normalization. Peroxidase-coupled goat anti-rabbit IgG (#31460, Thermo Fisher Scientific, Waltham, MA, USA, 1:5000) was used as secondary antibody. Signals were developed with the Extra Sensitive Chemiluminescent Substrate LiteAblot TURBO (Euroclone, Pero, Italy) and detected with the Amersham ImageQuant 800 Western blot imaging system (GE Healthcare, Chicago, IL, USA). Image J software (National Institutes of Health, Bethesda, MD, USA) was used to quantify protein bands. For iNOS expression, in some of the blots only, a band of poor intensity was present in DMSO sample; however, it was possible to quantify it and to express the protein level of LPS and PEA group in terms of relative expression. The experiments were repeated three independent times. Data were analyzed using GraphPad v6.0 software (San Diego, CA, USA) employing ANOVA followed by Tukey's test or by Kruskal–Wallis test and Dunn's multiple comparisons test for group comparison. $p < 0.05$ was considered statistically significant.

4.5. Immunofluorescence

N9 cells were seeded at a density of 1×10^5 cells/mL on porcine gelatin pre-treated coverslips. One day after seeding, cells were treated with 3 µg/mL LPS diluted in culture medium for 6 h. PEA (100 µM) was applied 1 h before LPS and maintained in contact with the cells throughout the whole LPS exposure. Cells were then stained with DiI (Sigma-Aldrich, St. Louis, MO, USA) to label cell membranes (according to the manufacturer's instructions) and fixed for 10 min with 3.7% paraformaldehyde in phosphate-buffered saline (PBS). Fluorescence images were captured with a Leica TCSSP2 confocal microscope (Wetzlar, Germany) equipped with a 63×/1.4 NA Plan-Apochromat oil immersion objective.

4.6. Morphological Analysis

Morphological analysis (skeleton, fractal analysis and hierarchical cluster analysis) were performed following procedures previously described by Fernández-Arjona [51] and Morrison [52]. Figures S2 and S3 illustrate the whole process, applied on a representative image for skeleton and fractal analysis, respectively. Parameters that we decided to eval-

uate in this work were summarized in Table S1. Regarding hierarchical cluster analysis (HCA), we decided to consider all parameters calculated with FracLac analysis even if multimodality index (MMI) was not higher than 0.55. Data were analyzed using GraphPad v6.0 software (San Diego, CA, USA) employing ANOVA followed by Tukey's test for group comparison. $p < 0.05$ was considered statistically significant.

4.7. Intracellular Calcium Mobilization Assay

Primary microglia cells and N9 cells were plated, respectively, at 50.000 and 20.000 cells/well into black walled, clear bottom 96-well plate (Greiner Bio One, Kremsmünster, Austria) and cultured up to 90–100% of confluence. Prior to assay, cells were incubated in dark conditions with 100 µL of Hank's Balanced Salt Solution (HBSS) containing 20 mM HEPES, 2.5 mM probenecid and 4.5 µM FLUO-4 NW (Molecular Probes, Eugene, OR, USA) at 37 °C and 5% CO_2 for 40 min. Fluorescence emissions were monitored with the multilabel spectrophotometer VICTOR^3 (Perkin Elmer, MA, USA) at 485/535 nm (excitation/emission filters) every 0.5 s for the 20 s preceding and the 60 s following the stimulation. Changes in fluorescence corresponded to changes in intracellular calcium levels. ATP was diluted in HBSS solution and injected into the wells by an automated injector system. Where indicated, PEA was added to the cells 1 h before the injection with the stimulus. All experiments were performed at 37 °C, and fluorescence values (F) were normalized against the baseline acquired immediately before stimulation (F0).

4.8. Electrophysiological Recordings by MEA System

Primary cortical neuron/astrocyte/microglia cultures were prepared as previously described [53] in MEA Petri dishes pre-coated with polyethyleneimine 0.1% (*w/v*, Sigma-Aldrich, St. Louis, MO, USA). After 3 h incubation, the plating medium was replaced by neurobasal medium (NB) with B27, 10 ng/mL basic fibroblast growth factor (bFGF) (all Thermo Fisher Scientific, Waltham, MA, USA), and 1 mM glutamine (Sigma-Aldrich, St. Louis, MO, USA). Cultures were covered with gas-permeable covers (MEA_MEM, Ala Scientific Instruments, Inc., Farmingdale, NY, USA) and were maintained for 12–22 days at 37 °C in a humidified atmosphere with 5% CO_2. Half of the medium volume was replaced every 3 days. Electrophysiological recordings were carried out at 12 to 16 days in vitro (DIV). Each MEA dish had a recording area of ~2 mm × 2 mm, constituted by 30 µm diameter ITO electrodes spaced 200 µm apart (Multichannels System, Reutlingen, Germany). In this area, the average number of neurons was ~6000, and astrocytes were about the same number. Drugs were added in volumes that were always < 1% of the total medium volume bathing the culture. As previously described [53,54], analog signals were recorded from the cultures at 36 °C in CO_2-controlled incubator by using MEA 1060BC or 1060INV pre-amplifiers (bandwidth 1–8000 Hz, Multichannel Systems, Reutlingen, Germany) connected to a MEA Work-station (bandwidth 100–8000 Hz, Plexon Inc., Dallas, TX, USA). Data were sorted as described in Gullo et al. [18,19]. Since our previous studies demonstrated that LPS causes the appearance of atypical events in the network, characterized by bursts with long duration, in this paper the burst duration (BD), and more precisely the value of BD at 95% of the cumulative distributions of BD (cumBD95), was used as the representative parameter of an overall increase in neuronal excitability. CumBD of the network was computed as previously described [18,19]. Briefly, a running window of duration from 10 ms to 1 s was applied to search for the start and the end of bursts. Each burst and each spike in the burst were precisely assigned to the neuron firing them. For each burst, the average time course (from its start to its end) was calculated, and to investigate the heterogeneity of the BD, we studied its distribution in the form of cumulative probabilities (cumBD) in each time of interest by performing a standard cumulative probability analysis. Data were analyzed and the figures were prepared using Neuroexplorer (v4.133, Plexon Inc., Dallas, TX, USA) (Figure 9A) and OriginPro 2018 (v9.5.193, OriginLab Corporation, Northampton, MA, USA) (Figure 9B). Data in Figure 9C are expressed as mean ± S.E.M. Normality of data were tested with GraphPad Prism (v6.0, San Diego, CA, USA), and statistical significance

of the difference of cumBD in LPS and in LPS after pretreatment with PEA was determined with multiple *t*-test corrected for multiple comparisons by using the Holm–Sidak method (GraphPad Prism v6.0).

4.9. TNF-α and BDNF Concentration Measurements

N9 cells were seeded at the concentration of 9×10^4 cells/well into a 12-well plate and then the day after were treated as described above. Levels of TNF-α released into the culture medium were quantified after 6 h by using the corresponding quantification ELISA kits (BMS607, Thermo Fisher Scientific, Waltham, MA, USA). In each MEA dish, small (150 µL) aliquots of the incubation medium were collected in control and at 6 h (representing the peak-time of LPS-induced TNF-α release [18]) after the addition of LPS (3 µg/mL) or PEA + LPS or SR144528 + PEA + LPS. Samples (50 µL) were analyzed in triplicate for murine TNF-α and BDNF with ELISA kits (BMS607, Thermo Fisher Scientific, Waltham, MA, USA) (KA0331 Abnova, Walnut, CA, USA) according to manufacturer's instructions. The data were expressed as pg/mL following interpolation on the basis of a standard curve. The experiments were repeated three independent times. Data were analyzed using GraphPad 6.0 software (San Diego, CA, USA) employing ANOVA followed by Tukey's test for group comparison. $p < 0.05$ was considered statistically significant.

4.10. SEAP Assay

THP-1 X-Blue and HEK-Blue hTLR4 cells were specifically designed for monitoring the NF-κB signal transduction pathway. Respectively, 8×10^4 and 3×10^4 cells/per well were seeded into a 96-well plate. Cells were then treated with 10 ng/mL LPS diluted in culture medium. PEA (100 µM) was applied 1 h before LPS and maintained in contact with the cells throughout the whole LPS exposure. Levels of SEAP in the supernatant were easily determined after 6 h with Quanti-Blue solution according to manufacturer's instructions (InvivoGen, San Diego, CA, USA). Activity of SEAP, expressed as OD, was normalized on value obtained by the control sample. Data was analyzed using GraphPad v6.0 software (San Diego, CA, USA) employing ANOVA followed by Tukey's test for group comparison. $p < 0.05$ was considered statistically significant.

Supplementary Materials: The following are available online at https://www.mdpi.com/1422-0067/22/6/3054/s1, Figure S1: Effect of PEAon Arg1 expression, Figure S2: Skeleton analysis of N9 microglia morphologies, Figure S3: FracLac for ImageJ to quantify cell complexity and shape, Table S1: Summary of microglia morphology parameters.

Author Contributions: Conceptualization, B.C. and A.T.; cell biology investigation, A.D., F.G., L.M., V.A., E.B., L.R., R.M. and S.C.; formal analysis, A.D. and L.M.; funding acquisition, A.T. and B.C.; MEA investigation, F.G. and M.L.; resources, B.C, M.C. and M.L.; supervision, B.C., M.L. and A.T.; validation, A.D., L.M., V.A., F.G., M.C., E.B., L.R. and R.M.; writing—original draft preparation, A.D., L.M., F.G., M.L., M.C., E.B., L.R., R.M. and B.C.; writing—review and editing, B.C., M.L., A.D., L.M. and A.T. All authors have read and agreed to the published version of the manuscript.

Funding: This research was supported in part by Fondo di Ateneo per la Ricerca of the University of Milano-Bicocca [FAR to A.T. and FAR to B.C.].

Institutional Review Board Statement: The study was conducted according to the guidelines of the Declaration of Helsinki, and approved by the Italian Ministry of Health (protocol No. 591/2017, 21/07/2017).

Informed Consent Statement: Not applicable.

Data Availability Statement: Not applicable.

Conflicts of Interest: The authors declare no conflict of interest.

References

1. Kettenmann, H.; Hanisch, U.-K.; Noda, M.; Verkhratsky, A. Physiology of microglia. *Physiol. Rev.* **2011**, *91*, 461–553. [CrossRef] [PubMed]
2. Ransohoff, R.M.; Perry, V.H. Microglial physiology: Unique stimuli, specialized responses. *Annu Rev. Immunol.* **2009**, *27*, 119–145. [CrossRef]
3. Kigerl, K.A.; Gensel, J.C.; Ankeny, D.P.; Alexander, J.K.; Donnelly, D.J.; Popovich, P.G. Identification of two distinct macrophage subsets with divergent effects causing either neurotoxicity or regeneration in the injured mouse spinal cord. *J. Neurosci. Off. J. Soc. Neurosci.* **2009**, *29*, 13435–13444. [CrossRef]
4. Mattace Raso, G.; Russo, R.; Calignano, A.; Meli, R. Palmitoylethanolamide in CNS health and disease. *Pharmacol. Res.* **2014**, *86*, 32–41. [CrossRef] [PubMed]
5. Facci, L.; Dal Toso, R.; Romanello, S.; Buriani, A.; Skaper, S.D.; Leon, A. Mast cells express a peripheral cannabinoid receptor with differential sensitivity to anandamide and palmitoylethanolamide. *Proc. Natl. Acad. Sci. USA* **1995**, *92*, 3376–3380. [CrossRef] [PubMed]
6. Redlich, S.; Ribes, S.; Schütze, S.; Nau, R. Palmitoylethanolamide stimulates phagocytosis of *Escherichia coli* K1 by macrophages and increases the resistance of mice against infections. *J. Neuroinflamm.* **2014**, *11*, 108. [CrossRef]
7. Guida, F.; Luongo, L.; Boccella, S.; Giordano, M.E.; Romano, R.; Bellini, G.; Manzo, I.; Furiano, A.; Rizzo, A.; Imperatore, R.; et al. Palmitoylethanolamide induces microglia changes associated with increased migration and phagocytic activity: Involvement of the CB2 receptor. *Sci. Rep.* **2017**, *7*, 375. [CrossRef]
8. McKimmie, C.S.; Fazakerley, J.K. In response to pathogens, glial cells dynamically and differentially regulate Toll-like receptor gene expression. *J. Neuroimmunol.* **2005**, *169*, 116–125. [CrossRef]
9. Marinelli, C.; Di Liddo, R.; Facci, L.; Bertalot, T.; Conconi, M.T.; Zusso, M.; Skaper, S.D.; Giusti, P. Ligand engagement of Toll-like receptors regulates their expression in cortical microglia and astrocytes. *J. Neuroinflamm.* **2015**, *12*, 244. [CrossRef]
10. Nomura, F.; Akashi, S.; Sakao, Y.; Sato, S.; Kawai, T.; Matsumoto, M.; Nakanishi, K.; Kimoto, M.; Miyake, K.; Takeda, K.; et al. Cutting edge: Endotoxin tolerance in mouse peritoneal macrophages correlates with down-regulation of surface toll-like receptor 4 expression. *J. Immunol.* **2000**, *164*, 3476–3479. [CrossRef]
11. Hines, D.J.; Hines, R.M.; Mulligan, S.J.; Macvicar, B.A. Microglia processes block the spread of damage in the brain and require functional chloride channels. *Glia* **2009**, *57*, 1610–1618. [CrossRef]
12. Buttini, M.; Limonta, S.; Boddeke, H.W. Peripheral administration of lipopolysaccharide induces activation of microglial cells in rat brain. *Neurochem. Int.* **1996**, *29*, 25–35. [CrossRef]
13. Karperien, A.; Jelinek, H.; Milosevic, N. Lacunarity Analysis and Classification of Microglia in Neuroscience. In Proceedings of the ESMTB 2011: 8th European Conference on Mathematical and Theoretical Biology, Krakow, Poland, 28 June–2 July 2011. [CrossRef]
14. Thorndike, R.L. Who belongs in the family? *Psychometrika* **1953**, *18*, 267–276. [CrossRef]
15. Domercq, M.; Vázquez-Villoldo, N.; Matute, C. Neurotransmitter signaling in the pathophysiology of microglia. *Front. Cell Neurosci.* **2013**, *7*, 49. [CrossRef]
16. Samuels, S.E.; Lipitz, J.B.; Dahl, G.; Muller, K.J. Neuroglial ATP release through innexin channels controls microglial cell movement to a nerve injury. *J. Gen. Physiol.* **2010**, *136*, 425–442. [CrossRef]
17. Wu, X.; Pan, L.; Liu, Y.; Jiang, P.; Lou, J.; Deversolc-Olerik, I.; Zhang, X.; Xu, J. Cell-cell communication induces random spikes of spontaneous calcium oscillations in multi-BV-2 microglial cells. *Biochem. Biophys. Res. Commun.* **2013**, *431*, 664–669. [CrossRef] [PubMed]
18. Gullo, F.; Amadeo, A.; Donvito, G.; Lecchi, M.; Costa, B.; Constanti, A.; Wanke, E. Atypical "seizure-like" activity in cortical reverberating networks in vitro can be caused by LPS-induced inflammation: A multi-electrode array study from a hundred neurons. *Front. Cell Neurosci.* **2014**, *8*, 361. [CrossRef] [PubMed]
19. Gullo, F.; Ceriani, M.; D'Alcia, A.; Wanke, E.; Constanti, A.; Costa, B.; Lecchi, M. Plant Polyphenols and Esendin-4 Prevent Hyperactivity and TNF-α Release in LPS-Treated In vitro Neuron/Astrocyte/Microglial Networks. *Front. Neurosci.* **2017**, *11*, 500. [CrossRef] [PubMed]
20. Zhang, P.; Liu, W.; Peng, Y.; Han, B.; Yang, Y. Toll like receptor 4 (TLR4) mediates the stimulating activities of chitosan oligosaccharide on macrophages. *Int. Immunopharmacol.* **2014**, *23*, 254–261. [CrossRef]
21. Ghosh, S.; Karin, M. Missing pieces in the NF-kappaB puzzle. *Cell* **2002**, *109*, 581–596. [CrossRef]
22. Karin, M.; Ben-Neriah, Y. Phosphorylation meets ubiquitination: The control of NF-[kappa]B activity. *Annu. Rev. Immunol.* **2000**, *18*, 621–663. [CrossRef]
23. Facchini, F.A.; Di Fusco, D.; Barresi, S.; Luraghi, A.; Minotti, A.; Granucci, F.; Monteleone, G.; Peri, F.; Monteleone, I. Effect of chemical modulation of toll-like receptor 4 in an animal model of ulcerative colitis. *Eur. J. Clin. Pharm.* **2020**, *76*, 409–418. [CrossRef] [PubMed]
24. D'Alcia, A.; Arrigoni, F.; Tisi, R.; Palmioli, A.; Ceriani, M.; Artusa, V.; Airoldi, C.; Zampella, G.; Costa, B.; Cipolla, L. Synthesis, Molecular Modeling and Biological Evaluation of Metabolically Stable Analogues of the Endogenous Fatty Acid Amide Palmitoylethanolamide. *Int. J. Mol. Sci.* **2020**, *21*, 9074. [CrossRef] [PubMed]

25. Howlett, A.C.; Barth, F.; Bonner, T.I.; Cabral, G.; Casellas, P.; Devane, W.A.; Felder, C.C.; Herkenham, M.; Mackie, K.; Martin, B.R.; et al. International Union of Pharmacology. XXVII. Classification of cannabinoid receptors. *Pharmacol. Rev.* **2002**, *54*, 161–202. [CrossRef] [PubMed]
26. Maresz, K.; Carrier, E.J.; Ponomarev, E.D.; Hillard, C.J.; Dittel, B.N. Modulation of the cannabinoid CB2 receptor in microglial cells in response to inflammatory stimuli. *J. Neurochem.* **2005**, *95*, 437–445. [CrossRef] [PubMed]
27. Ma, L.; Jia, J.; Liu, X.; Bai, F.; Wang, Q.; Xiong, L. Activation of murine microglial N9 cells is attenuated through cannabinoid receptor CB2 signaling. *Biochem. Biophys. Res. Commun.* **2015**, *458*, 92–97. [CrossRef] [PubMed]
28. Iannotti, M.A.; Di Marzo, V.; Petrosino, S. Endocannabinoids and endocannabinoid-related mediators: Targets, metabolism and role in neurological disorders. *Prog. Lipid Res.* **2016**, *62*, 107–128. [CrossRef] [PubMed]
29. Beggiato, S.; Tomasini, M.C.; Ferraro, L. Palmitoylethanolamide (PEA) as a potential therapeutic agent in Alzheimer's disease. *Front. Pharmacol.* **2019**, *10*, 821. [CrossRef]
30. Truini, A.; Biasiotta, A.; Di Stefano, G.; La Cesa, S.; Leone, C.; Cartoni, C.; Federico, V.; Petrucci, M.T.; Cruccu, G. Palmitoylethanolamide restores myelinated-fibre function in patients with chemotherapy-induced painful neuropathy. *CNS Neurol. Disord. Drug Targets* **2011**, *10*, 916–920. [CrossRef]
31. Lo Verme, J.; Fu, J.; Astarita, G.; La Rana, G.; Russo, R.; Calignano, A.; Piomelli, D. The Nuclear Receptor Peroxisome Proliferator-Activated Receptor-α Mediates the Anti-Inflammatory Actions of Palmitoylethanolamide. *Mol. Pharmacol.* **2005**, *67*, 15–19. [CrossRef] [PubMed]
32. Di Marzo, V.; Melck, D.; Orlando, P.; Bisogno, T.; Zagoory, O.; Bifulco, M.; Vogel, Z.; De Petrocellis, L. Palmitoylethanolamide inhibits the expression of fatty acid amide hydrolase and enhances the anti-proliferative effect of anandamide in human breast cancer cells. *Biochem. J.* **2001**, *358*, 249–255. [CrossRef] [PubMed]
33. Subhramanyam, C.S.; Wang, C.; Hu, Q.; Dheen, S.T. Microglia-mediated neuroinflammation in neurodegenerative diseases. *Semin. Cell Dev. Biol.* **2019**, *94*, 112–120. [CrossRef] [PubMed]
34. Block, M.L.; Zecca, L.; Hong, J.S. Microglia-mediated neurotoxicity: Uncovering the molecular mechanisms. *Nat. Rev. Neurosci.* **2007**, *8*, 57–69. [CrossRef] [PubMed]
35. Lawson, L.J.; Perry, V.H.; Dri, P.; Gordon, S. Heterogeneity in the distribution and morphology of microglia in the normal adult mouse brain. *Neuroscience* **1990**, *39*, 151–170. [CrossRef]
36. Ransohoff, R.M. A polarizing question: Do M1 and M2 microglia exist? *Nat. Neurosci.* **2016**, *19*, 987–991. [CrossRef] [PubMed]
37. Tang, Y.; Le, W. Differential Roles of M1 and M2 Microglia in Neurodegenerative Diseases. *Mol. Neurobiol.* **2016**, *53*, 1181–1194. [CrossRef]
38. Rivolta, I.; Binda, A.; Molteni, L.; Rizzi, L.; Bresciani, E.; Possenti, R.; Fehrentz, J.A.; Verdie, P.; Martinez, J.; Omeljaniuk, R.J.; et al. JMV5656, A Novel Derivative of TLQP-21, Triggers the Activation of a Calcium-Dependent Potassium Outward Current in Microglial Cells. *Front. Cell Neurosci.* **2017**, *11*, 41. [CrossRef]
39. Wang, X.; Li, C.; Chen, Y.; Hao, Y.; Zhou, W.; Chen, C.; Yu, Z. Hypoxia enhances CXCR4 expression favoring microglia migration via HIF-1alpha activation. *Biochem. Biophys. Res. Commun.* **2008**, *371*, 283–288. [CrossRef]
40. Ohto, U.; Fukase, K.; Miyake, K.; Satow, Y. Crystal structures of human MD-2 and its complex with antiendotoxic lipid IVa. *Science* **2007**, *316*, 1632–1634. [CrossRef]
41. Cotrina, M.L.; Lin, J.H.; López-García, J.C.; Naus, C.C.; Nedergaard, M. ATP-mediated glia signaling. *J. Neurosci. Off. J. Soc. Neurosci.* **2000**, *20*, 2835–2844. [CrossRef]
42. Schipke, C.G.; Boucsein, C.; Ohlemeyer, C.; Kirchhoff, F.; Kettenmann, H. Astrocyte Ca2+ waves trigger responses in microglial cells in brain slices. *Faseb J. Off. Publ. Fed. Am. Soc. Exp. Biol.* **2002**, *16*, 255–257. [CrossRef]
43. Verderio, C.; Matteoli, M. ATP mediates calcium signaling between astrocytes and microglial cells: Modulation by IFN-gamma. *J. Immunol.* **2001**, *166*, 6383–6391. [CrossRef]
44. Pires, M.; Raischel, F.; Vaz, S.H.; Cruz-Silva, A.; Sebastião, A.M.; Lind, P.G. Modeling the functional network of primary intercellular Ca2+ wave propagation in astrocytes and its application to study drug effects. *J. Biol.* **2014**, *356*, 201–212. [CrossRef] [PubMed]
45. Zeng, Y.; Lv, X.; Zeng, S.; Tian, S.; Li, M.; Shi, J. Sustained depolarization-induced propagation of [Ca2+]i oscillations in cultured DRG neurons: The involvement of extracellular ATP and P2Y receptor activation. *Brain Res.* **2008**, *1239*, 12–23. [CrossRef]
46. Santello, M.; Bezzi, P.; Volterra, A. TNFα controls glutamatergic gliotransmission in the hippocampal dentate gyrus. *Neuron* **2011**, *69*, 988–1001. [CrossRef] [PubMed]
47. Stellwagen, D.; Malenka, R.C. Synaptic scaling mediated by glial TNF-alpha. *Nature* **2006**, *440*, 1054–1059. [CrossRef] [PubMed]
48. Costello, D.A.; Lyons, A.; Denieffe, S.; Browne, T.C.; Cox, F.F.; Lynch, M.A. Long term potentiation is impaired in membrane glycoprotein CD200-deficient mice: A role for Toll-like receptor activation. *J. Biol. Chem.* **2011**, *286*, 34722–34732. [CrossRef]
49. Showalter, V.M.; Compton, D.R.; Martin, B.R.; Abood, M.E. Evaluation of binding in a transfected cell line expressing a peripheral cannabinoid receptor (CB2): Identification of cannabinoid receptor subtype selective ligands. *J. Pharmacol. Exp. Ther.* **1996**, *278*, 989–999. [PubMed]
50. Losurdo, M.; Pedrazzoli, M.; D'Agostino, C.; Elia, C.A.; Massenzio, F.; Lonati, E.; Mauri, M.; Rizzi, L.; Molteni, L.; Bresciani, E.; et al. Intranasal delivery of mesenchymal stem cell-derived extracellular vesicles exerts immunomodulatory and neuroprotective effects in a 3xTg model of Alzheimer's disease. *Stem Cells Transl. Med.* **2020**, *9*, 1068–1084. [CrossRef] [PubMed]

51. Fernández-Arjona, M.D.M.; Grondona, J.M.; Granados-Durán, P.; Fernández-Llebrez, P.; López-Ávalos, M.D. Microglia Morphological Categorization in a Rat Model of Neuroinflammation by Hierarchical Cluster and Principal Components Analysis. *Front. Cell Neurosci.* **2017**, *11*, 235. [CrossRef] [PubMed]
52. Morrison, H.; Young, K.; Qureshi, M.; Rowe, R.K.; Lifshitz, J. Quantitative microglia analyses reveal diverse morphologic responses in the rat cortex after diffuse brain injury. *Sci. Rep.* **2017**, *7*, 13211. [CrossRef]
53. Gullo, F.; Maffezzoli, A.; Dossi, E.; Wanke, E. Short-latency cross- and autocorrelation identify clusters of interacting cortical neurons recorded from multi-electrode array. *J. Neurosci. Methods* **2009**, *181*, 186–198. [CrossRef]
54. Gullo, F.; Mazzetti, S.; Maffezzoli, A.; Dossi, E.; Lecchi, M.; Amadeo, A.; Kranjeski, J.; Wanke, E. Orchestration of "presto" and "largo" synchrony in up-down activity of cortical networks. *Front. Neural Circuits* **2010**, *4*, 11. [CrossRef]

Appendix III

International Journal of *Molecular Sciences*

MDPI

Article

Synthesis, Molecular Modeling and Biological Evaluation of Metabolically Stable Analogues of the Endogenous Fatty Acid Amide Palmitoylethanolamide

Alessia D'Aloia [1,†], Federica Arrigoni [1,†], Renata Tisi [1,2], Alessandro Palmioli [1,2], Michela Ceriani [1], Valentina Artusa [1], Cristina Airoldi [1,2], Giuseppe Zampella [1], Barbara Costa [1,*] and Laura Cipolla [1,*]

[1] Department of Biotechnology and Biosciences, University of Milano-Bicocca, Piazza della Scienza 2, 20126 Milano, Italy; alessia.daloia@unimib.it (A.D.); federica.arrigoni@unimib.it (F.A.); renata.tisi@unimib.it (R.T.); alessandro.palmioli@unimib.it (A.P.); michela.ceriani@unimib.it (M.C.); v.artusa@campus.unimib.it (V.A.); cristina.airoldi@unimib.it (C.A.); giuseppe.zampella@unimib.it (G.Z.)

[2] Milan Center for Neuroscience (NeuroMI), University of Milano-Bicocca, P.zza dell'Ateneo Nuovo 1, 20126 Milano, Italy

* Correspondence: barbara.costa@unimib.it (B.C.); laura.cipolla@unimib.it (L.C.)

† These authors contributed equally to the work.

Received: 2 October 2020; Accepted: 26 November 2020; Published: 28 November 2020

check for updates

Abstract: Palmitoylethanolamide (PEA) belongs to the class of *N*-acylethanolamine and is an endogenous lipid potentially useful in a wide range of therapeutic areas; products containing PEA are licensed for use in humans as a nutraceutical, a food supplement, or food for medical purposes for its analgesic and anti-inflammatory properties demonstrating efficacy and tolerability. However, the exogenously administered PEA is rapidly inactivated; in this process, fatty acid amide hydrolase (FAAH) plays a key role both in hepatic metabolism and in intracellular degradation. So, the aim of the present study was the design and synthesis of PEA analogues that are more resistant to FAAH-mediated hydrolysis. A small library of PEA analogues was designed and tested by molecular docking and density functional theory calculations to find the more stable analogue. The computational investigation identified RePEA as the best candidate in terms of both synthetic accessibility and metabolic stability to FAAH-mediated hydrolysis. The selected compound was synthesized and assayed ex vivo to monitor FAAH-mediated hydrolysis and to confirm its anti-inflammatory properties. ^{1}H-NMR spectroscopy performed on membrane samples containing FAAH in integral membrane protein demonstrated that RePEA is not processed by FAAH, in contrast with PEA. Moreover, RePEA retains PEA's ability to inhibit LPS-induced cytokine release in both murine N9 microglial cells and human PMA-THP-1 cells.

Keywords: palmitoylethanolamide; fatty acid amide hydrolase; inflammation; PPAR-α receptor; metabolism; PEA analogues

1. Introduction

Fatty acid ethanolamides are a family of endogenous bioactive compounds abundant in the central nervous system, attracting great attention due to their physiological, pro-homeostatic, and therapeutic potential for the treatment of various pathological conditions, such as inflammation, neurodegenerative diseases, and neuropathic pain. Among this class of compounds, palmitoylethanolamide (PEA, *N*-(2-Hydroxyethyl)hexadecanamide) is particularly interesting. PEA acts through different

mechanisms affecting multiple pathways, both at the cellular and molecular level; however, arising evidence is demonstrating that one of the few identified mechanisms for anti-inflammatory PEA effects is due to peroxisome proliferator-activated receptor-α (PPAR-α) binding, resulting in the activation of PPAR-α-dependent gene transcription [1].

The main drawback of fatty acid ethanolamides as therapeutics is their poor in vivo metabolic stability, due to their fast hydrolysis by a series of hydrolytic enzymes, such as fatty acid amide hydrolase (FAAH), *N*-acylethanolamine acid amidase (NAAA), and monoacylglycerol lipase (MAGL). Concerning exogenous PEA as a drug, few data on its pharmacokinetics in humans or experimental animals are currently available; this issue has been recently reviewed by Rankin and Fowler who stated that "concerning the ADME of PEA there are large gaps in our knowledge" [2]. However, these data suggest that PEA produces limited systemic exposure levels, with plasma concentrations remaining in the nM range and with significant increases only for a short period; oral administration of PEA leads to a variable increase in plasma concentration, ranging from 2- to 9-fold from baseline [3]. The administration of 300 mg of ultramicronized PEA to healthy volunteers doubled the plasma level at 2 h with undetectable levels at 4 h [4]. FAAH-mediated metabolism may be, at least in part, responsible for the limited exposure of exogenous PEA. In fact, hydrolytic enzymes participate not only in the regulation of specific tissue levels of PEA but also in the first-pass effect, since the liver is the second organ, after the brain, in which FAAH shows the highest specific activity [5]. For these reasons, in the last decades a great deal of research has been focused on the design of ethanolamide analogues with increased stability to hydrolysis [5,6].

The key issue to ethanolamide analogues is maintaining the higher stability of hydrolytic enzymes while preserving the ability to bind to responsive receptors, such as PPAR-α. In this work, we propose the design of a small library of PEA analogues and an in silico study of PPAR-α ligands with hydrolytic stability towards FAAH and NAAA. The most promising compound was synthesized and preliminary biological evaluation is reported.

2. Results

2.1. Design of PEA-Analogues

PEA is a structurally simple amide constituted of palmitic acid as the acid component and the two carbon 2-aminoethanol as the amine moiety. Besides the amido group, the only additional functionality is the hydroxyl group, representing the polar head of the molecule. The aim of this work is to design PEA analogues that are still able to maintain biological activity and which possess longer life in vivo than their natural counterpart and are more stable to the hydrolytic action of FAAH. Both FAAH and NAAA exert their catalytic activity through a first nucleophilic attack of catalytic serine or cysteine, respectively, to the carbonyl group (vide infra); this first step towards hydrolysis may be influenced by stereoelectronic effects. Variation in the carbonyl group substituents can modify their propensity towards the nucleophilic attack of the catalytic amino acid, as well as steric hindrance. In order to modify carbonyl electrophilicity, modifications of the amidic bond are proposed: at first, the isosteric analogue **2** (RePEA, Figure 1), possessing a retroamide linkage between pentadecanamine and 2-hydroxypropanoic acid, was considered. In order to design PEA analogues with potentially increased stability, the amide bond was also substituted with an ester bond (**3**, Figure 1), with alkoxy amines, either with the alkoxy moiety as a mimic of the 2-aminoethanol polar head (compounds **4** and **7**, Figure 1) or as the apolar tail (**6**, Figure 1), and with acyl hydrazides (**5** and **8**, Figure 1). Finally, in order to evaluate the steric effect both on hydrolysis and PPAR-α affinity, two commercially available PEA analogues were also considered, (*R*)-palmitoyl-(1-methyl) ethanolamide (**9**, also referred to as MePEA1, Figure 1), which reproduces the presence of a methyl group similar to methanandamide [6] and (*R*)-palmitoyl-(2-methyl) ethanolamide (**10**, also referred to as MePEA2, Figure 1), where the methyl group is located on the *β*-carbon from the amidic group.

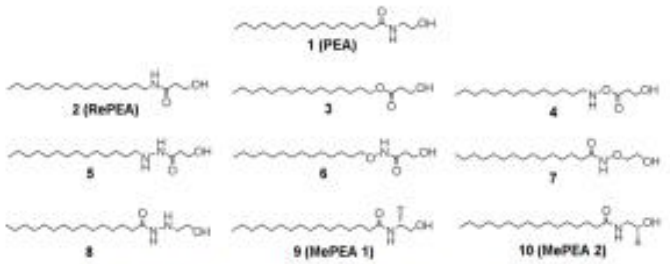

Figure 1. Chemical structures of PEA (palmitoylethanolamide) and its analogues.

2.2. Analogues of PEA Can Equally Bind PPAR-α Receptor

In the attempt of preserving the biological activity of PEA analogues, we took advantage of the availability of the X-ray crystal resolved PPAR-α receptor ligand-binding domain structure. All the ligands of the library have been designed purposefully to maintain the general PEA molecular scaffold (Figure 2A) to minimize the effect on yet uncharacterized sites of action. Molecular docking of PEA and its analogues to the binding domain of PPAR-α revealed a very similar binding mode (Figure 2B). Interestingly, even the top XP Glide scores of all ligands are rather close in energy, in a range from −6.0 to −8.4 kcal/mol.

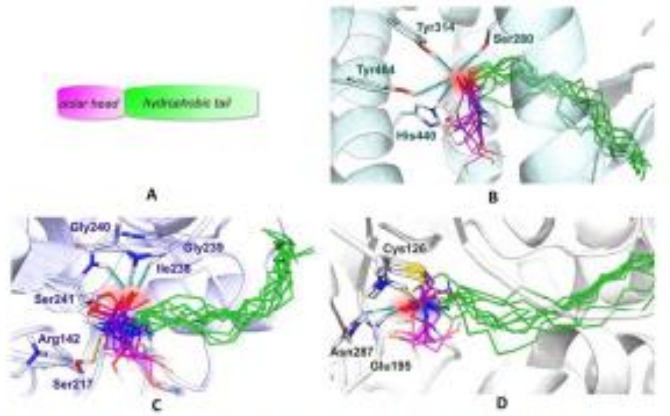

Figure 2. (**A**) Schematic scaffold of PEA and analogues **2**–**10**. They all feature a polar head, which is represented in pink, and a hydrophobic tail, in green. (**B**) Docking poses of PEA and analogues **2**–**10** into the PPAR-α (peroxisome proliferator-activated receptor-α) pocket. The side chains of key residues, Ser280, Tyr314, Tyr464, and His440 are shown as sticks. (**C**) Covalent docking poses of PEA and analogues **2**–**10** into the FAAH (fatty acid amide hydrolase) active site. All ligands are covalently bound to Ser241. The rest of the catalytic triad, formed by Ser217 and Arg142, together with the oxyanion hole, formed by Ser241, Gly240, Gly239, and Ile238, are shown as sticks. (**D**) Covalent docking poses of PEA

and analogues **2**–**10** into the NAAA active site. All ligands are covalently bound to Cys126. The oxyanion hole, formed by Asn287 and Glu195, is highlighted with stick representation. Oxygen, nitrogen, and sulfur atoms are colored in red, dark blue, and yellow, respectively. Significative non-bonding interactions are represented as black dotted lines. The ones involving the carbonyl group of ligands are highlighted in light blue, whereas the ones involving the amine group of ligands are highlighted in yellow. The different conformations of Ser241 (in (C)) and Cys126 (in (D)) result from covalent docking simulations, which imply geometry relaxation of the reactive residue, upon covalent bond formation.

The polar head and lipidic tail of each ligand are superimposed, occupying the arm I and arm II of the PPAR-α Y-shaped cavity, respectively (Supplementary Figure S1). This feature is essentially shared by most known PPAR full agonists [7,8]. Arm I is the only substantially polar cavity of PPAR-α and it extends toward the C-terminal helix12, referred to as AF2 (activation function-2) helix. The involvement of the latter in a conserved hydrogen bonds pattern has been proposed to be at the basis of PPAR agonism [9]. Particularly, the interaction between Tyr464 and the ligands has been found to be crucial for regulating the co-activator recruitment. Such an interaction, together with other H-bonds involving three polar residues that are highly conserved in the arm I of each PPAR isotype (Ser280, Tyr314, and His440 in PPAR-α) [10], has been proposed to hold the AF2 helix in the active conformation which is permissive for interactions with co-activators [11].

Remarkably, we found that these key interactions are intercepted by PEA and all of the docked analogues (Figure 2B). Indeed, Ser280, His440, and Tyr314 interact with the carbonyl group of the ligand amide bond, while in the lower energy poses Tyr464 interacts invariably with the carbonyl functionality or with the hydroxyl group of the ethanolamine portion.

In order to further assess the similarity of the designed ligands with PEA, in terms of their interaction with PPAR-α, we built Structural Interaction Fingerprints (SIFs), which capture the 3D information associated with a receptor–ligand complex into a 1D representation. This tool, generally used for docking-based virtual screening and poses clustering [12], allowed us to straightforwardly compare the interaction patterns provided by our docked ligands within the PPAR-α pocket (Figure 3). The SIFs obtained, considering the lowest energy pose of each compound, are all almost identical.

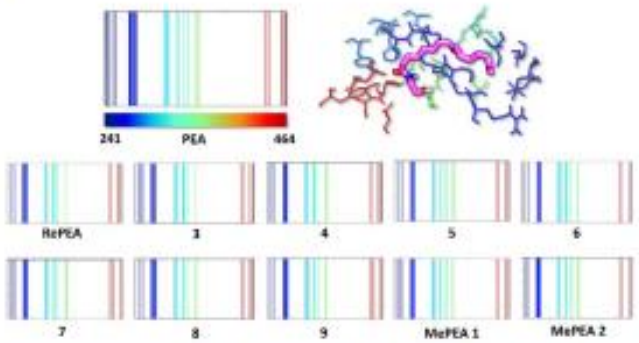

Figure 3. Structural Interactions Fingerprints (SIFs) of PEA and its analogues within the PPAR-α receptor. Each ligand is represented by a binary string encoding its interactions with the receptor residues, that are found between Ile241 and Tyr464. A solid-colored line in the SIFs indicates that the ligand is involved in one (or more) interaction(s) with the residue of the corresponding color (from dark blue to dark red).

This observation means that all the designed ligands interact with PPAR-α in a strictly analogous fashion, i.e., the same portion of each ligand generates essentially the same interactions with the same proximal residue(s). Since all the ligands also show a very similar predicted affinity for the receptor, we should expect, at least in principle, the triggering of the same biological response, at least as far as PPAR-α is involved. Moreover, the conservation of structural and molecular properties of PEA in all of the designed analogues suggests that they should retain interaction with other PEA targets as well.

2.3. All of the Designed Compounds Are Eligible as FAAH Substrate

Once verified that any structural modifications rationally introduced to PEA scaffold should not alter biological activity, we performed molecular docking on FAAH, to analyze the behavior of the ligands toward FAAH-mediated hydrolysis. Once more, covalent docking results suggest that PEA and its analogues should be similarly accommodated within the catalytic pocket (Figure 2C). In particular, their polar head directly interacts with the catalytic triad formed by Ser241, Ser217, and Lys142, while the hydrophobic chain occupies the acyl-chain binding pocket (ABP) [13]. This conformation should represent the pre-reactive pose for ligand hydrolysis [14,15]. According to the reported catalytic mechanism, the catalytic triad assists the proton transfer from Ser241 to the unprotonated Lys142, mediated by Ser217. Ser241 is thus responsible for the nucleophilic attack to the C=O bond of the ligand and the formed tetrahedral intermediate is stabilized by the oxyanion hole constituted by Ser241, Gly240, Gly239, and Ile238 [16,17]. Interestingly, the ligand interactions with the oxyanion hole are found in all of the best poses of each ligand, suggesting that they should undergo hydrolysis according to a general mechanism that is similar to the typical one proposed for fatty acid ethanolamides, such as PEA (see Supplementary Figure S2 for ligand-specific ligand interaction diagrams and scores). Other conserved interactions found in the docked ligand–protein complexes involve Ser217 and Met191, in line with previous investigations [18]. In particular, Ser217 interacts with the ligand amine functionality, prompted by the subsequent proton transfer that assists in leaving group release (ethanolamine in the case of PEA). The amine moiety is also involved in a H-bond interaction with the backbone of Met191. The latter is also found to interact through its sidechain with the hydroxyl head of some docked ligand. The CovDock results do not provide any structural or energetic rationale of hypothetical different stability of the docked ligands toward hydrolysis.

2.4. Identification of Analogues with a Higher Metabolic Stability

The structural variability introduced in the ligand set would tune the (i) amide electronic properties, (ii) effectiveness of protein–ligand interactions, and (iii) steric hindrance, all factors that could affect hydrolysis kinetic. To unravel this, we switched to a DFT (density functional theory) model (see Section 4), in order to characterize hydrolysis energy profiles (Figure 4). The approach consists of the construction of an all-QM (quantum mechanical) cluster model, starting from the CovDock poses obtained at the previous stage. The model comprises the catalytic triad and all the other residues (properly truncated) which interact with the docked ligands and/or limit the volume of the catalytic pocket. The proposed all-QM methodology is novel in the context of FAAH computational modeling and is an alternative to previously reported methodologies [19] falling in the QM-MM (quantum mechanics/molecular mechanics) framework [19–25]. In these works, the QM part, limited to the sole catalytic triad and to the polar head (plus a variable number of carbon atoms, depending on each case study) of the ligand, has been treated at a semiempirical level. The all-QM approach used in the present work explicitly includes the treatment of dispersion forces, allowing the quantification of the energetic contributions associated with both the covalent and non-covalent interactions at a higher accuracy level. This issue is crucial for the detection of eventual energy differences in the hydrolysis process resulting from ligands with very subtle structural differences. The calculated energy profiles depict only the first stage of hydrolysis, namely to the acyl enzyme intermediates, since it is reasonable to assume that the energy cost associated with enzyme de-acylation, assisted by a water molecule, would be identical for all of the ligands. The energy profiles have been calculated only for a selected

subset of representative ligands (PEA, RePEA, **4**, **6**, **7**, **8**, MePEA1, MePEA2), selected to verify the effects on hydrolysis kinetics and thermodynamics deriving from (i) inversion of the amide bond, thus going from PEA-like to RePEA-like ligands, (ii) addition of heteroatoms in proximity to the amide group, and (iii) introduction of a methyl substituent in the polar head.

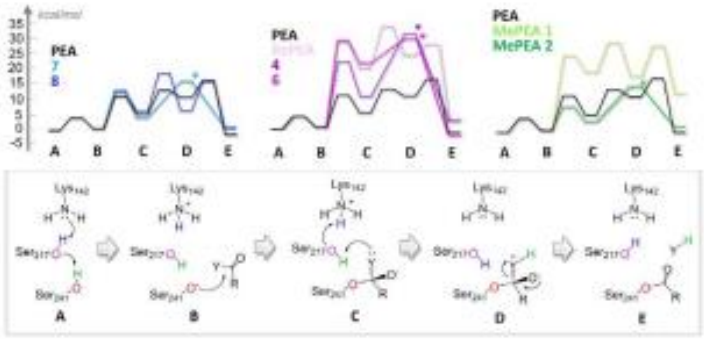

Figure 4. Top: energy profiles (kcal/mol) associated with the FAAH acylation phase of hydrolysis of PEA-like ligands (left blue shades), RePEA-like ligands (middle, purple shades), and MePEA ligands (right, green shades). The PEA hydrolysis profile (black lines) has been taken as a reference for each plot. If present, "*" indicates a concerted elementary reaction step from C to E (i.e., without passing through the formation of D. Bottom: reaction mechanism corresponding to the calculated energy profiles.

The lowest energy mechanism associated with FAAH acylation, as characterized by DFT calculations, is reported in Figure 4 and the results are compatible with previously proposed mechanisms [20,23]. The resting state (A) evolves through a concerted proton transfer, assisted by the catalytic triad, which ends with the deprotonation of Ser241 (B). The latter acts as a nucleophile attacking the amide carbonyl and forming the tetrahedral intermediate (C). A second concerted proton transfer (from Lys142 to Ser217) assists the leaving group protonation by Ser217 (D) and the acyl-enzyme is thus formed (E). Intermediate D is predicted to be transient, as expected, so for half of the tested ligands, it should not be formed at all along the catalytic cycle. This suggests that steps C→D and D→E can easily occur in a concerted manner, which also emerged from previous computational investigations [20]. The first step A→B represents an intermolecular proton transfer whose energy is independent from the nature of the ligand. This step is predicted to be facile, both kinetically and thermodynamically. Indeed, intermediate B is found to be rather stable, since the negatively charged Ser241 thiolate is strongly stabilized by interactions with the side chain of Ser217 and the backbone of Gly216. Interestingly, this result is novel with respect to previous theoretical investigations, which suggested A→B and B→C to be essentially concomitant [21,24]. The rate-determining step for PEA hydrolysis is the nucleophilic attack by Ser241, which also emerged from previous investigations on other ethanolamides, such as oleamide, although our calculated activation barrier is smaller (11.3 kcal/mol) than the one predicted for oleamide at different levels of theory (~18 kcal/mol) [22]. However, if considering the energetic span of the profile, calculated taking into account the energy separation between the lowest intermediate and the highest transition state, we obtained a value of 18.9 kcal/mol. Interestingly, this value is very close to the experimental activation barrier of 16 kcal/mol for the hydrolysis of oleamide, which is structurally related to PEA [26].

The calculated energy profiles suggest that two specific structural features should have a high impact on hydrolysis kinetics.

The first one is the inversion of the amide bond, going from PEA-like to RePEA-like ligands, which causes a doubling of the calculated catalysis energetic span (Figure 4, top, purple shades profiles). By reverting the amide bond, in fact, the oxyanion formed upon nucleophilic attack is not sufficiently stabilized by the oxyanion hole (Supplementary Figure S3A). This would translate into a more difficult hydrolysis process compared to the one of PEA.

A second structural feature that could hinder hydrolysis is the introduction of some steric bulk in the molecular structure, such as a methyl group, at the C-α of PEA. The calculated energy profile for MePEA1 lies, in fact, significantly higher in energy with respect to the one of PEA (Figure 4, top, light green energy profile). This result, which is in agreement with previous observations regarding anandamide vs. methanandamide behaviors [6], can be ascribed to the steric hindrance and electrostatic repulsion that are caused by introducing the methyl group (hydrophobic) in proximity to the oxyanion hole (hydrophilic) (Supplementary Figure S3B). This is supported by the fact that the shift of the methyl group in beta position, in MePEA2, is not predicted to alter hydrolysis kinetics with respect to PEA one (Figure 4, top, dark green energy profile), as a result of the absence of steric clashes with the protein matrix.

2.5. Ligand Binding to NAAA and Implications on Hydrolysis

To further investigate the behavior towards the hydrolysis of PEA and its analogues, we tested in silico their binding mode to human NAAA. According to the postulated mechanism, the N-terminal Cys126 participates in catalysis in zwitterionic form, as a Cys-S^-/Cys-NH_3^+ ion pair, being both the nucleophile and proton source [27,28]. First, the thiolate attacks the carbonyl, forming the tetrahedral oxyanion intermediate, and then the proton is transferred from the α-amino group of Cys126 to the ligand, allowing the release of the leaving group. Although the tetrahedral intermediate is supposed to be elusive [29], an active role has been proposed for the backbone of Glu195 and the sidechain of Asn287 in stabilizing the oxyanion formed upon nucleophilic attack [30].

The poses obtained upon covalent docking of PEA and analogues are very similar: the acyl chain is enclosed in a very narrow hydrophobic channel, while the polar head in the calyx-shaped cavity is exposed to the solvent (Figure 2D). In all the top score poses of each ligand, we find the expected H-bond pattern involving the oxyanion hole (Glu195, Asn287) and the negatively charged oxygen atom of the tetrahedral intermediate. These observations suggest that all the tested ligands can be recognized and similarly bound by NAAA (see Supplementary Figure S4 for further details on ligand interactions and scores). Another frequent interaction involves Asp145 and the ligand polar head, in line with the proposal that this residue should assist enzyme turnover by shuttling protons to/from Cys126 [27,29].

The simulated structure of PEA tetrahedral intermediate resembles the one modelled on the crystal structure of conjugated bile acid hydrolase (CBAH), another N-terminal cysteine hydrolase sharing with NAAA a highly conserved portion of the catalytic N-terminal region [31]. In PEA-like analogues, the amine of the ethanolamine head directly points toward Cys126-NH_2, a feature that should indicate a fast Cys126-to-ligand proton transfer (Figure 5A). If the amide bond is reverted, instead, as in RePEA-like analogues, the amine group of the ligand is shifted and located at a significant distance from to Cys126-NH_3^+ (Figure 5B). This would suggest that the Cys126-to-ligand proton transfer should be hindered unless we invoke important conformational rearrangements or alternative mechanisms for hydrolysis.

The computational investigation performed on the three targets suggests that the most strategic structural modifications to introduce in the PEA scaffold, in order to hinder hydrolysis, are reverting the amide bond and/or introducing steric bulkiness in the proximity of the amide. Particularly, among the RePEA-like compounds, RePEA is the best candidate in terms of both synthetic accessibility and metabolic stability to FAAH-mediated hydrolysis.

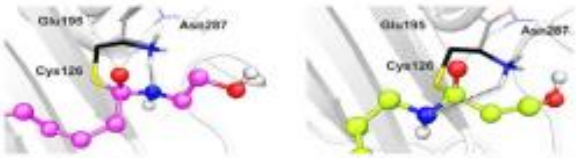

Figure 5. Comparison of the docking poses of PEA (**A**) and RePEA (**B**) into the NAAA pocket. In both cases, the oxyanion hole (Glu195 and Asn287) interacts with the negatively charged oxygen atom of the ligand. By reverting the amide bond, however, effective interaction between the NH_3^+ terminal of Cys126 and the leaving group of the ligand is hindered.

2.6. RePEA Is Stable When Exposed to FAAH-Containing Membranes

In order to validate DFT model predictions, PEA and RePEA hydrolysis, affording ethanolamine (EA) and 3-hydroxy-propionic acid (3-HPA), respectively (Figure 6), were monitored by ^{1}H-NMR spectroscopy over 24 h (Figure 7 and Supplementary Figure S5A,B).

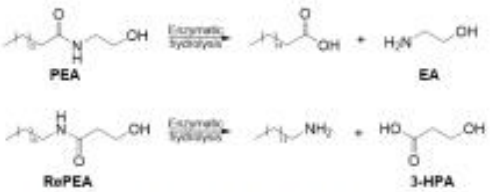

Figure 6. Enzymatic hydrolysis of PEA and RePEA affording ethanolamine (EA) and 3-hydroxypropionic acid (3-HPA), respectively.

To membrane samples purified from frozen primary cortical cultures (cerebral cortices) from postnatal mice and containing FAAH as an integral membrane protein (a representative spectrum of membrane samples is depicted in Figure 7A), 1 mM of either PEA (Figure 7B) or RePEA (Figure 7E) was added and the mixtures were incubated in deuterated PBS, pH 7.4 with 10% d_6-DMSO, at 37 °C. For each sample, a series of ^{1}H-NMR spectra was recorded in 30 min intervals over 24 h (Supplementary Figure S5) to check the formation of the hydrolysis products. EA and 3-HPA NMR resonances are clearly highlighted in reference spectra (Figure 7D,G respectively) acquired on membrane samples spiked with the two compounds at a concentration of 0.1 mM. While EA resonances are also detectable in spectra acquired on membrane samples incubated with PEA (Figure 7C and Supplementary Figure S5A), 3-HPA signals did not appear after the addition of RePEA to membrane samples (Figure 7F and Supplementary Figure S5B). These findings definitely indicate that, under the experimental conditions described, PEA is partially converted to EA by FAAH, in contrast with RePEA, which appears to be resistant to FAAH-mediated hydrolysis.

Notably, in both cases the NMR signal of glycerol and other small metabolites appeared in the NMR spectra over time, suggesting their slow release from the membrane during kinetic monitoring.

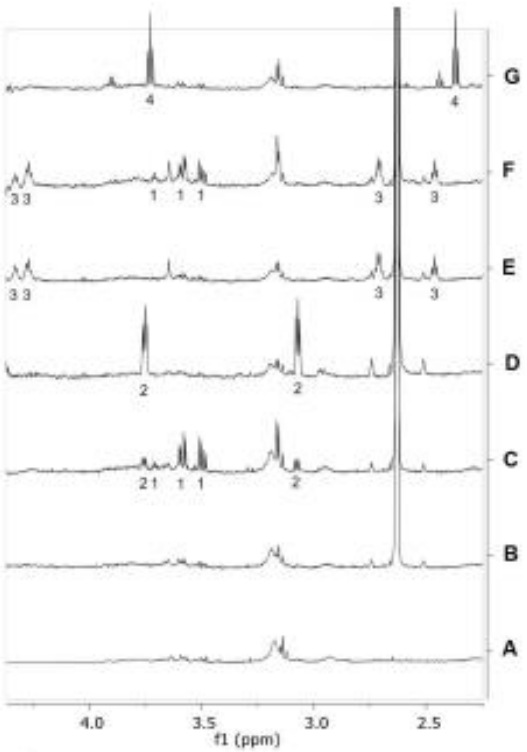

Figure 7. (**A**) ^{1}H NMR spectrum of a membrane sample dissolved in deuterated PBS, pH 7.4, 37 °C. (**B**,**C**) ^{1}H NMR spectra of the same sample after the addition of 1 mM PEA dissolved in d_6-DMSO. Number of scans (NS) = 64; spectrum B recorded at t = 0 s after PEA addition, spectrum C recorded after 12 h; (**D**) ^{1}H NMR spectrum of a membrane sample spiked with 0.1 mM ethanolamine (EA) dissolved in deuterated PBS, 10% d_6-DMSO, pH 7.4, 37 °C; (**E**,**F**) ^{1}H NMR spectra of the same sample after addition of 1 mM RePEA dissolved in d_6-DMSO; spectrum E recorded at t = 0 s after RePEA addition, spectrum F recorded after 12 h; (**G**) ^{1}H NMR spectrum of a membrane sample spiked with 0.1 mM 3-hydroxypropanoic acid (3-HPA) dissolved in deuterated PBS, 10% d_6-DMSO, pH 7.4 37 °C. PEA NMR resonances are not visible in spectra B and C due to PEA interaction in membranes. 1: glycerol, 2: EA, 3: RePEA, 4: 3-HPA.

2.7. PEA and RePEA Inhibits LPS-Induced Tumor Necrosis Factor-α (TNF-α) and Interleukin-6 (IL-6) Release in N9 Microglial Cells

To establish the bioactivity of PEA and its analogues, murine N9 microglial cells were used. The N9 microglia cells were developed by immortalizing primary microglia cells with the *v-myc* or *v-mil* oncogenes of the avian retrovirus MH2 [32] and are commonly used as an inflammatory model

as they upregulate the pro-inflammatory genes, including inducible nitric oxide synthase (iNOS), cyclooxygenase-2, TNF-a and interleukin-1β (IL-1β) [33].

In order to select the concentration of compounds to be used, we performed preliminary experiments showing that PEA treatment (1–100 nM for 24 h) did not induce significant cellular cytotoxicity on murine microglia cells. In addition, the same concentration of PEA demonstrated a significant modulatory effect on rat microglia [34]. Therefore, we also examined the toxicity of 100 nM PEA analogues (RePEA, MePEA1, MePEA2).

Murine N9 microglia cells were incubated for 1 h with 100 nM of each compound and after 24 h cell viability was analyzed by MTT assays. Cells treated with vehicle (DMSO) were used as control. As is shown in Figure 8, none of the compounds had any effects on cell viability and they were not cytotoxic.

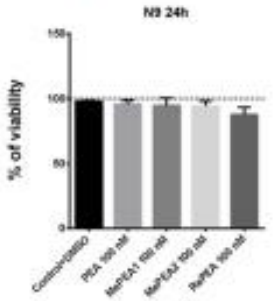

Figure 8. Cell viability in N9 murine microglial cells incubated for 1 h with 100 nM PEA and its analogues (MePEA1, MePEA2, RePEA). Then, medium was replaced with fresh IMDM supplemented with 5% FBS. Cell viability was quantified after 24 h. Data are presented as mean ± S.E.M. ($n = 3$ independent experiments).

To confirm MTT results, N9 cells were also analyzed by inverted microscopy (Figure 9 and Supplementary Figure S6) that revealed no changes in cell morphology between N9 cells treated with PEA or its analogues and cells not treated or treated with vehicle (DMSO).

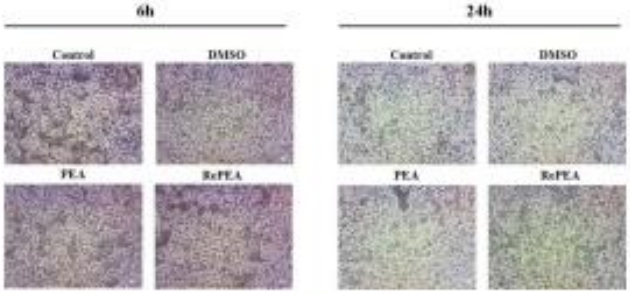

Figure 9. Cellular morphology of N9 cells incubated for 1 h with 100 nM PEA or RePEA. Then, medium was replaced with fresh IMDM supplemented with 5% FBS. After 6 or 24 h optical images were captured with an inverted Olympus CKX41 microscope. Representative images out of at least three separate experiments are shown. Scale bar: 10 μm.

Microglia responses in inflammation have been extensively triggered by the use of lipopolysaccharide (LPS), a wall component of Gram-negative bacterial cells; in particular, LPS binds the CD14/TLR4/MD2 receptor complex on cell membranes and induces responses such as release of inflammatory mediators, e.g., TNF-α IL-6, and IL-1β [35,36]. Initially, to test the ability of PEA and its analogues to inhibit TNF-α release, N9 cells were stimulated with LPS for 1 h; cells were then treated with 100 nM of PEA or with its analogues (1 h) and TNF-α release was examined at 3 h, 6 h, and 24 h. No effect was observed at 3 and 6 h time points (data not shown). After 24 h, PEA, MePEA1, and RePEA inhibited TNF-α release, while MePEA2 appeared to be less effective (Figure 10A).

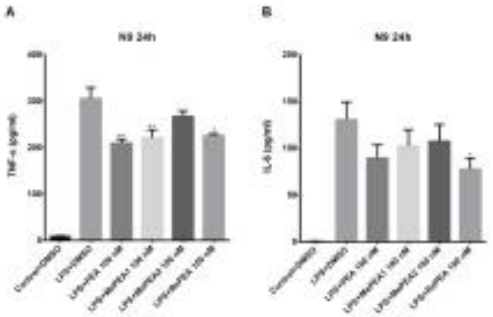

Figure 10. Release of TNF-α and of IL-6 at 24 h after LPS application. The mouse N9 microglial cells were stimulated with LPS at 10 ng/mL for 1 h; then, LPS-containing medium was removed and cells were incubated for 1 h with 100 nM PEA and its analogues (MePEA1, MePEA2, RePEA). Then, medium was replaced with fresh IMDM supplemented with 5% FBS. The amount of TNF-α (**A**) and of IL-6 (**B**) released into the culture medium was quantified after 24 h. Data are presented as mean ± S.E.M. ($n = 3$ independent experiments). Significant differences from LPS were determined using nonparametric one-way analysis of variance (ANOVA) with post hoc Dunnett's multiple comparison tests at * $p < 0.05$; ** $p < 0.01$.

Afterwards, the release of IL-6 and IL-1β was examined at 24 h. As it is shown in Figure 10B only RePEA was able to counteract the release of IL-6 and this result is statistically significant in respect of LPS. Unfortunately, IL-1β release was not detectable and the effect of PEA and its analogues could not be assessed. This is not surprising as the release of IL-1β from mouse microglial cells is a very inefficient process and needs two different treatments (LPS and ATP) to be detectable [37].

2.8. PEA and RePEA Effects on Nuclear Factor Kappa-Light-Chain-Enhancer of Activated B Cells (NF-κB) Activation in Human PMA-THP-1 X-Blue™ Cells

Often mouse and human cells give rise to different results. As PEA analogues have been generated to be used on human beings, the experiments previously performed on mouse N9 microglial cells were repeated on PMA-THP-1 X-Blue™ human cells. Moreover, between the proposed compounds, only RePEA functioned at different times in N9 cells therefore the assays were performed using only PEA and RePEA.

At first, viability assays (MTT assay) and morphology analyses were performed at 24 h, the time at which TNF-α release has given the best results. The experiments show that PEA and RePEA were not cytotoxic and the morphology was not influenced by their presence (Figure 11B and Supplementary Figure S7).

Although structurally different, TNF-α, IL-1β, and toll-like receptors (TLR) use similar signal transduction mechanisms that include activation of IkB kinase (IKK) and NF-κB [38]. In order to obtain further insight into the role of the TLR4/NF-κB axis in the previously observed inhibition of pro-inflammatory cytokines, NF-κB activation triggered by TLR4 stimulation was investigated in PMA-THP-1 X-Blue™ cells. PMA-THP-1 X-Blue™ cells were used as a tool to investigate whether PEA and/or RePEA act involving TLR4 directly. Cells were treated as described in Materials and Methods. As shown in Figure 11A, at 24 h, both PEA and RePEA inhibited NF-κB activation triggered by TLR4 stimulation in PMA-THP-1 X-Blue™. In particular, RePEA decreased SEAP (secreted embryonic alkaline phosphatase) release by 50% while PEA decreased it by about 30%.

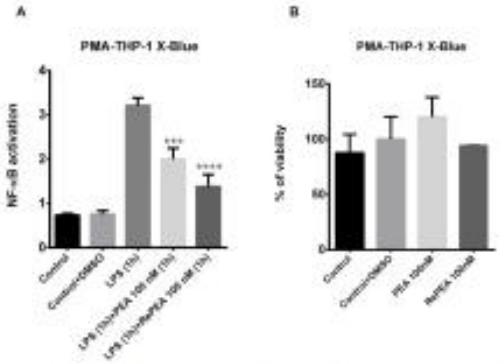

Figure 11. (**A**) Inhibition of NF-κB activation in LPS-stimulated PMA-THP-1 X-Blue™ cells by PEA and RePEA. PMA-THP-1 X-Blue™ cells were stimulated with LPS at 10 ng/mL for 1 h; then, the LPS-containing medium was removed and cells were incubated for 1 h with 100 nM PEA and RePEA. Then, the medium was replaced with fresh RPMI. The amount of SEAP (secreted embryonic alkaline phosphatase) released into the culture medium was quantified after 24 h as a measure of NF-κB activation. Data are presented as mean ± S.E.M. ($n = 3$ independent experiments), normalized on MTT data (the activity of SEAP, expressed as OD, was normalized on the MTT OD value of each corresponding well, as a measure of cell viability). Significant differences from LPS were determined using nonparametric one-way analysis of variance (ANOVA) with post hoc Dunnett's multiple comparison tests at *** $p < 0.001$, **** $p < 0.0001$. (**B**). Cell viability in PMA-THP-1 X-Blue™ cells incubated for 1 h with 100 nM PEA and RePEA. Then, medium was replaced with fresh RPMI. Cell viability was quantified after 24 h. Data are presented as mean ± S.E.M. ($n = 3$ independent experiments).

Furthermore, in order to test the ability of PEA and RePEA to counteract inflammation induced by LPS in PMA-THP-1 cells, macrophagic-release of TNF-α was evaluated. As shown in Figure 12, both PEA and RePEA decreased the amount of this cytokine triggered by LPS stimulation. Notably, RePEA inhibited TNF-α release compared to PEA in a very significant way. These results align with the hypothesis that RePEA is hydrolyzed slowly by FAAH. Finally, other cytokines associated with microglial activation were tested to confirm data obtained with TNF-α. In particular, IL-6 and IL-1β were analyzed. Released IL-6 and IL-1β cytokines were tested on PMA-THP-1 cells treated with LPS at 24 h. Cells were treated as described in Materials and Methods. As shown in Figure 12, IL-6 decreased significantly in respect of LPS both with PEA and RePEA treatments while IL-1β diminished only with RePEA treatment. These results confirmed previously obtained data and strengthened the potentiality of RePEA in the inhibition of pro-inflammatory cytokine release.

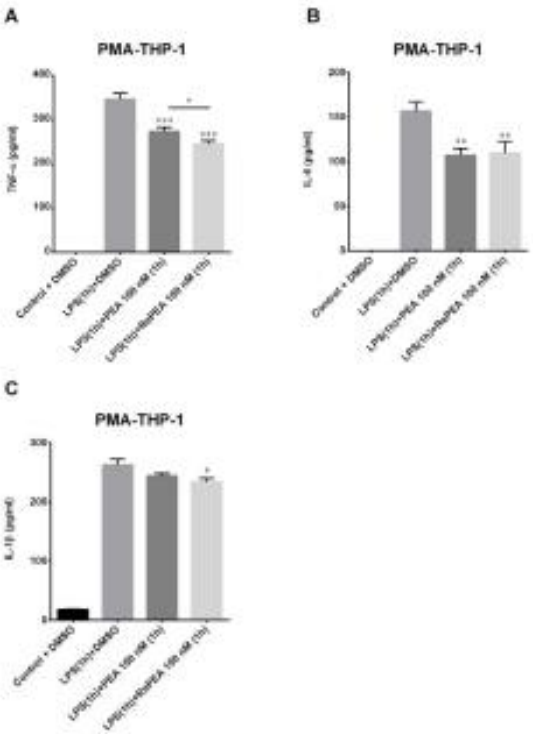

Figure 12. Release of TNF-α IL-6, and IL-1β at 24 h after LPS application. The human macrophages (PMA-THP-1) were stimulated with LPS at 10 ng/mL for 1 h; then, LPS-containing medium was removed and cells were incubated for 1 h with 100 nM PEA and its analogue, RePEA. Then, medium was replaced with fresh RPMI. The amount of TNF-α (**A**), IL-6 (**B**), and IL-1β (**C**) released into the culture medium was quantified after 24 h from LPS administration. Data are presented as mean ± S.E.M. ($n = 3$ independent experiments). Significant differences from LPS were determined using nonparametric one-way analysis of variance (ANOVA) with post hoc Dunnett's multiple comparison tests at * $p < 0.05$; ** $p < 0.01$; *** $p < 0.001$. Difference between treatment with PEA and RePEA was determined using unpaired *t*-test * $p < 0.05$.

3. Discussion

PEA is an endogenous lipid mediator which is not stored in cells, but is rather synthesized on demand from membrane phospholipid precursors; its endogenous levels are regulated by enzymes responsible for its degradation to fatty acid and ethanolamine. In particular, two enzymes are known to play a central role in the inactivation of PEA by hydrolysis: FAAH, an intracellular serine hydrolase [39], and NAAA, a cysteine hydrolase localized in the lysosomes [40]. FAAH also plays an important role in the hepatic metabolism of PEA when it is exogenously administered. In fact, it has

been recently proposed that whereas both FAAH and NAAA equally contribute to the catabolism of endogenous PEA, the FAAH-mediated degradation plays a predominant role in the metabolism of exogenously administered PEA [2]. The hydrolytic enzymes involved in PEA metabolism are expressed in the intestine and the liver [3] and the contribution of this pre-systemic metabolism strongly affects PEA bioavailability. This metabolic instability affects the pharmacokinetic properties of PEA which remain the main issue of therapeutic use in humans. In fact, in spite of the amelioration in the dissolution rate and absorption elicited by new oral formulations of PEA (such as micronized- and ultramicronized-PEA) [41], the metabolic inactivation is responsible for the short-lasting effects of the compound. A significant number of clinical trials suggest that systemic administration of PEA exerts anti-inflammatory, immunomodulatory, and neuroprotective effects, but it is especially evaluated for chronic pain management in humans [42–45]. Importantly, clinical trials prove that exogenous administration of PEA is well tolerated; in fact, the lack of side effects is a common finding in most clinical studies, as reported by a recent review carrying out a pooled meta-analysis based on data available from clinical trials about PEA employment in pain-suffering patients [46]. The efficacy and the tolerability of PEA explain why since 2008 it has been marketed in different countries as a nutraceutical food supplement.

Strategies aimed to ameliorate the in vivo use of PEA are required. One strategy to decrease PEA degradation could be the development of FAAH inhibitors; however, these compounds should increase the endogenous levels of other substrates of FAAH. On the other hand, an alternative strategy should be the development of PEA analogues, more stable to the enzymatic inactivation.

Different molecular mechanisms have been proposed so far to explain the biological effects of PEA. PEA can act through the so-called "entourage effect", increasing the level of other endocannabinoids which in turn activate cannabinoid receptors, or it can act via an allosteric modulation of TRPV1 receptors potentiating its activation by direct ligands [47]. Furthermore, it has been proposed that PEA can activate GPR55 receptor [48] even if this hypothesis awaits further evidence. Until now, the only direct target of PEA is PPAR-α receptor [1], which is considered the mediator of PEA anti-inflammatory effects. For this reason, we assessed whether the PEA analogues retain the ability to bind this pharmacological target of PEA.

Based on these issues, we designed a small library of PEA analogues, still able to maintain PPAR-α affinity and possessing longer life than their natural counterpart, being more stable to the hydrolytic action of FAAH. For comparison, we included in the analysis of the newly developed analogues PEA itself and two commercially available PEA analogues, i.e., MePEA1 and MePEA2.

Computational results suggest that MePEA1 and RePEA could be the ideal candidate to be hydrolyzed more slowly by FAAH, compared to PEA. As a matter of fact, methanandamide (Meth-AEA), a synthetic analogue of AEA, has a high resistance to enzymatic hydrolysis [6]. The same modification in PEA, yielding MePEA1, is expected to provide similar metabolic stability. Furthermore, it was reported that although RePEA cannot significantly inhibit FAAH [49], it can efficiently inhibit NAAA. This is probably related to the higher affinity of PEA analogues for NAAA [50], while anandamide analogues are preferred substrates for FAAH [51]. These data tally with computational results, suggesting that the DFT model was actually able to predict which compounds would be more resistant to hydrolysis. The major stability of RePEA was experimentally confirmed by its resistance when exposed to cell membranes. While PEA was prone to be partially hydrolyzed in 24 h, RePEA was persistent in the assay, confirming the robustness of the DFT model we proposed.

Molecular docking of PEA and its analogues to the binding domain of PPAR-α revealed a very similar binding mode, confirming that the modifications introduced to hinder hydrolysis of the amidic bond do not interfere with the affinity to the receptor. Although this result suggests that the analogues share with PEA the pharmacodynamic property of PPAR-α binding, research on the mechanism of action of these compounds is beyond the main aim of our work. Since many effects of PEA do not involve this receptor and various indirect mechanisms of action have been reported, we aimed to evaluate whether the compounds retained the ability of PEA to counteract inflammatory response in a

widely employed cellular setting. All the computational data revealed RePEA as the best candidate in terms of both synthetic accessibility and metabolic stability to FAAH-mediated hydrolysis. Since our results focused on the stability to hydrolysis catalyzed by FAAH, we cannot foresee the general in vivo metabolic stability of RePEA. Only further characterization aimed to evaluate the compound stability in plasma as well as the determination of metabolites produced in liver homogenate or in hepatic cell lines will allow us to propose RePEA as an in vivo metabolically stable compound. Thus, RePEA was synthesized and submitted to the biological assays in order to determine whether it was able to retain the anti-inflammatory properties of PEA.

It is well known that microglial cells, the phagocytic resident macrophages in the brain, play a key role in regulating cerebral inflammatory reactions [52]. In normal conditions, microglial cells are in "resting state". However, several agents can activate microglia to produce iNOS and pro-inflammatory factors which can induce neuron death [53]. In the present study, we used LPS to activate mouse N9 microglia cells and human macrophages and we evaluated the secreted TNF-α as the main pro-inflammatory marker. Other released pro-inflammatory cytokines were also evaluated, e.g., IL-6 and IL-1β. IL-6 is a cytokine with a dual effect; at some levels, it acts as a defense mechanism but, in chronic inflammation, it is rather proinflammatory. IL-6 has stimulatory effects on T- and B-cells and, in addition, in combination with its soluble receptor sIL-6Rα, tunes the transition from acute to chronic inflammation [54]. IL-1β is a potent pro-inflammatory cytokine that is crucial for host-defense responses to infection and injury [54,55]; it is involved in chronic inflammation such as rheumatoid arthritis, neuropathic pain, inflammatory bowel disease, osteoarthritis, vascular disease, multiple sclerosis, and Alzheimer's disease [56]. LPS is a constituent of the outer membrane of Gram-negative bacteria and has been widely used to induce experimental inflammatory reactions [53,57]. This agent is powerful enough to activate microglia into M1 state [58]. The mouse N9 microglial cell line used in this study, like primary microglia, can be polarized into M1 or M2 state and secrete the markers of microglial M1 and M2 states, such as iNOS, TNF-α, IL-1β and Arg-1, in the presence of a stimulus [59,60]. Microglia activation connected to pro-inflammatory responses has been considered detrimental in particular for neurons, and drugs able to stop microglia activation have been proposed for the treatment of a variety of diseases [61–64]. In our experiments, PEA, MePEA1, and RePEA inhibited TNF-α release after 24 h, whereas MePEA2 seemed to have few effects. Similar results were obtained measuring the level of another pro-inflammatory cytokine, IL-6. RePEA decreased IL-6, while PEA at the same concentration could not induce any decrease. These data suggest that RePEA still retains the ability of PEA to counteract LPS-induced inflammatory responses. More importantly, the evaluation of the same effect on human macrophages highlights a higher potency of RePEA in controlling inflammation than PEA.

Microglia and macrophages express a wide range of receptors, including TLRs, a subfamily of pattern-recognition receptors that recognize invading pathogens and endogenous harmful stimuli, to induce innate and adaptive immune responses [65]. Among TLRs, TLR4 is the major LPS receptor [66,67]. When expressed on the cellular membrane, TLR4 exists as a complex with the co-receptor myeloid differentiation protein-2 (MD-2), which is essential for LPS recognition by the TLR4–MD-2 complex [68,69]. Binding of LPS causes the TLR4–MD-2 complex dimerization [70], which results in the activation of downstream mediators, including the nuclear transcription factor NF-κB, which increases the production of pro-inflammatory molecules, such as cytokines (e.g., TNF-α, IL-1β, and IL-6), chemokines, enzymes, and reactive oxygen and nitrogen species [71]. NF-κB is a well-known master regulator of inflammation. In recent years, it has become clear that there are at least two separate pathways for NF-κB activation, the "canonical" and the "non-canonical" pathway. TLR4, TNF-α receptor, and IL-1β receptor are known to stimulate NF-κB through the "canonical" pathway, as activation of these receptors leads to phosphorylation of IKK [72] and this process is mediated by the adapter protein MyD88 [73]. In the "non canonical" pathway, NF-κB-inducing kinase (NIK) activates IKKα that phosphorylates p100, which is converted into p52/RelB heterodimers [72]. So, NF-κB dimers, released from the IκB complex, translocate to the nucleus and bind to specific DNA

sequences in the promoter of many genes [74,75]. Preclinical studies show the therapeutic effect of synthetic small molecules acting as TLR4 antagonists, both in vitro and in vivo, and confirm its central role in the regulation of inflammation [76]. Both PEA and even more RePEA inhibit NF-κB activation triggered by TLR4 stimulation. Moreover, no changes in cell morphology or viability were observed between N9 cells treated with PEA or its analogues, suggesting that none of the compounds are toxic.

In this work we proposed the design of a small library of PEA analogues and we developed a novel QM model that was able to predict the properties of the designed compounds and some commercial ones as far as FAAH-mediated hydrolysis is concerned. In conclusion, although the specific mechanism of action and the evaluation of in vivo metabolic stability awaits further investigation, RePEA represents a good candidate for pre-clinical studies in order to develop a compound with the same well-known therapeutic properties of PEA but with a better pharmacokinetic profile.

4. Materials and Methods

Palmitoylethanolamide (PEA, CAS N° 544-31-0), R-palmitoyl-(1-methyl) ethanolamide (MePEA1, CAS N° 142128-47-0), and R-palmitoyl-(2-methyl) ethanolamide (MePEA2, CAS N° 179951-56-5) were purchased from Cayman Chemical (Ann Arbor, MI, USA) with a declared purity ≥98%. 3-Hydroxy-*N*-pentadecylpropanamide (RePEA) was synthesized with a slight modification to methods previously reported in literature [49].

4.1. Chemical Procedures

Anhydrous solvents over molecular sieves were purchased from Acros Organics® (Thermo Fisher Scientific, Geel, Belgium) with a content of water ≤50 ppm. Thin-layer chromatography (TLC) was performed on Silica Gel 60 F_{254} plates (Merck, Darmstadt, Germany) and visualized using appropriate developing solutions. Automated flash chromatography was performed on a Biotage® Isolera™ (Biotage, Uppsala, Sweden). Prime system. NMR experiments were recorded on a Bruker Avance III 600 MHz equipped with cryo-probe instrument at 298 K. Chemical shifts (δ) are reported in ppm downfield from the residual solvent peak, whereas coupling constants (J) are stated in Hz. The ^{1}H and ^{13}C-NMR resonances of compounds were assigned by means of COSY and HSQC experiments. NMR data processing was performed with MestReNova v14.1.2 software (Mestrelab Research, Santiago de Compostela, Spain).

4.1.1. Synthesis of 3-Hydroxy-N-pentadecylpropanamide (RePEA)

A solution of pentadecylamine (100 mg, 0.44 mmol) in anhydrous dichloromethane (1 mL) kept at 0 °C was treated with β-propiolactone (83 µL, 1.32 mmol). The mixture was then allowed to return to room temperature and stirred overnight under argon atmosphere. Then, the reaction was quenched with MeOH and concentrated under reduced pressure and the crude was purified by automated flash chromatography (Hex:AcOEt gradient elution) obtaining pure compound RePEA (60 mg, 48% yield purity ≥95%). TLC (ethyl acetate) Rf = 0.25; ^{1}H NMR (600 MHz, $CDCl_3$) δ 6.02 (bs, 1H, NH), 3.92–3.87 (m, 2H, H_3), 3.27 (dd, = 6.8, 5.6 Hz, 2H, H_4), 2.48 (t, $J_{2,3}$ = 4.8 Hz, 2H, H_2), 2.38 (bs, 1H, OH), 1.51 (q, J = 6.8 Hz, 2H, H_5), 1.35–1.27 (m, 8H, CH_2), 1.25 (s, 16H, CH_2), 0.88 (t, J = 7.0 Hz, 3H, H_{16}). ^{13}C NMR (150 MHz, $CDCl_3$) δ 173.35 (CO), 59.04 (C_3), 40.15 (C_4), 37.57 (C_2), 32.07, 29.83, 29.74, 29.67, 29.51 (C_5), 29.40, 27.05, 22.84, 14.27 (C_{16}).

4.1.2. Sample Preparation

PEA, MePEA1, MePEA2, and RePEA were dissolved in dimethyl sulfoxide (DMSO) at a concentration of 67 mM, and then serially diluted in culture medium immediately prior to experiments. The final concentration of DMSO was less than 0.01% in the experiments. Lipopolysaccharides (LPS; Escherichia coli O55:B5) were obtained from ENZO Life Sciences (New York, NY, USA).

4.2. Computational Methods

4.2.1. Molecular Docking

Molecular recognition simulations were performed using the docking tools Glide [77–80] and CovDock [81], as available in Maestro 12.1 (Schrodinger Inc., LLC, New York, NY, USA). The X-ray crystal structures corresponding to the different PDB IDs of the investigated proteins (1I7G for PPAR-α, 6DXX for NAAA and 3K84 for FAAH) were edited for missing hydrogens and for assigning proper bond orders. Water molecules and co-crystallized ligands were removed, while protonation states of side chains were assigned running PROPKA, setting pH = 7. The H-bonds were then optimized using sample orientations. Finally, a restrained minimization of proteins was carried out using the OPLS3 force field, [82,83] until the RMSD between the starting structure and the minimized one reached 0.3 Å. PEA and its analogues were geometrically refined with the "Ligprep" module using OPLS3 force field. The (*R*)-stereochemistry for MePEA1 and MePEA2 was retained, for consistency with experiments. Receptor grids were all calculated with the OPLS3 force field as well. The receptor grid for PPAR-α was generated by selecting the crystal structure co-ligand AZ 242 ((2S)-2-ethoxy-3-[4-(2-[4-[(methylsulphonyl) oxy]phenyl]ethoxy)phenyl]propanoic acid) as centroid. The grid box for FAAH and NAAA, instead, were built selecting active site amino acids Gly240, Phe192, Ala490 and Cys126, Asn287, Phe174, Trp181, respectively. For PPAR-α, flexible ligand docking using the extra precision (XP) Glide module was performed [80], with no constraints on receptor–ligand(s) interactions. The docking performance was validated by re-docking the alpha-ketoheterocycle co-ligand ((9Z)-1-(5-pyridin-2-yl-1,3,4-oxadiazol-2-yl) octadec-9-en-1-one) and by comparing the lowest energy pose with the co-ligand position and conformation found in the crystal structure. Sidechains of key residues Tyr464, Tyr314, His440 and Ser280 were set as freely rotable during calculations. For FAAH and NAAA, instead, covalent docking with the CovDock workflow was carried out [81]. Ser241 (for FAAH) and Cys126 (for NAAA) were set as reactive residues and, in both cases, the reaction type was defined as a nucleophilic addition to a double bond. FAAH was chosen as a reference system to validate the CovDock procedure for this kind of ligand and chemical reaction.

4.2.2. Density Functional Theory Calculations

Quantum mechanical (QM) calculations were carried out in the density functional theory (DFT) framework, cutting off a cluster model from the FAAH crystal structure (PDB ID 3K84). The use of an all-QM cluster approach, instead of the alternative and more computationally costly hybrid QM-MM one (adopted for previous investigations on this theme) allowed us to treat at a more accurate DFT level a large portion of the protein active site, going beyond the sole catalytic triad.

The docking poses obtained with ligands covalent docking to FAAH were taken as the starting points to design the DFT model. In particular, we performed a cross-analysis of protein–ligand interactions found in the best poses of PEA and all the 10 analogues. In this way, we were able to identify crucial residues interacting with both the polar head and hydrophobic tail of our ligands. Since the structural variability among the ligands is introduced only in the polar head, the ligands' length was reduced by truncating their hydrophobic chain, so that they are overall characterized by a 11-atom-long chain (comprising both carbons and heteroatoms). The residues included in the DFT model are 16: Ser241, Lys142, Ser217, Ser218, Ser190, Met191, Phe192, Glu240, Gly239, Ile238, Gly235, Thr236, Leu278, Cys269, Val270, Try271 (Supplementary Figure S8). The last four residues do not interact with the ligands but have been introduced in order to sterically define the volume of the pocket accommodating their polar head (vide infra). Geometry optimizations were carried out at the BP86/DZP level [84–86], using the TURBOMOLE 2.1 suite [87]. The resolution-of-identity (RI) approximation was used to speed up calculations [88]. The Grimme's D3 corrections were added [89], in order to accurately account for the significant amount of dispersive protein–ligand interactions found in this system. Following a well-established approach, alpha carbons were kept frozen at the X-ray structure position. This constrained optimization is necessary to avoid unrealistic movements of

amino acids within the active site. Full vibrational analysis was carried out to characterize the nature of transition states, searching for the imaginary frequency associated with the reaction coordinate of interest. Solvent effect was implicitly treated according to the COSMO approach, [90,91] by simulating a continuum dielectric with $\varepsilon = 40$ (which is a good compromise for a system that is half water accessible and half hydrophobic). The hydrolysis starting points were modeled as van der Waals adducts, obtained by dissociating the Ser241-ligand complexes obtained with CovDock, and by restoring the reactants functional groups.

4.3. FAAH Assay

Membranes for FAAH assay were prepared as described by Jonsson et al. with minor modifications [92]. Briefly, frozen primary cortical cultures (cerebral cortices) stored at −80 °C from postnatal mice were thawed, homogenized on ice in cold PBS (PH 7.4) using an insulin syringe and centrifuged at 13,000 rpm for 30 min. The cell pellets were then washed twice with PBS and centrifuged at 13,000 rpm for 30 min. The pellets were suspended in cold PBS on ice and sonicated. Protein concentration was measured and samples were stored at −80 °C until use.

The hydrolysis of PEA and RePEA was followed by NMR spectroscopy, using a Bruker Avance III NMR spectrometer equipped with a QCI cryogenic probe.

For each NMR sample, 50 µL of membrane (167 µg of total protein) was resuspended in 148 µL of deuterated PBS 10 mM, pH 7.4, and transferred into a 3 mm NMR tube. A first proton was acquired at 37 °C using the pulse sequence noesygppr1d and 64 scans, a relaxation delay of 2 s, an acquisition time of 2 s and a receiver gain of 45.2. Then, the potential FAAH substrates PEA or RePEA were added immediately starting the reaction monitoring by applying the same acquisition parameters. Due to their very low water solubility, PEA and RePEA were added after dissolution in d6-DMSO, reaching a final substrate concentration of 1 mM and 10% of d6-DMSO. Spectra were acquired every 30 min over an interval of 24 h. They were processed using MestreNova software version 14.1.2-25024 (Mestrelab Research, Santiago de Compostela, Spain) by applying a line broadening of 0.3 Hz. Spectra were referenced to DMSO residual signal.

4.4. Cell Cultures

4.4.1. Murine N9 Microglial Cells

The murine microglial N9 cells were cultured in Iscove Modified Dulbecco's Medium (IMDM, Sigma-Aldrich, St. Louis, MO, USA) supplemented with 5% heat-inactivated fetal bovine serum (FBS), 100 IU/mL penicillin, 100 U/mL streptomycin, 2 mM L-glutamine (all Euroclone, Pero, Italy), and Mycozap™ prophylactic (Lonza, Walkersville, MD, USA) under standard cell culture conditions (37 °C, 5% CO_2).

4.4.2. THP-1 and THP-1 X-Blue™ Cells

THP-1 and THP-1 X-Blue™ cells were maintained in RPMI 1640 Medium without L-glutamine with phenol red (Euroclone, Pero, Italy), supplemented with 10% heat-inactivated fetal bovine serum (FBS) (Euroclone, Pero, Italy), 2 mM L-glutamine (Euroclone, Pero, Italy), and 100 U/mL penicillin/streptomicin (Euroclone, Pero, Italy). Before treatments, cells were seeded into a 96-well plate and differentiated into macrophages by 72 h incubation with 100 ng/mL phorbol 12-myristate 13-acetate (PMA, Enzo Life Sciences, New York, NY, USA) followed by 24 h incubation in RPMI medium.

4.5. Cell Viability Assay

N9 cells were seeded at the concentration of 3×10^4 cells/well into a 96-well plate and then the day after were incubated for 1 h with 100 nM PEA and its analogues (MePEA1, MePEA2, RePEA). Then, the medium was replaced with fresh IMDM supplemented with 5% FBS. After 24 h, cells were washed and incubated with fresh medium containing 3-(4,5-dimethylthiazol-2-yl)-2,5-diphenyltetrazolium

bromide (MTT) (0.5 mg/mL; Sigma-Aldrich, St. Louis, MO, USA) at 37 °C for 4 h. After, formazan crystals were dissolved in acidic isopropanol. The optical density was evaluated by spectrophotometric measurement of absorbance. All the experiments were done in triplicate and repeated for three independent measurements.

4.6. Morphological Analysis

N9 and THP-1 cells were seeded at the concentration of 9×10^4 cells/well and 8×10^4 cells/per well respectively into a 96-well plate. THP-1 cells were differentiated as described above. Cellular morphology of N9 and PMA-THP-1 cells was evaluated using inverted Olympus CKX41 microscope (Olympus Instruments, Tokyo, Japan), equipped with a Digital C-Mount Camera TP 5100. Cells were incubated for 1 h with 100 nM PEA and its analogues (MePEA1, MePEA2, RePEA). Then, medium was replaced with fresh IMDM supplemented with 5% FBS (N9 cells) or RPMI (PMA-THP-1 X-Blue™ cells). After 6 or 24 h optical images were captured with an inverted microscope (Olympus CKX41, Olympus Instruments, Tokyo, Japan).

4.7. LPS Treatment with and without PEA and Its Analogues

N9, PMA-THP-1 X-Blue™, and PMA-THP-1 cells were stimulated with LPS at 10 ng/mL for 1 h, then the medium that contained LPS was removed and cells were incubated for 1 h with 100 nM PEA and its analogues (MePEA1, MePEA2, RePEA). Then, the medium was replaced with fresh IMDM supplemented with 5% FBS (N9 cells) or RPMI (PMA-THP-1 X-Blue™ cells).

4.8. Pro-Inflammatory Cytokine Release

N9 cells were seeded at the concentration of 9×10^4 cells/well into a 12-well plate and then the day after were treated as described above. Levels of TNF-α released into the culture medium were quantified after 3, 6, and 24 h by using the corresponding quantification enzyme-linked immunosorbent assay (ELISA) kits (88-7324, Thermo Fisher Scientific, Monza, Italy) according to the manufacturer's instructions. Levels of IL-6 and IL-1β released into the culture medium were quantified after 24 h by using the corresponding quantification enzyme-linked immunosorbent assay (ELISA) kits (DY406, DY401, R&D systems, Minneapolis, MN, USA). PMA-THP-1 cells were seeded at a concentration of 8×10^4 cells/per well into a 96-well plate and differentiated as described above. Cells were then treated with 100 nM PEA or RePEA as indicated above. Levels of TNF-α, IL-6, and IL-1β released into the culture medium were quantified after 24 h by using the corresponding quantification enzyme-linked immunosorbent assay (ELISA) kits (DY210, DY206, DY201, R&D systems, Minneapolis, MN, USA) according to the manufacturer's instructions. The data were expressed as pg/mL following interpolation on the basis of a standard curve. The experiment was done in triplicate and repeated for three independent measurements.

4.9. SEAP Assay

THP-1 X-Blue™ NF-κB cells were specifically designed for monitoring the NF-κB signal transduction pathway in a physiologically relevant cell line. THP-1-Blue™ is derived from the human THP-1 monocyte cell line by stable integration of an NF-κB-inducible secreted embryonic alkaline phosphatase (SEAP) reporter construct. THP-1-Blue™ NF-κB cells are highly responsive to PRR agonists that trigger the NF-κB pathway. THP-1 X-Blue™ NF-κB cells express a SEAP reporter gene driven by an IFN-β minimal promoter fused to five copies of the NF-κB consensus transcriptional response element and three copies of the c-Rel binding site.

A total of 8×10^4 cells/per well were seeded into a 96-well plate and differentiated as described above. Cells were then treated with 100 nM PEA or RePEA as indicated above. As a result, PMA-THP-1 X-Blue™ NF-κB cells allow the monitoring of NF-κB activation by determining the activity of SEAP. Levels of SEAP in the supernatant have been easily determined after 24 h with Quanti-Blue™ solution according to manufacturer instructions (InvivoGen, San Diego, CA, USA). In addition, the cell density

of each well was analyzed by MTT assay as described above. Activity of SEAP, expressed as OD, was normalized on the MTT OD value of each corresponding well, as a measure of cell viability.

4.10. Statistical Analysis

Results are expressed as the mean ± SEM. All data were analyzed using the GraphPad Prism software (version 6.0) (San Diego, CA, USA). Differences between treatment groups were analyzed using one-way analysis of variance (ANOVA), followed by post hoc Dunnett's test or *t*-test. Difference between treatment with PEA and RePEA was determined using unpaired *t*-test. A p-value of less than 0.05 was considered statistically significant.

Supplementary Materials: Supplementary Materials can be found at http://www.mdpi.com/1422-0067/21/23/9074/s1.

Author Contributions: Conceptualization, B.C. and L.C.; methodology, F.A.; formal analysis, F.A.; validation, A.D., F.A. and C.A.; computational analysis, F.A. and G.Z.; NMR investigation, C.A.; cell biology investigation, A.D. and V.A.; organic chemistry investigation, A.P.; resources, M.C., B.C., L.C., C.A. and G.Z.; writing—original draft preparation, F.A., A.D., R.T., A.P., M.C., L.C., B.C.; writing—review and editing, R.T., G.Z. and B.C.; visualization, A.D., F.A. and C.A.; supervision, R.T., G.Z., L.C. and B.C.; funding acquisition, L.C., C.A. and B.C. All authors have read and agreed to the published version of the manuscript.

Funding: This research received no external funding.

Conflicts of Interest: The authors declare no conflict of interest.

Abbreviations

ABP	Acyl-chain Binding Pocket
AF-2	Activation function-2
DFT	Density Functional Theory
EA	Ethanolamine
FAAH	Fatty Acid Amide Hydrolase
HPA	Hydroxy-propionic acid
IL-1β	Interleukin-1β
IL-6	Interleukin-6
iNOS	inducible Nitric Oxide Synthase
LPS	Lipopolysaccharide
MAGL	Monoacylglycerol lipase
MD-2	Myeloid differentiation protein-2
MePEA	Methan-PEA
NAAA	*N*-acylethanolamine acid amidase
NF-κB	Nuclear Factor kappa-light-chain-enhancer of activated B cells
PEA	PalmitoylEthanolAmide
PPAR-α	Peroxisome Proliferator-Activated Receptor alpha
QM	Quantum Mechanical
QM-MM	Quantum Mechanics/Molecular Mechanics
RePEA	Retro-PEA
SEAP	Secreted embryonic alkaline phosphatase
SIFs	Structural Interaction Fingerprints
TLR	Toll Like Receptor
TNF-α	Tumor necrosis factor alpha

References

1. Lo Verme, J.; Fu, J.; Astarita, G.; La Rana, G.; Russo, R.; Calignano, A.; Piomelli, D. The Nuclear Receptor Peroxisome Proliferator-Activated Receptor-α Mediates the Anti-Inflammatory Actions of Palmitoylethanolamide. *Mol. Pharmacol.* **2005**, *67*, 15–19. [CrossRef] [PubMed]
2. Rankin, L.; Fowler, C.J. The Basal Pharmacology of Palmitoylethanolamide. *Int. J. Mol. Sci.* **2020**, *21*, 7942. [CrossRef] [PubMed]

3. Balvers, M.G.J.; Verhoeckx, K.C.M.; Meijerink, J.; Wortelboer, H.M.; Witkamp, R.F. Measurement of Palmitoylethanolamide and Other N-Acylethanolamines during Physiological and Pathological Conditions. *CNS Neurol. Disord. Drug Targets.* **2013**, *12*, 23–33. [CrossRef] [PubMed]
4. Petrosino, S.; Moriello, A.S.; Cerrato, S.; Fusco, M.; Puigdemont, A.; De Petrocellis, L.; Di Marzo, V. The anti-inflammatory mediator palmitoylethanolamide enhances the levels of 2-arachidonoyl-glycerol and potentiates its actions at TRPV1 cation channels. *Br. J. Pharmacol.* **2016**, *173*, 1154–1162. [CrossRef] [PubMed]
5. Desarnaud, F.; Cadas, H.; Piomelli, D. Anandamide amidohydrolase activity in rat brain microsomes. Identification and partial characterization. *J. Biol. Chem.* **1995**, *270*, 6030–6035. [CrossRef]
6. Abadji, V.; Lin, S.; Taha, G.; Griffin, G.; Stevenson, L.A.; Pertwee, R.G.; Makriyannis, A. (R)-methanandamide: A chiral novel anandamide possessing higher potency and metabolic stability. *J. Med. Chem.* **1994**, *37*, 1889–1893. [CrossRef]
7. Capelli, D.; Cerchia, C.; Montanari, R.; Loiodice, F.; Tortorella, P.; Laghezza, A.; Cervoni, L.; Pochetti, G.; Lavecchia, A. Structural basis for PPAR partial or full activation revealed by a novel ligand binding mode. *Sci. Rep.* **2016**, *6*, 34792. [CrossRef]
8. Wu, C.-C.; Baiga, T.J.; Downes, M.; La Clair, J.J.; Atkins, A.R.; Richard, S.B.; Fan, W.; Stockley-Noel, T.A.; Bowman, N.E.; Noel, J.P.; et al. Structural basis for specific ligation of the peroxisome proliferator-activated receptor δ. *Proc. Natl. Acad. Sci. USA* **2017**, *114*, E2563–E2570. [CrossRef]
9. Cronet, P.; Petersen, J.F.W.; Folmer, R.; Blomberg, N.; Sjöblom, K.; Karlsson, U.; Lindstedt, E.L.; Bamberg, K. Structure of the PPARα and -γ Ligand Binding Domain in Complex with AZ 242; Ligand Selectivity and Agonist Activation in the PPAR Family. *Structure* **2001**, *9*, 699–706. [CrossRef]
10. Yoshida, T.; Oki, H.; Doi, M.; Fukuda, S.; Yuzuriha, T.; Tabata, R.; Ishimoto, K.; Kawahara, K.; Obkubo, T.; Miyachi, H.; et al. Structural Basis for PPARα Activation by 1H-pyrazolo-[3,4-b]pyridine Derivatives. *Sci. Rep.* **2020**, *10*, 7623. [CrossRef]
11. Xu, H.E.; Lambert, M.H.; Montana, V.G.; Parks, D.J.; Blanchard, S.G.; Brown, P.J.; Sternbach, D.D.; Lehmann, J.M.; Wisely, G.B.; Willson, T.M.; et al. Molecular Recognition of Fatty Acids by Peroxisome Proliferator–Activated Receptors. *Mol. Cell.* **1999**, *3*, 397–403. [CrossRef]
12. Singh, J.; Deng, Z.; Narale, G.; Chuaqui, C. Structural interaction fingerprints: A new approach to organizing, mining, analyzing, and designing protein-small molecule complexes. *Chem. Biol. Drug Des.* **2006**, *67*, 5–12. [CrossRef] [PubMed]
13. Bracey, M.H.; Hanson, M.A.; Masuda, K.R.; Stevens, R.C.; Cravatt, B.F. Structural adaptations in a membrane enzyme that terminates endocannabinoid signaling. *Science* **2002**, *298*, 1793–1796. [CrossRef] [PubMed]
14. Tuo, W.; Leleu-Chavain, N.; Spencer, J.; Sansook, S.; Millet, R.; Chavatte, P. Therapeutic Potential of Fatty Acid Amide Hydrolase, Monoacylglycerol Lipase, and N-Acylethanolamine Acid Amidase Inhibitors. *J. Med. Chem.* **2017**, *60*, 4–46. [CrossRef] [PubMed]
15. Palermo, G.; Bauer, I.; Campomanes, P.; Cavalli, A.; Armirotti, A.; Girotto, S.; Rothlisberger, U.; De Vivo, M. Keys to Lipid Selection in Fatty Acid Amide Hydrolase Catalysis: Structural Flexibility, Gating Residues and Multiple Binding Pockets. *PLoS Comput. Biol.* **2015**, *11*, e1004231. [CrossRef] [PubMed]
16. Palermo, G.; Campomanes, P.; Cavalli, A.; Rothlisberger, U.; De Vivo, M. Anandamide hydrolysis in FAAH reveals a dual strategy for efficient enzyme-assisted amide bond cleavage via nitrogen inversion. *J. Phys. Chem. B.* **2015**, *119*, 789–801. [CrossRef]
17. McKinney, M.K.; Cravatt, B.F. Structure and function of fatty acid amide hydrolase. *Annu. Rev. Biochem.* **2005**, *74*, 411–432. [CrossRef]
18. Otrubova, K.; Ezzili, C.; Boger, D.L. The discovery and development of inhibitors of fatty acid amide hydrolase (FAAH). *Bioorg. Med. Chem. Lett.* **2011**, *21*, 4674–4685. [CrossRef]
19. Palermo, G.; Rothlisberger, U.; Cavalli, A.; De Vivo, M. Computational insights into function and inhibition of fatty acid amide hydrolase. *Eur. J. Med. Chem.* **2015**, *91*, 15–26. [CrossRef]
20. Tuberi-Brohman, I.; Acevedo, O.; Jorgensen, W.L. Elucidation of Hydrolysis Mechanisms for Fatty Acid Amide Hydrolase and Its Lys142Ala Variant via QM/MM Simulations. *J. Am. Chem. Soc.* **2006**, *128*, 16904–16913. [CrossRef]
21. Ledola, A.; Mor, M.; Rivara, S.; Christov, C.; Tarzia, G.; Piomelli, D.; Mulholland, A.J. Identification of productive inhibitor binding orientation in fatty acid amide hydrolase (FAAH) by QM/MM mechanistic modelling. *Chem. Commun.* **2008**, *2*, 214–216. [CrossRef] [PubMed]

22. Lodola, A.; Mor, M.; Hermann, J.C.; Tarzia, G.; Piomelli, D.; Mulholland, A.J. QM/MM modelling of oleamide hydrolysis in fatty acid amide hydrolase (FAAH) reveals a new mechanism of nucleophile activation. *Chem. Commun.* **2005**, *35*, 4399–4401. [CrossRef] [PubMed]
23. Lodola, A.; Mor, M.; Sirirak, J.; Mulholland, A.J. Insights into the mechanism and inhibition of fatty acid amide hydrolase from quantum mechanics/molecular mechanics (QM/MM) modelling. *Biochem. Soc. Trans.* **2009**, *37*, 363–367. [CrossRef] [PubMed]
24. Capoferri, L.; Mor, M.; Sirirak, J.; Chudyk, E.; Mulholland, A.J.; Lodola, A. Application of a SCC-DFTB QM/MM approach to the investigation of the catalytic mechanism of fatty acid amide hydrolase. *J. Mol. Model.* **2011**, *17*, 2375–2383. [CrossRef] [PubMed]
25. Lodola, A.; Capoferri, L.; Rivara, S.; Tarzia, G.; Piomelli, D.; Mulholland, A.; Mor, M. Quantum Mechanics/Molecular Mechanics Modeling of Fatty Acid Amide Hydrolase Reactivation Distinguishes Substrate from Irreversible Covalent Inhibitors. *J. Med. Chem.* **2013**, *56*, 2500–2512. [CrossRef] [PubMed]
26. McKinney, M.K.; Cravatt, B.F. Evidence for distinct roles in catalysis for residues of the serine-serine-lysine catalytic triad of fatty acid amide hydrolase. *J. Biol. Chem.* **2003**, *278*, 37393–37399. [CrossRef]
27. Scalvini, L.; Ghidini, A.; Lodola, A.; Callegari, D.; Rivara, S.; Piomelli, D.; Mor, M. N-Acylethanolamine Acid Amidase (NAAA): Mechanism of Palmitoylethanolamide Hydrolysis Revealed by Mechanistic Simulations. *ACS Catal.* **2020**, *20*, 11797–11813. [CrossRef]
28. Gorelik, A.; Gebai, A.; Illes, K.; Piomelli, D.; Nagar, B. Molecular mechanism of activation of the immunoregulatory amidase NAAA. *Proc. Natl. Acad. Sci. USA* **2018**, *115*, E10032–E10040. [CrossRef]
29. Lodola, A.; Rivara, S.; Mor, M. Insights in the Mechanism of Action and Inhibition of N-Acylethanolamine Acid Amidase by Means of Computational Methods. *Adv. Protein Chem. Struct. Biol.* **2014**, *96*, 219–234. [CrossRef]
30. Piomelli, D.; Scalvini, L.; Fotio, Y.; Lodola, A.; Spadoni, G.; Tarzia, G.; Mor, M. N-Acylethanolamine Acid Amidase (NAAA): Structure, Function, and Inhibition. *J. Med. Chem.* **2020**, *63*, 7475–7490. [CrossRef]
31. Solorzano, C.; Zhu, C.; Battista, N.; Astarita, G.; Lodola, A.; Rivara, S.; Mor, M.; Russo, R.; Maccarrone, M.; Antonietti, F.; et al. Selective N-acylethanolamine-hydrolyzing acid amidase inhibition reveals a key role for endogenous palmitoylethanolamide in inflammation. *Proc. Natl. Acad. Sci. USA* **2009**, *106*, 20966–20971. [CrossRef] [PubMed]
32. Righi, M.; Mori, L.; De Libero, G.; Sironi, M.; Biondi, A.; Mantovani, A.; Donini, S.D.; Ricciardi-Castagnoli, P. Monokine production by microglial cell clones. *Eur. J. Immunol.* **1989**, *19*, 1443–1448. [CrossRef] [PubMed]
33. Fleisher-Berkovich, S.; Filipovich-Rimon, T.; Ben-Shmuel, S.; Hülsmann, C.; Kummer, M.P.; Heneka, M.T. Distinct modulation of microglial amyloid β phagocytosis and migration by neuropeptides (i). *J. Neuroinflammation.* **2010**, *7*, 61. [CrossRef] [PubMed]
34. Guida, F.; Luongo, L.; Boccella, S.; Giordano, M.E.; Romano, R.; Bellini, G.; Manzo, I.; Furiano, A.; Rizzo, A.; Imperatore, R.; et al. Palmitoylethanolamide induces microglia changes associated with increased migration and phagocytic activity: Involvement of the CB2 receptor. *Sci. Rep.* **2017**, *7*, 375. [CrossRef] [PubMed]
35. Rivest, S. Molecular insights on the cerebral innate immune system. *Brain Behav. Immun.* **2003**, *1*, 13–19. [CrossRef]
36. Cohen, J. The immunopathogenesis of sepsis. *Nature* **2002**, *420*, 885–891. [CrossRef] [PubMed]
37. Sanz, J.M.; Di Virgilio, F. Kinetics and mechanism of ATP-dependent IL-1 beta release from microglial cells. *J. Immunol.* **2000**, *164*, 4893–4898. [CrossRef] [PubMed]
38. Ghosh, S.; Karin, M. Missing pieces in the NF-kappaB puzzle. *Cell* **2002**, *109*, 581–596. [CrossRef]
39. Cravatt, B.F.; Giang, D.K.; Mayfield, S.P.; Boger, D.L.; Lerner, R.A.; Gilula, N.B. Molecular characterization of an enzyme that degrades neuromodulatory fatty-acid amides. *Nature* **1996**, *384*, 83–87. [CrossRef]
40. Ueda, N.; Yamanaka, K.; Yamamoto, S. Purification and Characterization of an Acid Amidase Selective for N-Palmitoylethanolamine, a Putative Endogenous Anti-inflammatory Substance. *J. Biol. Chem.* **2001**, *276*, 35552–35557. [CrossRef]
41. Petrosino, S.; Cordaro, M.; Verde, R.; Schiano Moriello, A.; Marcolongo, G.; Schievano, C.; Siracusa, R.; Piscitelli, F.; Peritore, A.F.; Crupi, R.; et al. Oral Ultramicronized Palmitoylethanolamide: Plasma and Tissue Levels and Spinal Anti-hyperalgesic Effect. *Front. Pharmacol.* **2018**, *9*, 249. [CrossRef] [PubMed]
42. Chirchiglia, D.; Chirchiglia, P.; Signorelli, F. Nonsurgical lumbar radiculopathies treated with ultramicronized palmitoylethanolamide (umPEA): A series of 100 cases. *Neurol. Neurochir. Pol.* **2018**, *52*, 44–47. [CrossRef] [PubMed]

43. Passavanti, M.B.; Fiore, M.; Sansone, P.; Aurilio, C.; Pota, V.; Barbarisi, M.; Fierro, D.; Pace, M.D. The beneficial use of ultramicronized palmitoylethanolamide as add-on therapy to Tapentadol in the treatment of low back pain: A pilot study comparing prospective and retrospective observational arms. *BMC Anesthesiol.* **2017**, *17*, 171. [CrossRef] [PubMed]
44. Marini, I.; Bartolucci, M.L.; Bortolotti, F.; Gatto, M.R.; Bonetti, G.A. Palmitoylethanolamide versus a nonsteroidal anti-inflammatory drug in the treatment of temporomandibular joint inflammatory pain. *J. Orofac. Pain* **2012**, *26*, 99–104.
45. Truini, A.; Biasiotta, A.; Di Stefano, G.; La Cesa, S.; Leone, C.; Cartoni, C.; Federico, V.; Petrucci, M.T.; Cruccu, G. Palmitoylethanolamide restores myelinated-fibre function in patients with chemotherapy-induced painful neuropathy. *CNS Neurol. Disord. Drug Targets* **2011**, *10*, 916–920. [CrossRef]
46. Paladini, A.; Fusco, M.; Cenacchi, T.; Schievano, C.; Piroli, A.; Varrassi, G. Palmitoylethanolamide, a Special Food for Medical Purposes, in the Treatment of Chronic Pain: A Pooled Data Meta-analysis. *Pain Physician.* **2016**, *19*, 11–24.
47. Di Marzo, V.; Melck, D.; Orlando, P.; Bisogno, T.; Zagoory, O.; Bifulco, M.; Vogel, Z.; De Petrocellis, L. Palmitoylethanolamide inhibits the expression of fatty acid amide hydrolase and enhances the anti-proliferative effect of anandamide in human breast cancer cells. *Biochem. J.* **2001**, *358*, 249–255. [CrossRef]
48. Ryberg, E.; Larsson, N.; Sjögren, S.; Hjorth, S.; Hermansson, N.-O.; Leonova, J.; Elebring, T.; Nilsson, K.; Drmota, T.; Greasley, P.J. The orphan receptor GPR55 is a novel cannabinoid receptor. *Br. J. Pharmacol.* **2007**, *152*, 1092–1101. [CrossRef]
49. Vandevoorde, S.; Tsuboi, K.; Ueda, N.; Jonsson, K.-O.; Fowler, C.J.; Lambert, D.M. Esters, Retroesters, and a Retroamide of Palmitic Acid: Pool for the First Selective Inhibitors of N-Palmitoylethanolamine- Selective Acid Amidase. *J. Med. Chem.* **2003**, *46*, 4373–4376. [CrossRef]
50. Tsuboi, K.; Sun, Y.-X.; Okamoto, Y.; Araki, N.; Tonai, T.; Ueda, N. Molecular characterization of N-acylethanolamine-hydrolyzing acid amidase, a novel member of the cholylglycine hydrolase family with structural and functional similarity to acid ceramidase. *J. Biol. Chem.* **2005**, *280*, 11082–11092. [CrossRef]
51. Katayama, K.; Ueda, N.; Katoh, I.; Yamamoto, S. Equilibrium in the hydrolysis and synthesis of cannabimimetic anandamide demonstrated by a purified enzyme. *Biochim. Biophys. Acta* **1999**, *1440*, 205–214. [CrossRef]
52. Kreutzberg, G.W. Microglia: A sensor for pathological events in the CNS. *Trends Neurosci.* **1996**, *19*, 312–318. [CrossRef]
53. Brown, G.C.; Bal-Price, A. Inflammatory neurodegeneration mediated by nitric oxide, glutamate, and mitochondria. *Mol. Neurobiol.* **2003**, *27*, 325–355. [CrossRef]
54. Gabay, C. Interleukin-6 and chronic inflammation. *Arthritis Res. Ther.* **2006**, *8*, S3. [CrossRef] [PubMed]
55. Dinarello, C.A. Biologic basis for interleukin-1 in disease. *Blood* **1996**, *87*, 2095–2147. [CrossRef]
56. Braddock, M.; Quinn, A. Targeting IL-1 in inflammatory disease: New opportunities for therapeutic intervention. *Nat. Rev. Drug Discov.* **2004**, *3*, 330–339. [CrossRef]
57. Reutershan, J.; Chang, D.; Hayes, J.K.; Ley, K. Protective effects of isoflurane pretreatment in endotoxin-induced lung injury. *Anesthesiology* **2006**, *104*, 511–517. [CrossRef]
58. Jung, W.-K.; Lee, D.-Y.; Park, C.; Choi, Y.H.; Choi, I.; Park, S.-G.; Seo, S.H.; Lee, S.W.; Yea, S.S.; Ahn, S.C.; et al. Cilostazol is anti-inflammatory in BV2 microglial cells by inactivating nuclear factor-kappaB and inhibiting mitogen-activated protein kinases. *Br. J. Pharmacol.* **2010**, *159*, 1274–1285. [CrossRef]
59. Tang, Y.; Li, T.; Li, J.; Yang, J.; Liu, H.; Zhang, X.J.; Le, W. Jmjd3 is essential for the epigenetic modulation of microglia phenotypes in the immune pathogenesis of Parkinson's disease. *Cell Death Differ.* **2014**, *21*, 369–380. [CrossRef]
60. Liu, H.-C.; Zheng, M.-H.; Du, Y.-L.; Wang, L.; Kuang, F.; Qin, H.-Y.; Zhang, B.-F.; Han, H. N9 microglial cells polarized by LPS and IL4 show differential responses to secondary environmental stimuli. *Cell Immunol.* **2012**, *278*, 84–90. [CrossRef]
61. Aisen, P.S. The potential of anti-inflammatory drugs for the treatment of Alzheimer's disease. *Lancet Neurol.* **2002**, *1*, 279–284. [CrossRef]
62. Block, M.L.; Hong, J.-S. Microglia and inflammation-mediated neurodegeneration: Multiple triggers with a common mechanism. *Prog Neurobiol.* **2005**, *76*, 77–98. [CrossRef] [PubMed]
63. Gao, H.M.; Liu, B.; Zhang, W.; Hong, J.S. Novel anti-inflammatory therapy for Parkinson's disease. *Trends Pharmacol. Sci.* **2003**, *24*, 395–401. [CrossRef]

64. Rock, R.B.; Peterson, P.K. Microglia as a pharmacological target in infectious and inflammatory diseases of the brain. *J. Neuroimmune Pharmacol.* **2006**, *1*, 117–126. [CrossRef] [PubMed]
65. Kawai, T.; Akira, S. The role of pattern-recognition receptors in innate immunity: Update on Toll-like receptors. *Nat. Immunol.* **2010**, *11*, 373–384. [CrossRef] [PubMed]
66. Poltorak, A.; He, X.; Smirnova, I.; Liu, M.Y.; Van Huffel, C.; Du, X.; Birdwell, D.; Alejos, E.; Silva, M.; Galanos, C.; et al. Defective LPS signaling in C3H/HeJ and C57BL/10ScCr mice: Mutations in Tlr4 gene. *Science* **1998**, *282*, 2085–2088. [CrossRef] [PubMed]
67. Park, B.S.; Lee, J.-O. Recognition of lipopolysaccharide pattern by TLR4 complexes. *Exp. Mol. Med.* **2013**, *45*, e66. [CrossRef] [PubMed]
68. Shimazu, R.; Akashi, S.; Ogata, H.; Nagai, Y.; Fukudome, K.; Miyake, K.; Kimoto, M. MD-2, a molecule that confers lipopolysaccharide responsiveness on Toll-like receptor 4. *J. Exp. Med.* **1999**, *189*, 1777–1782. [CrossRef]
69. Ohto, U.; Fukase, K.; Miyake, K.; Satow, Y. Crystal structures of human MD-2 and its complex with antiendotoxic lipid IVa. *Science* **2007**, *316*, 1632–1634. [CrossRef]
70. Park, B.S.; Song, D.H.; Kim, H.M.; Choi, B.-S.; Lee, H.; Lee, J.-O. The structural basis of lipopolysaccharide recognition by the TLR4-MD-2 complex. *Nature* **2009**, *458*, 1191–1195. [CrossRef]
71. Bryant, C.E.; Spring, D.R.; Gangloff, M.; Gay, N.J. The molecular basis of the host response to lipopolysaccharide. *Nat. Rev. Microbiol.* **2010**, *8*, 8–14. [CrossRef] [PubMed]
72. Gerondakis, S.; Fulford, T.S.; Messina, N.L.; Grumont, R.J. NF-κB control of T cell development. *Nat. Immunol.* **2014**, *15*, 15–25. [CrossRef] [PubMed]
73. Laird, M.H.W.; Rhee, S.H.; Perkins, D.J.; Medvedev, A.E.; Piao, W.; Fenton, M.J.; Vogel, S.N. TLR4/MyD88/PI3K interactions regulate TLR4 signaling. *J. Leukoc. Biol.* **2009**, *85*, 966–977. [CrossRef] [PubMed]
74. Hayden, M.S.; Ghosh, S. Signaling to NF-kappaB. *Genes Dev.* **2004**, *18*, 2195–2224. [CrossRef]
75. Oeckinghaus, A.; Ghosh, S. The NF-kappaB family of transcription factors and its regulation. *Cold Spring Harb. Perspect. Biol.* **2009**, *1*, a000034. [CrossRef]
76. Facchini, F.A.; Di Fusco, D.; Barresi, S.; Luraghi, A.; Minotti, A.; Granucci, F.; Monteleone, G.; Peri, F.; Monteleone, I. Effect of chemical modulation of toll-like receptor 4 in an animal model of ulcerative colitis. *Eur. J. Clin. Pharmacol.* **2020**, *76*, 409–418. [CrossRef]
77. Halgren, T.A.; Murphy, R.B.; Friesner, R.A.; Beard, H.S.; Frye, L.L.; Pollard, W.T.; Banks, J.L. Glide: A new approach for rapid, accurate docking and scoring. 2. Enrichment factors in database screening. *J. Med. Chem.* **2004**, *47*, 1750–1759. [CrossRef]
78. Friesner, R.A.; Banks, J.L.; Murphy, R.B.; Halgren, T.A.; Klicic, J.J.; Mainz, D.T.; Repasky, M.P.; Knoll, E.H.; Shelley, M.; Perry, J.K.; et al. Glide: A new approach for rapid, accurate docking and scoring. 1. Method and assessment of docking accuracy. *J. Med. Chem.* **2004**, *47*, 1739–1749. [CrossRef]
79. Repasky, M.P.; Shelley, M.; Friesner, R.A. Flexible Ligand Docking with Glide. *Curr. Protoc. Bioinformatics* **2007**. [CrossRef]
80. Sherman, W.; Friesner, R. Glide XP fragment docking and structure-based pharmacophores. *Chem. Central J.* **2009**. [CrossRef]
81. Zhu, K.; Borrelli, K.W.; Greenwood, J.R.; Day, T.; Abel, R.; Farid, R.S.; Harder, E. Docking covalent inhibitors: A parameter free approach to pose prediction and scoring. *J. Chem. Inf. Model.* **2014**, *54*, 1932–1940. [CrossRef] [PubMed]
82. Harder, E.; Damm, W.; Maple, J.; Wu, C.; Reboul, M.; Xiang, J.Y.; Wang, L.; Lupyan, D.; Dahlgren, M.K.; Knight, J.L.; et al. OPLS3: A Force Field Providing Broad Coverage of Drug-like Small Molecules and Proteins. *J. Chem. Theory Comput.* **2016**, *12*, 281–296. [CrossRef] [PubMed]
83. Jorgensen, W.L.; Maxwell, D.S.; Tirado-Rives, J. Development and Testing of the OPLS All-Atom Force Field on Conformational Energetics and Properties of Organic Liquids. *J. Am. Chem. Soc.* **1996**, *118*, 11225–11236. [CrossRef]
84. Becke, A.D. Density-functional exchange-energy approximation with correct asymptotic behavior. *Phys. Rev. A Gen. Phys.* **1988**, *38*, 3098–3100. [CrossRef]
85. Perdew, J.P. Density-functional approximation for the correlation energy of the inhomogeneous electron gas. *Phys. Rev. B Condens. Matter* **1986**, *33*, 8822–8824. [CrossRef]
86. Dunning, T.H. Gaussian basis functions for use in molecular calculations. Contraction of (12s9p) atomic basis sets for the second row atoms. *Chem. Phys. Lett.* **1970**, *7*, 423–427. [CrossRef]

87. Balasubramani, S.G.; Chen, G.P.; Coriani, S.; Diedenhofen, M.; Frank, M.S.; Franzke, Y.J.; Furche, F.; Grotjahn, R.; Harding, M.E.; Hattig, C.; et al. TURBOMOLE: Modular program suite for ab initio quantum-chemical and condensed-matter simulations. *J. Chem. Phys.* **2020**, *152*, 184107. [CrossRef]
88. Eichkorn, K.; Weigend, F.; Treutler, O.; Ahlrichs, R. Auxiliary basis sets for main row atoms and transition metals and their use to approximate Coulomb potentials. *Theor. Chem. Acta* **1997**, *97*, 119–124. [CrossRef]
89. Grimme, S.; Antony, J.; Ehrlich, S.; Krieg, H. A consistent and accurate ab initio parametrization of density functional dispersion correction (DFT-D) for the 94 elements H-Pu. *J. Chem. Phys.* **2010**, *132*, 154104. [CrossRef]
90. Klamt, A. Conductor-like Screening Model for Real Solvents: A New Approach to the Quantitative Calculation of Solvation Phenomena. *J. Phys. Chem.* **1995**, *99*, 2224–2235. [CrossRef]
91. Klamt, A. Calculation of UV/Vis Spectra in Solution. *J. Phys. Chem.* **1996**, *100*, 3349–3353. [CrossRef]
92. Jonsson, K.-O.; Vandevoorde, S.; Lambert, D.M.; Tiger, G.; Fowler, C.J. Effects of homologues and analogues of palmitoylethanolamide upon the inactivation of the endocannabinoid anandamide. *Br. J. Pharmacol.* **2001**, *133*, 1263–1275. [CrossRef] [PubMed]